



3 1293 00908 5733

This is to certify that the
dissertation entitled
Metabolic Engineering of Product Formation During Carbon
Monoxide Fermentation by Butyribacterium methylotrophicum

presented by

Andrew Jacob Grethlein

has been accepted towards fulfillment
of the requirements for

Doctor of Philosophy degree in Chemical Engineering

Robert Mark Worden

Major professor

Date 8/2/91

LIBRARY
Michigan State
University

PLACE IN RETURN BOX to remove this checkout from your record.
TO AVOID FINES return on or before date due.

DATE DUE	DATE DUE	DATE DUE
_____	_____	_____
_____	_____	_____
_____	_____	_____
_____	_____	_____
_____	_____	_____
_____	_____	_____
_____	_____	_____

**METABOLIC ENGINEERING OF PRODUCT FORMATION DURING CARBON
MONOXIDE FERMENTATION BY *BUTYRIBACTERIUM METHYLOTROPHICUM***

By

Andrew Jacob Grethlein

A DISSERTATION

**Submitted to
Michigan State University
in partial fulfillment of the requirements
for the degree of**

DOCTOR OF PHILOSOPHY

Department of Chemical Engineering

1991

ABSTRACT

METABOLIC ENGINEERING OF PRODUCT FORMATION DURING CARBON MONOXIDE FERMENTATION BY *BUTYRIBACTERIUM METHYLOTROPHICUM*

By

Andrew Jacob Grethlein

The regulation of carbon monoxide (CO) gas metabolism was examined in the anaerobic bacterium *Butyribacterium methyilotrophicum* using continuous fermentation and batch bottle studies. A cell recycle system was integrated with a chemostat to increase cell density and bias the cell population towards the stationary (resting) state. Culture media was optimized to support high cell densities and maintain CO as a limiting substrate. This system was operated at fermentation pH values between 5.1 and 7.2. Results indicated three metabolic regimes for this system. Between pH values of 6.0 and 7.2, steady-state operation was achieved, and a 5-10 fold increase in acid and alcohol production was observed relative to chemostat operation. Between pH values of 5.5 and 6.0, oscillations in butyrate and acetate production were observed, with butanol as the major product over a 72 hour period during an initial start-up period. Between pH values of 5.1 and 5.5, the cells exhibited a death phase response.

Under conditions of decreasing pH and high acetate concentration in batch culture, *B. methyilotrophicum* exhibited consumption of both CO and acetate, or CO and butyrate, with net production of butyrate or acetate, butanol and ethanol. The tolerance to both ethanol and butanol was less than 5 g/L. Hydrogen sulfide was toxic above partial pressures of 2%. These studies indicate that regulation of CO metabolism in *B. methyilotrophicum* can be achieved using a variety of environmental conditions.

A metabolic model, based on a linear system of equations for the known pathways of CO metabolism, was developed to analyze the fermentation data. The model was accurate compared to other methods of data analysis. The metabolic analysis showed decreasing

ATP yields with decreasing fermentation pH for steady-state cultures. For unsteady-state results, oscillations in ATP production were shown concomitant with oscillations in substrate consumption and product formation. From the modeling results, low fermentation pH was concluded to cause a decrease in the net ATP yields between steady-state and unsteady state systems, primarily via decreases in acetate production, inhibition of cell formation, and by decreasing the overall rate of CO metabolism.

ACKNOWLEDGMENTS

This work would not have been possible without the unwavering support of the staff at the Michigan Biotechnology Institute, and I wish to express my deepest appreciation to all of the employees and associates at MBI. I am particularly indebted to both Dr. Rathin Datta and Dr. Mahendra Jain for their advice and support during the course of this work. Special thanks also goes out to all of my friends and peers at both MBI and MSU, including Detlef Schartges, Ali Siahpush, and Cathy McGowan. I would especially like to thank Greg Reid for his steadfast friendship during the last 5 years, as well as for frequent reality checks. Finally, the success of this entire undertaking was due in large part to my thesis advisor, Dr. R. Mark Worden, who allowed me the freedom to pursue my own interests, and who consistently supported my efforts with advice, critique, and most of all, with enthusiasm.

TABLE OF CONTENTS

LIST OF TABLES:	vii
LIST OF FIGURES:	ix
INTRODUCTION:	1
CHAPTER 1: TECHNICAL AND SCIENTIFIC REVIEW:	5
1.1. Synthesis Gas Chemical Technology:	5
1.1.1. The Case for Coal Utilization:	5
1.1.2. Direct versus Indirect Liquefaction:	7
1.1.3. Gasification and Synthesis Gas Production:	9
1.1.4. Purification of Synthesis Gas:	14
1.1.5. Synthesis Gas Utilization:	22
1.1.6. Application of Synthesis Gas-Derived Compounds:	34
1.1.7. Future Prospects:	37
1.2. Microbial Metabolism of Synthesis Gas Components:	38
1.2.1. Principles of 1-Carbon Metabolism:	38
1.2.2. Carbon Monoxide, Carbon Dioxide, and Hydrogen Metabolizing Bacteria:	41
1.2.3. Principles of Acetogenic Metabolism:	47
1.2.4. Potential Application of Acetogenic Bacteria:	53
1.3. Physiology and Metabolism of <i>Butyribacterium methylotrophicum</i> :	56
1.3.1. Origin and General Characteristics of the CO Strain:	56
1.3.2. Heterotrophic Metabolic Characteristics:	57
1.3.3. Autotrophic Metabolic Characteristics:	59
1.4. Biological Processing of Coal-Derived Gases:	63
1.4.1. Potential Advantages of Biological Processing:	64
1.4.2. Potential Disadvantages of Biological Processing:	65
1.4.3. The MBI Indirect Liquefaction Process:	66
1.4.4. Objectives and Scope of the Present Work:	70
CHAPTER 2: EXPERIMENTAL MATERIALS AND METHODS:	72
2.1. Microorganism and Culture Conditions:	72
2.2. Culture Media and Gases:	72
2.3. Fermentation Equipment:	74
2.4. Fermentation Conditions:	76

2.5. Fermentation Broth Analysis:	77
2.6. Fermentation Product Analysis:	78
CHAPTER 3: METABOLIC TOLERANCE AND REGULATION STUDIES:	80
3.1. Objectives:	80
3.2. Effect of Alcohols on Growth and Product Formation:	81
3.3. Effect of Acids on Growth and Product Formation:	90
3.4. Effect of Sulfide on Growth and Product Formation:	100
3.5. Media Development Studies:	110
CHAPTER 4: CELL RECYCLE FERMENTATION STUDIES:.....	114
4.1. Objectives:	114
4.2 System Set-up and Design:	117
4.3. Results for Continuous Cell Recycle CO Fermentations:	120
4.3.1. Steady-State Results:	121
4.3.2. Unsteady-State Results:	130
4.3.3. Death Phase Results:	137
4.3.4. Cosubstrate Results:	137
4.4. Summary Discussion of Fermentation Results:	138
CHAPTER 5: METABOLIC MODELING AND FERMENTATION ANALYSIS:	140
5.1. Objectives and Principles of the Model:	140
5.2. Development of the Metabolic Model:	141
5.3. Application to Chemostat Results:	148
5.4. Application to Steady-State Cell Recycle Fermentation Results:	153
5.4.1. Case 1: Uniquely Specified System; No Cell Mass Production:	153
5.4.2. Case 2: Uniquely Specified System:	160
5.4.3. Cases 3-5: Overspecified Systems:	166
5.5. Application to Unsteady-State Cell Recycle Fermentation Results: ...	168
5.6. Limitations of the Model:	177
CHAPTER 6: CONCLUSIONS AND RECOMMENDATIONS:	180
APPENDIX:	184
LIST OF REFERENCES:	187

LIST OF TABLES

Table 1. Synthesis gas compositions from commercial and near-commercial coal gasification processes:	13
Table 2. CO/H ₂ ratios of direct synthesis routes for chemicals from synthesis gas:	30
Table 3. Properties of various fuel oxygenates:	36
Table 4. Reactions in the unicarbonotrophic and autotrophic pathways for acetyl-CoA synthesis in the acetogens <i>B. methylotrophicum</i> and <i>C. thermoaceticum</i> :	50
Table 5. 1-Carbon catabolic transformations observed with <i>B. methylotrophicum</i> :	60
Table 6. Components of the phosphate buffered basal medium:	73
Table 7. Balanced carbon and available electron equations for batch incubation in the presence of ethanol during growth on CO gas:	84
Table 8. Balanced carbon and available electron equations for batch incubation in the presence of butanol during growth on CO gas:	84
Table 9. Effect of increasing alcohol concentration on cell density and product formation during growth on CO gas:	85
Table 10. Effect of increasing alcohol concentration on cell growth and CO consumption during growth on CO gas:	85
Table 11. Balanced carbon and available electron equations for batch incubation of stationary phase cells in the presence of alcohols during growth on CO gas:	87
Table 12. Balanced carbon and available electron equations for batch incubation in the presence of acetate during growth on CO gas:	95
Table 13. Balanced carbon and available electron equations for batch incubation in the presence of butyrate during growth on CO gas:	95
Table 14. Theoretical molar ATP and electron yields from substrate-level phosphorylation for products derived during CO metabolism in <i>Butyribacterium methylotrophicum</i> :	98
Table 15. Experimental pH profiles showing dynamics of H ₂ S dissolution:	102

Table 16. Effect of liquid phase sulfide concentration on cell growth of <i>B. methylotrophicum</i> grown on CO gas at an initial pH of 7.0:	109
Table 17. Continuous, steady-state CO fermentation stoichiometries as a function of pH for <i>B. methylotrophicum</i> :	116
Table 18. Continuous, steady-state CO fermentation product concentrations as a function of pH for <i>B. methylotrophicum</i> :	116
Table 19. Overall culture response as a function of fermentation pH during cell recycle fermentation:	121
Table 20. Steady-state fermentation stoichiometries as a function of pH for continuous fermentation of CO gas:	122
Table 21. Continuous, steady-state CO fermentation molar yield coefficients as a function of pH for <i>B. methylotrophicum</i> :	122
Table 22. Continuous, steady-state CO fermentation carbon partitioning as a function of pH for <i>B. methylotrophicum</i> :	124
Table 23. Continuous, steady-state CO fermentation electron partitioning as a function of pH for <i>B. methylotrophicum</i> :	124
Table 24. Continuous, steady-state CO fermentation parameters, product concentrations, and CO consumption rates as a function of pH for <i>B. methylotrophicum</i> :	126
Table 25. Continuous, steady-state CO fermentation CO consumption rates as a function of fermenter volume and culture OD for <i>B. methylotrophicum</i> :	126
Table 26. Unsteady-state, initial fermentation stoichiometries as a function of pH for cell recycle fermentation of CO gas:	133
Table 27. Continuous, initial unsteady-state CO fermentation carbon partitioning as a function of pH for <i>B. methylotrophicum</i> :	136
Table 28. Continuous, initial unsteady-state CO fermentation electron partitioning as a function of pH for <i>B. methylotrophicum</i> :	136
Table 29. Continuous, steady-state CO fermentation carbon and electron partitioning at a pH of 5.9 in the presence of acetate for <i>B. methylotrophicum</i> :	138
Table 30. Standard free energies of reaction for CO conversion:	139
Table 31. Comparison of CO:CO ₂ ratios from chemostat culture between metabolic model and carbon and electron balancing calculations:	151
Table 32. Comparison of CO:CO ₂ ratios from steady-state cell recycle culture between metabolic model and carbon and electron balancing calculations for Case 2:	161

LIST OF FIGURES

Figure 1. Schematic of typical sulfur recovery and removal operations during catalytic conversion of coal-derived synthesis gas:	21
Figure 2. Potential industrial uses of fuels and chemicals from coal-derived synthesis gas:	23
Figure 3. Specific uses for 1-carbon compounds from coal-derived synthesis gas:	27
Figure 4. General process scheme for SASOL Fischer-Tropsch synthesis plant, Sasolburg, South Africa (Dry, 1987):	29
Figure 5. General pathway for unicarbonotrophic, acetogenic metabolism:	49
Figure 6. General mechanism for electron transport-coupled phosphorylation (ETP):	52
Figure 7. Potential biological routes for fuels and chemicals production from synthesis gas components:	54
Figure 8. Proposed bioconversion scheme for production of fuel alcohols from coal-derived synthesis gas:	68
Figure 9. Effect of increasing ethanol concentration during growth of <i>B. methylotrophicum</i> on CO gas:	82
Figure 10. Effect of increasing butanol concentration during growth of <i>B. methylotrophicum</i> on CO gas:	82
Figure 11. Effect of increasing ethanol concentration during growth of <i>B. methylotrophicum</i> on CO gas:	86
Figure 12. Effect of increasing butanol concentration during growth of <i>B. methylotrophicum</i> on CO gas:	86
Figure 13. Effect of increasing acetate concentration during growth of <i>B. methylotrophicum</i> on CO gas:	93
Figure 14. Effect of increasing butyrate concentration during growth of <i>B. methylotrophicum</i> on CO gas:	94
Figure 15. Effect of increasing NaCl concentration during growth of <i>B. methylotrophicum</i> on CO gas:	97

Figure 16. Effect of initial H ₂ S gas phase concentration during growth of <i>B. methylotrophicum</i> on CO gas:	104
Figure 17. Effect of increasing H ₂ S concentration on acetate production during growth of <i>B. methylotrophicum</i> :	104
Figure 18. Acetate yields as a function of initial H ₂ S concentration during growth of <i>B. methylotrophicum</i> on CO gas:	105
Figure 19. Effect of initial sulfide concentration during growth of <i>B. methylotrophicum</i> on CO gas:	107
Figure 20. Effect of initial sulfide concentration during growth of <i>B. methylotrophicum</i> on CO gas:	107
Figure 21. Specific and molar yields as a function of initial sulfide concentration during growth of <i>B. methylotrophicum</i> on CO gas:	108
Figure 22. Specific and molar yields for product formation during growth of <i>B. methylotrophicum</i> on CO gas:	108
Figure 23. Effect of media supplements on the growth of <i>B. methylotrophicum</i> on CO gas:	113
Figure 24. Effect of increasing yeast extract concentration on the growth of <i>B. methylotrophicum</i> on CO gas:	113
Figure 25. Schematic diagram of continuous, cell recycle CO fermentation system:	118
Figure 26. Molar product ratios as a function of pH during continuous cell recycle fermentation:	125
Figure 27. Product concentrations during continuous cell recycle CO fermentation at a pH of 5.75:	131
Figure 28. Product concentrations during continuous cell recycle CO fermentation at a pH of 5.5:	132
Figure 29. Theoretical and measured washout curves for butyrate during cell recycle fermentation at a pH of 5.5:	134
Figure 30. Known and proposed metabolic pathways for carbon and electron flow during CO metabolism in <i>B. methylotrophicum</i> :	145
Figure 31. Molar consumption and production rates for CO and CO ₂ gas as a function of fermentation pH during continuous, steady-state culture:	150
Figure 32. Molar product ratios as a function of fermentation pH during steady-state, continuous culture:	150

Figure 33. Theoretical molar ATP yield via electron-transport phosphorylation and substrate-level phosphorylation as a function of fermentation pH during continuous culture:	152
Figure 34. Steady-state CO consumption, cell production, and optical density as a function of pH for continuous cell recycle fermentation:	156
Figure 35. Normalized CO consumption rates for continuous cell recycle fermentation as a function of pH:	156
Figure 36. Normalized molar gas consumption and production rates as a function of pH during steady-state, continuous cell recycle fermentation: Case 1:	157
Figure 37. Molar product ratios as a function of pH during steady-state, continuous cell recycle fermentation: Case 1:	157
Figure 38. Theoretical molar ATP yield via electron-transport phosphorylation and substrate-level phosphorylation vs. pH during steady-state cell recycle fermentation: Case 1:	158
Figure 39. Molar electron yields as a function of fermentation pH during steady-state cell recycle fermentation: Case 1:	159
Figure 40. Normalized molar gas consumption and production rates as a function of pH during steady-state cell recycle fermentation: Case 2:	162
Figure 41. Molar product ratios as a function of pH during steady-state cell recycle fermentation: Case 2:	162
Figure 42. Theoretical molar ATP yield via electron-transport phosphorylation and substrate-level phosphorylation vs. pH during steady-state cell recycle fermentation: Case 2:	163
Figure 43. Molar electron yields as a function of fermentation pH during steady-state cell recycle fermentation: Case 2:	165
Figure 44. Electron-transport phosphorylation and total ATP yields as a function of ETP H^+ /ATP ratio during steady state, continuous cell recycle fermentation:	167
Figure 45. Molar CO consumption for Cases 2-5 as a function of pH during steady-state cell recycle fermentation:	169
Figure 46. Molar product ratios for Cases 2-5 as a function of pH during steady-state cell recycle fermentation:	169
Figure 47. Theoretical molar ATP yields for Cases 2-5 as a function of pH during steady-state cell recycle fermentation:	170
Figure 48. Theoretical molar electron yields for Cases 2-5 as a function of pH during steady-state cell recycle fermentation:	170

Figure 49. Normalized molar gas consumption and production rates as a function of time during unsteady-state cell recycle fermentation at a pH of 5.5:	174
Figure 50. Molar yield of acetate during unsteady-state cell recycle fermentation at a pH of 5.5:	175
Figure 51. Molar yield of butyrate during unsteady-state cell recycle fermentation at a pH of 5.5:	175
Figure 52. Theoretical molar ATP yield via electron-transport phosphorylation and substrate-level phosphorylation during unsteady-state cell recycle fermentation at a pH of 5.5:	176

INTRODUCTION

The potential advantages of bioprocessing compared to catalytic processing of coal-derived synthesis gas stem primarily from the specificity of biological conversion systems and the associated low temperature and low pressure operating conditions. One of the major drawbacks with using coal-derived synthesis gas as a feedstock for chemical catalysis is the presence of sulfur gases such as hydrogen sulfide and carbonyl sulfide, both of which are potent catalyst poisons. Removal of these contaminants is an energy-intensive process that can add significantly to the final product cost, particularly for coals with a high sulfur content. In biological processing, the conversion is conducted in an aqueous media which can reduce direct contact of microorganisms to harmful sulfide species. By employing sulfur-tolerant microorganisms, this effect can be further minimized, and thus stringent and costly synthesis gas purification steps can be avoided. Furthermore, since most biological reactions occur at relatively low pressures and temperatures, and exhibit a high degree of selectivity and efficiency, the cost of operation during gas conversion can potentially be much less expensive for a biological process. These key advantages distinguish the biological synthesis gas conversion concept and offer a unique niche for production of oxygenated fuels or chemicals via fermentation of coal-derived gases.

The inherent disadvantages with biological systems are mainly slow reaction rates and difficulties associated with maintenance of microbial populations in desired growth and metabolic states. Therefore, any bioconversion scheme for synthesis gas must be designed for maximization of reaction rates and for maintaining long-term, stable cultures. Such a potential process scheme has been proposed by the Michigan Biotechnology Institute (MBI). Briefly, the concept employs a two-stage fermentation for production of liquid

fuels such as butanol and ethanol using anaerobic bacteria. The first stage is an acidogenic conversion where the CO present in the synthesis gas, with or without methanol, is converted to a mixture of primarily butyric and acetic acids. The hydrogen atoms required for this reaction come from water. The acids, along with the hydrogen gas, are then converted in a second stage fermentation to butanol, ethanol and acetone. Cell recycling is used in each stage to maintain high cell densities and thus high productivity. An energy-efficient distillation unit is proposed for efficient, cost-effective separation of the dilute alcohols. The first stage CO conversion is expected to be rate-limiting and requires an organism capable of both butyrate and acetate production directly from CO gas. Such an organism is *Butyribacterium methylotrophicum*, an anaerobic, sulfide-tolerant bacterium with the ability to metabolize a wide range of 1-carbon compounds, including CO and methanol.

The focus of this dissertation was to investigate the potential of *B. methylotrophicum* for use in the MBI bioconversion scheme. A major goal of this investigation included the design and operation of a cell recycle fermentation system for use with a gas phase substrate. Determining the regulatory effect of fermentation pH on CO metabolism in studies with the cell recycle system was a key objective of those experiments. Results from those fermentations raised several questions which were best addressed in batch metabolic regulation studies, such as product tolerance and acid uptake phenomena. Determining the effects of end-products and sulfide on CO metabolism was a another objective. Results from the metabolic and fermentation studies indicated that the cellular energetics could potentially be as significant a factor as fermentation pH in regulating the flow of carbon and electrons during CO metabolism. To this end, a metabolic model was developed to address the energetic hypothesis and attempt to elucidate a probable mechanism for the pH effect, based on the results obtained in the cell recycle systems. Specifically, the key objectives were:

1. Increase CO fermentation productivity and effluent product concentrations.

2. Operate continuously at low fermentation pH values, where butyrate and alcohol production are favored.
3. Regulate CO metabolism away from acetate and towards other products.
4. Develop a liquid media capable of supporting high cell densities.
5. Elucidate pathways for alcohol production from CO in *B. methylotrophicum*.
6. Investigate effect of fermentation products on CO metabolism.
7. Identify possible mechanism(s) of metabolic regulation during CO metabolism.
8. Determine the organism's tolerance for sulfide species that may be present in coal-derived synthesis gas .
9. Determine the overall mechanism of the pH effect on CO metabolism.

The overall objective of this work was thus to attempt to identify the mechanism of the pH effect, both by experimentation and by modelling analysis.

The textual organization of this dissertation reflects the three major thrusts of this work: regulation of metabolism, fermentation development, and metabolic modeling. Chapter 1 is a scientific and technical review of the current chemical technology for synthesis gas production, purification, and utilization. The fundamentals of anaerobic, acetogenic bacteria are then discussed, including a review of the most widely known organisms capable of metabolizing the major synthesis gas components. The origin, physiology, and metabolism of *B. methylotrophicum* are then reviewed, followed by a description of the MBI process for biological conversion of coal-derived synthesis gas.

Chapter 2 is a description of the materials and techniques used during the experimental portion of this work. Chapter 3 presents the microbiological studies conducted in anaerobic bottle systems. These studies included the effect of all major CO fermentation products, including acetate, butyrate, ethanol, and butanol, on CO metabolism during growth. The effect of sulfide species on CO metabolism during cell growth is then described. Finally, the development of a culture medium for use in the cell recycle fermentations is presented.

Chapter 4 encompasses the cell recycle fermentation studies conducted with *B. methylotrophicum*. This chapter is divided into sections based on the observed metabolic responses to fermentation pH, mainly steady-state responses, oscillatory responses, and cell death. These results are discussed in light of the current hypothesis for the mechanism of the pH effect on CO metabolism, including the possibility of energetic limitations during CO fermentation. Experiments relating to the use of cosubstrates during CO fermentation are then presented.

Chapter 5 presents the development and analysis of results of the metabolic model for CO metabolism, based on the cell recycle fermentation data. The basic principles and objectives of the model are outlined. The model is then applied to previously derived chemostat data, the results evaluated, and the modeling approach evaluated. The steady-state cell recycle fermentation results are then analyzed with the model. The energetics of CO metabolism are discussed in light of the fermentation analysis. A preliminary analysis of the unsteady-state fermentation data is then presented. A short discussion on the limitations of the modelling method concludes this chapter. The findings from Chapters 3-5 are summarized and discussed further in Chapter 6, with a focus on the pH effect and its likely mechanism. Finally, the work is concluded with a statement concerning the potential for a bioconversion process based on the presented results, and with some recommendations on areas and aspects for further investigation.

CHAPTER 1

TECHNICAL AND SCIENTIFIC REVIEW

1.1. Synthesis Gas Chemical Technology

1.1.1. The Case for Coal Utilization

The cultural and political volatility and instability of the world's major petroleum producing regions as well as the predicted future shortages in petroleum resources has stimulated both discussion and research on alternate forms of energy and their utilization. Whether these issues and many others are sufficient to motivate the United States to implement policy changes towards a major energy transition remains to be seen. Diversification of energy resources instead of the current heavy dependence on a petroleum based energy and fuels economy would certainly be advantageous from a domestic standpoint. However, the competitive advantage of petroleum versus other energy forms, based on its abundance, and based on the dependence of the current infrastructure on its use, makes diversification a difficult and arduous process. The ultimate degree of diversification obtainable depends on development of policy, technology, and also on efficient application of the technology, to modify and refocus the current structure of the industry. Social and environmental factors will also have an important influence on the degree of diversification possible. Such non-technical factors have even been described as the major obstacles towards commercialization of new processes (Conn, 1981). Finding substitutes for petroleum to serve as sources for fuel, energy, and chemicals production is thus an important, difficult, and far-reaching endeavor.

The use of coal as direct energy source or as a raw material for fuels and chemicals production is an existing and increasingly attractive alternative to petroleum-based processes. In 1990, U.S. coal production surpassed 1 billion tons for the first time (Lepkowski, 1991), and is predicted to surpass 2 billion by the year 2000 (Exxon Co.,

1979). Currently, coal-fired plants account for 56% of domestic power generation, with utility companies consuming approximately 80% of the total mined coal (Haggin, 1991). Another major industry based on coal is the coking industry, in which carbonization of coal via destructive distillation produces coke, which has a principal use as a fuel in blast furnaces, with wide application in the steel industry. In the fuels and chemicals sector, coal's contribution is much less evident, with the majority of fuels and chemicals production currently arising from natural gas and petroleum utilization. The domestic abundance of coal, its comparative cost, and a relatively large processing technology base are some of the advantages associated with its use. Environmental issues and transportation costs are a few of the major disadvantages.

In general, coals are ranked or categorized by their relative aromaticity and their moisture and volatile matter content, with anthracite, semi-anthracite, low-volatile bituminous, medium-volatile bituminous, high-volatile bituminous, sub-bituminous, and lignite coals comprising the major classifications. These types are listed in order of increasing moisture content and volatile matter content and decreasing aromatic content. A high rank coal is thus one in which the fixed carbon to volatile carbon ratio, with fixed carbon in the form of an aromatic ring structure, is very high. The above list is also indicative of the overall energy content for combustion, most commonly listed in the units of Btu/lb, where lignitic coal has the lowest calorific value and anthracitic coal the highest. It follows that lignitic coal is typically cheaper in comparison, mainly because the price is generally determined by the application, which for coal is mainly in its combustion for electric power generation. Low-rank coals have thus become a focal point for synthetic fuels and chemicals research, because of their relatively low cost.

The complexity and diversity of coal has been one of the limiting factors in development of new technology for specific applications. The diversity of structure stems primarily from the diversity of carbonaceous plant life that was fossilized, the geologic environment in which the fossilization occurred, and on the age of the coal. All of these

factors are reflected in the composition of both the organic and inorganic structure. Although the fine organic structure of coal is a topic still under debate and investigation, it can generally be described with an empirical formula containing carbon, hydrogen, oxygen, nitrogen, and sulfur such as $\text{CH}_{0.7}\text{O}_{0.6}\text{N}_{0.2}\text{S}_{0.1}$ for bituminous coal (Datta and Andrews, 1991). The inorganic fraction is typically in the form of discrete mineral inclusions. Contained in both the organic and inorganic fractions are sulfur compounds, present primarily as inorganic iron pyrite or covalently bound organic thiols, sulfides/disulfides, and mercaptans (Young and Finnerty, 1991). The overall sulfur content of coal is one of the key characteristics in determining its value and utility, since these sulfur compounds will result in the formation of sulfur oxides during combustion, which will have a direct impact on air quality and emissions during processing.

These factors have been one of the key influences in the definition and implementation of the U.S. Department of Energy's clean-coal program, which has been focused on increasing the uses and applications of coal in the national energy strategy. Although this effort has been primarily based on restructuring and redesigning existing technology for using coal in electric power generation, other areas are also under investigation. One area which is very active is the development of lower rank coal and coal-based processes for synthetic fuels and chemicals/feedstocks production. Most of this developmental research is in optimization of technology for design of commercial facilities and plants (Bassler and Sperhac, 1986). These routes involve coal liquefaction technology.

1.1.2. Direct versus Indirect Liquefaction

Coal utilization and processing for synthetic fuels and chemicals production can be categorized under 4 generic coal liquefaction methods, which are pyrolysis, direct hydroliquefaction, solvent extraction, and indirect synthesis. If synthesis gas is produced as an intermediate, then indirect synthesis is referred to as indirect liquefaction, while all the others are referred to as direct liquefaction. Hydroliquefaction is generally accepted to be the preferred direct liquefaction route, and is a technology that has its roots in coal

pyrolysis. Solvent extraction is not currently under serious development, particularly on the pilot and commercial scales. Indirect liquefaction has been shown to be a commercially viable technology, albeit under specific circumstances, as discussed below.

Coal pyrolysis, also known as destructive distillation, is a process by which the coal is thermally decomposed to form a mixture of gases, liquids, tars, char, and coke. The principle mechanism is first removal of the volatile fraction, and then generation of organic free radicals, which subsequently react with the solid structure to form a mixture of volatile liquids and gases. A carbonaceous char is the resulting solid structure, which is typically reacted or gasified further. A major limitation is the availability of hydrogen, which during pyrolysis comes from the coal itself. In the absence of available hydrogen, polymerization and aromatization of the reactive free radical coal fragments occurs, resulting in excessive coke formation (Mills, 1976). The regulation of destructive coal distillation is thus dependent on the relative rates of free radical generation and on the rates of hydrogen transfer to the free radical reactive intermediates; balanced rates will favor volatile hydrocarbon formation, low rates of hydrogen donation and transfer will favor coke formation. Some pilot-scale processes which demonstrate pyrolysis technology are the COED process, the TOSCOAL process, and the Occidental (Garrett Coal Pyrolysis) process (Kalfadelis and Shaw, 1980).

In direct hydroliquefaction, which is also called coal hydrogenation, coal is thermally liquified in the presence of catalyst and high pressure hydrogen. The basic mechanism is the same as for pyrolysis, only in hydroliquefaction, external hydrogen helps to minimize the reactive polymerization of the free radicals, which thus minimizes coke and char formation. This hydrogen can come from molecular hydrogen, or more typically from a hydrogen-donating solvent added to the reaction mixture. Balancing the reaction temperature, which as it is increased promotes free radical formation, with the reaction pressure, which as it is increased allows for higher hydrogen availability until catalyst saturation, is a key issue in these processes. Some representative technologies are the

Synthoil process, the H-Coal process, and the Exxon donor-solvent coal liquefaction process (Mangold et al., 1982).

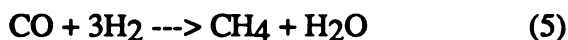
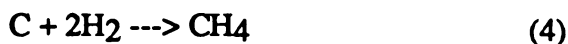
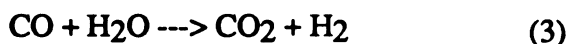
Indirect liquefaction is a technology based on intermediate formation of synthesis gas by coal gasification, and then further catalytic reaction to produce the desired liquid products. Coal is gasified by thermal reaction in the presence of oxygen and water to produce carbon monoxide (CO) and hydrogen (H₂) gases. These gases can then serve as precursors for several different reaction chemistries, either direct or indirect themselves, including Fischer-Tropsch synthesis, Roelen chemistry, which is also known as oxo-processes or hydroformylation, and many indirect methanol chemistry routes. These technologies have a long history, are currently in use commercially, and are discussed in more detail in a subsequent section.

1.1.3. Gasification and Synthesis Gas Production

Indirect coal liquefaction requires gasification of coal to form synthesis gas, primarily a mixture of CO and H₂ gases. Although synthesis gas for fuels and chemicals production is presently produced primarily by catalytic steam reformation of natural gas or by partial oxidation of heavy oil fractions (Heubler and Janka, 1980), coal gasification to form synthesis gas has a future potential because of the relative abundance, availability, and cost of coal. Coal gasification in the U.S. between the turn of the century and until the 1950's was an attractive technology, with extensive production of gaseous fuels occurring in plants which operated generally at low capacity and low efficiency (Spencer et al., 1982). This technology, however, was superseded by the availability of low cost natural gas and petroleum after the Second World War.

The revitalization of coal gasification technology depends on the redesigning of old methods to produce more economically and environmentally attractive processes. With gasification becoming a more prominent step in electric power generation from coal, the electric power industry has served to develop gasification technology to a relatively high level, technology which can directly translate to synthetic fuels and chemical production

via indirect liquefaction. Typically, synthesis gas is produced from coal by steam gasification, where coal, water, and oxygen (O₂) are combined at high temperature and pressure under conditions promoting an O₂ limited system. The resulting synthesis gas is primarily a mixture of CO and H₂, with carbon dioxide (CO₂), methane (CH₄), hydrogen sulfide (H₂S), and H₂O being the remaining components. The composition of the synthesis gas depends mainly on the type of gasifier and the resulting reaction conditions. The conditions directly affect 5 main reactions occurring in the gasifier (Mangold et al., 1982):



The relative rates of these reactions will determine the exit synthesis gas composition. Under oxygen limited conditions, reaction (1) becomes rate limiting thus making incomplete or partial combustion of coal a fundamental step. Reaction (3) is often referred to as the water-gas shift reaction, and is the main regulatory reaction in determining the final CO:H₂ ratio. This reaction also favors H₂ at lower temperatures. Reaction (5) is what has been referred to above as steam reformation of natural gas, and is a reaction which regulates CH₄ formation in the presence of steam (H₂O). The final synthesis gas composition desired depends on the application; for substitute natural gas (SNG) production, one wants to maximize CH₄ and H₂ formation and minimize CO formation. For electric power generation, one wants to maximize the CO:H₂ ratio, and for chemical and fuels production, a specific CO:H₂ based on the stoichiometry based on the product-forming reaction is usually desired. These objectives are most commonly achieved by the choice of gasifier system, whether it be a fixed- or moving-bed, a fluidized-bed, or an entrained flow gasifier (Wilson et al, 1988).

The design and performance of the main gasifier types are based primarily on the physical and mechanical aspects of contacting the coal with the O_2 and H_2O . Fixed/moving-bed gasifiers operate with countercurrent flow of coal and reacting gases, generally operate below $1000^\circ F$, and exhibit a very non-uniform temperature profile in the reactor. These systems generally cannot react the coal fines, and produce heavy by-product tars (Spencer et al., 1982). Relatively high solid residence times are required, and the mechanical strength of the coal must be high (Verma, 1978a). Entrained-bed gasifiers use cocurrent flow of coal and reactant gases, generally operate between $2300^\circ F$ and $2700^\circ F$, and exhibit a very uniform temperature profile. Reaction of coal and carbon fines in these systems is possible. Methane and tar formation are not observed because of the high temperature of operation. Fluidized-bed systems exhibit rapid and complete gas-solids mixing, operate between $1000^\circ F$ and $1700^\circ F$, and exhibit a relatively uniform temperature profile. The characteristics described above are critical in determining the final synthesis gas composition (Wilson et al., 1988).

The application of these reactor types and their development has resulted in a so-called second generation of coal-gasification systems on a world-wide basis. Only a few types and modifications of these have been commercially proven, such as the Wellman-Galusha, Winkler, Koppers-Totzek, and Lurgi type gasifiers, but many others are at the pilot scale of development and testing. Most of the systems were designed initially for production of gases in a particular heating value range, but current technology now allows a certain degree of versatility in this regard. All of these types were invented in Germany over 50 years ago.

The Wellman-Galusha gasifier is a fixed-bed configuration designed specifically for the production of low-Btu gases. The reactant gas stream is a mixture of steam and air, and thus nitrogen is typically a significant portion of the resulting synthesis gas. Operating pressures are atmospheric or slightly above atmospheric pressure. The temperatures of

operation are in the range of 1000-1200°F (Verma, 1978a). A major operating advantage of this design is its ability to process all types and ranks of coal.

The Winkler gasifier is a fluidized-bed type unit in which crushed coal is fed by screw feeder to the bottom of a fuel bed, where the gas stream is introduced and the reacting mixture fluidized. The fluidizing gas used is usually a mixture of steam and air or O₂. The unit typically operates at 1500-1850°F and at atmospheric pressure (Verma, 1978a). Conversion of carbon in the coal is relatively low. The Winkler process was one of the first applications of fluidized-bed technology, but has been transcended by competing technology in recent times. However, a version of this type of gasifier, called the High Temperature Winkler (HTW) or Rheinbraun process is under development at the pilot and demonstration plant scales. This version of the conventional Winkler technology uses a high pressure gasification system nearing 10 atm (Simbeck, et al., 1982).

The Koppers-Totzek (K-T) gasifier is an entrained-bed type where dried and finely crushed coal is conveyed into a mixing nozzle, where it is contacted by a jet of steam and O₂ and entrained into the gasifier. Reaction pressures are nominally above atmospheric, with reaction temperatures nearing 2600°F. Carbon conversion is relatively high. The K-T process is one of the most recent gasifiers to be proven commercially, with the primary application in the production of synthesis gas for ammonia formation (Simbeck et al., 1982). There are several offshoots of the K-T process under development at the pilot and demonstration scales, most notably of which is the Shell-Koppers process, which uses a pressurized version of the K-T gasifier (Simbeck et al., 1982).

The Lurgi gasifier is perhaps the most successful of the commercialized gasifier technologies. Its configuration is an O₂/steam blown, high pressure, moving-bed. Operating temperatures are in the range of 1150-1400°F. The countercurrent flow configuration results in various reaction regimes in the gasifier, with zones of combustion, gasification, carbonization, and drying occurring. The primary examples of commercial application are in the South African Coal, Oil, and Gas Corporation, or SASOL, where

Lurgi gasifiers are used to produce synthesis gas for subsequent Fischer-Tropsch processing and liquid fuels production. Lurgi gasifiers are also employed at the Great Plains Coal Gasification Plant, in North Dakota (Imler, 1985). A version of the Lurgi which reduces steam requirements by slagging the ash produced in the gasifier, called the BGC/Lurgi process, is in the demonstration scale of development (Simbeck et al., 1982).

Current developments in gasifier technology are coming mostly in the areas of reduced utilities requirements and improved capacities. A wide range of synthesis gas compositions are obtainable as shown in Table 1; these compositions are not only dependent on the gasifier design and operating conditions but also on the type of coal used.

Table 1. Synthesis gas compositions from commercial and near-commercial coal gasification processes.

Process	Gas Composition (vol %)					
	CO	H ₂	CO ₂	H ₂ O	CH ₄	H ₂ S + COS
Wellman-Galusha ^a	22.8	22.8	11.4	0.0	0.0	(43.0 N ₂)
Winkler ^a	36.0	42.0	17.7	0.0	3.2	0.1
Koppers-Totzek ^a	52.5	39.0	10.0	0.0	0.0	0.5
Lurgi ^a	21.0	41.0	27.5	0.0	8.8	-
Shell-Koppers ^b	64.0	31.6	0.8	1.5	0.0	1.4
BGC Lurgi ^c	55.5	28.3	5.1	0.0	6.3	3.0
Texaco ^d	54.0	34.0	11.0	0.0	0.01	0.3
Underground Gasification ^e	19.6	31.1	33.0	-	16.3	-

^a From Verma, 1978a.

^b From McCullough et al., 1982.

^c From Development Status of Key Emerging Foreign Gasification Systems, TRW Report. Sept., 1980.

^d From Schafer et al., 1988.

^e From Bloomstran and Davis, 1984.

Several large energy corporations, including Texaco (Kolaian and Schlenger, 1982) and Shell (McCullough, 1982), are currently developing demonstration scale variations of the

basic types of gasifiers listed above (Spencer et al., 1989; Schafer et al., 1988). However, gasifier development is not the only area of technology advancement for coal gasification. For specific applications, mainly in the production of low-Btu gases, underground coal gasification *in situ*, for deep coal seams where mining is either impractical or impossible, has undergone favorable field tests in recent years (Hammesfahr and Winter, 1984; Bloomstran and Davis, 1984). This technology, first developed in the Soviet Union over 60 years ago, employs air or O₂ and steam injection through bore holes drilled into the coal seam. The drilling process and the gas flow properties in coal strata are the major obstacles to commercial development (Verma, 1978b).

1.1.4. Purification of Synthesis Gas

The production of synthesis gas from coal is a technically complex process. The complicated structure and composition of coal results in a variety of contaminant species being formed during gasification, most of which are sulfur and nitrogen compounds. Formation of CO₂ in conventional gasifiers, as shown previously in Table 1, can account for anywhere between 1-30% by volume of the synthesis gas mixture. These impurities, or contaminants, must be removed prior to catalytic synthesis, because of catalyst poisoning limitations. There are also many corrosion and environmental/safety issues involved in sulfur and acid gas processing. Separation and removal is not the only concern, however. Once the synthesis gas has been purified, the contaminant streams must be recovered, recycled, or disposed of in some way. The magnitude of these operations is enormous when the processing rate of most commercial gasifiers is realized.

The presence of sulfur compounds in coal can vary widely, with the sulfur content range between 0.5-11% by weight for U.S. coals (Young and Finnerty, 1991). Inorganic sulfur pyrites (FeS₂) are generally removed in density-dependent pretreatment processes prior to gasification, since these compounds are generally present as distinct mineral inclusions. It is thus the organic sulfur in coal that contributes during gasification to the formation of contaminating sulfur species. The reducing conditions of the typical

gasification process result in most of the sulfur in coal ending up as hydrogen sulfide (H_2S) or carbonyl sulfide (COS), with the vast majority as H_2S . As shown previously in Table 1, these compounds can typically account for between 0-3% by volume of synthesis gas mixtures, with the final concentration highly dependent on the composition of the coal gasified. Other sulfur compounds that are often observed in much lower amounts are carbon disulfide (CS_2), thiophenes, mercaptans, and several alkylated sulfide species (Cumare et al., 1984).

Nitrogen contaminants in synthesis gas can be of particular concern if the gasification process is using air and steam instead of pure O_2 and steam. The nitrogen species from operation with air are typically NO_x type species, including N_2O , NO and NO_2 . The use of O_2 instead of air will generally limit formation of these oxidized nitrogen compounds (Cumare et al., 1984). Organic nitrogen contained in the coal will be liberated during gasification in the form of ammonia (NH_3), hydrogen cyanide (HCN), and elemental nitrogen (N_2). Since the nitrogen content of coal, on the average, is between 1-2% by weight, these impurities are less prevalent than sulfur impurities.

The necessity and stringency of contaminant removal for synthesis gas processing is determined primarily by catalyst poisoning issues, the vast majority of which concern the concentration of sulfides in the reactant synthesis gas. As detailed in the next section, both production of substitute natural gas (SNG) and conventional Fischer-Tropsch chemistry are catalyst-dependent. These processes have different sulfur tolerance levels based on the catalyst composition. Catalysts which have been determined to be active in CO hydrogenations such as those observed during Fischer-tropsch synthesis include most of the Type VIII metals, namely iron, cobalt, nickel, ruthenium, platinum, and also rhodium. Of the above metals used in synthesis gas processing, iron is the most common and the best characterized.

Specifically, the poisoning of Type VIII metal catalysts is due primarily to the reactivity of the two unshared electron pairs present in a molecule of H_2S , which contribute to

stability during metal-poison interactions (Lee, 1985). The strength of these interactions is explained in part by a high heat of adsorption for sulfide on most of the metals listed above. Besides the issue of active site poisoning, there is evidence from work with platinum for decreased CO binding energy with increased sulfur coverage, possibly due to electronic interactions between the adsorbed sulfur and the adsorbing CO (Bonzel and Ku, 1973). This same study, using flash desorption techniques, determined that sulfur and CO compete for the same active sites on platinum catalysts. The negative effect due to sulfur poisoning on the binding energy of CO is partially a consequence of a weakening of the electronic density in sites adjacent to that of the adsorbed sulfur molecule, a result stemming from its highly electronegative nature (Oudar, 1980). In the case of surface reactions characterized by a Langmuir-Hinshelwood mechanism, the presence of chemisorbed sulfur is detrimental, a likely effect of decreased active species mobility (Hegedus and McCabe, 1984).

The actual permissible sulfur concentrations in a typical synthesis gas feedstock are quite low. For iron at 400°C, 1.6 ppm is the tolerance limit, and for nickel at 550°C, the limit is 2.5 ppm (Rostrup-Nielsen, 1971). Current industrial standards aim at an order of magnitude less than these values, to maintain quality control and long catalyst life (Dry, 1981). These low levels are obtainable by employing advanced sulfur removal technology, as described below.

The predominant contaminant species H_2S and CO_2 , also known as the acid gases, account for the majority of synthesis gas separation and removal technology, with removal of COS and CS_2 occurring simultaneously. H_2S removal is necessary to prevent corrosion of process equipment, to protect downstream catalytic reactors from poisoning, and to maintain safety and environmental quality in the plant. Removal of CO_2 is necessary during production of high-Btu synthesis and fuel gases. There are two basic commercial technologies for removal of these compounds, either solvent absorption or chemical conversion. The choice between these system depends heavily on the partial pressures of

acid gases in the synthesis gas stream. Solvent absorption processes can be further separated by the nature of the solvent used, with chemical, physical, and hybrid solvent absorption strategies all being commercially available. The chemical solvents allow chemisorption with acid gas compounds. These solvents usually have high heats of reaction with acid gases, and possess high heats of absorption for the same compounds (Eickmeyer and Gangriwala, 1981). The physical solvent processes exhibit a much different equilibrium curve than chemical solvents, and are useful at high pressures and higher acid gas partial pressures. Hybrid solvent systems are mixtures of both chemical and physical solvents and attempt to combine the best characteristics of each, and are used when very specific absorption characteristics are required.

The majority of chemical absorption systems are amine-based solutions which are weakly alkaline. The alkanolamines such as monoethanolamine (MEA), diethanolamine (DEA) are the most common, with DEA usually preferred because of the negative effect of COS on MEA (Cumare, 1984). The use of amine-based solvent systems is limited by the temperature-equilibrium curve for the acid gas components; increasing temperature results in a sharp increase in the CO₂ back pressure for these chemisorption systems (Eickmeyer and Gangriwala, 1981). The heat transfer issues during removal are thus paramount when employing amine-based systems. Other possible solvents include diglycolamine (DGA), a primary amine which is similar to MEA but more soluble in water. The secondary amine diisopropanolamine (DIPA) is specific for H₂S removal, and is also used in various hybrid solvents. The tertiary amine methyldiethanolamine (MDEA) is also selective for H₂S over CO₂, and is used in acid gas separations. In general, one positive feature of all amine-based chemical absorption systems is the low solubility of hydrocarbons in the aqueous amine-water solvents (Cumare, 1984). When the operating pressure and the partial pressures of the acid gas contaminants are adequately high, chemical solvents based on aqueous hot potassium carbonate solutions are preferable, because of the lower heats of absorption for CO₂ and thus lower utility costs (Eickmeyer and Gangriwala, 1981). When

a catalyst is added, called promoted hot carbonate solutions, the rate of CO₂ absorption is increased even more. These systems also exhibit low solubilities for hydrocarbon absorption. Commercial hot carbonate processes include the Catacarb, Flexsorb HP, and Benfield processes.

Absorption of acid gas constituents in physical solvents is applicable at higher pressures and higher partial pressures of acid gases. High acid gas loading in physical solvents allows higher acid gas removal capacities and lower solvent circulation rates (Cumare et al., 1984). One major drawback of using physical solvents is the absorption of heavier hydrocarbons compared to chemical solvents (Cumare et al., 1984). The use of physical solvents is often determined by the process heat requirements and availability of process heat for regeneration of the solvent, mainly because steam stripping is required for removal of H₂S (Eickmeyer and Gangriwala, 1981). Representative commercial physical solvent processes include Selexol, Rectisol, Purisol, Sepasolv MPE, and Catasol, the selection of which can depend on which acid gas component is more critical for removal, although all of the above will absorb both H₂S and CO₂ to a certain degree (Cumare et al., 1984).

Hybrid solvents are a combination of chemical and physical solvent systems and exhibit properties of both. Shell's Sulfinol is perhaps the best known, which is a combination of DIPA and the physical solvent Sulfolane. Hybrid solvents generally have a lower water content than amine-based chemical solvents and thus allow treatment of acid gases at higher partial pressures (Eickmeyer and Gangriwala, 1981). Other commercial examples are Amisol and Flexsorb PS.

There are several purification processes that are currently in the development and testing phases of research to explore more innovative and economical purification technologies. The use of pressure-swing adsorption phenomena to separate individual coal gas components is one such approach. Application of specific ion-exchange membranes is another. Dissolving chemical coordination complexes in an organic solvent for specific

synthesis gas component separation is also a current approach. One of the most intriguing methods is the use of specific gas separation membranes for CO and H₂ purification and separation, with application in controlling CO:H₂ ratios for synthesis gas processing. These membranes can operate at very high pressure, can employ cryogenic, catalytic, and pressure swing adsorption phenomena, and are relatively simple to operate (Spillman and Sherman, 1990). The preliminary economics of these membrane-based separation systems are favorable compared to conventional gas separation schemes (Spillman, 1989). In general, all of these novel ideas are still in the exploratory phases of research and development, but can potentially offer substantially reduced operating and capital costs compared to the present separation and purification technologies available (Wilson et al., 1988).

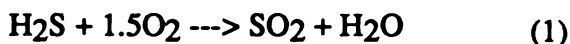
Chemical conversion processes to remove acid gases and other synthesis gas contaminants are designed either for direct removal or for sulfur recovery following direct removal by solvent-based systems. The use of chemical conversion processes for direct sulfur removal requires synthesis or raw gas streams with low H₂S partial pressures where high H₂S selectivity is required (Cumare et al., 1984). When these conditions are present, direct chemical conversion is possible by using commercially available processes such as the Stretford process, and the Takahax process. Generally, these types of chemical conversion require less than 10% H₂S in the gas stream and are used when CO₂ removal is not necessary or warranted. The Stretford process is a catalytic vanadium oxidation of hydrosulfide ion, with very high purification capability. The Takahax process is similar in design but uses napthoquinone (Cumare et al., 1984). When necessary, specific catalytic processes for conversion of COS gas to H₂S gas can be employed, such as the CKA COS hydrolysis reaction catalyst (Udengarrd and Berzins, 1984).

The typical process flow for synthesis gas purification is thus dependent on the composition of H₂S, CO₂, and COS in the raw synthesis gas, and upon whether or not higher-Btu fuel gases are desired. Low sulfide containing raw gases with no requirement

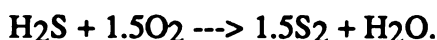
for CO₂ removal can be treated directly by chemical conversion and the sulfide species removed. Synthesis gas streams requiring CO₂ and H₂S removal are first treated using either chemical or physical solvent absorption systems, typically physical solvent systems for moderate to high H₂S contents, and chemical solvent systems for moderate to low H₂S contents. The resulting acid gas stream, which is a mixture primarily of H₂S, CO₂, and other sulfide species, is then treated to selectively remove the CO₂ from the H₂S, a degree of removal which is ultimately dependent on the type of sulfur recovery technology employed downstream. Figure 1 outlines a typical synthesis gas purification process flow concept.

Sulfur recovery technology is based on the proportion of H₂S in the separated acid gas stream. The original chemistry for converting H₂S to elemental sulfur was invented by Carl Friedrich Claus, an English scientist working in the late nineteenth century. In the late 1930's, German scientists redesigned and improved the Claus process and developed what is now known as the modified Claus process. It is estimated that the Claus process accounts for approximately 90-95% of the world's recovered sulfur (Goar, 1986). Typically, the Claus process can recover 95-97% of the feed H₂S. However, recent advances and new processes and modifications have increased the obtainable recovery to over 99% (Goar, 1986).

The Claus and modified Claus process are basically catalytic combustions of H₂S in the presence of O₂, governed by the two reactions,



which are called the Burns and Claus reactions, for reactions 1 and 2, respectively. The overall reaction taking place is thus,



Numerous side reactions are possible and do occur during the combustion reactions, including formation of carbonyl sulfides, carbon disulfides, and various oxidized sulfur

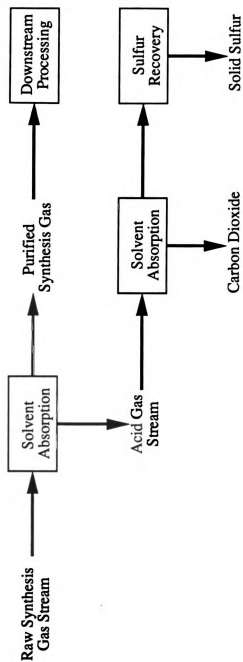


Figure 1. Schematic of typical sulfur recovery and removal operations during catalytic conversion of coal-derived synthesis gas.

species. The typical process scheme is to have several Claus reactors in series for increasing recovery.

The limitations of the Claus technology are in the minimum H_2S concentration required for efficient operation, which was previously 30% but has been steadily improved over the last 50 years (Cumare et al., 1984). These improvements to the Claus process have included preheating of both air and fuel, sulfur recycling and burning, and integration with selective solvent absorption units to increase the fraction of H_2S . Such modifications have allowed recovery of sulfur from gas streams between 5-30% H_2S (Cumare, 1984). For acid gas streams less than 5%, a more recent technology called the Selectox process is typically used, in which the entire recovery process is catalytic and no combustion of H_2S to SO_2 is done (Goar, 1986).

After a majority of the sulfur is recovered by the Claus or Selectox processes, the remaining gases are either vented to the atmosphere or proceed downstream to tail gas clean up processes, depending on the sulfur composition of the exit gas. Tail gas clean up is typically a wet scrubbing or a dry bed process, where the remaining sulfur compounds are either oxidized or reduced and subsequently reacted again. Therefore, tail gas clean up technology is usually a refined extension of conventional modified Claus sulfur recovery technology (Cumare et al., 1984).

1.1.5. Synthesis Gas Utilization

The uses and potential applications of synthesis gas are widespread. Electric power generation, substitute natural gas production, methanol synthesis, and a host of fuels, fuel additives, fuel oils, and chemicals are obtainable from 1-carbon chemistry and synthesis reactions from CO and H_2 . These potential routes are outlined in Figure 2. Many of these technologies have long, proven histories, others are new, as yet commercially unproven processes, and still others are modifications to existing technologies. Whatever the application, the employment and economics of coal-derived synthesis gas technologies are ultimately dependent on the limitations of coal as an energy source, as discussed earlier.

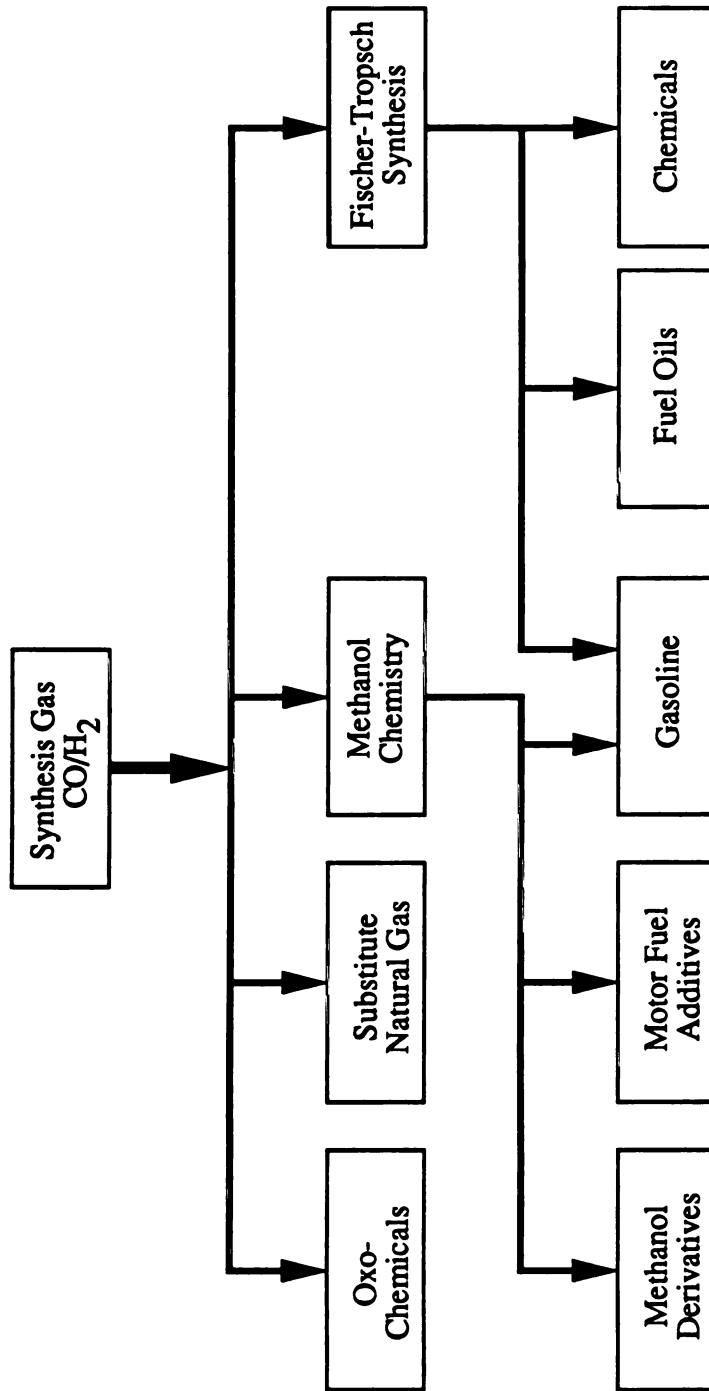


Figure 2. Potential industrial uses of fuels and chemicals from coal-derived synthesis gas.

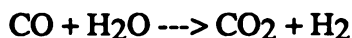
The electric utility industry has by far been the major consumer of coal in the U.S., but fluctuating natural gas and petroleum prices, restrictive environmental regulations in the form of compliance issues for emissions reduction and control, and aging plant hardware problems have been pushing the industry towards a financial crisis (Spencer et al., 1982; Haggin, 1991). Consequently, a restructuring of the industry has been taking place to streamline the economics of electricity generation, in order to stay competitive while meeting environmental requirements. The major effort in this restructuring has been a shift from conventional coal-fired plants with oxidized sulfur scrubbers to integrated coal gasification combined-cycle (IGCC) technology.

IGCC technology is generally in the site-testing and demonstration phases of commercial development, and the outlook is favorable, particularly because of the differences in sulfur emissions problems arising from plant operation (Spencer et al., 1989). The basic process design is to gasify the coal to form a CO-rich synthesis gas, from which heat is removed to produce high-pressure, saturated steam from process water. The steam is then superheated in heat recovery steam generators, from which it then goes to steam turbines to produce electricity. The cooled synthesis gas, which has a high sensible heat content, passes through sulfur and nitrogen purification steps, as described in the previous section. The clean synthesis gas is then expanded and combusted in gas turbines, producing electricity and providing more heat for low-quality steam generation. Technical improvements in both gasifier and gas turbine systems have enhanced the potential for IGCC electric power generating systems, although the gas cleaning and environmental emissions compliance are still a significant portion of both the capital and total cost (Haggin, 1991).

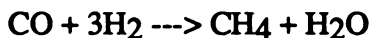
An interesting design modification to the basic IGCC plant design, and one which reflects the versatility of C₁ chemistry, is cogenerating or coproducing power plants which produce both electricity and medium to high-Btu gas or chemicals. These designs split the synthesis gas stream entering the gas turbines for processing to SNG, for sale "over the

fence" as medium-Btu fuel gas, or for catalytic, onsite production of methanol (Spencer et al., 1982). The methanol can then be used as a fuel on site or sold as a commodity. In general, these potential modifications have not yet been adequately tested, but are indicative of the overall flexibility and future for IGCC power plants.

The Btu content of coal-derived synthesis gas is dependent on the gasification process, which is usually dictated by the application. One route for energy generation from coal is in the production of high-Btu SNG from synthesis gas. This process involves first gasification and then methanation, and requires synthesis gas with a low CO:H₂ ratio. Such a ratio is controlled by regulation of the water-gas shift reaction,



both in the gasifier and in downstream shift conversion reactors. Typically, a 3:1 H₂ to CO ratio is required prior to methanation, and the ratio is controlled by splitting the synthesis gas stream and remixing shifted and unshifted streams to obtain the final proportion. One of the current topics of gasifier development for this technology is in the design of coal gasification systems which are high in their CH₄ and H₂ compositions relative to CO, in order to minimize the requirements for a methanation step. The synthesis gas stream, once the required CO:H₂ ratio has been obtained, is then cooled, purified, and passed to the methanation units, where the exothermic reaction,



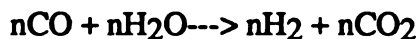
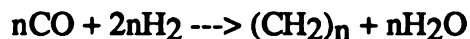
is mediated using a nickel catalyst to produce SNG (Verma, 1978a). The heat of reaction for this methanation step is used to generate process steam, which is subsequently superheated and used to drive turbines for compressor duty.

The best commercial example for this technology is the Great Plains Coal Gasification Plant, in Mercer County, North Dakota, which is designed to produce pipeline quality SNG from lignite coal. This plant employs 12 Lurgi Mark IV gasifiers and uses a Rectisol unit for sulfur and CO₂ purification (Imler, 1985). An adjacent coal-fired power plant provides the electricity for the gasification and purification operations. One of the largest

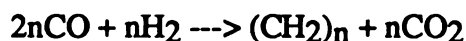
grassroots facilities in the U.S., the Great Plains Coal Gasification Project was the nations first commercial synthetic fuels plant based on coal conversion technology (Imler, 1985).

For producing liquid fuels and chemicals from synthesis gas, the available technology can be separated into direct and indirect synthesis routes. The most notable direct synthesis routes are the Fischer-Tropsch synthesis and the oxonation (hydroformylation) or Roelen chemistry synthesis. Indirect routes are typically through methanol chemistry, or by using methanol (CH₃OH) plus CO/H₂ synthesis schemes. Between the direct and indirect synthesis routes, the potential applications of C₁ chemistry technology based on coal-derived synthesis gas are widespread, as outlined in Figure 3. The chemistry of these direct and indirect synthesis routes are discussed in more detail below, including the current commercial applications.

The Fischer-Tropsch synthesis is a catalytic conversion of CO and H₂ to variety of paraffinic, olefinic, and oxygenated compounds. These routes were developed in the 1920's and 1930's by Franz Fischer and Hans Tropsch in Germany, using iron catalysts at high pressure for oxygenate production, and cobalt catalysts at intermediate pressure for liquid hydrocarbons and paraffin production. In general, the mechanism is a reductive oligomerization of CO following a geometric progression in chain growth (Haggin, 1986). The defining reactions can be described by the formation of linear alkanes (and/or alkenes),



which sum to give the overall reaction,



for which the paraffin to olefin ratio is mainly a function of the catalyst used and of the initial CO/H₂ ratio. One of the main limitations of conventional Fischer-Tropsch synthesis technology is the lack of catalyst selectivity, with product fractions typically including a C₃ to C₄ fraction, a gasoline fraction in the C₃ to C₁₀ range, and a diesel oil fraction as

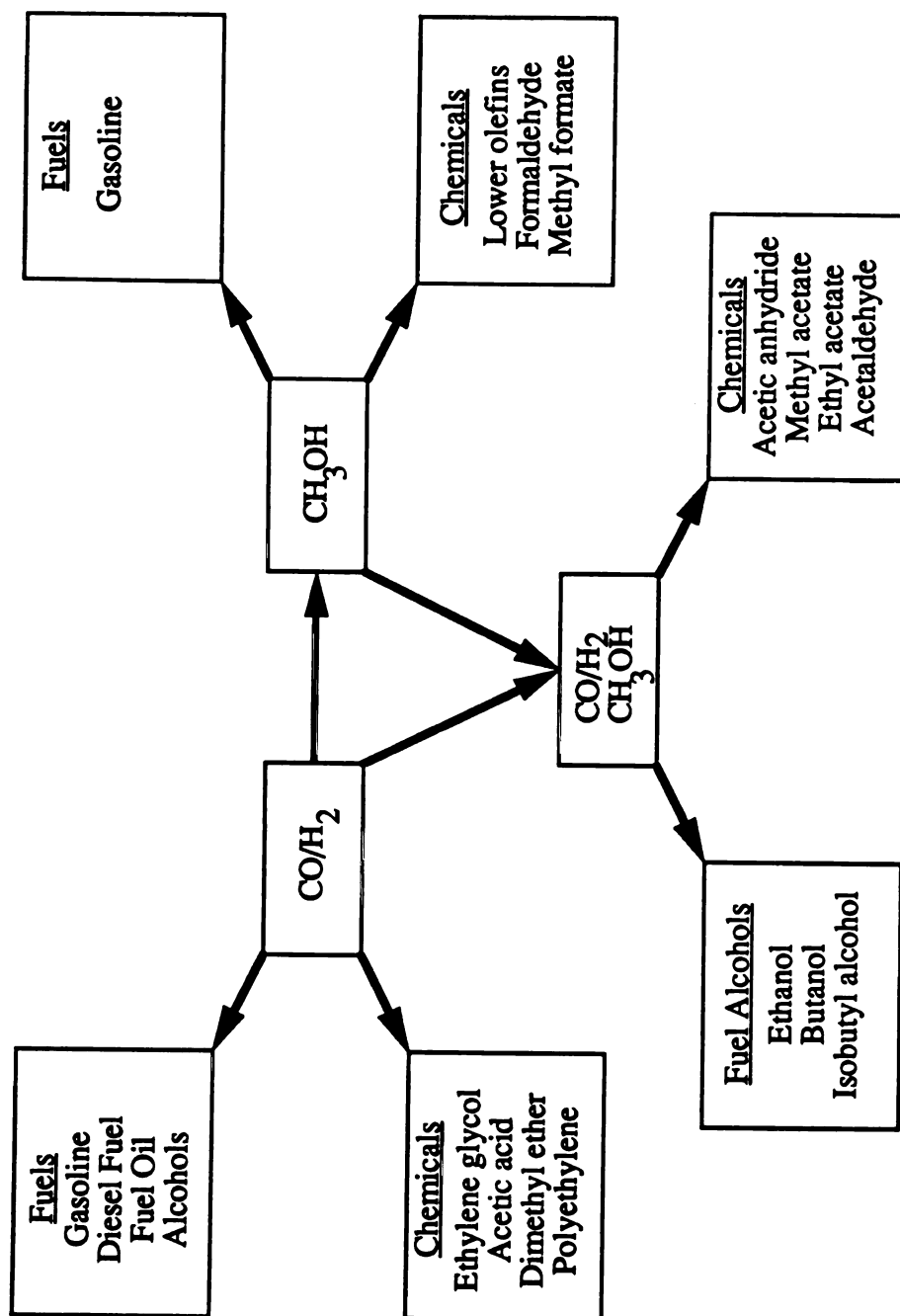


Figure 3. Specific uses for 1-Carbon compounds derived from coal-derived synthesis gas.

well (Haggin, 1981a). The wide product distribution is a function of the type of catalyst metal, which are normally Type VIII heavy metals, the pressure and temperature of reaction, the CO/H₂ ratio, and the presence of catalytic promoters (King et al., 1981). Only the C₁ compounds can be produced with 100% selectivity, i.e., methanol and methane formation (King et al., 1981), although not until recently have detailed catalytic studies elucidated the specific reaction mechanism for methanol synthesis (Chinchen et al., 1990).

In general, the Fischer-Tropsch reaction can be compared to a chain polymerization process and will thus exhibit a product distribution identical to a Schulz-Flory distribution (King et al., 1981). Revitalization of Fischer-Tropsch technology has therefore focused on the selectivity issue and has been based on catalyst improvement and development. These efforts to more accurately control product distribution center on catalyst modification, such as the addition of zeolites to heavy metal catalysts (Haggin, 1981b). Another area is in the use of catalyst promoters, either metal oxides like alumina or energetic promoters such as alkali carbonates (Haggin, 1981b). Interception of surface-level intermediates during reaction and physical regulation of hydrocarbon chain growth by catalyst pore size restriction mechanisms are other exploratory efforts (King et al., 1981).

The only commercially proven Fischer-Tropsch synthesis plants for fuel production using synthesis gas from coal are in South Africa, known as SASOL I, II, and III. These plants are geared predominantly towards production of gasoline and diesel fuels, but a significant amount of chemicals are also produced in both the gasification and synthesis steps (Dry, 1987). These plants use Lurgi gasifiers for a synthesis gas with a low CO/H₂ ratio, use fluidized bed reactors with iron catalysts for the Fischer-Tropsch synthesis, remove sulfur and other contaminants using Rectisol technology, and employ nickel bed catalysts in the steam reformation reactors (Dry, 1987). A generalized Sasol process scheme, from Dry, (1987), is shown in Figure 4. Several specific factors attributed to the success of the SASOL plants include the availability of nearby, inexpensive coal, the lack

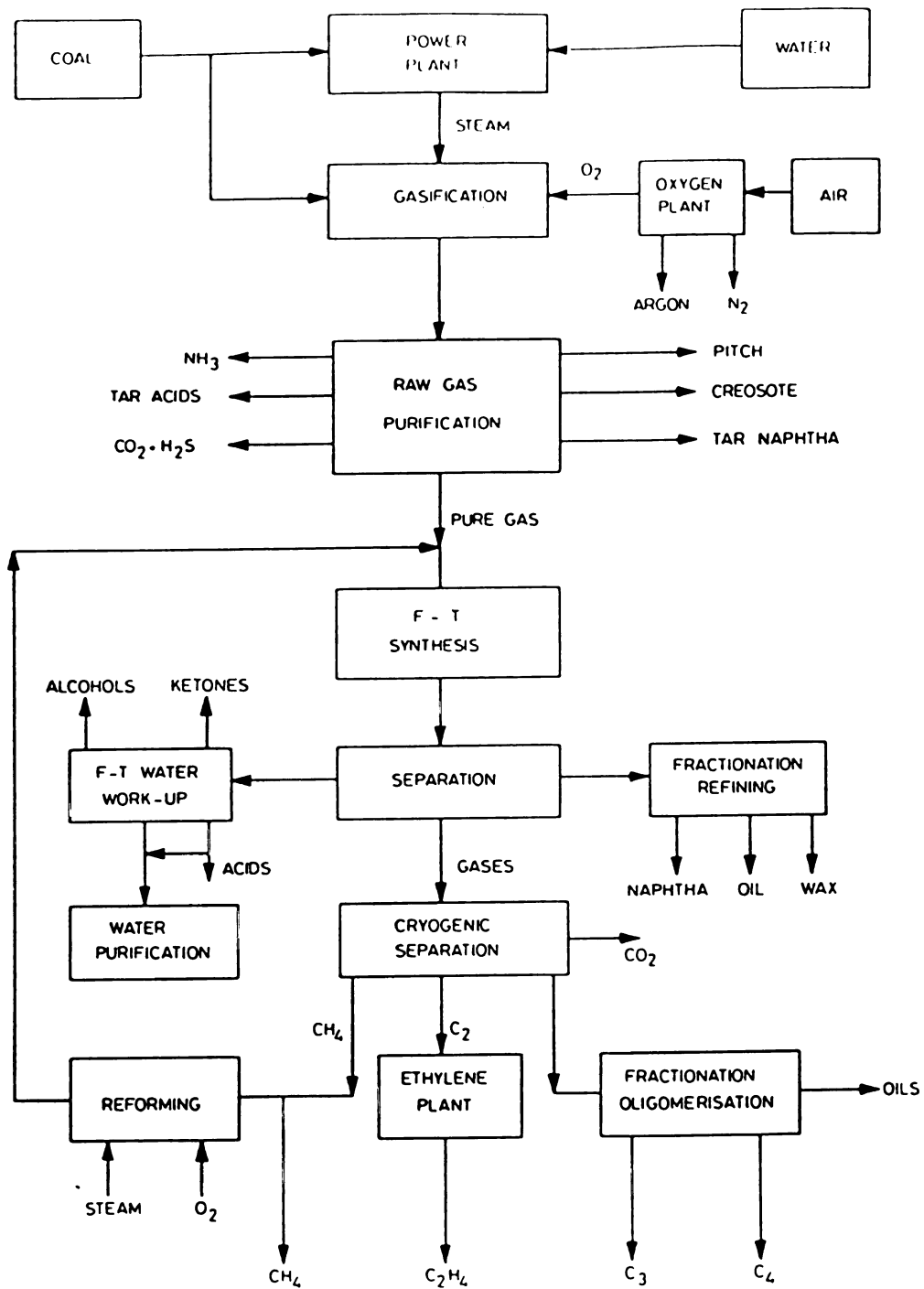


Figure 4. General process scheme for SASOL Fischer-Tropsch synthesis plant, Sasolburg, South Africa (Dry, 1987).

of a domestic petroleum industry, and an industrial market far from the coast and thus far from potential petroleum import stations (Dry, 1987). The specific economic and industrial situation in South Africa is therefore the primary reason for SASOL's continued success.

One factor of concern in direct synthesis routes is the required CO/H₂ ratio and the corresponding losses of CO₂ and H₂O during many synthesis reactions. Some representative direct routes which are in various stages of development are shown in Table 2, along with the reaction stoichiometry and the required CO/H₂ ratio. The commercial potential of these direct synthesis routes, except for the methanol route, which is has been proven commercially, is still being explored. Japanese researchers, as part of the Japanese C₁ Chemistry National Project, have done considerable development in both catalysis/reaction control and reaction/process design for production of ethylene glycol,

Table 2. CO/H₂ ratios of direct synthesis routes for chemicals from synthesis gas.

Product	Reaction Stoichiometry	CO/H ₂ Ratio
Methanol	$\text{CO} + 2\text{H}_2 \rightarrow \text{CH}_3\text{OH}$	1:1
Acetic Acid	$2\text{CO} + 2\text{H}_2 \rightarrow \text{CH}_3\text{COOH}$	1:1
Ethanol	$2\text{CO} + 4\text{H}_2 \rightarrow \text{C}_2\text{H}_5\text{OH} + \text{H}_2\text{O}$	1:2
Propanol	$3\text{CO} + 6\text{H}_2 \rightarrow \text{C}_3\text{H}_7\text{OH} + \text{H}_2\text{O}$	1:2
Ethylene	$2\text{CO} + 4\text{H}_2 \rightarrow \text{CH}_2\text{CH}_2 + 2\text{H}_2\text{O}$	1:2
Ethylene Glycol	$2\text{CO} + 3\text{H}_2 \rightarrow \text{HOC}_2\text{H}_4\text{OH}$	2:3

ethanol, acetic acid, and olefins (Nakamura, 1990). Production of C₁ to C₆ alcohols is the primary mission of the Research Association for Petroleum Alternative Development (RAPAD), which is an international organization with a strong membership base in both France and Japan. Up to 99% of C₁ to C₆ alcohols has been achieved in bench scale tests, with up to a 30% weight fraction of C₂ to C₆ alcohols (Haggin, 1986). The

question of whether these syntheses are better performed in a direct or indirect fashion is an ongoing issue, although the current technology greatly favors the indirect synthesis routes; direct synthesis of these chemicals has been described as technology for the next century (Ehrler and Juran, 1983).

A direct synthesis route which was originally a spin off of the Fischer-Tropsch synthesis reactions are oxonation or hydroformylation reactions. These "oxo" routes are also known as Roelen chemistry, after Otto Roelen, who invented the technology in Germany over 50 years ago. The principle is based on reacting CO and H₂ with an unsaturated hydrocarbon, primarily olefins, to produce aldehydes and ultimately longer-chain alcohols. Cobalt is generally the catalyst used, although iron, rhodium, and ruthenium have exhibited similar properties (Haggin, 1981a). The aldehydes produced by hydroformylation are most often hydrogenated to form alcohols, such as in the formation of butyraldehyde and finally n-butanol and isobutanol from propylene; 2-ethylhexyl alcohol is also produced by this route (Ehrler and Juran, 1983).

Another indirect synthesis route is carbonylation, in which CO reacts with unsaturated and nucleophilic compounds to yield carboxylic acid derivatives. The typical catalysts for these reactions are nickel, iron, and cobalt, and also rhodium, ruthenium, and palladium to a lesser extent (Haggin, 1981a). The Monsanto process for acetic acid production from methanol is an example of carbonylation. Besides methanol, other common nucleophiles used in carbonylation are water, ammonia, alcohols, and carboxylic acids (Haggin, 1981a).

Many experts agree that indirect synthesis routes via methanol from synthesis gas comprise the major future of using coal-derived gases for synthetic fuels and chemicals production (Frank, 1982). The potential of methanol chemistry lies in both synthetic fuels and chemicals production, including transportation fuels, diesel fuels, ethylene glycol, acetic acid, acetic anhydride, and a host of others. The direct applications of methanol itself are also of importance, both in its solvent and fuel properties.

One of the most recent triumphs in C₁ chemistry development has been the Mobil process for gasoline production from methanol, via zeolites. In the Mobil process, coal is gasified to produce synthesis gas, which is then reacted to produce methanol at near 100% selectivity by conventional methods. The methanol is then catalytically reacted to form high octane gasoline and light hydrocarbons (C₂ to C₄ olefins and C₆ to C₁₀ aromatics) using the Mobil ZSM-5 shape-selective zeolite catalyst (King et al., 1981; Keim, 1987). This is a fully developed commercial technology, with operating plants in New Zealand (Haggin, 1986). An extension of this technology is a two-stage approach for conversion of methanol to olefins, and then selective conversion of the olefins to gasoline, a route which produces more premium transportation fuels (Haggin, 1986). The methanol to olefin technology is of itself industrially important; under certain reaction conditions ethylene and propylene can comprise almost the entire product spectrum (Haggin, 1981a).

For the the indirect synthesis of chemicals from synthesis gas via methanol, there are basically 3 major routes: carbonylation, reductive carbonylation, and oxidative carbonylation. In general, the normal carbonylation route is a commercial technology, while the reductive and oxidative carbonylation routes are still under development (Keim, 1987). The Monsanto process for acetic acid production, as mentioned previously, is the prime example of commercial technology for carbonylation and indirect methanol chemistry. The reaction scheme is,



and both reactions are highly selective and proceed under low pressure conditions (Ehrler and Juran, 1983).

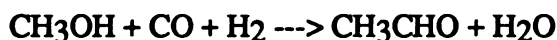
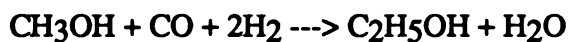
By reacting methanol and acetic acid, methyl acetate can be obtained, which upon further reaction with CO will yield acetic anhydride. This indirect route is the basis for commercial technology employed by the Tennessee Eastman Company, in Kingsport, Tennessee. The process feeds a portion of the total coal-derived synthesis gas into a

cryogenic separator, where a pure CO stream is created for the acetic anhydride plant and an H₂-rich stream is created for adjustment of the CO/H₂ synthesis gas ratio for methanol production. The methanol is sent to a methyl acetate plant, where it is reacted with acetate to form methyl acetate, which is then passed to the acetic anhydride plant to combine with CO and produce acetic anhydride. The acetic anhydride is subsequently reacted with cellulose in an acetylation step to form cellulose acetate. This reaction releases acetate, which is recycled to the methyl acetate plant. (Mayfield and Agreda, 1986). The entire process reaction scheme is basically,



where reaction (1) is the coal gasification step, reaction (2) is the methanol synthesis step, reaction (3) is the methyl acetate synthesis step, reaction (4) is the acetic anhydride synthesis step, and reaction (5) is the final product formation step (Agreda, 1988). This innovative chemistry is the result of 20 years of effort, and is a prime example of technology diversification from a process that was formerly based on natural gas and petroleum fuel gases (Agreda, 1988).

There are several promising but commercially unproven technologies based on reductive and oxidative carbonylation of methanol. Reductive carbonylation, or homologation, can yield ethanol or acetaldehyde from methanol and CO/H₂, by the reactions,



which have yielded 80% selectivity for acetaldehyde over complex cobalt catalysts (Keim, 1987). Reductive carbonylation of methyl acetate can yield ethyl acetate or ethylidene

diacetate, which is a precursor to vinyl acetate (Haggin, 1986). Oxidative carbonylation of methanol can yield dimethyl carbonate or dimethyl oxalate, which is a precursor to ethylene glycol (Keim, 1987).

Other indirect routes include formaldehyde and methyl formate chemistry. Methyl formate can be obtained by carbonylation of methanol, dehydration of methanol, methanol oxydehydrogenation, by formaldehyde disproportionation, or by direct CO hydrogenation. An application for methyl formate is as an intermediate in the synthesis of formaldehyde, but other reactions are possible to yield a variety of fine chemicals (Keim, 1987). Formaldehyde derived from synthesis gas can also be used as an intermediate in indirect processing, with synthesis of compounds such as glycol anhydride, glycolic acid, and methyl methacrylate possible. The potential, however, for formaldehyde as an important intermediate in synthesis gas utilization is doubtful (Haggin, 1986; Keim, 1987).

1.1.6. Application of Synthesis Gas-Derived Compounds

The previous section has detailed some of the potential routes for synthesis gas in the production of gaseous fuels (SNG), liquid fuels, electricity (IGCC), and a wide variety of chemicals and chemical feedstocks obtained both by direct and indirect processing routes. The ultimate application of these products and their processes will depend on their market value, market share, and many other economic considerations. For the purposes of this review, it suffices to state that all of the listed commercial and near-commercial technologies have existing markets and relatively clear applications as feedstocks, intermediates, or final products. The applications which are not entirely clear are for the oxygenate fuels and their derivatives. It is these compounds that are the focus of this section.

A major disparity in the U.S. energy situation as far as the extent of its diversification is in the transportation sector. With 20% of the nation's energy consumption occurring in cars, trucks, and buses and 98% of that energy being derived from petroleum, the

transportation industry is particularly sensitive to fluctuations and shortages in the supply and flow of imported oil (Moore and Shadis, 1984). There has thus been ongoing research and development pertaining to synthetic fuels and fuel additives, and their potential application in the transportation sector to decrease the present petroleum-dependent nature of the industry. But complete substitution of petroleum-based gasoline and diesel fuels with synthetic fuels and alcohols will be a long-term endeavor. A more immediate problem is the effort to increase octane ratings because of the phasing out of both lead and tetraethyl or tetramethyl lead as octane enhancers.

The octane rating of a motor fuel is expressed as the octane number, a reflection of the gasoline quality which most current automobile engines require in high amounts for efficient operation. Specifically, it is a reflection of the anti-knock property of a fuel, expressed as a percentage of isooctane that must be mixed with n-heptane to equal the knock intensity of the tested fuel. There are several kinds of octane numbers, including the research octane number (RON), the motor octane number (MON), and the road octane number (RdON). The RON is a test for fuels used in spark-ignition engines at low speed and low temperatures. The MON is a test for fuels used in high speed, high temperature conditions. The RdON is for intermediate applications, and is tested under actual driving conditions. The average of the RON and MON values is the anti-knock index, or blending octane number, and is used as a substitute value for an actual road test octane number. The typical gas station pump octane value is the blending octane number.

The phasing-out of environmentally hazardous octane enhancers has created new markets and potential applications for oxygenates such as alcohols and their ether derivatives as clean burning blending agents, octane enhancers, and direct motor fuels. These new, potentially coal-derived oxygenates include methanol, ethanol, n-butanol, and ethers such as methyl tert-butyl ether (MTBE) and ethyl tert-butyl ether (ETBE). The chemical and fuel properties of these compounds compared to conventional gasoline motor fuels are shown in Table 3. One of the most favorable properties of oxygenates is their

Table 3. Properties of various fuel oxygenates^a.

Product	RON	MON	Blending Octane	ΔH_{comb} (kBtu/lb)	Boiling Point (°C)
Methanol	111	91	101	9.77	64.6
Ethanol	108	91	100	11.59	78.5
n-Butanol	101	87	94	15.02	117
MTBE	116	99	108	17.22	55.4
ETBE	117	105	111	18.79	72.8
Gasoline	91	83	87	20.13	Range

^aFrom Ecklund and Mills, 1989a; Iborra et al., 1988.

octane number. The other more favorable properties of alcohols and ethers are their high miscibility in gasoline and higher blending octane values compared to conventional motor fuels.

The application of oxygenates as octane enhancers depends on several factors, including the miscibility in gasoline, the vapor pressure, the blending octane number, and the burn characteristics. When comparing various oxygenates, methanol is generally the base of comparison. The ethers, which are formed from the reaction of either methanol or ethanol with isobutylene, have greater octane values and higher heats of combustion compared to methanol (Piel, 1988; Ecklund and Mills, 1989b; Iborra, 1988). The higher alcohols, in the C₂ to C₄ range, also have higher heats of combustion, higher octane values, and can also inhibit phase separation when used as cosolvents in methanol-gasoline mixtures (Ecklund and Mills, 1989b). In general, there is great potential for increased usage of oxygenates as gasoline octane enhancers, extenders, and blending components for use with motor fuels.

1.1.7. Future Prospects

The development of coal gasification technology, of integrated coal-based power and chemical plants, and of synthesis gas reactor and catalyst technology has served to revitalize and refocus the synthetic fuels and chemicals industry, even in the advent of inexpensive petroleum. The cultural bias against coal and coal-fired plants has to a certain extent been steadily eroded due to adherence to strict environmental compliance issues, long-term uncertainty and instability of petroleum supplies, and the potential economic advantages arising from a diversified industry based on domestic resources and labor.

However, the obstacles to commercialization are somewhat more complex than mere social, political, and environmental issues. Long-term dependence on petroleum has created an infrastructure committed to that resource, and which will require significant restructuring and far-sighted investment in order to diversify the energy supply base in the face of short-term, profit-directed corporations, both on the supply (petroleum companies) and the demand (automotive and transportation companies) sides of the industry. Without the assistance of another major crisis in the flow of petroleum imports, these obstacles will be difficult to surmount. The potential for diversification is not in doubt, as a look at the global examples in South Africa (commercial Fischer-Tropsch synthesis from coal) and in Brazil (ethanol from biomass) will attest. Yet the factors arising to the success of these few and often cited examples were not only technical, indeed, the supplies of coal in South Africa and biomass in Brazil were a large piece of the success equation, as were government subsidies and public acceptance. It therefore can be concluded that for successful commercialization of coal-based processes, the technical, political, environmental, and social climates must all be conducive.

Methanol from coal, although by no means a synthetic fuels and chemicals panacea, has been one of the major developments in recent times. Finding new uses for methanol and methanol derived products, as well as serving existing ones, has been an important aspect of the technology development. The current outlook for methanol is considered to be very

promising (Frank, 1982; Ecklund and Mills, 1989a). One aspect of the commercial promise of methanol as a product or as an intermediate is the specificity of its formation from synthesis gas, with almost 100% yields obtainable, as described previously. This specificity is also apparent in other areas of C₁ chemistry, and will continue to be a major advantage of indirect synthesis gas processing routes via methanol (Ehrler and Juran, 1983).

In order to substitute an existing petroleum based product or industry with a coal-based product or industry in the absence of a cohesive and focused national energy strategy, the potential niches for application will have to be well worked out, as can be seen in the examples at Tennessee Eastman and the Great Plains Coal Gasification project. Alternatives to existing fuels and chemicals that are presented as environmentally sound will be received favorably in the existing industrial climate, as are the above examples. It is thus in this light that clean-burning, alternative motor fuels and fuel additives have future potential, first by diversifying the energy sources for such products (coal and biomass versus petroleum), and second, by presenting environmentally "friendly" alternatives (oxygenates versus lead compounds) to the industry.

1.2. Microbial Metabolism of Synthesis Gas Components

1.2.1. Principles of 1-Carbon Metabolism

The ongoing discovery of 1-carbon metabolizing bacteria and their diversity in nature has led to a somewhat confusing and sometimes redundant terminology for classification of the organisms. Autotrophy refers to organisms which use CO₂ as their sole carbon source and which grow in the absence of organic matter. Heterotrophy refers to organisms which grow on organic carbon and energy sources. Methyлотrophy refers to organisms capable of growth on organic compounds containing no carbon-carbon bonds, such as methanol. Mixotrophy refers to cosubstrate metabolism. When classifying microorganisms by their carbon sources, autotrophs and heterotrophs are presently the accepted terms, and

thus classification of CO-utilizing organisms requires either further definition or a broadening of the current classifications. The term unicarbonotrophy has been suggested for organisms capable of growth on 1-carbon compounds as their sole carbon and energy sources (Zeikus, 1983a).

For the purposes of this review, the term unicarbonotroph will be used for organisms capable of growth on CO, and the use of the terms autotroph and methylotroph will be restricted to their literal definitions above. This terminology emphasizes the great diversity of several bacterial species, outlined below, such as the anaerobic bacterium *Butyribacterium methylotrophicum*, which is capable of heterotrophic growth on glucose, autotrophic growth on H₂ and CO₂, methylotrophic growth on methanol, unicarbonotrophic growth on CO, and mixotrophic growth on CH₃OH and CO₂.

The major mechanisms for CO₂ fixation in autotrophic microorganisms include the ribulose diphosphate carboxylase cycle, or Calvin cycle, the reverse di- or tricarboxylic acid cycles, or reductive carboxylic acid cycles, and the acetyl-CoA pathway, which is a uni-directional mechanism. The Calvin cycle involves fixation of CO₂ via ribulose diphosphate, yielding 2 molecules of 3-phosphoglyceric acid for every CO₂ molecule consumed. The 3-phosphoglyceric acid is then further reacted in an ATP and electron-consuming reaction to form glyceraldehyde-3-phosphate, as well as to regenerate ribulose diphosphate, which is the intermediate used for subsequent catabolic reactions, including cell synthesis (Brock et al., 1984). This cycle, a C₃ cycle, functions in all aerobic photosynthetic organisms, in some anaerobic phototrophs, and in several carboxydotrophs, or aerobic CO-utilizing bacteria (Meyer and Schlegel, 1983).

The reverse di or tricarboxylic acid cycles are C₄ pathways which use acetyl-CoA as the initial CO₂ acceptor through ferredoxin-mediated carboxylation to pyruvate, and then further phosphorylation and carboxylation to oxaloacetate. In the reverse dicarboxylic acid cycle, the oxaloacetate is then further reduced, either to malate, fumarate, or succinate, and the acetyl-CoA regenerated to complete the cycle. The net CO₂ fixation is thus 2 moles per

mole of oxaloacetate formed. In the reverse tricarboxylic acid (TCA) cycle, the carbon and electron flow proceeds with more carboxylation reactions from oxaloacetate ultimately to citrate, which is cleaved to regenerate acetyl-CoA and oxaloacetate, resulting in a net CO₂ fixation of 4 moles per mole of oxaloacetate formed (Brock et al., 1984).

The acetyl-CoA pathway has been studied in both acetogenic and methanogenic bacteria, and is the fundamental metabolic pathway operating in the bacterium used in the present study. This mechanism is basically a catabolic reduction process, where reducing equivalents from a variety of dehydrogenated compounds (H₂, H₂O) are used to form the methyl and carboxyl groups of acetate, via acetyl-CoA as an intermediate (Fuchs, 1986). The ubiquitous enzyme in this transformation is carbon monoxide dehydrogenase (CODH), also known as acetyl-CoA synthase, a multi-component enzyme complex of varying homology in several species of acetogenic bacteria (Fuchs, 1986). Although initially conceived by Wood over 40 years ago, the elucidation of this pathway for both CO and CO₂-utilizing bacteria has been ongoing, particularly in the last decade, and current research trends are focused on the energetics of acetogenic metabolism and the mechanism for ATP generation during autotrophic and unicarbonotrophic growth.

A variety of microorganisms representing a diverse cross section of the bacteria division of the kingdom procaryotae are capable of 1-carbon compound metabolism, primarily by one of the three major mechanisms of carbon fixation listed above. However, in the context of potential industrial application for conversion of the major synthesis gas components, the characteristics of anaerobic bacteria, specifically unicarbonotrophic anaerobic bacteria, represent the most promising route for production of fuels and chemicals (Datta and Zeikus, 1982; Zeikus, 1983b; Linden, 1988). Anaerobic metabolism conserves the chemical energy content of the substrate very efficiently in the absence of O₂ and oxidation, a characteristic which provides unicarbonotrophs with a metabolic efficiency greater than all other biosynthetic life forms (Zeikus, 1983b). The autotrophic and unicarbonotrophic organisms outlined in the following pages thus represent

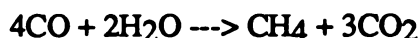
specifically those organisms capable of anaerobic oxidation of CO or anaerobic utilization of H₂ and CO₂. In the majority of these organisms, particularly the acidogenic bacteria, it is the Wood or acetyl-CoA pathway that is the mechanism for 1-carbon compound utilization, and thus this pathway is discussed in more detail below.

1.2.2. Carbon Monoxide, Carbon Dioxide, and Hydrogen Metabolizing Bacteria

Attaining a unifying theme for organisms capable of metabolizing the primary synthesis gas components CO, H₂, and CO₂ is a difficult problem because of the phylogenetic diversity of the many species. For this review, the anaerobic bacteria capable of such metabolism are classified as either methanogenic, sulphidogenic, phototrophic, or acidogenic. The emphasis is thus on metabolic similarity as opposed to taxonomic or phylogenetic similarity.

Methanogenic bacteria are obligate anaerobes and members of the procaryotic group *Archaeobacteria*, family *Methanobacteriaceae*. Typically, CO₂ is the terminal electron acceptor and H₂ the electron donor during methanogenesis. These organisms are considered to play an important role in the carbon cycle, with approximately 80% of the atmospheric methane believed to have a biological origin (Brock et al., 1984). There is no direct evidence for the existence in methanogens for either the Calvin cycle or cytochromes, and novel metabolic mechanisms have been proposed which include a propensity of corrinoid species, unique coenzymes, and coenzyme factors (Zeikus, 1983b; Zeikus et al., 1985; Linden, 1988). Several methanogenic species of bacteria are capable of metabolizing CO and/or H₂ and CO₂, abilities which have in most cases been achieved only after long periods of culture adaptation (Zeikus, 1983b). In general, the energy-yielding metabolism of methanogenic bacteria is defined by the oxidation of H₂ and the reduction of CO₂ to form methane. The most well characterized species capable of unicarbonotrophic growth are in the genera *Methanobacterium* and *Methanosarcina*, which are genera readily distinguished by cell morphology and ultrastructure analysis (Zeikus and Bowen, 1975).

Methanobacterium thermoautotrophicum and *Methanobacterium formicicum* are rod-shaped, gram-positive bacteria with a high guanine and cytosine (G+C) content in the DNA (>50%) and numerous intracytoplasmic membranes (Zeikus, 1977). Both of these organisms are nonmotile and use H₂ and CO₂ as substrates for methanogenesis. *Methanobacterium thermoautotrophicum*, a thermophilic, filament-forming organism isolated from heat exchanger sewage sludge (Zeikus and Wolfe, 1972), is considered to be the most prolific methogen known, and but is not an obligate autotroph, since growth on acetate has been observed (Linden, 1988). Doubling times as low as 2 hr have been observed on H₂ and CO₂ in ammonium-limited continuous culture studies (Kenealy et al., 1982). Adaptation of *M. thermoautotrophicum* to grow with CO as the sole carbon source, with following the reaction



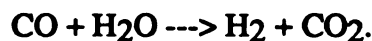
has been achieved in CO atmospheres up to 30%, albeit at substantially reduced rates of growth (approximately 1%) compared to H₂ and CO₂ (Daniels et al., 1977). Growth was completely inhibited at CO partial pressures approaching 60% during these studies (Daniels et al., 1977).

Another species of bacteria, which has been described as the most metabolically versatile methanogen known, is *Methanosarcina barkeri*. This bacterium is a gram-positive, packet-forming cocci, with a G+C content over 50% (Zeikus, 1977). *M. barkeri*, of which there are several distinct strains, is capable of either autotrophic, unicarbonotrophic, or mixotrophic growth on a variety of compounds as either the sole carbon or sole carbon and energy sources. Autotrophic growth on H₂ and CO₂ or methylotrophic growth on CH₃OH has been observed with doubling times of 11 hr and 8 hr, respectively (Weimer and Zeikus, 1978). Mixotrophic growth on H₂/CO₂/CH₃OH is also possible during methanogenesis (Weimer and Zeikus, 1978). Methane formation from acetate has also been observed, but with almost a 40 hr doubling time and an extremely long adaptation period (Zeikus, 1983a). Growth on CO as the sole carbon

source with a doubling time of 65 hr in the presence of H₂ has been reported (O'Brien et al., 1984).

1-Carbon compound metabolism in sulphidogenic bacteria, which comprise an extremely diverse group of organisms, has been documented specifically for CO or H₂ and CO₂, although the specific physiological concepts have not been well determined. Such organisms include *Desulfovibrio vulgaris*, *Thermodesulfotobacterium commune*, and *Desulfovibrio desulfuricans* (Zeikus, 1983a). Growth of *D. vulgaris* with CO as the sole electron source for cell mass production and sulfate reduction was achieved at partial pressures up to 4%, but was inhibited at greater concentrations of CO in the gas headspace (Lupton et al., 1984). Uptake of dilute CO gas has also been observed by *D. desulfuricans*, but at very low rates of metabolism and with no apparent energy-generating mechanism (Uffen, 1981). *Thermodesulfotobacterium commune* has exhibited growth on H₂ and CO₂ in the presence of acetate, although prolonged periods of cultural adaptation were required (Zeikus, 1983a). In general, metabolism of synthesis gas components in sulphidogenic organisms, although having been documented in a few specific cases, is not nearly as defined as in methanogenic or acetogenic bacteria, and is only included here in order to exemplify the diversity of species capable of such metabolism.

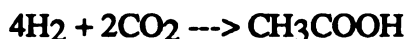
Similarly, photosynthetic bacteria such as *Rhodospirillum rubrum* and *Rhodopseudomonas gelatinosa* have also been documented with CO metabolizing ability following the overall water-gas shift reaction,



R. rubrum is known to metabolize CO gas anaerobically and in the dark, although growth cannot be supported on CO alone (Uffen, 1981). *R. gelatinosa*, also under dark conditions, is capable of growth with CO as the sole carbon and energy source, although addition of trypticase was required to achieve the reported doubling time of 6.7 hr (Uffen, 1976). As for the sulphidogenic bacteria described above, CO metabolism in phototrophs is also poorly characterized and not well understood.

The occurrence of 1-carbon metabolism is perhaps best-characterized and understood in acidogenic, anaerobic bacteria, primarily acetogenic bacteria in the family *Bacillaceae* genus *Clostridium* and family *Propionibacteriaceae* genus *Eubacterium*. Unicarbonotrophy has only recently been recognized in homoacetogens, and in general, acidogenic bacteria are the most interesting because of the potential for acetate, ethanol, butyrate, and butanol synthesis from CO or H₂ and CO₂ found in this diverse collection of microorganisms. It is important to stress the distinction between the terms acidogen and acetogen, which are often confused and thus misused. Acidogen refers to the products from metabolism, in this case mainly acetic acid, with a usage similar to that of the term methanogen. Acetogen is a term which specifically refers to catabolic pathways which are based on formation of acetyl-CoA as an intermediate, with homoacetogens being organisms with acetyl-CoA as the sole intermediate for all catabolic reactions, whether from heterotrophic, autotrophic, or unicarbonotrophic mechanisms.

Clostridium thermoaceticum, a spore-forming thermophile, is probably the most intensely studied and well known homoacetogenic bacterium. This organism has a G+C content of 54%, and grows on both CO, with a 16 hr doubling time, or H₂ and CO₂, with an 18 hr doubling time, but is not capable of growth on CH₃OH (Kerby and Zeikus, 1983). Growth on CO was reported not to be inherent but was obtained after a prolonged adaptation period (Kerby and Zeikus, 1983). Interestingly, the capacity for CO oxidation was first observed during heterotrophic growth on glucose (Diekert and Thauer, 1978). Both growth on CO and on H₂ and CO₂ yielded acetic acid, with theoretical product formation stoichiometries of



calculated from batch growth results (Kerby and Zeikus, 1983). Several key enzymes and electron carriers have been discovered and characterized in *C. thermoaceticum*, including the first evidence for heme-prosthetic groups, such as cytochromes and menaquinones, as

opposed to strictly corrinoid-based electron carriers (Gottwald et al., 1975), a discovery which still has widespread implications when discussing electron flow in acetogenic organisms. Recent evidence suggests that the menaquinone in *C. thermoaceticum* is the same as for *Clostridium thermoautotrophicum*, discussed below (Das et al., 1989). Electron carrying ferredoxin proteins have also been isolated (Elliott and Ljungdahl, 1982), as has a nickel-based CO dehydrogenase enzyme (Drake et al., 1980) and hydrogenase enzyme (Drake, 1982b).

Several more recent physiological discoveries with *C. thermoaceticum* include the existence of a membrane bound ATPase complex, supporting the increasingly widespread belief that homoacetogenic bacteria require active electron-transport phosphorylation mechanisms. This ATPase complex, which functions based on the proton-motive force, has been characterized and purified to homogeneity (Mayer et al., 1986; Ivey and Ljungdahl, 1986). Membrane vesicles containing CO dehydrogenase have also been shown to generate a proton gradient when exposed to CO, which is another piece of physiological evidence for a complete electron-transport phosphorylation mechanism in *C. thermoaceticum* (Hugenholtz and Ljungdahl, 1989).

Other *Clostridia* have also shown either CO or H₂ and CO₂ metabolizing ability. *Clostridium pasteurianum* exhibited CO oxidation in cell-free extracts (Thauer et al., 1974), and while growing on glucose (Fuchs et al., 1974), although growth with CO as the sole carbon source was not reported. The CO dehydrogenase enzyme was determined to be nickel-dependent in *C. pasteurianum*, and similar to that present in *C. thermoaceticum* (Diekert et al., 1979; Drake, 1982a). *Clostridium thermoautotrophicum* has a G+C content of 54%, and exhibits an autotrophic metabolism similar to that of *C. thermoaceticum*, with growth on H₂ and CO₂ observed at a doubling time of 8 hr and at the same 4:2:1 H₂:CO₂:acetate stoichiometry (Wiegel et al., 1981). Growth on CH₃OH was also reported, as was a G+C content of approximately 54% (Wiegel et al., 1981). Similarly, CO dehydrogenase and hydrogenase enzyme were found to play important roles

in acetate synthesis from H_2 and CO_2 (Clark et al., 1982). Another species exhibiting H_2 and CO_2 metabolism is *Clostridium aceticum*, which has a G+C content of 33%, and but does not exhibit growth on CH_3OH (Braun et al., 1981). A recently discovered bacteria, now known as *Clostridium ljungdahlii*, was originally isolated from chicken waste, and is capable of both ethanol and acetate synthesis from CO gas (Barik et al., 1988). However, the specific physiological characteristics of this organism have not yet been determined.

Acetobacterium woodii is a rod-shaped, mesophilic bacterium isolated from a marine environment, which possesses a G+C content of 39%, and is capable of growth on CO, H_2 and CO_2 , and CH_3OH and CO_2 to produce acetate (Tanner et al., 1978; Kerby et al., 1983). The 1-carbon metabolism in *A. woodii* is considered to be very similar to that of *C. thermoaceticum* because of the presence of corrinoids, a nickel dependent CO dehydrogenase, and other key enzymes associated with 1-carbon transformations in acetogens (Ragsdale et al., 1983b; Kerby et al., 1983).

Peptostreptococcus productus strain U-1 was originally isolated from sewage digester sludge and is perhaps the fastest growing bacteria exhibiting CO metabolism, with a 1.5 hr doubling time in a 50% CO atmosphere and doubling times less than 2 hr for CO atmospheres approaching 90% (Horowitz and Bryant, 1984). This organism produces acetate and CO_2 from CO, and is also capable of H_2 and CO_2 metabolism to form acetate with a doubling time of 5 hr in an 80% atmosphere (Horowitz and Bryant, 1984). Growth on methanol has not been observed, nor has growth on formate (Ljungdahl, 1986). *P. productus* is one of the few CO-utilizing bacteria for which extended batch and continuous fermentations have been conducted, including extensive fermentation kinetic analyses during acetate production from CO in both batch and chemostat systems (Vega et al., 1989a; Vega et al., 1989b).

A sheep rumen isolate, *Eubacterium limosum* is capable of both acetate and butyrate production depending on the 1-carbon substrate. This organism is considered to be a newer isolate of what was formerly known as *Butyribacterium rettgeri*. When grown on

H₂ and CO₂, *E. limosum* exhibits a 14 hr doubling time, producing acetate and minor amounts of butyrate (Sharak Genthner et al., 1981). Faster growth (7 hr doubling time) was observed on CH₃OH with equimolar production of acetate and butyrate, but only in the presence of acetate and CO₂ (Sharak Genthner et al., 1981). The ratio of CH₃OH to CO₂ is critical in determining the product ratio, regulation occurring specifically due to the bicarbonate ion concentration (Pacaud et al., 1985). Growth on 50% CO was observed with a 7 hr doubling time and sole production of acetate, this doubling time increased to 18 hr at a CO concentration of 75%, which was the highest partial pressure tested (Sharak Genthner and Bryant, 1982). Butyric acid fermentation schemes using CH₃OH and CO₂ have been proposed using *E. limosum*, schemes which depend on feedback inhibition mechanisms, optimization of substrate ratios, and ultrafiltration technology for homobutyric acid production (Loubiere et al., 1986).

Probably the most versatile of unicarbonotrophic, anaerobic bacteria, *Butyribacterium methylotrophicum* is capable of both acetate and butyrate production depending on the substrate used. Growth on H₂ and CO₂ produces acetate with a 9 hr doubling time, while growth on CH₃OH in the presence of acetate and CO₂, also at a 9 hr doubling time, produces butyrate in a 4:1 methanol:butyrate ratio (Zeikus et al., 1980; Lynd and Zeikus, 1983). Product formation and fermentation rates in *B. methylotrophicum* during growth on CH₃OH and CO₂ were also found to be dependent on the substrate ratio, as for *E. limosum* (Datta and Ogletree, 1983). A mutant strain of this organism, the CO strain, was adapted to grow with a 12 hr doubling time on 100% CO gas, producing acetate and minor amounts of butyrate (Lynd et al., 1982). The specific origin, physiology and biochemistry of *B. methylotrophicum* are discussed in more detail in the next section.

1.2.3. Principles of Acetogenic Metabolism

The specific mechanism of acetogenic metabolism in both the unicarbonotrophic and autotrophic pathways of *C. thermoaceticum* and *B. methylotrophicum* have recently been elucidated, particularly the role played by CO dehydrogenase in the formation of acetyl-

CoA (Zeikus et al., 1985; Kerby and Zeikus, 1987b; Fuchs, 1986; Wood and Ljungdahl, 1991). Figure 5, adapted from Zeikus et al., (1985), and Wood and Ljungdahl, (1991), is a condensed outline of the autotrophic acetyl-CoA pathway for CO and CO₂ utilization by these organisms. Key steps for CO metabolism include the reaction of CO and H₂O with CO dehydrogenase to yield CO₂, the production of formate from CO₂ via formate dehydrogenase, several tetrahydrofolate mediated transformations ultimately resulting in a methyl-corrinoid complex, the reaction of CO with CO dehydrogenase to form a bound carbonyl moiety, and finally the synthesis of acetyl-CoA, from both the methyl and carbonyl groups bound to the CO dehydrogenase complex. Metabolism of H₂ and CO₂ occurs by the same mechanism, with H₂ being used to reduce CO₂ to bound CO, or [CO], in a ferredoxin dependent reaction, and the resulting carbonyl group reacting with the methyl-corrinoid species via CO dehydrogenase, to ultimately form acetyl-CoA.

The specific reactions and the mediating enzymes and enzyme complexes are detailed in Table 4. It is important to note the versatility of the CO dehydrogenase complex in that it potentially mediates 5 distinct reactions, including the oxidation of CO to CO₂, the binding of CO, the reduction of CO₂ to form a bound [CO] group, the binding of a methyl group from the corrinoid protein, and the condensation reaction of the carbonyl group, the methyl group, and the CoA ester to form acetyl-CoA.

The properties of carbon monoxide dehydrogenase have been recently reviewed (Diekert et al., 1985), and the enzyme has been purified from both *C. thermoaceticum* and *A. woodii* (Ragsdale et al., 1983a; Ragsdale et al., 1983b). The 440,000 MW enzyme isolated from *C. thermoaceticum* contains 2 different subunits of three copies each in the form $\alpha_3\beta_3$, with molecular weights of 78,000 and 71,000, respectively (Ragsdale et al., 1983b). The enzyme is a nickel-containing, iron-sulfur protein which reduces ferredoxin and cytochrome b in the presence of CO (Drake et al., 1980; Drake, 1982a). The iron exists in the active site as clusters of Fe₂S₄, which are reduced by reaction with CO and oxidized by reaction with CO₂ (Diekert et al., 1985). The condensation of bound

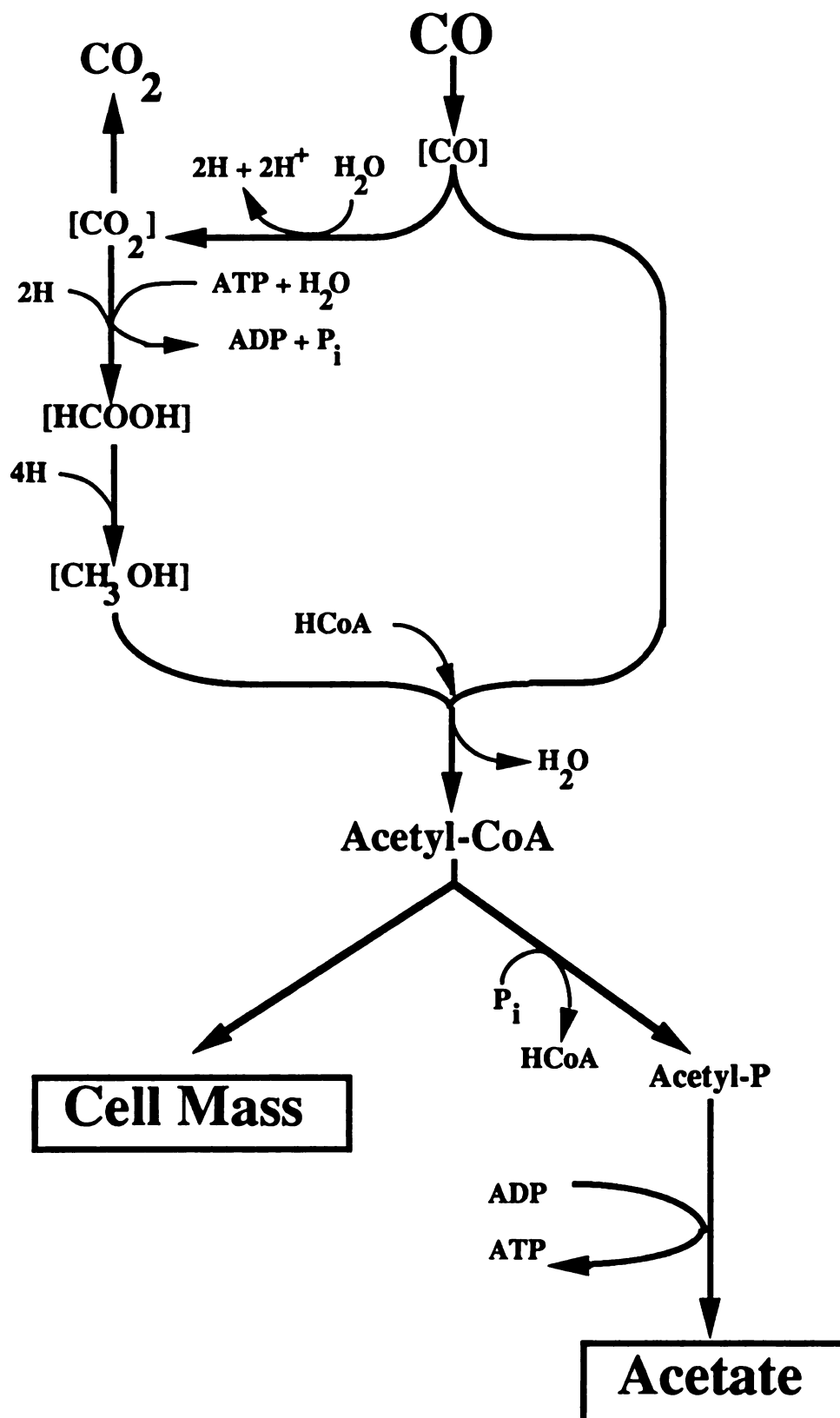


Figure 5. General pathway for unicarbonotrophic, acetogenic metabolism.

Table 4. Reactions in the unicarbonotrophic and autotrophic pathways for acetyl-CoA synthesis in the acetogens *B. methylotrophicum* and *C. thermoaceticum*^a.

Reaction	Mediating Enzyme
Formation of the Methyl Group ^b :	
$\text{CO} + \text{H}_2\text{O} \rightarrow \text{CO}_2 + 2\text{H}^+ + 2\text{e}^-$	Carbon Monoxide Dehydrogenase
$\text{CO}_2 + 2\text{e}^- \rightarrow \text{HCOOH}$	Formate Dehydrogenase
$\text{HCOOH} + \text{ATP} + \text{THF} \rightarrow \text{HCO-THF} + \text{ADP} + \text{H}_2\text{O}$	Formyl-THF Synthetase
$\text{HCO-THF} + \text{H}^+ \rightarrow \text{HC-THF}$	Methenyl-THF Cyclohydrase
$\text{HC-THF} + 2\text{e}^- \rightarrow \text{H}_2\text{C-THF}$	Methylene-THF Dehydrogenase
$\text{H}_2\text{C-THF} + \text{Fd:2e}^- \rightarrow \text{H}_3\text{C-THF}$	Methylene-THF Reductase
$\text{H}_3\text{C-THF} + \text{Co-E} \rightarrow \text{H}_3\text{C-Co-E}$	Corrinoid Protein
Formation of the Carbonyl Group:	
$\text{CO} + \text{CODH} \rightarrow \text{CO-CODH}$	Carbon Monoxide Dehydrogenase
$\text{H}_2 + \text{Fd} \rightarrow \text{Fd:2e}^- + 2\text{H}^+$	Hydrogenase
$\text{Fd:2e}^- + \text{CO}_2 + \text{CODH} \rightarrow \text{CO-CODH} + \text{Fd}$	Carbon Monoxide Dehydrogenase
Formation of the Acetyl-CoA Group:	
$\text{H}_3\text{C-Co-E} + \text{CO-CODH} \rightarrow \text{H}_3\text{C-CO-CODH} + \text{Co-E}$	
$\text{H}_3\text{C-CO-CODH} + \text{CoASH} \rightarrow \text{CH}_3\text{CO-CoA}$	Carbon Monoxide Dehydrogenase

^aDerived from Zeikus et al., 1985; Kerby and Zeikus, 1987b; Wood and Ljungdahl, 1991.

^bTHF = tetrahydrofolate; Fd = ferredoxin; Co-E = Corrinoid protein; CODH = Carbon monoxide dehydrogenase.

carbonyl, methyl, and CoA groups catalyzed by this enzyme has recently been verified in several different bacteria, including *C. thermoaceticum* (Ragsdale and Wood, 1985), *Methanosarcina thermophila* (Abbanat and Ferry, 1990), and *A. woodii* (Diekert and Ritter, 1982).

The other major components in the acetogenic pathway are tetrahydrofolate and corrinoid protein(s). Tetrahydrofolate participates in the reduction of formate to a methyl group, by serving as the carrier during catalysis by the 4 sequential enzymatic reactions; these reactions are reversible depending on the substrate utilized (CO/CO₂ or CH₃OH) (Zeikus et al., 1985). The corrinoid protein is a cobalt containing carrier protein, also known as cobamides, with 3 reduction states, and participates not only in the methyl

group transfer to CO dehydrogenase, but also in amino acid synthesis and in ferredoxin oxidation (Ljungdahl, 1986).

The principles of metabolic energy generation in acetogens are based on both substrate-level (SLP) and electron-transport (ETP) phosphorylation mechanisms. Energy conservation by SLP is a mechanism which couples exergonic chemical reactions to the synthesis of energy-rich intermediates such as thioesters or acid anhydrides, the hydrolysis of which allow formation of ATP from ADP and inorganic phosphate (Thauer et al., 1977). In autotrophic, acetogenic bacteria, this energy-rich intermediate is primarily acetyl-CoA. However, metabolism of CO or H₂ and CO₂ to produce acetate does not produce any net ATP via SLP because an ATP is consumed in the activation of the formyltetrahydrofolate synthetase reaction for every acetyl-CoA formed, and an ATP is produced for every acetate formed from acetyl-CoA, as shown in Table 4. For production of cell mass, another source of ATP generation must be present, and a chemiosmotic mechanism (ETP) to couple the proton motive force to ATP synthesis has often been hypothesized to account for the ATP generation required for cell growth and other metabolic reactions (Zeikus et al., 1985; Fuchs, 1986). The basic mechanism of electron-transport phosphorylation is given in Figure 6, where soluble, membrane bound, and intermembrane electron carriers facilitate the ejection of protons outside of the cell into the environment, generating a proton gradient across the cell membrane. This gradient, or proton-motive force, can then serve as the driving force to allow protons to re-enter the cell, the potential energy of which is captured in the form of ATP synthesis. The electron-transport pathway thus serves to link catabolic oxidation and reduction reactions to the proton-motive force. Both physiological and structural results supporting such a mechanism in acetogenic bacteria have been increasing over the last 6 years, and an ATP synthase and corresponding electron carriers have been isolated in *C. thermoaceticum*, as described previously. Soluble and membrane-bound electron carriers have been isolated from *B. methylotrophicum*, including ferredoxins, rubredoxins, cytochrome b and

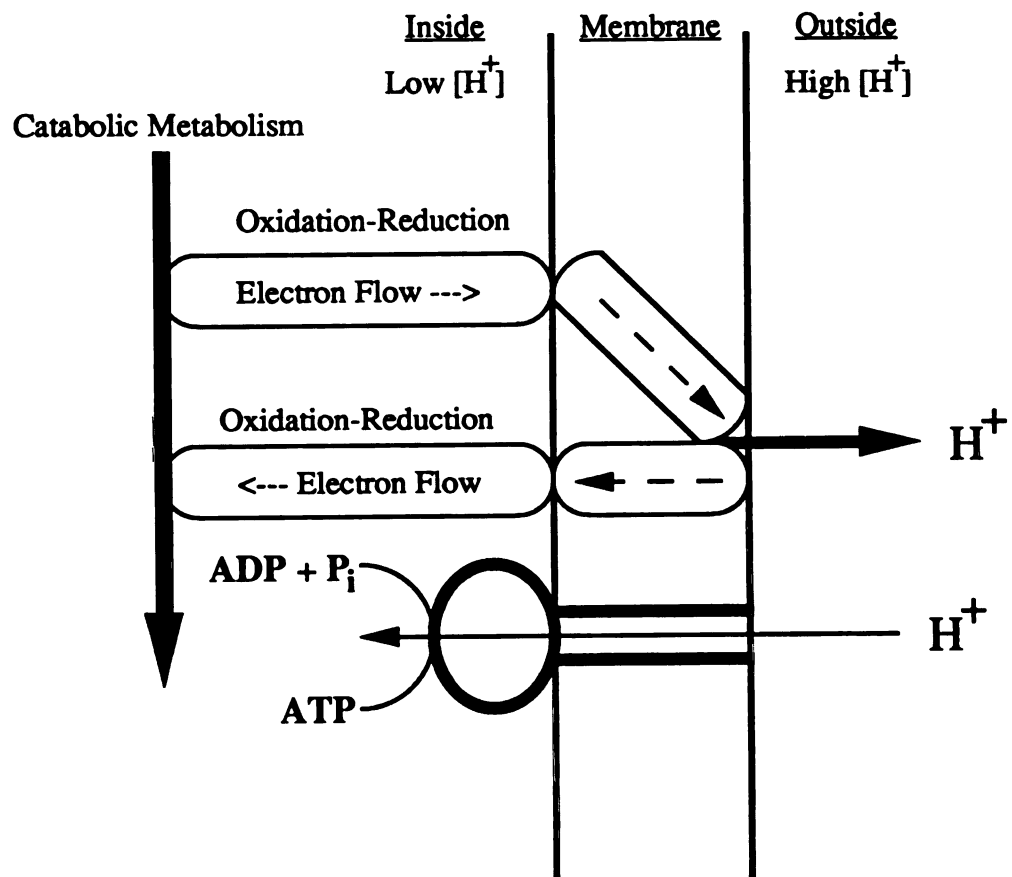


Figure 6. General mechanism for electron transport-coupled phosphorylation (ETP).

menaquinones, but the complete electron-transport system has yet to be ascertained (Zeikus et al., 1985; Saeki et al., 1989a; Saeki et al., 1989b).

Unfortunately, without the complete picture for energy generation in autotrophic and unicarbonotrophic acetogens, the specific energy yields for various substrates and metabolic reactions will be very difficult to verify, as discussed in later chapters. Furthermore, other mechanisms of ATP synthesis are possible, including transport-coupled phosphorylation (TCP), which as of this writing has only one known example in *P. modestum* (J. Kemner, pers. comm.). Such a hypothesis would inevitably raise questions of the possibilities for other, non-proton based ATP synthase enzymes, such as sodium based ATPases. These questions are currently under investigation; *C. thermoaceticum* has been determined to be sodium-independent during growth, but *A. woodii* has been found to be quite sodium-dependent during growth (Wood and Ljungdahl, 1991). In summary, it is now generally accepted that ETP mechanisms do exist in homoacetogens, and that they play an important role in energy generation, but the specific mechanisms and electron flow pathways have yet to be elucidated in many bacteria, as do the membrane-associated ATP synthase components.

1.2.4. Potential Application of Acetogenic Bacteria

The traditional feedstocks for anaerobic fermentation have been carbohydrates, but a resurgence in industrial coal utilization would provide ample and inexpensive 1-carbon feedstocks for fermentation by selected unicarbonotrophic and autotrophic organisms. The major synthesis gas components, CO, H₂ and CO₂, and also CH₃OH, are all readily available through coal gasification, or coal gasification and reaction in the case of CH₃OH. A general schematic for potential uses of 1-carbon fermentation technology in processing these compounds is shown in Figure 7, with several routes available for production of fuels, chemicals, and other feedstocks or commodity biological products.

The biological conversion of synthesis gas to methane, analogous to industrial catalytic SNG production from coal via steam reformation, is a reaction well-suited to some of the

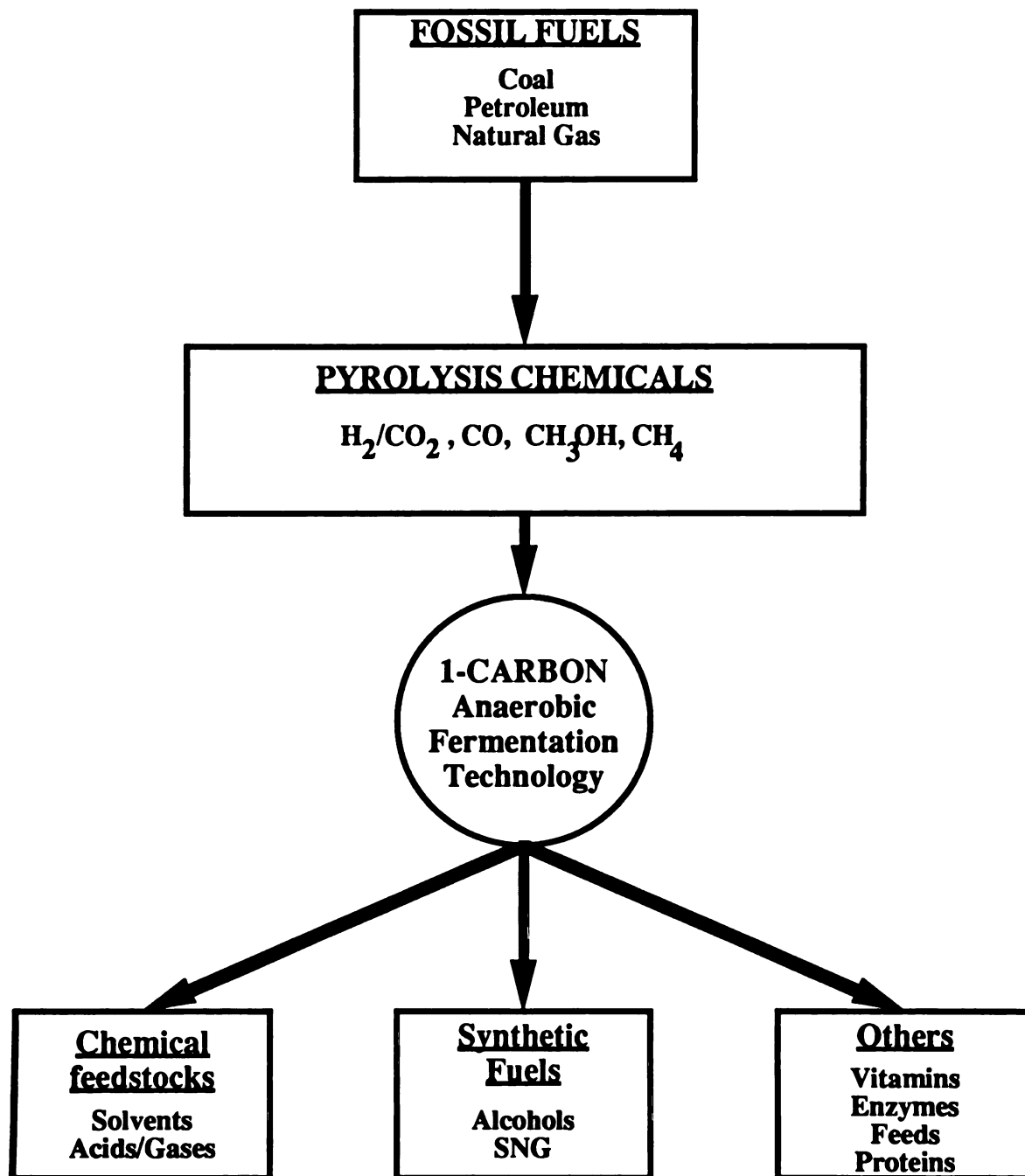


Figure 7. Potential biological routes for fuels and chemicals production from synthesis gas components.

methanogenic organisms listed previously. Such reactions are typically referred to as biomethanation processes; inherent in this definition is a potential for secondary product formation such as short-chain fatty acids. The basic tenet of biomethanation is upgrading the Btu content of synthesis gas, and studies with mixed cultures have shown CO₂ formation from CO, and CH₄ formation from H₂ and CO₂ (Wise et al., 1978). Enhancement of methane product yields, bacterial growth rates, and improvement of rate limiting metabolic steps including gas-liquid mass transfer have been identified as areas requiring more detailed study (Zeikus, 1983b), an indication that this technology is still in the exploratory stages of development. Regardless of the potential for biotechnology in this area, competition with available natural gas reserves and with industrially available routes for SNG production from coal could seriously limit the application of microorganisms for methane production from synthesis gas.

Acidogenic bacteria have the potential for production of short-chain organic acids, 2- and 4-carbon alcohols, and perhaps even single-cell protein from synthesis gas components. The potential for acetic or butyric acid production by acetogens has been well-documented, and product yields are particularly favorable (Zeikus, 1980). However, acetic acid is presently a large-volume industrial chemical, and commercial technology for acetic acid production from CO and CH₃OH is readily available, as discussed previously for the Monsanto process. Butyric acid, although not produced in nearly as large quantities as acetic acid, is a potential precursor to butanol, or for esterification in order to produce other chemical intermediates (Datta, 1981).

The recent discoveries of direct ethanol and butanol production from synthesis gas components via unicarbonotrophic, anaerobic bacteria have created a potential application for such organisms in the production of fuels, fuel additives, and industrial solvents. Ethanol has current potential as a direct gasoline additive, in addition to its chemical uses and solvent properties. Butanol is a so-called plasticizer alcohol, and can serve either as a chemical feedstock for production of butyl acetate or butyl acrylate, or can be potentially

be used as a gasoline octane enhancer or fuel additive. In general, application of 1-carbon metabolizing anaerobic bacteria for conversion of synthesis gas could ultimately depend on the discovery of a specific industrial niche based on the 4 most readily available products acetate, butyrate, ethanol, and butanol, or more likely on processes using these products as intermediate chemical feedstocks.

1.3. Physiology and Metabolism of *Butyribacterium methylotrophicum*

1.3.1. Origin and General Characteristics of the CO Strain

The original strain of *Butyribacterium methylotrophicum* (ATCC33266), known as the Marburg strain, was isolated by Zeikus and coworkers in 1980 from sewage digester sludge in Marburg, Federal Republic of Germany. *B. methylotrophicum* is a mesophilic, gram-positive, non-motile, rod-shaped bacterium isolated on a mineral salts medium containing 0.05% yeast extract, methanol, and acetate (Zeikus et al., 1980). The morphology is pleomorphic, with single or branched rod structures predominating. The importance of this organism was that it was the first acidogenic bacterium which used methanol as the sole carbon and energy source, producing a mixture of acetate and butyrate during growth.

Several fundamental characteristics of the Marburg strain were determined by Zeikus and coworkers in 1980, including a G+C content of approximately 49% and a very high level of corrinoids when grown on methanol. The strain is also an obligate anaerobe, with spore structures observed during heat shock treatment (Zeikus et al., 1980). Besides O₂, penicillin, streptomycin, tetracycline, and chloramphenicol were found to potent inhibitors during growth on carbohydrates. Glucose, CH₃OH, CH₃OH and acetate, and H₂ and CO₂ were all found to be usable energy sources, with a mixture of acetate and butyrate being produced during growth except for H₂ and CO₂, where only acetate was produced during growth (Zeikus et al., 1980). *B. methylotrophicum* is thus capable of growing

heterotrophically, autotrophically, or methylotrophically; abilities which provide it with an extremely diverse range of possible substrates (Moench and Zeikus, 1983).

B. methylotrophicum was originally placed in the family Propionibacteriaceae, grouped in the genus *Butyribacterium* after a similar organism, *Butyribacterium rettgeri*, which has been isolated 40 years before (Barker, 1944). *B. rettgeri*, however, was later found to actually be *Eubacterium limosum*, and thus some confusion, or contention, currently exists (Sharak Genthner et al., 1981) as to whether *B. methylotrophicum* is also not a separate genus but actually in the genus *Eubacteria*. The ongoing controversy has centered on morphological and physiological characteristics such as spore-formation, pleomorphism, vitamin requirements, and product spectrum. Interestingly, the high levels of corrinoids found in *B. methylotrophicum* have raised the issue of whether this organism is more suitable than other *Propionibacteria* for production of vitamin B₁₂ (cobalamin), which is difficult to synthesize chemically, although many species, including *B. methylotrophicum* have been used for vitamin production (Hatanaka et al., 1988).

The CO strain of *B. methylotrophicum* was developed in 1981 by Lynd, Kerby and Zeikus by first growing cells of the Marburg strain on glucose, pyruvate, and CH₃OH in the presence of a 100% CO gas headspace. Through repeated transfers on CH₃OH and acetate in the presence of CO and then on 100% CO and 0.05% yeast extract without alternate carbon sources, a culture was obtained which gradually adapted to use CO as the sole carbon and energy source, which was subsequently designated the CO strain (Lynd et al., 1982). The ability to use CO gas was retained through repeated back-transfers on other substrates in the absence of CO gas, thus confirming the stability of the adapted metabolism in the presence of selective pressure (Lynd et al., 1982).

1.3.2. Heterotrophic Metabolic Characteristics

Heterotrophic growth of *B. methylotrophicum* on substrates such as glucose proceeds via the Emden-Meyerhof-Parnas pathway to produce pyruvate, which is then converted to

acetyl-CoA by pyruvate dehydrogenase. The overall products from glucose metabolism are CO₂, acetate, butyrate, H₂, and cell mass, following the reaction,



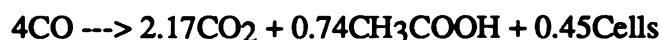
with a cell yield of 42.7 g cells (dry weight) per mole of glucose consumed (Lynd and Zeikus, 1983). An empirical formula for *B. methylotrophicum* of C₁H_{1.82}O_{0.50}N_{0.21} was also derived from an elemental analysis (Lynd and Zeikus, 1983). This carbon-balanced reaction stoichiometry was calculated using carbon and available electron balances (Erickson et al., 1978; Erickson and Oner, 1983), and was found to close within 0-1% for growth on glucose in a complex medium and to within 9-10% for growth on glucose with a defined medium (Lynd and Zeikus, 1983). These balancing methods are detailed in the Appendix. A doubling time on glucose of 3-4 hr was calculated from the batch growth data, and more than 25% of the consumed carbon was assimilated into cell mass, as shown in the fermentation equation. Hydrogen production during glucose metabolism is due to the activity of a hydrogenase enzyme, which gains electrons via an NADH-linked ferredoxin (G. J. Shen and J. G. Zeikus, unpublished results). This ferredoxin has been purified and its properties determined (Saeki et al., 1989a; Saeki et al., 1989b).

Activities for some of the major 1-carbon compound metabolizing enzymes such as CO dehydrogenase and formate dehydrogenase have been detected on glucose, pyruvate, or lactate grown cells, indicating that these enzymes are still synthesized in the absence of CO (G. J. Shen and J. G. Zeikus, unpublished results). The metabolic pathways for acetate and butyrate production have also been elucidated during growth on glucose (G. J. Shen and J. G. Zeikus, unpublished results), a pathway which also operates during growth on CO and which is detailed in the next chapter. In general, the specific mechanisms of carbon and electron flow have been investigated for heterotrophic metabolism of glucose, lactate, and pyruvate, but at the time of this writing these results have not been completely analyzed or published.

1.3.3. Autotrophic Metabolic Characteristics

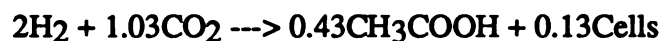
Metabolism of 1-carbon compounds in *B. methylophilum* has been elucidated both in batch bottle experiments and in larger, laboratory scale batch and continuous fermentations. The basic microbiology of this metabolism was determined by Zeikus and coworkers in the early 1980's. The CO strain exhibits acetogenic metabolism, as described previously, with formation of all cell mass and fermentation products arising from an acetyl-CoA intermediate. The versatility of this organism is outlined Table 5 and is described below.

Unicarbonotrophic metabolism of CO gas proceeds in batch culture by the carbon-balanced reaction



with an doubling time of approximately 12 hr. Carbon and electron recoveries during CO metabolism were within 3%. Slight variations on this CO fermentation stoichiometry have been observed, variations which include trace formation of butyrate during growth on CO (Lynd and Zeikus, 1983). Activities for CO dehydrogenase and formate dehydrogenase have been obtained during growth on CO, indicating that both of these enzymes participate in unicarbonotrophic metabolism. Interestingly, the specific activity of CO dehydrogenase is higher for CH₃OH and CO₂ grown cells of the Marburg strain or the CO strain than for CO grown cells of the CO strain, a strong reflection on the multipurpose nature of CO dehydrogenase in acetogenic metabolism (Lynd et al., 1982; Kerby and Zeikus, 1987b).

Growth on H₂ and CO₂ produces acetate and cell mass with a 9 hr doubling time, and exhibits the batch stoichiometry



with trace butyrate formation also observed (Lynd and Zeikus, 1983). Carbon and electron recoveries were within 2-3% for this fermentation. As shown, the approximate H₂:CO₂ consumption ratio is 2:1 during growth. Consumption of H₂ and CO₂ in the presence of

Table 5. 1-Carbon catabolic transformations observed with *B. methylotrophicum*^a.

Carbon/Energy Source	Reaction Stoichiometry ^b	Carbon Recovery (%)	Electron Recovery (%)	Doubling Time (hrs)	Yield ^c (g/mol)
H ₂ -CO ₂	:1.00H ₂ + 0.517CO ₂ ----> 0.216CH ₃ COOH + 0.002C ₃ H ₇ COOH + 0.063Cells	97	102	10	1.7
CO	:1.00CO ----> 0.497CO ₂ + 0.172CH ₃ COOH + 0.001C ₃ H ₇ COOH + 0.129Cells	97	97	12	3.4
CH ₃ OH-CO ₂ ^d	:1.00CH ₃ OH + 0.183CO ₂ ----> 0.016CH ₃ COOH + 0.234C ₃ H ₇ COOH + 0.284Cells	105	100	8	7.6
CH ₃ OH-CO	:1.00CH ₃ OH + 0.183CO ---->0.475CH ₃ COOH + 0.097C ₃ H ₇ COOH + 0.104CO ₂ + 0.327Cells	93	91	11	4.6

^aAdapted from Lynd and Zeikus, 1983; Kerby et al., 1983; Zeikus et al., 1985.

^bCalculated with a corresponding cell formula of [C₁H_{1.82}O_{0.50}N_{0.21}]; hydrogen and nitrogen balances omitted.

^cIn units of grams cells produced per mole substrate consumed.

^dObtained during fermentation in the presence of CH₃COOH.

CO is fully inhibited, and only proceeds after a majority of the CO is consumed in cultures incubated on CO, H₂, and CO₂ (Kerby and Zeikus, 1987a).

Growth of *B. methylotrophicum* with formate (HCOOH) as the sole substrate in batch culture follows the stoichiometry



with carbon and electron recovery within 3-5% and a 16 hr doubling time (Kerby and Zeikus, 1987a). During this metabolism, H₂ was first produced and then later consumed, furthermore, the overall growth on HCOOH compared to CO or H₂ and CO₂ was significantly reduced. However, cosubstrate fermentation of HCOOH plus H₂ and CO₂ yielded a carbon balance of



with an elimination in the fluxes for H₂ production and consumption, and a carbon and electron recovery within 10% (Kerby and Zeikus, 1987a). Cosubstrate fermentation with HCOOH and CO yielded a carbon balance of



within a 6% recovery for carbon and electrons (Kerby and Zeikus, 1987a). The absence of H₂ production or consumption during growth on HCOOH and CO suggests that CO is a strong inhibitor of the production hydrogenase enzyme, in that growth on HCOOH in the absence of CO results in significant H₂ production (Kerby and Zeikus, 1987a). When taken with the results for studies using CO, H₂, and CO₂, which suggest that CO is a strong inhibitor of uptake hydrogenase activity, there is strong indirect evidence for inhibition of both uptake and consumption hydrogenase by CO; however, this inhibition is not complete, since H₂ uptake was observed in the presence of low CO partial pressures (Kerby and Zeikus, 1987a) and low hydrogenase activity was observed in CO grown cells (Lynd et al., 1982). This inhibition may play a key role in the electron flow during CO metabolism, with ferredoxin oxidation proceeding via reduction of NADH as opposed to via production hydrogenase and subsequent production of H₂ gas (G. J. Shen, pers.

comm.). Determining the specific inhibition kinetics of CO on the hydrogenase enzyme is thus an important and as yet uninvestigated area of unicarbonotrophic metabolism.

B. methylotrophicum is also capable of growth on CH₃OH in the presence of acetate, with a batch carbon balance of



with a 9 hr doubling time and a carbon and electron recovery within 5% (Lynd and Zeikus, 1983). The principle of adding acetate during batch fermentation of CH₃OH in this study was to regulate the acetate:butyrate product ratio; an increase in exogenous acetate serves to decrease net acetate production and increase net butyrate production. This stoichiometry is thus not the "true" carbon balance for methylotrophic metabolism. Such experiments have also been conducted in the presence of acetate for cosubstrate fermentations of CH₃OH and CO, and CH₃OH and HCOOH, with acetate produced in the former and butyrate produced in the latter (Kerby et al., 1983). The ratio of CH₃OH to CO₂, or specifically to bicarbonate ion, is also a key parameter in regulating the acetate:butyrate product ratio, with increasing concentrations of bicarbonate resulting in increasing acetate production (Datta and Ogletree, 1983). Presumably, these phenomena are due to product inhibition, changes in the energetics of growth, and to changes in the relative fluxes of various pathways, all of which are subjects investigated in this study.

Results during extended batch CO fermentations with this organism have established that fermentation pH directly influences the relative production of acetate and butyrate during unicarbonotrophic growth on CO. At a pH of 6.8, acetate production was favored over butyrate production with a molar ratio of approximately 32:1, whereas at a pH of 6.0, acetate and butyrate were formed in equimolar amounts (Worden et al., 1989). Continuous, steady-state fermentations using *B. methylotrophicum* at several pH values yielded similar results, with minor butanol and ethanol production occurring at lower pH values (Grethlein et al., 1990). In this study, cell washout was observed at pH values below 5.5.

The effect of fermentation pH on product formation was also investigated during extended batch fermentation of CO, CO₂, and CH₃OH, and the same effect observed to a lesser extent, with a 2-fold decrease in the acetate to butyrate ratio observed between pH values of 6.8 and 6.0; however, acetate was still the primary product (Grethlein, 1989). A preliminary investigation as to the overall effect of fermentation pH on key catabolic enzymes was also initiated, and a 22% increase in the specific activity of butyrate kinase observed between pH values of 6.8 and 6.0 (Grethlein, 1989). Although not by any means a conclusive result, this preliminary enzymatic study suggested that the overall effect of fermentation pH in regulation of CO metabolism includes regulation of specific enzyme activities. Confirmation of this hypothesis has since been obtained for the key enzymes involved in acetate, butyrate, ethanol, and butanol formation during CO metabolism (J. S. Sheih, unpublished results).

1.4. Biological Processing of Coal-Derived Gases

The use of coal-derived synthesis gas as an industrial feedstock for production of fuels and chemicals has provided an increasingly attractive alternative to present petroleum-based processes stemming from recent developments in C₁ chemistry and coal gasification technology. One of the major drawbacks in using coal-derived synthesis gas is the required stringent removal of catalyst poisons such as H₂S, COS, and other trace contaminants. The levels of these sulfur contaminants can vary between 0-2% of the synthesis gas. Removal of these sulfur species requires energy-intensive purification steps which add significantly to the cost of the final product, particularly when the high sulfur content of most U.S. coals is recognized (Wilson et al., 1988).

Biological processing of synthesis gas, a potential option to conventional catalytic processing, is focused on a reduction in the amount of purification and synthesis gas preparation steps required for efficient conversion to fuels and chemicals. Research in this area is presently in the exploratory phase and is focused on characterization and

development of microorganisms and anaerobic fermentations for conversion of synthesis gas components. Some of the key motivations and obstacles in a biological processing approach, as well as a process concept for synthesis gas bioconversion, are described in this section.

1.4.1. Potential Advantages of Biological Processing

The main advantage to be gained by employing a biological route for coal-derived synthesis gas conversion is in reduced requirements for sulfur gas removal and clean-up prior to conversion. The sulfur, or more specifically sulfide, tolerance of anaerobic microorganisms capable of CO and H₂/CO₂ metabolism has been documented as at or above a concentration 2% H₂S or COS (Vega et al., 1990; Grethlein et al., 1991a). With sulfide tolerant microorganisms, raw or unpurified synthesis gas can potentially serve as the feedstock for fermentation, without the intensive sulfur purification that is typically a major part of conventional synthesis gas processing. Operating costs for production of clean synthesis gas, including the coal preparation, gasification, and gas purification, can account for over half of the total operating costs for coal-based processes such as at SASOL (Dry, 1987). The potential savings in a biological route will thus be realized in reduced capital and operating costs for purification equipment and energy requirements.

The other major advantage of biological processing is in the area of synthesis gas composition. The specificity of chemical reactions based on reactant stoichiometry requires set CO/H₂ ratios in the synthesis gas prior to catalytic reaction. Obtaining this set composition requires separate gas-shifting reactors, which frequently operate under high pressure, in order to modify the CO/H₂ ratio via the water-gas shift reaction. These shift-conversion operations often require gas recompression, high temperatures, and reactor equipment. In biological fermentations, a set CO/H₂ ratio is not of importance with respect to the metabolic reactions. Substantial savings in both operating and capital equipment costs could thus be realized by the removal of gas-shifting operations from the synthesis gas conversion process.

Fermentations at relatively low temperature and pressure will bring advantages in operating costs for the actual synthesis gas reactors, temperatures and pressures which are generally at least an order of magnitude less than those required in catalytic reactors using synthesis gas as a feedstock. The efficiency of anaerobic fermentations, the specificity of most biological reactions, and the high product yields of anaerobic bacteria are also specific advantages of biological routes in comparison to typical chemical processing.

1.4.2 Potential Disadvantages of Biological Processing

When comparing biological routes for synthesis gas conversion to chemical or catalytic routes, the most prevalent disadvantages are in the achievable reaction rates, the product separations costs based on typically aqueous, dilute fermentation broths, and the issues of culture maintenance, stability, and sterility. The intrinsic biological reaction rates for CO or H₂ vary greatly depending on the microorganism, but the achievable reaction rates will depend on the mass-transfer characteristics of aqueous fermentations, based on sparingly soluble gases such as CO and H₂. Achieving high mass transfer rates could potentially require high energy input and thus incur high operating costs.

Separation of aqueous fermentation products, particularly alcohols, typically requires energy intensive distillation unit operations, for which the operating costs increase as the concentration of alcohol decreases. There is also a practical minimum limit for separating ethanol or butanol from water, generally in the range of 10-15 g/L. The productivity and product concentrations resulting from a bioconversion process based on coal-derived synthesis gas will thus be critical in the assessment of its potential. Fermentation and process sterility is also a significant concern when working with biological systems; contaminated systems can result in uncontrolled reactions, decreases in product yields, and a potential for the desired organism to be out-competed for substrates and nutrients.

Development of fundamental scientific knowledge and fermentation technology for the types of unique biological systems which would potentially be employed for processing of coal-derived synthesis gas is thus a challenging endeavor from both a biological and an

engineering standpoint. None of the potential disadvantages associated with biological systems in this context are so overwhelming as to discount the entire concept, since separations, reaction control, and process stability issues will be present regardless of whether a biological or chemical route is used. However, the issues of reaction rate and product concentration are probably the most pervasive when discussing the limitations of a biological route. The advantages of biological systems are much more distinguishing in that all catalytic systems presently known are highly susceptible to sulfide poisoning, whereas in biological systems, particularly for anaerobic bacteria, many species are known to be sulfide tolerant. The degree of tolerance, however, varies from organism to organism. Similarly, regulation of the water-gas shift reaction as a prelude to chemical processing is an integral aspect of all current chemical routes, whereas, in general, the synthesis gas composition requirements for biological routes can be met in the gasifier itself, and will not be a function of the microorganism. These features have thus prompted government funding of two exploratory research efforts, at the University of Arkansas and at the Michigan Biotechnology Institute, for investigation of the potential for biological conversion of coal-derived synthesis gas.

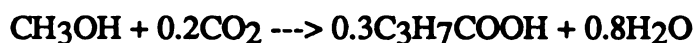
1.4.3. The MBI Indirect Liquefaction Process

With support from the U.S. Department of Energy, and more recently by the Center for Research on Sulfur in Coal and the Illinois Coal Development Board, the Michigan Biotechnology Institute (MBI), in Lansing, MI, has been developing a bioconversion process for coal-derived synthesis gas, of which the present work is an integral part. This process is aimed at biological production of fuel oxygenates, specifically alcohols, from the CO and H₂ in synthesis gas. The overall goals of the MBI process are to establish a fundamental knowledge base for high productivity, continuous, anaerobic fermentations based on CO and based on the possible fermentation products from CO.

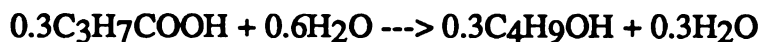
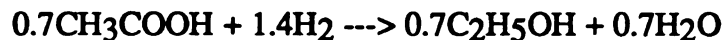
The original MBI process scheme consisted of a two-stage anaerobic fermentation of coal-derived synthesis gas plus methanol to produce an aqueous mixture of butanol,

ethanol, and acetone, followed by energy efficient distillation recovery. This process scheme is outline in Figure 8, where the synthesis gas mixture of CO and H₂, plus methanol, enters the first stage, which is an acidogenic fermentation based on CO gas. This fermentation produces a mixture of acetic and butyric acids, which are then transferred to the second stage where a solventogenic fermentation converts the acids to the corresponding alcohols ethanol and butanol, plus minor amounts of acetone. The chosen organisms for these fermentation stages were the CO strain of *B. methylotrophicum* for the acidogenic stage, and a mutant strain of *Clostridium acetobutylicum* for the solventogenic stage. The hydrogen gas is presumably consumed in the second stage fermentation to provide electrons for solventogenesis. Cell recyling is used for maintaining high cell density fermentations in both stages of the process.

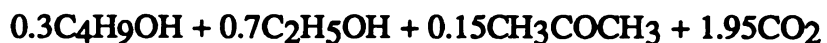
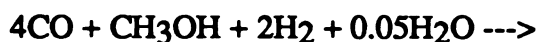
The overall theoretical conversion reactions in the acidogenic stage are



where methanol is introduced to promote butyrate formation. The exit streams from the first stage will thus be gaseous H₂ and an aqueous mixture of acetic and butyric acids. The acids then enter the second, solventogenic stage, where the theoretical reactions



result in mixture of butanol, ethanol, and acetone. The overall process theoretical fermentation balance is thus



With an improved mutant adapted for decreased acetone formation, that product can potentially be eliminated from the solventogenic fermentation step.

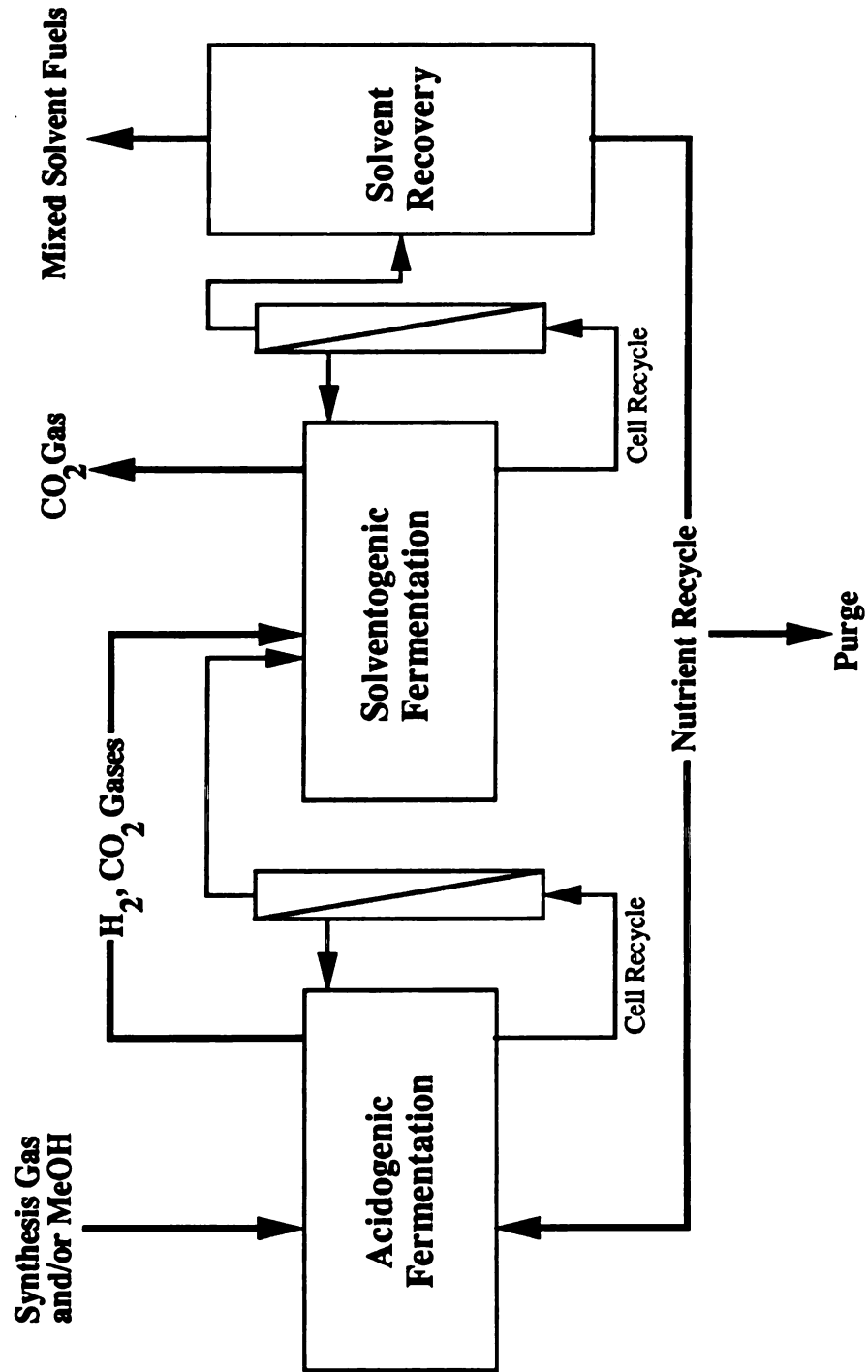


Figure 8. Proposed bioconversion scheme for production of fuel alcohols from coal-derived synthesis gas.

The proposed energy efficient solvent recovery scheme comprises a patented distillation process (IHOSR), based on heat recovery via vapor recompression and optimal side-stream return (Grethlein and Lynd, 1986). This distillation technology has exhibited dramatic energy savings for binary ethanol-water systems, and is expected to offer similar savings in a multicomponent mixture such as for the MBI bioconversion process. The use of pervaporation technology directly applied to the solventogenic fermentation has also been proposed. Overall, some of the most unique aspects of the MBI bioconversion concept include direct conversion of raw synthesis gas, conversion of high CO/H₂ ratio synthesis gases to liquid oxygenates, and an integrated, energy-efficient product separation.

Since its inception in 1987, the MBI process has undergone a significant amount of development and changes based on fermentation and microbiology research for both the acidogenic and solventogenic stages. As described previously, The CO strain of *B. methylotrophicum* has exhibited butyrate formation from CO (Worden et al., 1989), as well as a capacity for butanol and ethanol production directly from CO gas. However, alcohol production was observed only in trace quantities less than 0.1 g/L (Grethlein et al., 1990). A continuous fermentation for CO gas was developed, and operation at long-term, steady-state conditions was achieved (Grethlein et al., 1990). Fermentation pH was found to be a key regulatory factor in the overall CO metabolism of this organism during these studies. Other key developments include application of cell recycling to the solventogenic fermentation, with a 3 fold increase in the rate of solvent production observed. Uptake of butyrate by *C. acetobutylicum* has also been demonstrated under a variety of conditions.

There were several key issues for the biocoverion process upon which the initial objectives of the exploratory research effort were based; issues which still had significant bearing at the beginning of this work. These were,

1. Low rates of product formation and growth by anaerobic, CO-utilizing bacteria.
2. Low rates of organic acid uptake by solventogenic bacteria.

3. Difficulties of long-term, steady-state maintenance of anaerobic fermentations.
4. Low solubilities and mass transfer limitations of CO and H₂.
5. Product inhibition by alcohols and acids during anerobic fermentation.
6. High energy requirements for separation of dilute aqueous solvent mixtures.

These issues have been important in focusing MBI's research efforts towards obtaining fundamental knowledge of the particular microbial systems, as well advancing the technical aspects of the bioconversion process concept.

1.4.4. Objectives and Scope of the Present Work

The work in this dissertation is focused on the research and development of the first stage, acidogenic CO fermentation, which uses the CO strain of *B. methylotrophicum*. Based on previous results from batch and chemostat systems, the overall objectives for the fermentation and process development were:

1. Increase CO fermentation productivity and effluent product concentrations.
2. Operate continuously at low fermentation pH values, where butyrate and alcohol production are favored.
3. Regulate CO metabolism away from acetate and towards other products.
4. Develop a liquid media capable of supporting high cell densities.

In conjunction with these development objectives were several research objectives:

1. Elucidate pathways for alcohol production from CO in *B. methylotrophicum*.
2. Investigate effect of fermentation products on CO metabolism.
3. Identify possible mechanism(s) of metabolic regulation during CO metabolism.
4. Determine the organism's tolerance for sulfide species that may be present in coal-derived synthesis gas .
5. Determine the overall mechanism of the pH effect on CO metabolism.

The research effort is thus concerned both with the technical development of the CO fermentation as well as with increasing the scientific knowledge of CO metabolism and its regulation. The challenge of this system is particularly apparent in its novelty, for there

were no previous examples of similar studies with CO fermentations to be used as guidelines for the present work. The ultimate goal was to determine the potential for a biological fermentation based on CO from coal-derived synthesis gas, and to obtain a fundamental understanding of this specific biological system. Such an understanding allows identification of the important parameters and limitations, regardless of the specific microorganism or fermenter configuration used.

CHAPTER 2

EXPERIMENTAL MATERIALS AND METHODS

2.1. Microorganism and Culture Conditions

The CO strain of *B. methylotrophicum* was originally obtained from a frozen stock culture at the Michigan Biotechnology Institute (courtesy of Dr. M. K. Jain) in Lansing, Michigan, USA. A stock culture was maintained in 152 mL serum bottles (Wheaton, Millville, NJ) sealed with butyl rubber bungs (Bellco Biotechnology, Vineland, NJ) and aluminum crimp caps (Bellco Biotechnology, Vineland, NJ). These bottles contained 50 mL of phosphate buffered medium under an initial gas headspace of 100% CO gas at approximately 2.1 atm total pressure. When applicable, 28 mL pressure tubes (Bellco Biotechnology, Vineland, NJ) were substituted for the bottles, containing 10 mL of liquid media. The stock culture was grown in the dark at 37°C on a shaking platform (New Brunswick G10 Gyrotory Shaker, New Brunswick Scientific Co., Edison, NJ) at 100 rpm. The culture were transferred to fresh bottles every 2-3 weeks. Periodically, cells from a fermentation experiment were substituted for transferred cells in the continuation of the stock culture, so that any cellular adaptations resulting from long-term fermentation could be maintained. Twice during the course of this work, a complete set of 5 mL glycerol containing cell culture bottles was frozen at -70°C for extended storage of the cell line. Fermentation studies were initiated by inoculation with a 0.5% - 2.0% (v/v) actively growing *B. methylotrophicum* stock culture.

2.2. Culture Media and Gases

A phosphate buffered basal medium was adapted from Lynd et al., (1982), and used for maintenance of the stock culture as well as in all bottle experiments and batch

fermentation experiments. The pre-autoclaving components of this media are shown in Table 6. Trace Mineral II solution is a aqueous mineral salts addition containing 12.8 g/L

Table 6. Components of the phosphate buffered basal medium.

Component	Amount (per Liter)
Double Distilled water	1 L
NaCl	0.9 g
MgCl ₂ •2H ₂ O	0.2 g
CaCl ₂ •2H ₂ O	0.1 g
NH ₄ Cl	1.0 g
Trace Mineral II	10 mL
0.2% Resazurin	1.0 mL

nitrilotriacetic acid, 0.10 g/L FeSO₄•7H₂O, 0.10 g/L MnCl₂•4H₂O, 0.17 g/L CoCl₂•6H₂O, 0.10 g/L CaCl₂•2H₂O, 0.10 g/L ZnCl₂, 0.02 g/L CuCl₂•2H₂O, 0.01 g/L H₃BO₃, 0.01 g/L sodium molybdate, 1.0 g/L NaCl, 0.017 g/L Na₂SeO₃, and 0.026 g/L NiSO₄•6H₂O. The nitrilotriacetic acid is not a carbon source, but serves to prevent precipitation of iron in the form of FeS. Resazurin is a colorometric indicator of dissolved oxygen in the pH range of 5-8.

After autoclaving, 10 mL/L of a 10% w/v DIFCO bacto yeast extract (Difco laboratories, Detroit, MI) solution and 25mL/L of an aqueous phosphate buffer containing 150 g/L KH₂PO₄ and 290 g/L K₂HPO₄ were added. Also added was 10 mL/L of an aqueous vitamin solution containing 0.002 g/L Biotin, 0.002 g/L Folic acid, 0.010 g/L B₆•HCl (pyridoxine), 0.005 g/L B₁•HCl (thiamine), 0.005 g/L B₂ (riboflavin), 0.005 g/L

nicotinic acid, 0.005 g/L pantothenic acid, 0.0001 g/L crystalline B₁₂ (cyanocobalamin), 0.005 g/L PABA (para-aminobenzoic acid). The final addition was 25 mL/L of a 2.5% w/v Na₂S•9H₂O aqueous reducing aqueous solution. All the post-autoclaving additions above were sterilized separately, either by autoclaving or filter sterilization. This media thus consists of mostly inorganic salts, minerals, yeast extract, and vitamins, and contains no carbon source except for the small amount present in the yeast extract. The continuous fermentation experiments were conducted with the above media but with 10 mL/L phosphate buffer added instead of 25 mL/L, and with 10 mL/L of an aqueous cysteine-sulfide reducing solution containing 12.5 g/L cysteine sulfide and 12.5 g/L Na₂S•9H₂O substituted for the 25 mL/L Na₂S solution. The continuous cell recycling fermentations were conducted with a 2-fold increase in the amount of yeast extract added, a 5-fold increase in the amount of Trace Mineral II solution added, and a 10-fold increase in the amount of vitamin solution. These fermentations also used 1.98 g/L (NH₄)₂SO₄ and 10mL/L of a modified ammonium phosphate buffer containing 150 g/L KH₂PO₄, 116 g/L K₂HPO₄, and 132 g/L (NH₄)₂HPO₄ in double distilled water.

The CO, CO₂, N₂, and COS gases used in this study were obtained either from Linde (Linde Division, Union Carbide, Co., Warren, MI), Airco (Airco Industrial Gases, Royal Oak, MI), or from AGA (AGA Gas Inc., Cleveland, OH). Gas purities averaged 99.0% for CO, 99.99% for CO₂, 99.99% for N₂, and 98.5% for COS. H₂S gas was generated by adding a Na₂S solution to an excess of HCl under a vacuum headspace. The approximate purity of this synthesized H₂S gas was 90%.

2.3. Fermentation Equipment

All fermentation systems were designed for pure culture operation in an anaerobic environment. Nitrogen gas was used to initially flush the systems prior to inoculation. Substrate gases were passed through a hydrogen-reduced copper catalyst oven (Sargent Welch Scientific Co., Skokie IL) to remove any trace oxygen from the gas. Sample ports

were stoppered with butyl rubber bungs and crimped aluminum caps. All of the fermentation systems typically used Masterflex food grade Norprene tubing (Cole Parmer Instrument Co., Chicago, IL) for gas and liquid lines, and sealed connections with Dennison 7.5 inch Bar-lok cable ties (Dennison Manufacturing Co., Fastener Division, Framingham, MA). Fermentation vessels and attached external parts were autoclaved for a minimum of 30 minutes, and up to 95 minutes for the continuous systems with large liquid media reservoir volumes. Batch systems were autoclaved with the liquid media already in the fermenter, continuous systems were autoclaved separately from the media. External CO gas concentration was monitored for safety using both an SMC Series 2006 Carbon Monoxide Monitor and an SMC Series 2001 Combustible Gas Monitor (Sierra Monitor Corporation, Millipitas, CA), with both sensors calibrated in the toxic range of 50 ppm CO gas.

The continuous cell recycle fermentations were conducted in 2 L Multigen fermenters (New Brunswick Scientific Co., Edison, NJ, USA) with working volumes of either 1.2 or 1.4 L. A New Brunswick TM-100 Series Mega-Flow Filtration System (New Brunswick Scientific Co., Edison, NJ, USA) using an Amicon YM30 0.3 μm pore size cellulosic membrane (Amicon Corporation, Danvers, MA, USA) was used for cell microfiltration. Gas recycling was conducted using a Cole Parmer Masterflex peristaltic pump (Cole Parmer Instrument Co., Chicago, IL). A porous, stainless steel frit was used to reduce gas bubble size into the liquid from this gas recycle stream. Fermentation pH was automatically controlled by addition of 2N NaOH solution, using an Ingold Type 465 pH electrode (Ingold Electrodes Inc., Wilmington, MA) in conjunction with either a New Brunswick Model pH-40 Automatic pH controller (New Brunswick Scientific Co., Edison, NJ) or a Chemcadet pH Meter/Controller (Cole Parmer Instrument Co., Chicago, IL). Liquid flows were established using Gilson Minipuls 2 peristaltic pumps (Gilson Electronics, Middleton, WI). The liquid media reservoirs were prepared in 16 L batches using 20 L PYREX solution bottles (Corning, Inc., Corning, NY). Outlet gas flow rates

were measured using Cole Parmer series N062-01 or Series N032-41 rotameters (Cole Parmer Instrument Co., Chicago, IL).

2.4. Fermentation Conditions

In general, bottle experiments were conducted on a shaking platform in the dark as described previously for the stock culture maintenance. Bottles were initially at a pH of between 7.0 and 7.1 with a 100 % CO gas atmosphere. The pH was not controlled in these systems. Gas phase components such as H₂S gas were added by volume to the bottles prior to inoculation. Liquid phase components such as organic acids and alcohols were also added by volume from stock solutions prior to inoculation. Both gas and liquid samples were taken on a daily basis in these systems. Test tube growth experiments measured optical density by direct insertion into the spectrophotometer, and did not involve any external assays.

The experiments involving acids and alcohols were conducted in 152 mL sealed, anaerobic bottles with 50 mL liquid media and an initial 100% CO gas headspace at 2-2.2 atm, thus achieving a 2:1 gas to liquid volume ratio. Initial concentration ranges of approximately 0-12 g/L for alcohols were achieved by volumetric addition of either ethanol or n-butanol directly to the anaerobic bottles. Initial concentration ranges of approximately 0-10 g/L for acetate or butyrate were achieved by volumetric addition of stock solutions containing either 4 M acetic acid or 3 M butyric acid. The broth pH was adjusted prior to inoculation during organic acid tolerance experiments by equimolar volumetric addition of 10 N NaOH solution. To determine the effect of sodium on the growth of *B. methylotrophicum*, 28 mL sealed, anaerobic culture tubes, each with 10 mL of phosphate-buffered media under an 18 mL 100% CO gas headspace at 1.5-1.6 atm total pressure were used. A concentration range of 0 to 0.5 M sodium was generated by volumetric addition of sodium from a stock 5 M NaCl solution. All growth phase tolerance experiments were initiated by the addition of a 2% v/v mid-log phase *B. methylotrophicum*

stock culture. All bottle experiments were conducted in duplicate. Samples for cell density, broth pH, CO gas, CO₂ gas, and all liquid phase products were taken on a daily basis.

For experiments testing sulfide tolerance, varying sulfide concentrations were generated by directly adding H₂S gas or by addition of a stock 2.5 % Na₂S solution to 152 mL anaerobic bottles containing 50 mL of phosphate-buffered media with a 100% CO gas headspace at 2-2.2 atm. Initial equilibrium concentrations of the total liquid sulfide species were calculated for each experiment. Control experiments were always conducted with the standard total sulfide concentration of 0.083 g/L (based on the pre-equilibration concentration). All bottle experiments were conducted in duplicate. Experiments were initiated by the addition of a 2% v/v mid-log phase *B. methylotrophicum* stock culture. Samples for cell density, pH, CO gas, CO₂ gas, and all liquid phase products were taken on a daily basis.

The continuous cell recycle fermentations had a CO gas addition rate of 40 mL/min, with a gas recycling rate from the headspace into the liquid broth at 150 mL/min. Fermentation parameters for these experiments included a dilution rate of 0.015 hr⁻¹, an impeller speed of 450 rpm, a temperature of 37°C. This specific system is diagrammed in detail in Chapter 4.

2.5. Fermentation Broth Analysis

Liquid samples were taken using N₂-flushed, sterile syringes inserted into the butyl rubber bungs in either the bottles or fermenter sample ports. Approximately 1-5 mL liquid volume was taken, depending on the experiment. Gas volume samples were taken using gas tight glass syringes with a sample volume of 1.0 mL. Cell density was measured by determining optical density at 660 nm on a Sequoia-Turner Model 340 spectrophotometer (Sequoia-Turner Corporation, Mountain View, CA). Samples with an optical density greater than 0.6 were diluted 10 fold with distilled water. Those with an optical density greater than 6.0 were diluted 100 fold. Cell mass determinations for *B. methylotrophicum*

were made using a previously derived dry weight versus optical density calibration curve (Lynd et al., 1982). This curve was periodically reproduced in order to ensure accuracy for the cell mass calculations based on a value of 0.344 g cell mass/L•OD (Lynd et al., 1982). Undiluted samples were observed microscopically for general viability and contamination and subsequently transferred to 1.5 mL Eppendorf polypropylene micro test tubes (Brinkmann Instruments, Inc., Westbury, NY), centrifuged for 2 minutes at 12,000 rpm in an Eppendorf Centrifuge 5415 (Brinkmann Instruments, Inc., Westbury, NY), and the pH checked to provide external calibration for the experiments.

2.6. Fermentation Product Analysis

Concentrations of organic acids and alcohols were determined on a Hewlett-Packard 5890A Gas Chromatograph in tandem with a 3392A auto-sampler and 3392A integrator (Hewlett-Packard Co., Avon, PA), equipped with a 1.2 m Chromosorb 101 80/100 mesh column and a flame-ionization detector. The N₂ carrier gas flow rate was 30 mL/min. Operating temperatures were 190°, 220°, and 250°C for the column, injector, and detector, respectively. All samples were centrifuged, acidified with 3N phosphoric acid (1 part acid /10 parts sample) and then transferred to sealed injection vials. All samples were automatically injected in duplicate using the autosampler. Samples were compared to 10 mM standards run concurrently.

Analysis of organic acids and alcohols was alternately conducted on a Hewlett-Packard 5890A Gas Chromatograph in tandem with a 7673A auto-sampler and 3392A integrator (Hewlett-Packard Co., Avon, PA), equipped with a 1.2 m Carbopack C 80/100 mesh column and a flame-ionization detector. The N₂ carrier gas flow rate was 15 mL/min. Operating temperatures were 125°, 150°, and 220°C for the column, injector, and detector, respectively. All samples were centrifuged, acidified with 20 % (v/v) formic acid (1 part acid /10 parts sample) and then transferred to sealed injection vials. All samples

were automatically injected in duplicate using the autosampler. Samples were compared to 10 mM standards run concurrently.

The analysis of butanol and ethanol was confirmed periodically by high-performance liquid chromatography using a Waters 410 differential refractometer (Waters Instruments, Division of Millipore, Milford, MA, USA) with an Aminex ion exclusion HPX 87H column at 40°C, and in an outside laboratory by gas chromatography-mass spectroscopy using a Hewlett-Packard 5840 gas chromatograph and Hewlett-Packard 5895 Quadrapole Mass Spectrometer (Hewlett-Packard Co., Avondale, PA, USA) with a Chromosorb 101 80/100 mesh column at 190°C.

CO, CO₂, N₂ and H₂S gases were analyzed by gas chromatography in a GowMac Series 580 Gas Chromatograph (GowMac Instrument Co., Bridgewater, NJ) using a 1.8 m Carbosphere 80/100 mesh column and a thermal conductivity detector. Column, injector, and detector temperatures were 100°, 115°, and 150°C, respectively. A helium carrier gas was used with a flow rate of 50 mL/min. The detector current was 200 mA. All injections were 0.4 mL volume and at atmospheric pressure. Samples were compared to a calibrated standard curve constructed from pure gas responses.

CHAPTER 3

METABOLIC TOLERANCE AND REGULATION STUDIES

3.1. Objectives

The primary objective of the research described in this chapter was to investigate the effects of the known CO fermentation products on CO metabolism in *B. methylotrophicum*. These questions arose from the results obtained during the continuous cell recycling fermentation experiments described in Chapter 4, and thus chronologically these experiments would actually follow those results. The key objectives of these metabolic regulation and tolerance experiments were to determine the potential for alcohol or acid inhibition, the potential for acid uptake, the overall effect, if any, of these compounds on CO metabolism, and also, from a processing standpoint, the limits of sulfide tolerance. Also, an enhanced media was developed for use in the high cell density fermentations described in Chapter 4. These microbiological studies are presented prior to the fermentation studies, to allow a complete discussion of the results in Chapter 4.

Overall, the majority of the experiments described in this chapter were focused on elucidating mechanisms for manipulation or regulation of product formation during CO metabolism. The choice of an experimental system for these studies was thus critical, since the ultimate application of the information obtained was towards analyzing fermenter results. The impracticality of conducting controlled variable, microbiological experiments in a lab-scale set-up, particularly for an organism with a 12 hr doubling time, prompted the choice of batch bottles as an experimental system for these experiments. The advantages of this set-up include the ability to conduct experiments with controls and experimentals in duplicate or triplicate runs, high practicality in the number of experiments possible at one time, and in the short-term duration of the experiments. However, several limitations of the batch bottles must be recognized, particularly the difficulties in controlling only one

variable, and in extrapolating batch growth results for analysis of continuous fermenter data. Furthermore, the limits of the bottle system allowed only growth phase experiments to be conducted, and this origin must be considered when analyzing stationary phase fermenter results.

3.2. Effect of Alcohols on Growth and Product Formation

Although *B. methylotrophicum* produced butanol and ethanol from CO in concentrations ranging from 0.005 to 0.01 g/L during chemostat operation (Grethlein et al., 1990), concentrations which are not likely to be inhibitory either to growth or to product formation, the possibility during a high productivity CO fermentation for alcohol or even acid inhibition definitely exists. There is a strong potential for gradual adaptation of this organism towards alcohol production during prolonged, low pH fermentation of CO, and such adaptation would be limited, in part, by any potential product inhibition effects. A 10-20 fold increase (an optimistic but not unrealistic goal) in the alcohol concentration during a cell recycle fermentation could influence the cellular metabolism. Alcohol tolerance is, therefore, a potentially rate-limiting aspect of high cell density CO fermentations. Thus, in order to investigate any possible inhibition by butanol and ethanol during CO fermentation, several experiments were conducted and the rates of cell growth and product formation were measured both with and without the presence of butanol or ethanol. The results from these studies have a direct impact on the feasibility of any acid or alcohol-producing fermentation for *B. methylotrophicum* using CO gas as the sole carbon and energy source.

The effect of ethanol and butanol on the fermentation pattern during growth of *B. methylotrophicum* using CO as the sole carbon and energy source was determined in batch, anaerobic bottles. Time-course growth curves for the culture optical density as a function of alcohol concentration between 0-12 g/L are shown in Figures 9 and 10 for the ethanol and butanol experiments, respectively. Carbon and available electron balances

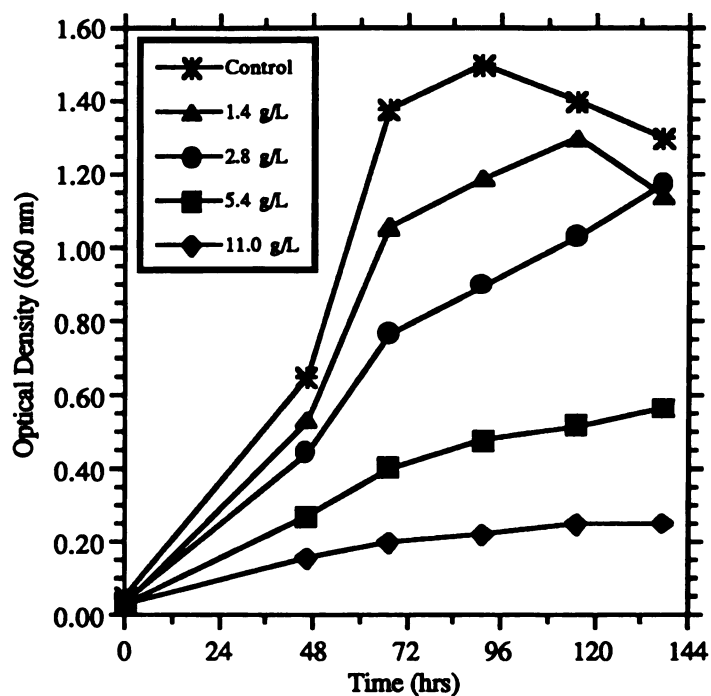


Figure 9. Effect of increasing ethanol concentration during growth of *B. methylotrophicum* on CO gas.

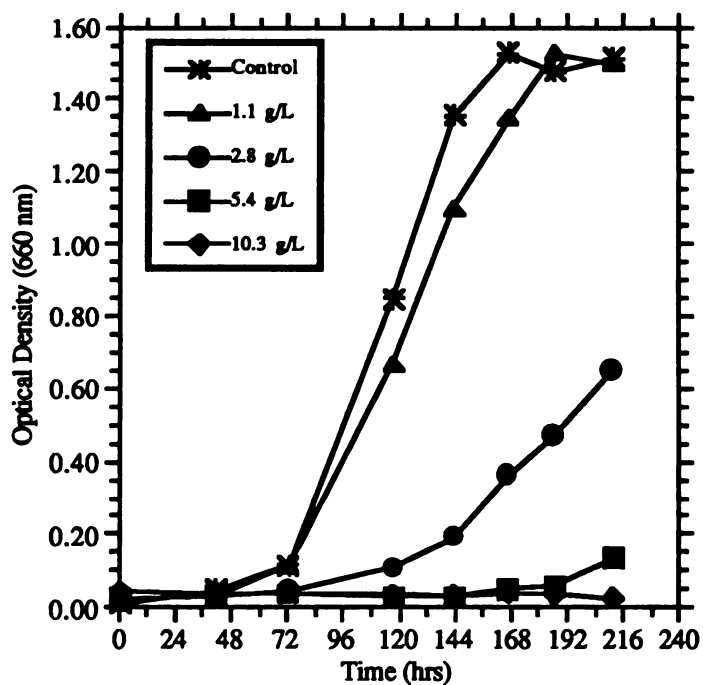


Figure 10. Effect of increasing butanol concentration during growth of *B. methylotrophicum* on CO gas.

(Erickson, et al., 1978; Erickson and Oner, 1983), calculated assuming 100% conservation during these experiments, are shown in Tables 7 and 8. These balances have been shown to be accurate to within 3-5% in similar experimental systems using this organism grown on CO gas (Lynd et al., 1983). Table 9 shows several observed and calculated variables as a function of alcohol concentration, including the maximum cell density obtained as a function of the control experiment (no exogenous alcohol added), cell density, the total drop in pH, the final acetate and butyrate concentrations observed, and the corresponding acetate to butyrate concentration ratio. Table 10 shows the observed doubling time during mid-log phase and also the total consumption of CO gas. For ethanol, concentrations of 5 g/L and above significantly inhibit both growth and product formation. For butanol, the tolerance level is somewhat lower, with significant inhibition of cell growth occurring at butanol concentrations of 2.8 g/L and higher.

The same effect over the concentration range of 0-2.5 g/L was examined in pressure tubes, with time-course measurement of optical density during experiments with either ethanol or butanol. Results for these experiments are shown in Figures 11 and Figure 12. These data show no significant effect of either alcohol between 0-1.0 g/L on the rates of cell growth, but with some decrease in the growth rate at concentrations of 2.5 g/L for both alcohols, an effect more significant for butanol, where a marked decrease in the final cell density is also observed, relative to the other experimentals and to the control. These findings are consistent with the trends observed in the previous bottle experiments, showing butanol to be somewhat more toxic than ethanol to cell growth.

The stationary phase response to exogenous ethanol and butanol was also examined. Fermenter grown cells were transferred at the onset of the stationary phase to batch bottles and incubated under CO gas headspaces in the presence of 7.1 g/L ethanol or 5.3 g/L butanol. These experiments were inoculated from separate fermentation cultures. Table 11 shows the carbon and available electron balanced fermentation stoichiometries calculated over these 3 day experiments. Initial concentrations of acetate and cell mass were 3.9 and

Table 7. Balanced carbon and available electron equations for batch incubation in the presence of ethanol during growth on CO gas.

Ethanol Concentration. (g/L)	Fermentation Stoichiometry^a
0.0 g/L	$4\text{CO} \rightarrow 2.16\text{CO}_2 + .48\text{AC} + .10\text{BU} + .03\text{EH} + .40\text{CM}$
1.4 g/L	$4\text{CO} \rightarrow 2.17\text{CO}_2 + .45\text{AC} + .13\text{BU} + .02\text{EH} + .36\text{CM}$
2.8 g/L	$4\text{CO} \rightarrow 2.18\text{CO}_2 + .43\text{AC} + .15\text{BU} + .01\text{EH} + .35\text{CM}$
5.4 g/L	$4\text{CO} \rightarrow 2.07\text{CO}_2 + .71\text{AC} + .05\text{BU} + .31\text{CM}$
11.0 g/L	$4\text{CO} \rightarrow 2.01\text{CO}_2 + .87\text{AC} + .25\text{CM}$

^aSymbols used: AC = Acetate; BU = Butyrate; EH = Ethanol; CM = Dry Cell Mass.

Table 8. Balanced carbon and available electron equations for batch incubation in the presence of butanol during growth on CO gas.

Butanol Concentration. (g/L)	Fermentation Stoichiometry^a
0.0 g/L	$4\text{CO} \rightarrow 2.16\text{CO}_2 + .42\text{AC} + .12\text{BU} + .01\text{EH} + .47\text{CM}$
1.1 g/L	$4\text{CO} \rightarrow 2.19\text{CO}_2 + .36\text{AC} + .14\text{BU} + .02\text{EH} + .48\text{CM}$
2.8 g/L	$4\text{CO} \rightarrow 2.15\text{CO}_2 + .51\text{AC} + .04\text{BU} + .09\text{EH} + .50\text{CM}$
5.4 g/L	$4\text{CO} \rightarrow 2.03\text{CO}_2 + .73\text{AC} + .52\text{CM}$
10.3 g/L	$4\text{CO} \rightarrow 2.00\text{CO}_2 + .99\text{AC} + .03\text{CM}$

^aSymbols used: AC = Acetate; BU = Butyrate; EH = Ethanol; CM = Dry Cell Mass.

Table 9. Effect of increasing alcohol concentration on cell density and product formation during growth on CO gas.

Alcohol% Concentration	Maximum OD Obtained	pH Change (Δ pH)	Final Concentration (mM)		Product Ratio (Ac:Bu)
			Acetate	Butyrate	
Ethanol:					
Control	100	0.94	23.8	4.8	5.0
1.4 g/L	86.7	0.92	21.8	6.5	3.4
2.8 g/L	78.0	0.84	19.4	6.6	2.9
5.4 g/L	37.9	0.65	17.1	1.3	13.2
11.0 g/L	17.0	0.28	10.5	0.0	∞
Butanol:					
Control	100	0.97	19.0	5.6	3.4
1.1 g/L	98.9	0.90	15.8	6.1	2.6
2.8 g/L	43.0	0.47	9.0	0.7	12.9
5.4 g/L	9.0	0.09	2.3	0.0	∞
10.3 g/L	2.0	0.00	0.5	0.0	∞

Table 10. Effect of increasing alcohol concentration on cell growth and CO consumption during growth on CO gas.

Alcohol Concentration	% Maximum OD Obtained	Total CO Consumption (μ moles)	Observed Doubling Time ^a (hrs)
Ethanol:			
Control	100	10,500	12.8
1.4 g/L	86.7	10,200	11.7
2.8 g/L	78.0	9,400	13.1
5.4 g/L	37.9	5,100	16.1
11.0 g/L	17.0	2,500	21.0
Butanol:			
Control	100	9,400	15.8
1.1 g/L	98.9	9,200	17.9
2.8 g/L	43.0	3,700	28.2
5.4 g/L	9.0	700	>30
10.3 g/L	2.0	100	>30

^aCalculated from initial growth phase data

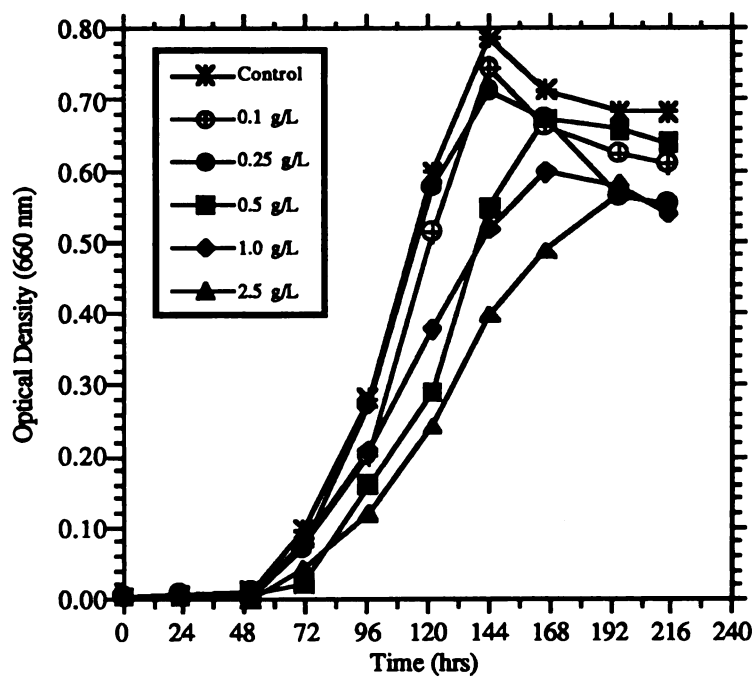


Figure 11. Effect of increasing ethanol concentration during growth of *B. methylotrophicum* on CO gas.

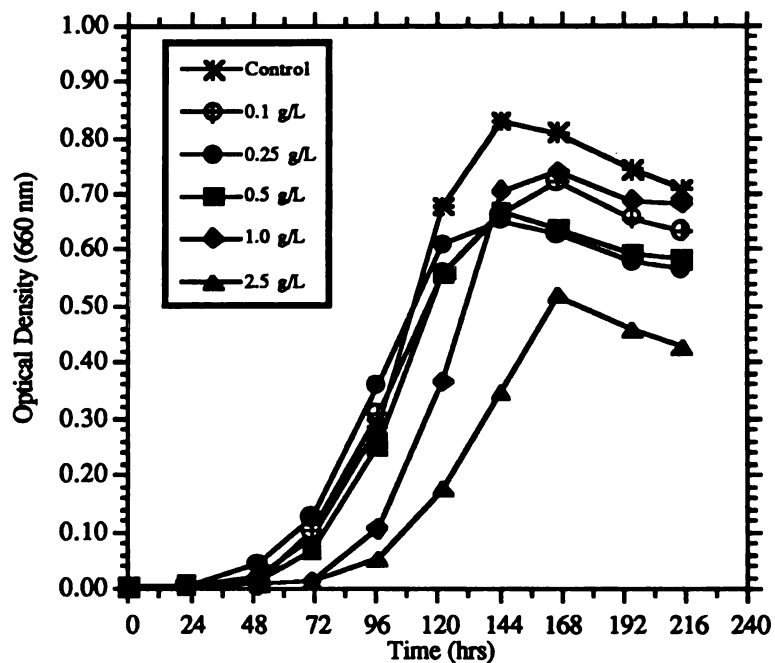


Figure 12. Effect of increasing butanol concentration during growth of *B. methylotrophicum* on CO gas.

Table 11. Balanced carbon and available electron equations for batch incubation of stationary phase cells in the presence of alcohols during growth on CO gas.

Alcohol Concentration	Fermentation Stoichiometry ^a
Ethanol:	
0.0 g/L	$4\text{CO} + .39\text{AC} \rightarrow 2.59\text{CO}_2 + .48\text{BU} + .03\text{EH} + .04\text{BH}$
5.3 g/L	$4\text{CO} + .38\text{AC} \rightarrow 2.62\text{CO}_2 + .44\text{BU} + .08\text{BH}$
Butanol:	
0.0 g/L	$4\text{CO} + .20\text{AC} \rightarrow 2.48\text{CO}_2 + .33\text{BU} + .06\text{EH} + .04\text{BH} + .31\text{CM}$
7.1 g/L	$4\text{CO} + .30\text{AC} \rightarrow 2.52\text{CO}_2 + .48\text{BU} + .14\text{EH} + .35\text{CM}$

^aSymbols used: AC = Acetate; BU = Butyrate; EH = Ethanol; BH = Butanol; CM = Dry Cell Mass.

1.2 g/L (dry weight) for the ethanol experiment, and 5.6 g/L and 2.1 g/L for the butanol experiment, respectively. The ethanol experiment also had initial concentrations of 0.3 g/L ethanol and 0.9 g/L butyrate in the fermenter grown cells prior to transferring to the CO bottles. A cosubstrate metabolism using both CO gas and the acetate present in the broth is evident from these calculated balances. These results indicate a potential for continued stationary phase CO metabolism in the presence of alcohol concentrations which severely inhibit cell growth and division. Furthermore, the data verify a mechanism in *B. methylotrophicum* for exogenous acid uptake. However, as indicated, these experiments exhibited a cosubstrate metabolism, and thus CO gas was not the sole carbon and energy source. Another important qualification to these stationary phase results is necessary. For the experiment using butanol, cell production was observed concomitant with a pH drop during the first day, and then the optical density declined moderately over the final 2 days (data not shown). For the experiment using ethanol, no cell production was observed (data not shown). This ambiguity is likely a result of the fermenter grown cells in the experiment involving ethanol having been harvested and subsequently transferred after

they had already entered the stationary phase and exhibited a slight decrease in optical density.

The effect of ethanol and butanol on the growth and performance of *B. methylotrophicum* during growth on CO gas is directly relevant to any potential alcohol-producing synthesis gas fermentation. Using continuous cell recycling, this organism has exhibited a transient capability for production of butanol as the primary product from CO metabolism in concentrations as high as 2.7 g/L (Grethlein et al., 1991b), a result detailed in Chapter 4. The effects of high alcohol concentration are important if such a response is to be optimized towards a steady-state fermentation scheme, particularly with respect to any possible inhibition mechanism(s) on cell growth or CO metabolism. The results for alcohol inhibition during batch cell growth clearly indicate the inhibitory effects of both butanol and ethanol above 2 and 5 g/L, respectively, with decreases in the total CO consumption, the total acetate and cell production, and the observed growth rates.

The precise mechanism for this effect on *B. methylotrophicum* was not investigated, but a general mechanism can perhaps be inferred from published alcohol tolerance studies with *C. acetobutylicum*, which are quite numerous. The major effect of alcohols, particularly butanol, on a bacterial cell is in the cell membrane, where high butanol concentrations have been shown to increase the membrane fluidity of *C. acetobutylicum*, a phenomenon for which the cellular response is to increase the ratio of saturated to unsaturated fatty acyl hydrocarbons (Vollherbst-Schneck et al., 1984; Baer et al., 1987). This membrane fluidization effect of butanol has several consequences, including a disruption of the nutrient transport and energy-generation systems in the cell membrane (Moreira et al., 1981), specific inhibition of ATPase activity (Soucaille et al., 1987), and destabilization of the internal pH (Bowles and Ellefson, 1985). This loss of energy generation thus results in slower growth rates and increased lag times (Bowles and Ellefson, 1985; Moreira et al., 1981; Bajpai and Iannotti, 1988). The relative toxicity of butanol compared to ethanol in *C. acetobutylicum* is approximately tenfold, a trend which

was observed during this study but not nearly to the same degree, and which is attributed to the increased hydrophobicity of butanol compared to ethanol (Moreira et al., 1981). Although the physical nature of these effects can be extrapolated to *B. methylotrophicum*, it should be kept in mind that *C. acetobutylicum* is an alcohol-producing bacterium, with total solvent production capacities in the 1-2% range; thus one would expect the cellular tolerance, membrane-maintenance systems, and growth mechanisms in the presence of butanol to be much more fully developed than for *B. methylotrophicum*.

Results for the stationary phase alcohol experiments are somewhat inconclusive, particularly in light of the inoculum conditions, as described previously. There is not a significant difference in the response to ethanol between the control and the 5.0 g/L ethanol experiment, indicating that the observed cosubstrate metabolism of acetate and CO uptake was due not to the influence of added ethanol but to either the initial presence of acetate or the lower starting pH of 6.4 rather than 7.0-7.1, as was used for the growth experiments. Three variables affect the stationary phase experiments: the culture pH, the acetate concentration, and the alcohol concentration, and distinguishing the effects of one of these variables is not possible from this single series of experiments. The experimental evidence does conclusively show, however, that although growth of *B. methylotrophicum* is severely inhibited by increasing alcohol concentrations, the stationary phase CO metabolism is not sensitive to concentrations up to 5.0 g/L of either ethanol or butanol. This result is relevant to the future potential of an alcohol fermentation using *B. methylotrophicum* with CO gas as the sole carbon and energy source, where a fermentation system designed to bias the cell population towards a stationary phase response would minimize the effects of product inhibition due to high concentrations of ethanol and butanol.

The production of alcohols as primary products from CO metabolism will require major research efforts to increase the tolerance and productivity, as this study has shown concentrations of 2-5 g/L to be inhibitory to cell growth. Since 10-15 g/L can be

considered a minimum concentration range required for efficient alcohol separation (H. E. Grethlein, pers. comm.), the overall feasibility of an alcohol fermentation directly from CO gas is quite low. Strain improvement and adaptation research could aid in increasing the attractiveness of these unique biological pathways, improvements which in *C. acetobutylicum* have focused on alcohol tolerance via temperature-induced membrane stabilization (Baer et al., 1987), increases in internal stabilization factors (Soucaille et al., 1987), and isolation of tolerant mutants by application of various mutagenic factors and adaptation mechanisms (Hermann et al., 1985).

3.3. Effect of Acids on Growth and Product Formation

As for the alcohols, the possibility for inhibition by either acetate or butyrate exists during a high cell density CO fermentation. However, the nature of this issue is different for the acids, particularly acetate, in lieu of product desirability. Due to the emphasis of this research on production of fuel and fuel enhancer compounds, alcohol production was considered more desirable than acid production, not only because alcohols are volatile, combustible fuels or fuel additives, but also because of separation issues. Therefore, although acetate and butyrate inhibition of cell growth would be detrimental, feedback inhibition of these products, particularly acetate, could be a possible mechanism for controlling the production of alcohols during CO fermentation. If the acetate forming pathway were inhibited by a high external acetate concentration, the cellular "pool" of acetyl-CoA would exhibit a net increase and more acetyl-CoA would be available for ethanol or butyryl-CoA formation. The same logic also would apply for butyrate, with a net increase in the pool of butyryl-CoA providing more substrate for butanol production.

Another potential issue intimately involved with the acid regulation question is that of acid uptake during growth. The optimization of *B. methylotrophicum* for use in a CO fermentation has primarily depended on the regulation of CO metabolism by changes in external pH. Although previously thought to produce only acetate from CO, decreasing the

fermentation pH has since been shown to regulate carbon and electron flow away from acetate and towards butyrate and butanol in extended batch fermentation (Worden et al., 1989), continuous fermentation (Grethlein et al., 1990), and continuous fermentation with cell recycling (See Chapter 4). Yet in all of these previous pH studies, the relative proportioning of carbon and electrons towards the various products could only be moderately affected, and the complete shutdown of one or more of the pathways was not observed (Worden et al., 1989; Grethlein et al., 1990; Grethlein et al., 1991a). During these acid tolerance studies, the overall objective was to determine if more complete regulation could be achieved by exploiting any end-product inhibition mechanisms present in *B. methylotrophicum* during growth on CO gas. Specifically, the primary objective was to inhibit acetate formation and increase butyrate or butanol formation.

The enzymes for acetate and butyrate formation from their corresponding CoA precursors have been examined and studied as a function of pH (Grethlein, 1989). The two pathways consist of an acetyl (butyryl) phosphotransferase enzyme, and an acetate (butyrate) kinase enzyme, which are known to be reversible *in vitro*; assays involved in measuring these enzyme activities are usually performed in reverse direction (Grethlein, 1989). With or without the influence of a mass action type phenomena, it is conceivable that conditions can be met during CO fermentation for these enzyme pathways to operate in the reverse direction and for the cells to take up acetate and/or butyrate and produce either ethanol or butanol (or even butyrate, in the case of acetate uptake). It should be emphasized, however, that such uptake would not necessarily be a reversal of the known pathways, separate mechanisms could exist for production and consumption, as has been suggested for *C. acetobutylicum* (Hartmanis et al., 1984). The benefits of acid uptake ability, if it were stable, would be numerous. Most importantly, it would allow operation a two-stage fermentation in which acids were produced in one stage with the effluent serving as the feedstock for alcohol production in the second stage. The potential complexity of such uptake phenomena is unclear but most likely the conditions are very

stressful to the cell, since ATP consumption would be required, as opposed to the normal acid-forming routes, which produce ATP.

These questions were investigated in *B. methylotrophicum* for both acetate and butyrate in batch bottle experiments similar to those described for the alcohol tolerance studies listed above. The growth of *B. methylotrophicum* on CO with initial acetate and butyrate in concentrations ranging from 0 to 12 g/L was monitored. Cell growth and product formation were measured, and net acid production calculated. Time-course growth curves for *B. methylotrophicum* cells grown in the presence of increasing acetate or butyrate concentrations are shown in Figures 13 and 14, respectively. Balanced equations for these experiments are given in Tables 12 and 13. As shown, the trends of acid uptake are evidence for a cosubstrate fermentation mechanism in this organism for simultaneous consumption of CO gas and either acetate or butyrate. The pH changes depicted in Figure 3 are consistent with the acetate or butyrate uptake trends shown in Table 12 ; at higher acetate concentrations, acid uptake is observed and the media is essentially deacidified, thus resulting in less of a pH decrease during the course of the experiment. Similarly, the trends shown in Table 13 are consistent with the pH changes observed in Figure 14, where at higher butyrate concentrations, a relative increase in the uptake of butyrate is observed concomitant with an increase in acetate production, and thus a decrease in the medium pH. These experiments are further evidence for the existence of either reversible pathways for acetate and butyrate production or distinct production and consumption mechanisms in *B. methylotrophicum*, with the formation and uptake reactions both exhibiting a strong dependence on the corresponding external acid concentration.

To test the effect of increased osmotic stress due to the experimental set-up, where to attain a constant initial pH of 7.0-7.2, the bottles containing acetic and butyric acid were pH-adjusted with NaOH solution, the effects of sodium on the growth of *B. methylotrophicum* were investigated. The molar addition of sodium was a maximum at an acetate concentration of 12.3 g/L, or 0.205 M, which corresponds to an addition of

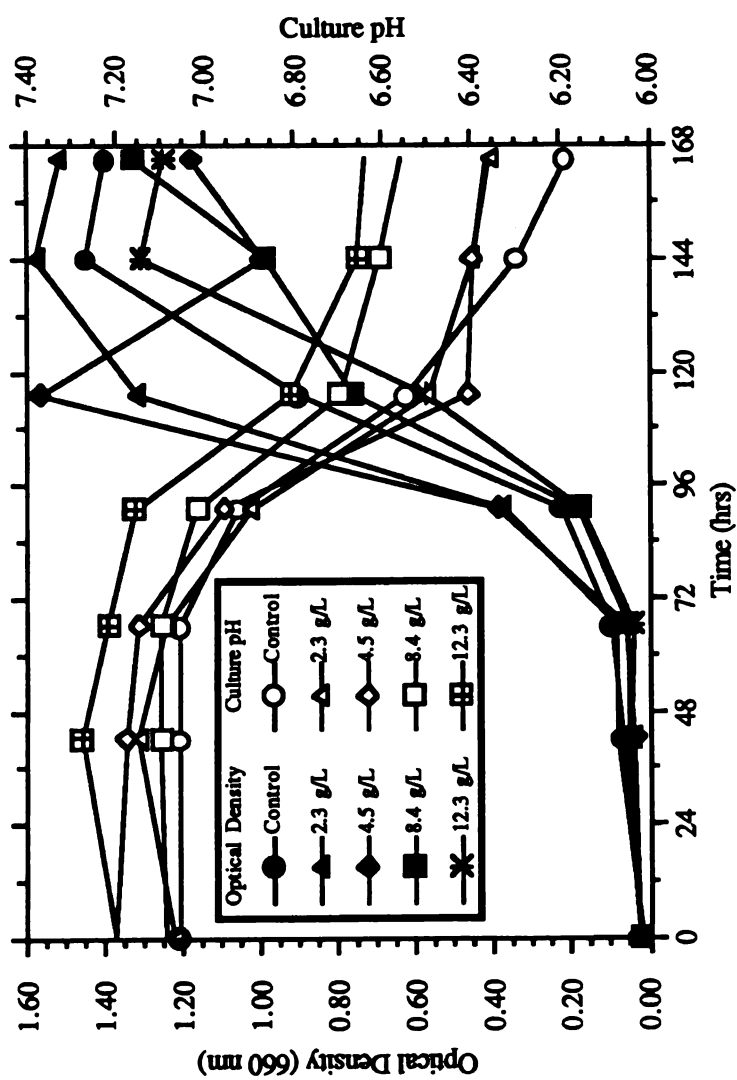


Figure 13. Effect of increasing acetate concentration during growth of *B. methylotrophicum* on CO gas.

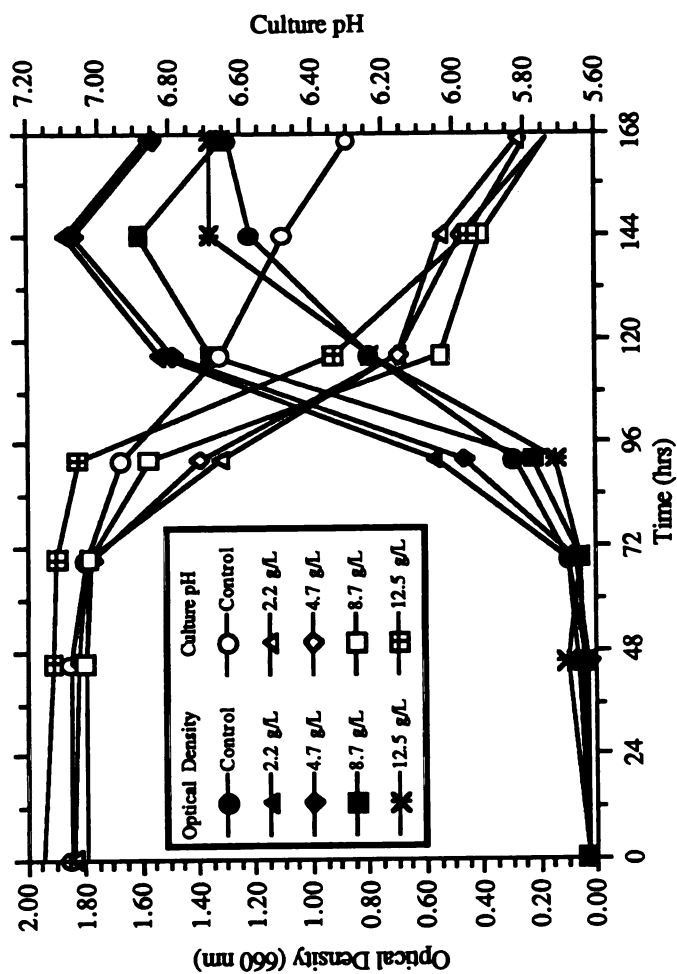


Figure 14. Effect of increasing butyrate concentration during growth of *B. methylotrophicum* on CO gas.

Table 12. Balanced carbon and available electron equations for batch incubation in the presence of acetate during growth on CO gas.

Acetate Concentration. (g/L)	Fermentation Stoichiometry ^a
0.0 g/L	$4\text{CO} \rightarrow 2.08\text{CO}_2 + .61\text{AC} + .04\text{BU} + .01\text{IBU} + .03\text{EH} + .50\text{CM}$
2.3 g/L	$4\text{CO} \rightarrow 2.21\text{CO}_2 + .30\text{AC} + .14\text{BU} + .02\text{IBU} + .02\text{EH} + .52\text{CM}$
4.5 g/L	$4\text{CO} \rightarrow 2.20\text{CO}_2 + .29\text{AC} + .15\text{BU} + .01\text{IBU} + .01\text{EH} + .55\text{CM}$
8.4 g/L	$4\text{CO} + .11\text{AC} \rightarrow 2.38\text{CO}_2 + .32\text{BU} + .02\text{IBU} + .03\text{EH} + .45\text{CM}$
12.3 g/L	$4\text{CO} + .18\text{AC} \rightarrow 2.41\text{CO}_2 + .34\text{BU} + .02\text{IBU} + .03\text{EH} + .44\text{CM}$

^aSymbols used: AC = Acetate; BU = Butyrate; IBU = Isobutyrate; EH = Ethanol;
CM = Dry Cell Mass.

Table 13. Balanced carbon and available electron equations for batch incubation in the presence of butyrate during growth on CO gas.

Butyrate Concentration. (g/L)	Fermentation Stoichiometry ^a
0.0 g/L	$4\text{CO} \rightarrow 2.10\text{CO}_2 + .57\text{AC} + .06\text{BU} + .01\text{IBU} + .01\text{EH} + .48\text{CM}$
2.2 g/L	$4\text{CO} + .07\text{BU} \rightarrow 2.01\text{CO}_2 + .85\text{AC} + .01\text{IBU} + .02\text{EH} + .02\text{BH} + .42\text{CM}$
4.7 g/L	$4\text{CO} + .28\text{BU} \rightarrow 1.84\text{CO}_2 + 1.25\text{AC} + .02\text{IBU} + .02\text{EH} + .03\text{BH} + .57\text{CM}$
8.7 g/L	$4\text{CO} + .34\text{BU} \rightarrow 1.77\text{CO}_2 + 1.44\text{AC} + .01\text{IBU} + .02\text{EH} + .03\text{BH} + .52\text{CM}$
12.5 g/L	$4\text{CO} + .42\text{BU} \rightarrow 1.69\text{CO}_2 + 1.68\text{AC} + .01\text{IBU} + .02\text{EH} + .03\text{BH} + .44\text{CM}$

^aSymbols used: AC = Acetate; BU = Butyrate; IBU = Isobutyrate; EH = Ethanol;
BH = Butanol; CM = Dry Cell Mass.

0.0102 acid equivalents. Thus, to neutralize this acid, a minimum of 0.012 base equivalents was required, in the form of NaOH. In 50 mL liquid, this is equivalent to 0.24 mol Na/L, or, in the form of NaCl, approximately 0.25 mol NaCl/L. An experiment testing the effect of NaCl was thus conducted over the concentration range of 0-1.0 g/L, and the effect on the growth on *B. methylotrophicum* determined during CO metabolism in pressure tubes. Results from this experiment are shown in Figure 15, where only at a NaCl concentration of 1.0 g/L is significant inhibition of cell growth observed, mostly in the form of an increased lag phase, a result also seen at 0.75 g/L NaCl. Therefore, from these results, the effect of osmotic stress from Na addition was determined not to influence cell growth during the tolerance studies with acetate and butyrate.

A metabolic precedent for the phenomenon of acid uptake can be found in *E. limosum* grown on methanol, where the production of acetate can be decreased by adding acetate to the growth medium, with higher concentrations reversing the reaction and causing acetate uptake (Pacaud et al., 1986a; Pacaud et al., 1986b). Furthermore, the same effect has been observed with butyrate, with increasing butyrate concentrations causing an increase in the relative production of acetate (Loubiere et al., 1986), a trend observed here for butyrate uptake by *B. methylotrophicum*. Similar phenomena have also been observed for *Clostridium tyrobutyricum* grown on glucose (Michel-Savin et al., 1990). The authors of these studies state that the observed acid uptake occurred by reversal of the acid-forming pathways, although no enzyme activity studies were conducted.

The uptake of external acetate and butyrate during batch growth of *B. methylotrophicum* raises the important question of the potential for a steady-state uptake response over long time periods, since this mechanism would place additional stress on the cellular energetics. Assuming the uptake of external acids proceeds via a reversal of the known production pathways, the uptake of acetate, on a basis of acetyl-CoA formation, requires 1 ATP for every 1 acetate consumed or 1/2 an ATP for every 1 butyrate consumed. With this stoichiometry, one would predict that acetate production from

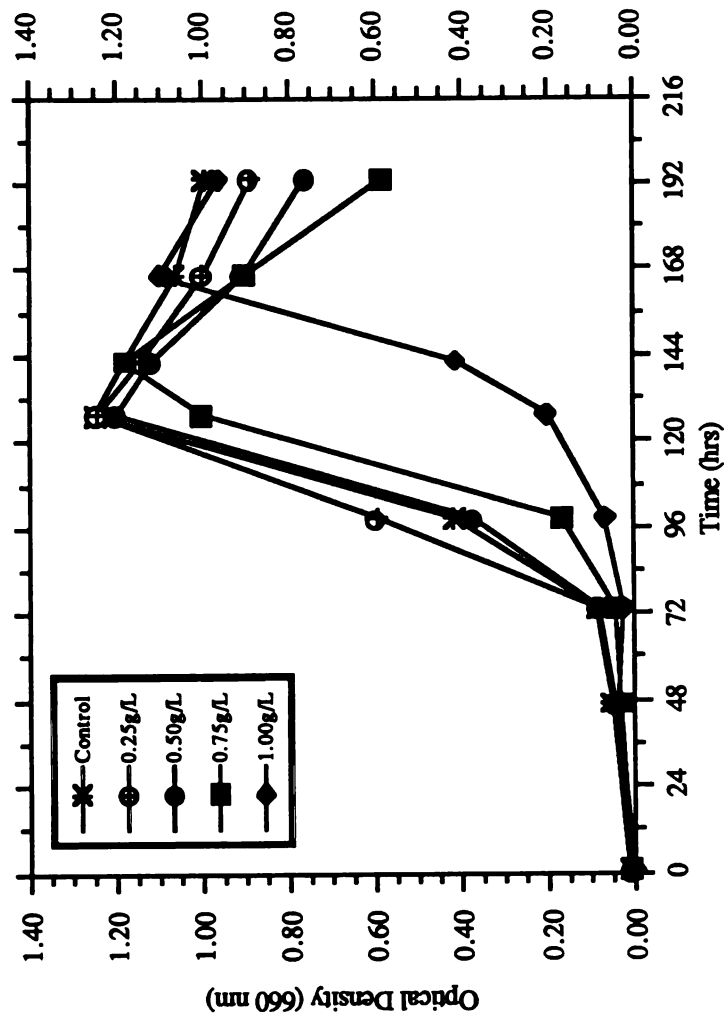


Figure 15. Effect of increasing NaCl concentration during growth of *B. methylotrophicum* on CO gas.

butyrate uptake would be more favorable than butyrate production from acetate uptake, if only from an ATP formation standpoint (based on SLP only). This trend is consistent with the experimental data, which indicate a higher affinity for butyrate uptake, observed at 2.2 g/L and above, than for acetate uptake, observed at 8.4 g/L and above. This hypothesis may also explain why a major increase in butanol production is not observed during butyrate uptake, since the butanol pathway from butyrate yields no ATP, but conversion of butyrate to acetate does. The importance of energetics during CO metabolism can be seen in the metabolic pathways for 1-carbon metabolism (Zeikus et al, 1985) as well as acid and alcohol formation from CO (Grethlein et al., 1991b) , which have been previously elucidated for *B. methylotrophicum*. The ATP consuming reaction in the CO pathway is the formation of formyl-H₄folate, and thus ultimately the methyl group of acetyl-CoA, which is catalyzed by formyl-H₄folate synthetase (Kerby and Zeikus, 1987b). The ATP producing steps are the kinase reactions for formation of acetate and butyrate. From these known pathways, the molar ATP and electron yields arising from substrate-level CO metabolism can be calculated, as shown in Table 14. A critical

Table 14. Theoretical molar ATP and electron yields^a from substrate-level phosphorylation for products derived during CO metabolism in *Butyribacterium methylotrophicum*.

Product	ATP Yield	Electron Yield
Acetate	0	0
Butyrate	-1	-2
Ethanol	-1	-2
Butanol	-2	-4

^aMoles ATP and Electrons per Mole of Product.

observation arising from these calculations is that only acetate production requires no net input of energy or electrons; all other products from CO metabolism consume ATP and electrons. This observation is strong indirect evidence for the existence of an electron transport phosphorylation mechanism in *B. methylotrophicum*, since products other than acetate, including cell mass, are observed from CO metabolism. Preliminary evidence has been obtained to support the existence of such an ATP generating mechanism based on ETP (Zeikus et al., 1985), but conclusive experimental evidence has not yet been obtained. The required electrons for production of butyrate, alcohols, and cell mass from CO presumably arise from the oxidation of CO to CO₂, which would explain the increase in CO₂ yields observed experimentally (Grethlein et al., 1990) as CO metabolism is regulated away from acetate production and towards butyrate (or alcohol) production.

The growth experiments to determine the effect of external acid concentration on *B. methylotrophicum* during CO metabolism have provided a possible mechanism to regulate carbon and electron flow away from acetate production. A capacity for both acetate and butyrate uptake was observed as a function of increasing acid concentration during growth of the organism on CO gas. This observed acid uptake thus yielded a cosubstrate fermentation profile, with either CO and acetate or CO and butyrate serving as the carbon and energy sources. The uptake of acids was furthermore observed concomitant with CO consumption, and thus it is reasonable to assume that acetate and butyrate serve as precursors for acetyl-CoA and butyryl-CoA formation, but not as energy sources for oxidation of acetyl-CoA to CO₂, since this would reverse the carbon and electron flow observed *in situ* during CO metabolism (Kerby et al., 1983).

This study has further shown the metabolic versatility of *B. methylotrophicum* with the observed ability for acetate and butyrate cosubstrate fermentations with CO gas. These acid uptake mechanisms could have significant impact on the design of a butyric acid fermentation using CO gas, with a first stage fermentation producing acetic acid from CO, and a second stage fermentation producing butyric acid from CO and acetic acid. Such a

scheme could be more favorable than a direct CO to butyric acid fermentation, where complete termination of acetic acid formation has proven to be extremely difficult.

3.4. Effect of Sulfide on Growth and Product Formation

An attractive advantage of biological synthesis gas conversion is that intensive sulfur gas removal and synthesis gas upgrading may not be required. With sulfur-tolerant microorganisms such as *B. methylotrophicum*, the 0.5-2 volume % sulfur gases present in a typical coal-derived synthesis gas will potentially pass through the process as inert components. Because the CO (and H₂ in the MBI Process) will be removed from the CO gas stream, a reduced volume of gas having a higher H₂S concentration will exit the process. Sulfur removal costs will thus be reduced, because the mass transfer driving force will be greater, while the volume to be processed will be less. Furthermore, *B. methylotrophicum* does not require a strict CO/H₂ ratio, and thus gas shift operations would potentially be unnecessary.

Although anaerobic media requirements provide a high level of sulfate and sulfide-containing chemical species, the specific effects, if any, of H₂S gas on *B. methylotrophicum* during growth and product formation are unknown. Therefore the effects of H₂S gas was determined during batch growth on CO, with initial mole fractions of H₂S between 0.005 and 0.02--a range typical of actual compositions in coal-derived synthesis gas mixtures (Verma, 1978a; McCullough et al., 1984). In order to quantify the sulfur-tolerance of *B. methylotrophicum*, the growth and product-formation properties during CO metabolism were determined in the presence of sulfide. These results are necessary to evaluate the potential economic benefits of the synthesis gas bioconversion process.

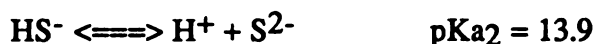
To determine the effects of sulfide in an experimental biological system, the equilibrium partitioning and dissociation chemistry of sulfide species must be addressed. The liquid-phase concentration of H₂S in equilibrium with a given H₂S partial pressure (pH₂S) can

be estimated accurately for pressures less than two atmospheres using Henry's Law (Carroll, 1990):

$$[\text{H}_2\text{S}] = (K_H)(p_{\text{H}_2\text{S}}).$$

Values for the Henry's law constant (K_H) published in the International Critical Tables and Perry's Chemical Engineer's Handbook were found to be incorrect by several orders of magnitude. However, correct values were estimated using a published correlation (Carroll, 1990) and were used for calculations made during these experiments.

In aqueous solution, H_2S acts as a diprotic acid, as shown below,



where the ratios of the various sulfide species may be calculated using the Henderson-Hasselbach equation:

$$\text{pH} = \text{pK}_{a1} + \log([\text{HS}^-]/[\text{H}_2\text{S}]) \quad \text{pH} = \text{pK}_{a2} + \log([\text{S}^{2-}]/[\text{HS}^-]).$$

Because *B. methylotrophicum* operates in a pH range of 5.5 to 7.2, the concentration of S^{2-} will be negligibly small. Based on these relationships, the following equation was developed to give C, the total equilibrium sulfide concentration (including all species) in the liquid phase following an initial loading of n moles of sulfide:

$$C = \frac{n[1 + 10(\text{pH} - \text{pK}_{a1})]}{V_G/K_HRT + V_L[1 + 10(\text{pH} - \text{pK}_{a1})]}$$

where V_G and V_L are the volumes of the gas and liquid phases, respectively. The absolute temperature is represented as T, and the gas constant as R. This equation is valid regardless of the form of sulfide added (e.g., H_2S or Na_2S). At the low pressures involved in these experiments, the number of moles of H_2S added can be estimated using the ideal gas law with the appropriate volume of gas added. The liquid-phase concentrations of individual species may also be calculated, as shown below:

$$[\text{H}_2\text{S}] = C/[1 + 10(\text{pH} - \text{pK}_{a1})]$$

$$\text{HS}^- = C - [\text{H}_2\text{S}]$$

$$\text{pH}_2\text{S} = [\text{H}_2\text{S}]/K_{\text{H}}$$

The equations used to calculate sulfide concentrations in the gas and liquid phases are based on the assumption of phase equilibrium. To determine whether this assumption was reasonable during the sulfur-tolerance studies, a batch experiment was conducted to estimate the time required for equilibrium to occur after the addition of H_2S to gas headspaces in bottles containing distilled water. This experiment was performed in pressure bottles, which were well mixed by shaking after addition of H_2S gas. As the H_2S partitions into the liquid phase and dissociates, the pH of the distilled water would be expected to decrease. Equilibrium was assumed to have occurred when the pH stopped decreasing. The results for this experiment are shown in Table 15, for duplicate bottles initially containing 2%, 5%, and 10% H_2S gas in the headspace (by volume). For all of the concentrations tested, the pH ceased decreasing after 15 minutes, with over 90% of the pH change occurring during the first 2 minutes. This is a rapid change relative to the 120-160 hr duration of the growth experiments with the sealed bottle systems. Therefore

Table 15. Experimental pH profiles showing dynamics of H_2S dissolution.

Time (min)	pH of Sample		
	2% H_2S	5% H_2S	10% H_2S
0	6.43	6.46	6.51
2	5.52	5.42	5.24
15	5.50	5.41	5.20
30	5.56	5.43	5.19
45	5.65	5.43	5.26
60	5.71	5.54	5.42
90	5.76	5.55	5.44
120	5.80	ND	5.44

ND denotes "not determined"

the assumption of phase equilibrium was deemed valid for the sulfur tolerance experiments.

The sulfur tolerance of *B. methylotrophicum* grown on CO gas was investigated from the standpoint of total liquid-phase sulfide concentration. This organism requires a media reducing agent to maintain anaerobic conditions, and in the phosphate-buffered media, Na₂S is typically used during batch culture (Lynd et al., 1982). The standard amount of sulfide initially added to the liquid is 0.083 g/L, which corresponds to an equilibrium liquid phase sulfide concentration of 1.7 mmol/L. This value is an amount equivalent to contacting a 102 mL 3.2% H₂S gas phase with a non-reduced liquid media volume of 50 mL, which are the standard experimental conditions. The resulting equilibrium H₂S gas phase concentration arising from the control addition would be 1.13%. Thus, this organism is inherently tolerant to sulfide species.

Using an initial liquid-phase sulfide concentration of 1.7 mmol/L as a control value, three distinct sulfide tolerance experiments were conducted: the first using the control amount of Na₂S plus addition of increasing amounts of H₂S gas, the second using increased amounts of Na₂S relative to the control, and the third using decreased amounts of Na₂S relative to the control. These experiments were all conducted at an initial pH of 7.0. The equilibrium liquid phase sulfide concentration at this initial pH can be considered to be a maximum, since during the course of the CO fermentation the pH decreases, and thus promotes formation of H₂S gas as determined by the dissociation chemistry. Figures 16 and 17 show the growth and acetate production time-course profiles for batch growth of *B. methylotrophicum* during the first experiment. The values of percent H₂S gas indicate initial equilibrium gas phase concentrations. The additional sulfide severely inhibited both cell growth and acetate production in the 3.2%, 5.2%, and 8.0% runs. Molar and specific yield values for acetate production during this experiment are shown in Figure 18. As the initial equilibrium sulfide concentrations increased, and the resulting cell

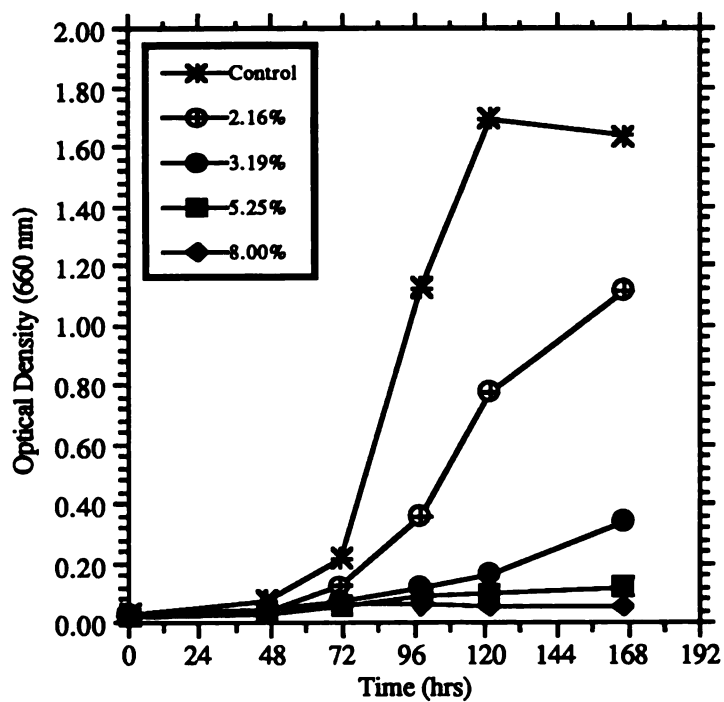


Figure 16. Effect of initial H_2S gas phase concentration during growth of *B. methylotrophicum* on CO gas.

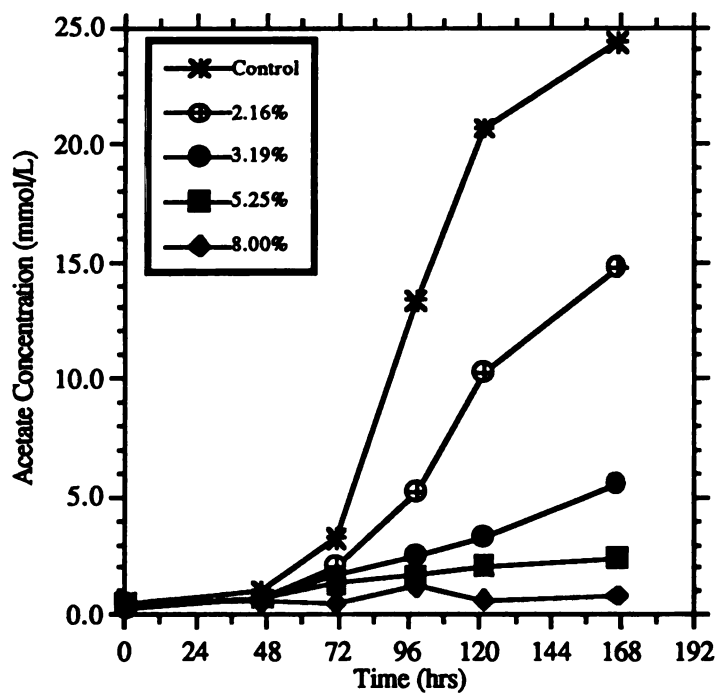


Figure 17. Effect of increasing H_2S concentration on acetate production during growth of *B. methylotrophicum*.

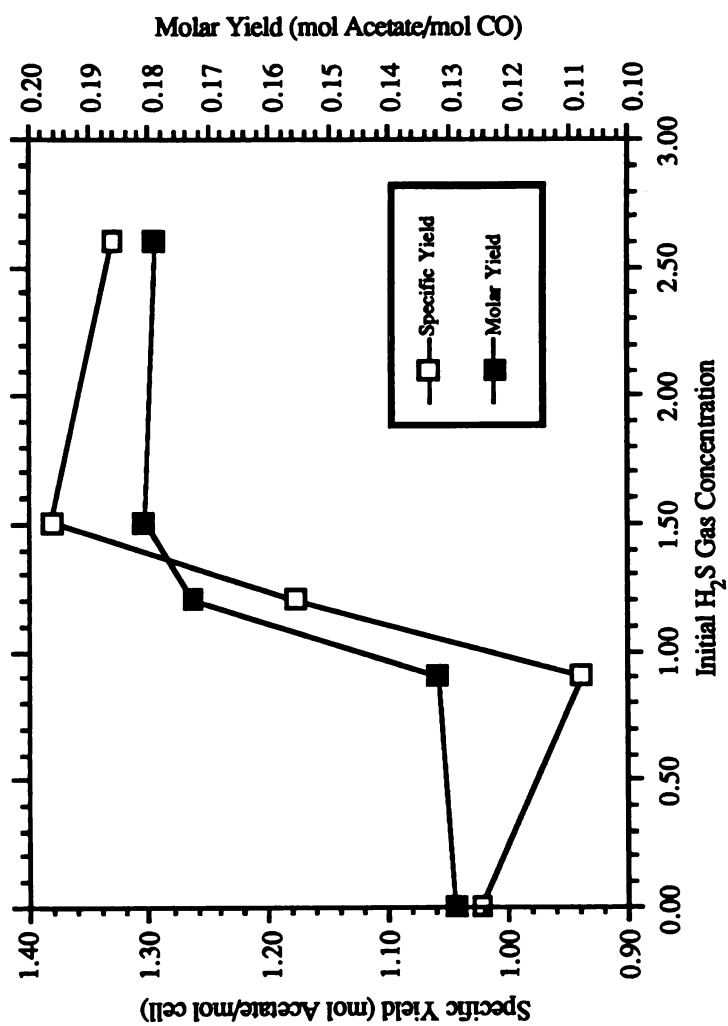


Figure 18. Acetate yields as a function of initial H_2S concentration during growth of *B. methylotrophicum* on CO gas.

growth rates decreased, the specific and molar yields for acetate increased by approximately 50%.

For the second experiments, the time-course profiles for cell density are shown in Figures 19 and 20. The initial liquid sulfide concentrations shown in these figures are pre-equilibrium values, calculated assuming no equilibrium partitioning. At concentrations below the control (0.083 g/L) value, shown in Figure 19, there was no significant effect on cell growth, except that the lowest concentration tested did show a slight increase in the growth rate. At concentrations above the control, shown in Figure 20, the growth rate and corresponding cell densities decreased with increasing sulfide concentration. The data for acetate, and minor butyrate, formation during these experiments paralleled the trends for cell density and cell growth and are therefore not shown. However, the specific and molar yields of acetate and butyrate were significantly influenced by the concentration of sulfide, and are shown in Figures 21 and 22. The two experiments are shown in separate figures because of the separate control runs for each experiment. As the sulfide concentration was increased, the acetate yields initially decreased, reached a minimum, and then increased. The butyrate yields exhibited the opposite trend.

A summary of the results which used Na₂S as the sulfide source is shown in Table 16, which relates the total initial, equilibrium, liquid-phase sulfide concentration to the relative cell growth and corresponding gas phase H₂S concentrations. Initial equilibrium gas phase concentrations approaching 1.4% did not significantly inhibit cell growth. Reduced rates of growth were observed between 1.4% and 3.3%, and concentrations above 3.3% were toxic to *B. methylotrophicum*.

The experimental results for sulfide tolerance obtained with both H₂S gas and Na₂S serving as the sulfur sources have determined a practical concentration limit for liquid phase sulfide species during cell growth and metabolism. The growth results for *B. methylotrophicum* were based upon the initial liquid concentration of sulfide species that is typically used as a reducing agent in the phosphate-buffered media (1.7 mmol/L). The

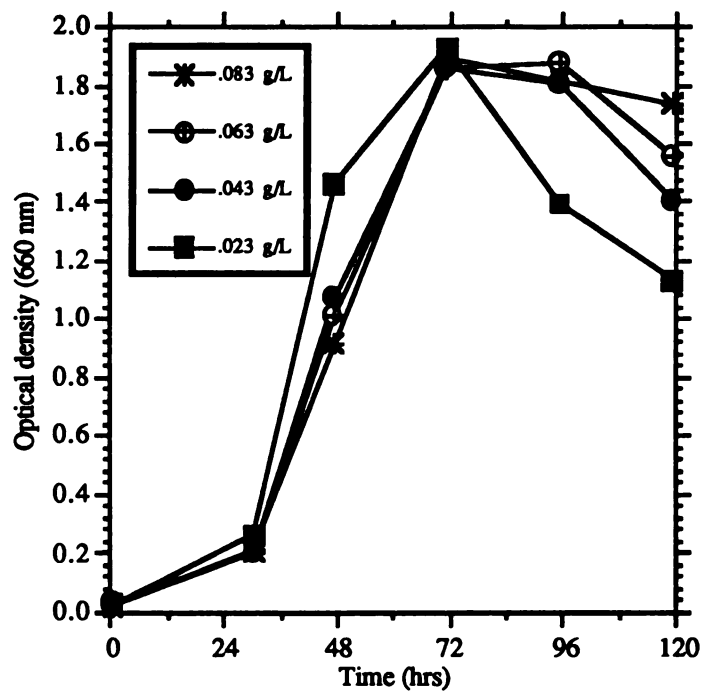


Figure 19. Effect of initial sulfide concentration during growth of *B. methylotrophicum* on CO gas.

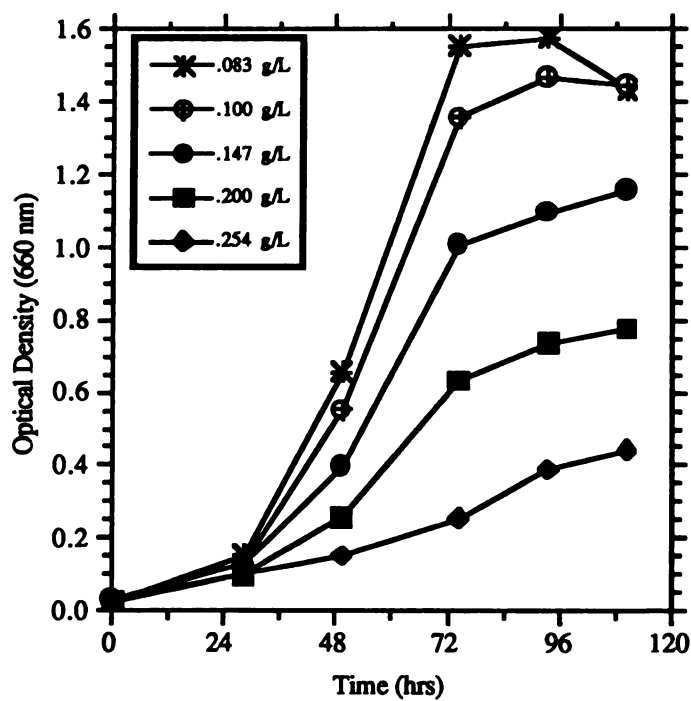


Figure 20. Effect of initial sulfide concentration during growth of *B. methylotrophicum* on CO gas.

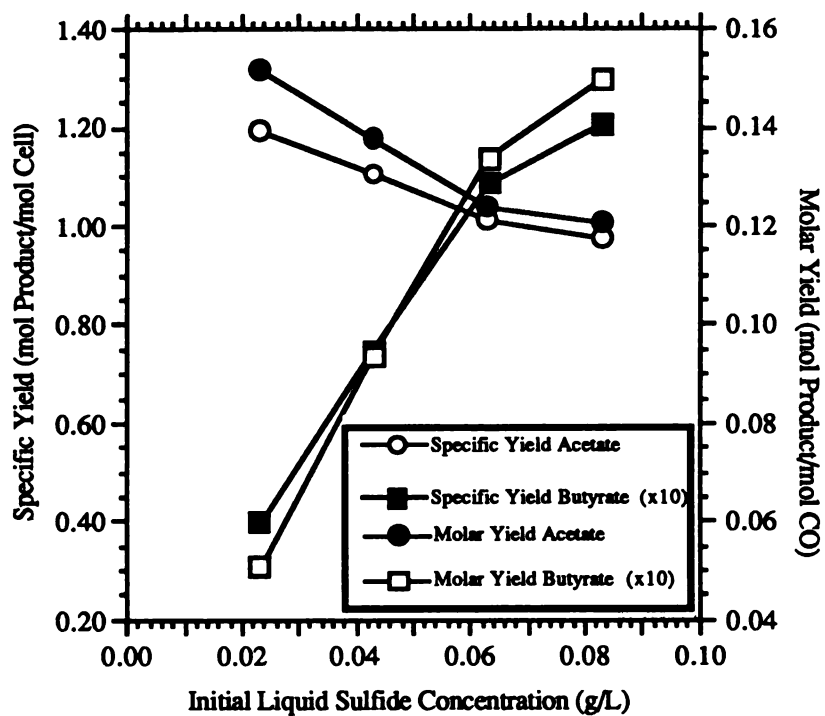


Figure 21. Specific and molar yields as a function of initial sulfide concentration during growth of *B. methylotrophicum* on CO gas.

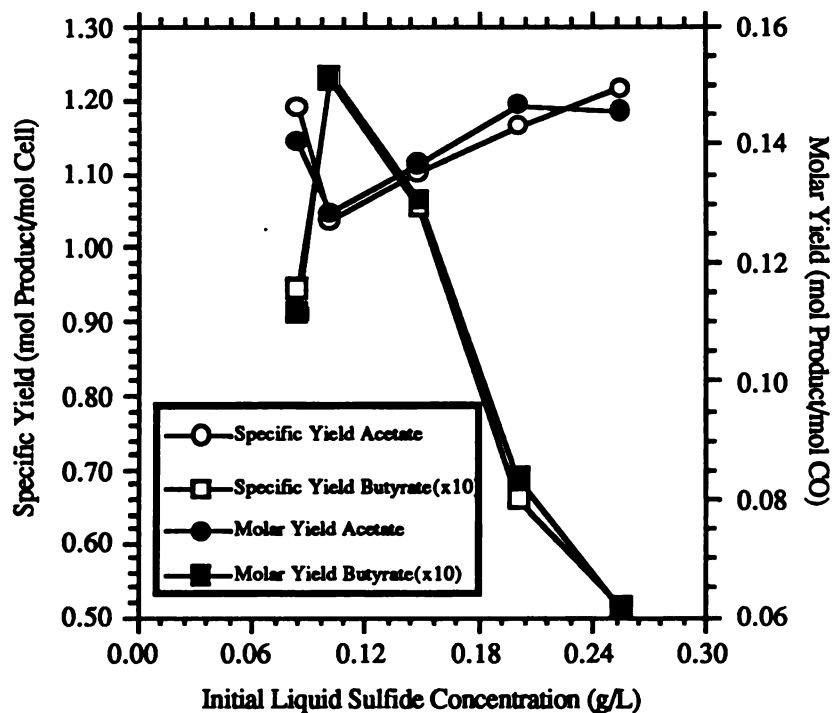


Figure 22. Specific and molar yields for product formation during growth of *B. methylotrophicum* on CO gas.

Table 16. Effect of liquid phase sulfide concentration on cell growth of *B. methylotrophicum* grown on CO gas at an initial pH of 7.0.

Total Sulfide Species in Liquid Phase (mmol/L)	Equilibrium Gas Phase H ₂ S Concentration (mol %)	% Maximum OD Obtained (% Control)
0.479	0.32%	~102%
0.890	0.59%	~100%
1.301	0.86%	~100%
1.711	1.13%	100%
2.053	1.36%	~93%
3.012	1.99%	~72%
4.107	2.71%	~48%
5.203	3.32%	~27%

experiment with excess addition of H₂S gas to the control media showed severe inhibition of cell growth in the presence of greater than 2% H₂S gas. The specific mechanism of this inhibition is not clear, but an effect on the molar and specific yields is apparent from the data presented in Figure 18, where high sulfide concentrations appear to favor acetate formation. This result is most likely a cellular response to the toxic effects of high sulfide concentrations, a response which may require more metabolic energy and thus would favor acetate production at the expense of cell mass production. Whatever the specific mechanism, it is evident that the overall effect of sulfide is dependent on the physiology of the bacteria; studies with *P. productus* and *R. rubrum* have shown almost an order of magnitude greater sulfide tolerance, although under somewhat different experimental conditions (Vega et al., 1990).

The data obtained using Na₂S as the sulfur source show that the initial, pre-equilibrium control concentration of 0.083 g/L total sulfide is on the border between tolerance and

inhibition, with lower concentrations having little or no effect on cell growth (Figure 19), and with higher concentrations leading to inhibition of cell growth (Figure 20). The specific and molar yields of acetate and butyrate, plotted in Figures 21 and 22, are affected by sulfide concentration in a complicated manner. At low sulfide concentrations, the acetate yields are higher, decrease to a minimum at an intermediate concentrations, and then increase again as the sulfide concentration is increased further. The butyrate specific and molar yields exhibit the opposite trend. Currently these trends cannot be adequately explained.

It has been previously shown that Na_2S addition to *C. acetobutylicum* cultures results in a metabolic shift resulting in enhanced butyrate production (Rao and Mutharasan, 1988). The addition of Na_2S to *Thermoanaerobacter ethanolicus* cultures has also been shown to inhibit cell growth at high concentrations (Rao et al., 1987). These findings are consistent with our findings for *B. methylotrophicum*, where the liquid phase sulfide concentrations above 3.0 mmol/L significantly reduce cell growth and product formation. However, the effects of sulfide on stationary phase CO metabolism could potentially be much less severe, as was observed for high alcohol concentrations which inhibited growth during the exponential phase but allowed CO metabolism to proceed during the stationary phase. Regardless of this speculation, since the equilibrium partial pressures of H_2S gas above these liquid concentrations are in the range of 1-2%, with proper process design the influence of H_2S on the growth and metabolism of *B. methylotrophicum* should not create any problems during coal-derived synthesis gas conversion, and should substantially reduce the requirements for stringent sulfur gas removal prior to the fermentation, relative to the typical chemical process requirements.

3.5. Media Development Studies

To apply cell recycling technology to a continuous fermenter for increasing cell densities and volumetric productivities during CO fermentation, as detailed in Chapter 4, a

modified phosphate-buffered medium was needed to ensure that during high cell density culture, CO gas-liquid mass transfer is still the rate limiting factor. Without such modifications, nutrient limitations could drastically alter the observed kinetics and make comparison with previously obtained chemostat data extremely difficult. However, the potential enhancement must not interfere with the premise that CO is the sole carbon and energy source during *B. methylotrophicum* metabolism. A media development effort was therefore conducted in order to increase the amount of nutrients and minerals in the fermentation media, without adding alternate sources of carbon or energy.

The original phosphate-buffered basal medium used for culturing *B. methylotrophicum* was detailed in Chapter 2. Carbon, in the form of CO, was chosen as the limiting nutrient. For *B. methylotrophicum*, the H₂ is obtained from H₂O, and phosphorous will not be limiting in a phosphate-buffered environment. Approximate cellular elemental compositions of nitrogen (14% w/w) and sulfur (1% w/w) were obtained from available *E. coli* data (Bailey and Ollis, 1986). Total required concentrations of these elements in a 1 OD broth solution can then be calculated by multiplying by the dry weight concentration of 0.334g/L•OD (Lynd et al., 1982), yielding 0.00334 g/L sulfur and 0.04816 g/L nitrogen required. The original phosphate-buffered medium contains .0156 g/L and .252 g/L of these elements, respectively. Thus, assuming a 10-fold increase obtained in cell density, the required amounts of these elements would be 0.0334 g/L sulfur and 0.4816 g/L nitrogen. Therefore, as a minimum, the concentrations of these two elements should be doubled in the enhanced medium. From the available chemicals, the concentration of sulfur was approximately tripled using ammonium sulfate, and the concentration of nitrogen was approximately doubled using ammonium sulfate and ammonium phosphate, with the ammonium phosphate added to the phosphate buffer as a partial substitute for dibasic potassium phosphate. Arbitrarily, the concentration of vitamins was increased 10-fold, and the concentration of trace minerals was increased 5-fold. A 2-fold increase in the yeast extract concentration was also included, as determined below.

Experiments to determine the effect of these modifications on the growth of *B. methylotrophicum* were conducted in batch bottles with a control of the original medium, experimentals for each of the separate additions, and with all of the additions together. The time-course growth curves are shown in Figure 23 for the various medium supplements, and in Figure 24 for the tests with increasing concentrations of yeast extract. The cell growth rates in the presence of all the supplements shown in Figure 23 are similar, and only the 2-fold nitrogen test indicated a significant increase in the final cell density relative to the control. The lag phase on some of the additions are slightly increased. It was thus determined that these additions do not significantly effect the typical growth response of *B. methylotrophicum* when grown on CO gas. The effect of increasing yeast extract, however, was significant, as shown in Figure 24, particularly for the 3-fold and 5-fold increases, which exhibited reduced lag phases, slightly increased growth rates, and higher cell densities. The 2-fold increase exhibited a similar growth rate and final OD relative to the control, but with a reduced lag time. It was thus decided to incorporate a 2-fold increase in the yeast extract concentration, from 0.1% (w/v) to 0.2% (w/v). This increase, particularly in view of anticipated 10-fold increases in cell density during cell recycle fermentations, will result in a net decrease in the mass ratio of yeast extract to cells, and thus cannot be argued to support cell growth alone, an argument which was refuted previously for cells grown on CO gas and 0.05% yeast extract (Lynd et al., 1982).

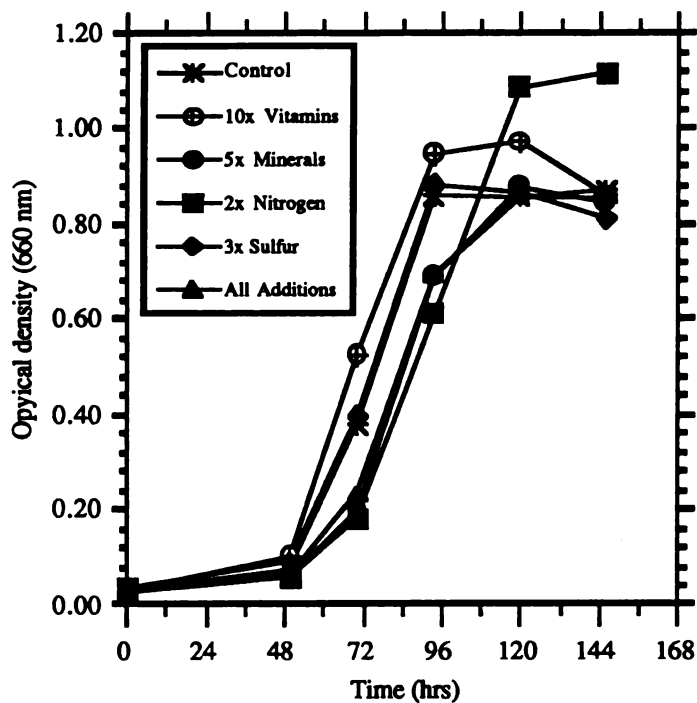


Figure 23. Effect of media supplements on the growth of *B. methylotrophicum* on CO gas.

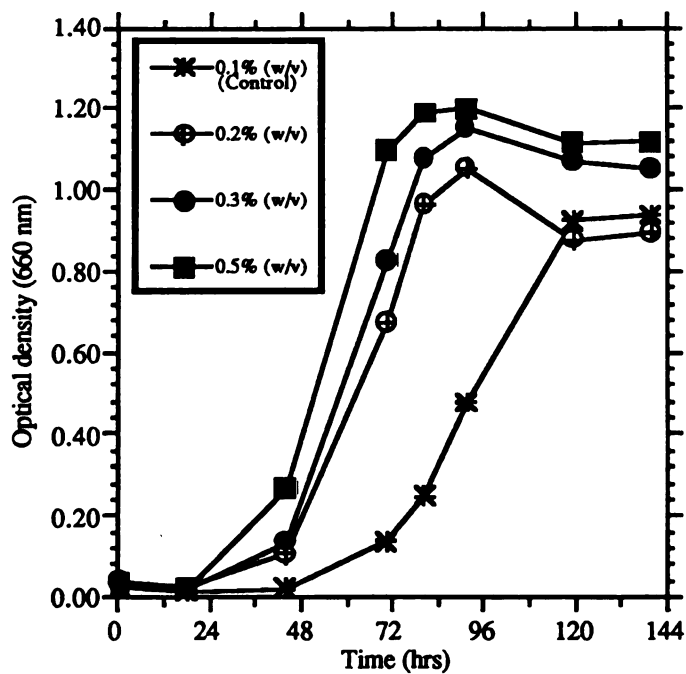


Figure 24. Effect of increasing yeast extract concentration on the growth of *B. methylotrophicum* on CO gas.

CHAPTER 4

CELL-RECYCLE FERMENTATION STUDIES

4.1. Objectives

Biological processing of synthesis gas requires the application of microorganisms capable of both efficient metabolism and sustained growth on CO, with the objective of producing organic acids or alcohols. Research over the last few years in several laboratories has identified the few critical problem areas which must be addressed and overcome for the ultimate success of a bioconversion concept. These areas include low rates for gas-liquid mass transfer of both CO and H₂, low specific rates of growth, and also a potentially wide range of multiple products resulting from CO metabolism. Another disadvantage with biological systems is the difficulty associated with maintenance of microbial populations in desired metabolic states, particularly if these states are not optimal for cell growth and viability. These issues all affect fermenter productivity, which has been consistently shown to be much too low for an economically viable process. The major objective of the cell recycling studies contained in this chapter was to address these concerns.

As discussed below, the previous continuous culture results suggested that to maximize butyrate production, long-term operation of the acidogenic CO fermentation at low pH values is required. These key issues were addressed by incorporation of both gas and cell recycle systems into the chemostat CO fermentation system. Such a system, when used during continuous CO fermentation, potentially allows operation at low pH, attains much higher cell densities than with conventional chemostat systems, and thus can achieve large increases in fermenter productivity.

Extended batch fermentations with *B. methylophilicum* determined that fermentation pH has a significant influence on the relative proportion of acetate and butyrate produced

from CO or CH₃OH and CO (Worden et al., 1989; Grethlein, 1989). Continuous, steady-state CO fermentations at pH values between 5.5 and 6.8 also showed this trend, with butanol and ethanol production occurring at lower pH values (Grethlein, 1990). These continuous results, showing butanol and ethanol formation directly from CO, identified a potential mechanism for direct bioconversion of synthesis gas to alcohols. Carbon and electron balance calculations, based on the broth product composition as a function of fermentation pH during steady-state operation, yielded several significant trends for these experiments. As shown in Tables 17 and 18, there was a trend towards more reduced product formation, specifically butyrate and butanol, as the fermentation pH was reduced. Also evident was a drop in the cell growth as the pH was reduced to a value of 6.0 with further reduction observed at a pH of 5.5 (washout was observed at a pH of 5.0). These trends define the major experimental obstacles for fermentation development of this biological system: low fermentation pH induces butyrate and alcohol formation but inhibits cell growth and thus reduces fermenter productivity.

The low specific growth rate of this organism, as indicated by a 12 hour doubling time, required a very low dilution rate for steady-state operation during previous continuous culture. Thus, although this operation was achieved, volumetric productivities for acids and alcohols were very low, ranging approximately between 0.001 g/L hr for the alcohols and 0.015 g/L hr for the acids. Production of acids and alcohols was achieved at concentrations of approximately 0.05% to 0.1% (w/v) for the acids and 0.005% to 0.01% (w/v) for the alcohols (Grethlein et al., 1990), concentration levels which are of scientific interest only. Higher dilution rates and cell densities are therefore required in order to increase product concentrations and volumetric productivities.

This dissertation research was focused on fermentation development in order to achieve a stable, long-term, and highly productive CO fermentation with *B. methylotrophicum*. As described above, the major method used to achieve this objective was the application of cell recycle membrane technology to a conventional continuous fermentation system. This

Table 17. Continuous, steady-state CO fermentation stoichiometries as a function of pH for *B. methylotrophicum*^a.

pH	Fermentation Stoichiometry
6.8	$4\text{CO} \rightarrow 2.09\text{CO}_2 + .63\text{CH}_3\text{COOH} + .043\text{C}_3\text{H}_7\text{COOH} + .027\text{C}_2\text{H}_5\text{OH} + .43\text{Cells}$
6.5	$4\text{CO} \rightarrow 2.13\text{CO}_2 + .56\text{CH}_3\text{COOH} + .082\text{C}_3\text{H}_7\text{COOH} + .026\text{C}_2\text{H}_5\text{OH} + .37\text{Cells}$
6.0	$4\text{CO} \rightarrow 2.27\text{CO}_2 + .30\text{CH}_3\text{COOH} + .161\text{C}_3\text{H}_7\text{COOH} + .032\text{C}_2\text{H}_5\text{OH}$ $+ .029\text{C}_4\text{H}_9\text{OH} + .31\text{Cells}$
5.5	$4\text{CO} \rightarrow 2.18\text{CO}_2 + .40\text{CH}_3\text{COOH} + .154\text{C}_3\text{H}_7\text{COOH} + .40\text{Cells}$

^aFrom Grethlein et al., 1990.

Table 18. Continuous, steady-state CO fermentation product concentrations as a function of pH for *B. methylotrophicum*^a.

pH	Product Concentrations (g/L)				Cells
	CH ₃ COOH	C ₃ H ₇ COOH	C ₂ H ₅ OH	C ₄ H ₉ OH	
6.8	0.860	0.086	0.028	ND	0.248
6.5	1.055	0.227	0.037	Trace	0.284
6.0	0.689	0.536	0.056	0.081	0.286
5.5	0.475	0.266	Trace	Trace	0.196

^aFrom Grethlein et al., 1990. Trace indicates amounts < 0.5 mmol/L, ND = Not Detected.

technology allows high cell densities by restricting cell washout during continuous operation, while allowing soluble fermentation products to leave the system. In general, the application of cell recycling allowed operation at a wider range of physical and environmental conditions without any washout restrictions, compared to conventional chemostat culture.

4.2. System Set-up and Design

To increase the overall productivity of the CO fermentation at low pH values, and to bias the cell population towards a stationary (resting) state metabolism, a cell recycling system was integrated with a continuous fermentor, as shown in Figure 25. This system was designed for higher CO gas mass transfer by using a pump to continuously remove the headspace gas and sparge it into the fermentor broth. CO gas was provided to the fermentation continuously. An enhanced phosphate buffered media, modified by increasing the vitamin, mineral, and nutrient contents as described in Chapter 3, was used to support higher cell densities while still maintaining CO as the limiting nutrient, as in all previous studies. Experiments were conducted at a wide range of pH values, in order to achieve high cell density, steady-state CO fermentations. Steady-state was defined as liquid product concentration deviations of not more than 15% from the mean value over a period of 2-3 residence times, or approximately 6-9 days.

In order to adequately supply the fermentation with enough CO to support the expected increases in cell density, high mass transfer rates for CO were obtained by using a high impeller speed and with a CO gas recycle pump. These developments allowed high gas flows into the liquid and provided increased dispersion of the dissolved gas. Furthermore, macroporous frits were used to minimize bubble size for the sparged CO gas.

The major investigation using the cell recycle fermentation system described above was the effect of fermentation pH. This variable had already been shown to be highly influential on production rates and product specificity during CO metabolism. Cell

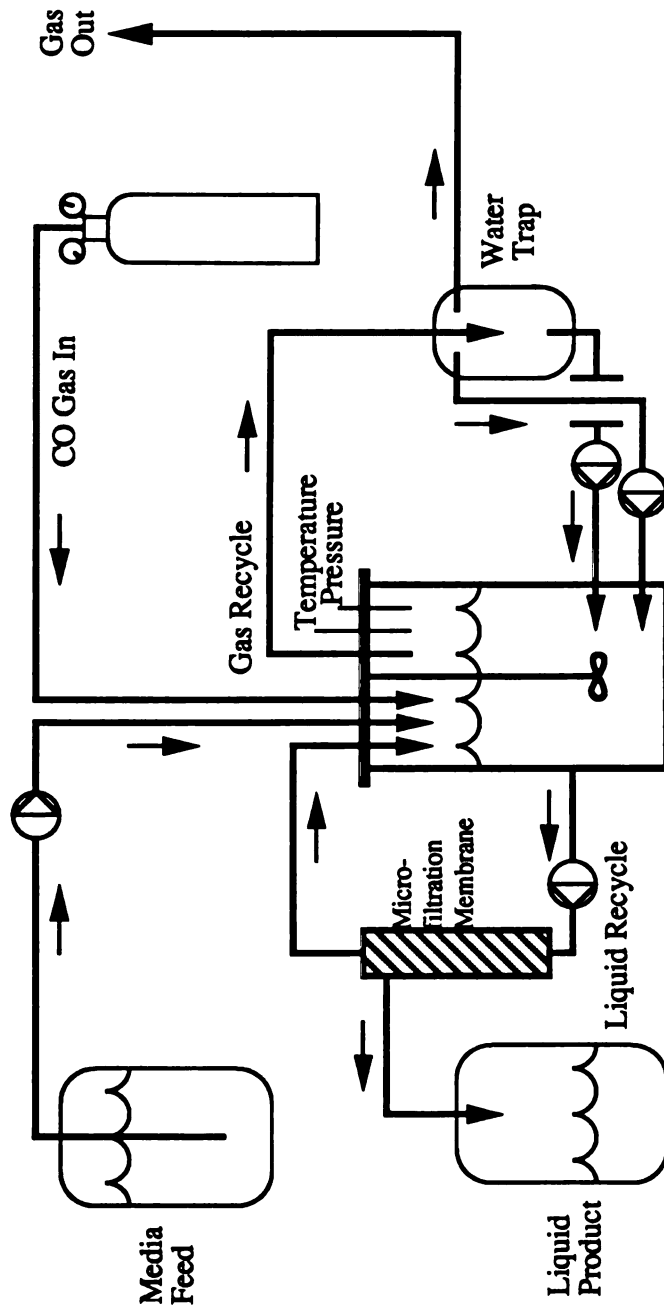


Figure 25. Schematic diagram of continuous, cell recycle CO fermentation system.

recycling allowed investigation at pH values lower than those obtainable during conventional continuous culture, where reductions in the specific growth rate of *B. methylotrophicum* at pH values below 6.0 were previously observed (Grethlein et al., 1990). Fermentations were conducted at a range of pH values from 5.0 to 6.8 and the fermentation profile measured, including product formation and cell density. Emphasis during the cell recycle experiments was on achieving steady-state response at each pH value tested. The dilution rate for these studies was 0.015 hr^{-1} , which is the same as for the previous chemostat experiments, in order to allow direct comparison. All of the fermentations were operated at a conversion rate of approximately 20%, with approximately 5-7% deviation from this value observed. Product formation data allowed calculation of overall stoichiometries, yield coefficients, volumetric productivities, and other kinetic parameters.

A major limitation with the experimental system design was with the reliance on the carbon and electron balances for calculation of cell production and CO consumption. The use of these balances assumes 100% conservation of carbon and electrons calculated from the fermentation data. Thus, since all of the experimental data is ultimately normalized to the CO consumption, any error in the system or in the analytical methods will ultimately be reflected in the calculated values for cell mass production. These limitations were somewhat voluntarily accepted; the methods for measuring direct CO consumption (gas phase tie-component analysis) and for measuring direct cell production (viability plate assays) are very labor intensive and were deemed impractical during this study.

Another important point concerning this experimental system is the nature of its development and operation over long-term time periods. With a 12 hour doubling time, each fermentation conducted required approximately 3 weeks just to raise the cell density high enough before adjusting the controlled variable, whether it was fermentation pH or the addition of a cosubstrate. Achieving steady-state was then a matter of precise monitoring and control (and also luck) since small fluctuations in operating conditions

over days of operation could cause significant perturbations in the system. The end result was that for each fermentation, an average of 6-8 weeks was required either to achieve steady-state, or to obtain a complete picture of the fermentation response. Since only 1 and sometimes 2 experiments were conducted at a time, there was some amount of operating expertise gained over the course of this study, which is generally reflected in the cell densities for the fermentations (the later experiments exhibited higher cell densities and generally greater stability). These limitations and experimental characteristics must therefore be taken into account when comparing the results from the various cell recycle fermentations. In general, the analysis of experimental results in this chapter reflects this point, and relies more heavily on fermentation stoichiometries than on direct comparison of product concentrations.

One aspect of typical cell recycle systems which was not a factor during these studies was the problem of membrane fouling or life. The mineral salts nature of the phosphate medium and the lack of extracellular slime or polymer production by *B. methylotrophicum* contributed to "clean" fermentation broths which did not have a great affinity for the cellulosic membranes. Even in systems which were operated for up to 6-8 weeks, backflushing and membrane cleaning operations were not required. Of course, the lack of fouling was largely due to a very low flux through the membrane, since the liquid residence times of the CO fermentations were approximately 67 hr.

4.3. Results for Continuous Cell Recycle CO Fermentations

The cell-recycle system was operated between fermentation pH values of 5.1 and 7.2. Three distinct metabolic regimes were observed, as presented in Table 19. At pH values of 7.2, 6.8, 6.4, and 6.0, steady-state was achieved. At pH values of 5.75 and 5.5, oscillations in the concentrations of several fermentation products were observed. A viable culture could not be maintained during operation at pH values below 5.5. The results for each of these regimes are discussed in detail below.

Table 19. Overall culture response as a function of fermentation pH during continuous cell recycle fermentation.

<u>Fermentation pH</u>	<u>Culture Response</u>
7.2	Steady-State
6.8	Steady-State
6.4	Steady-State
6.0	Steady-State
5.75	Oscillations
5.5	Oscillations
5.35	Death
5.1	Death

4.3.1 Steady-State Results

The steady-state CO fermentations exhibited trends in product composition similar to previous experiments without cell recycling (Grethlein et al., 1990). Table 20 shows the steady-state fermentation stoichiometries for these experiments. The coefficients were determined using carbon and available electron balances. A consistent trend of decreasing acetate production and increasing butyrate and alcohol production is evident as the pH decreases from 7.2 towards 6.0. At a pH of 6.0, a shift from acid to alcohol production is indicated, since the proportional amounts of both acetate and butyrate decrease while the relative alcohol production increases. By dividing the coefficients for the products by the coefficient for CO in the fermentation stoichiometries shown in Table 20, the molar yield coefficients can be obtained. These are shown in Table 21. The relative production for each compound can be seen as a function of decreasing pH, with decreasing acetate and cell yields, increasing butyrate yields, and at a pH of 6.0, and a 40-50% increase in the alcohol yields, presumably at the expense of the corresponding acids. These trends are further exemplified by the partitioning of carbon and energy (electrons) available in the CO

Table 20. Steady-state fermentation stoichiometries as a function of pH for cell recycle fermentation of CO gas.

pH	Fermentation Stoichiometry
7.2	$4\text{CO} \rightarrow 2.21\text{CO}_2 + .410\text{CH}_3\text{COOH} + .105\text{C}_3\text{H}_7\text{COOH} + .019\text{C}_2\text{H}_5\text{OH} + .032\text{C}_4\text{H}_9\text{OH} + .387\text{CELLS}$
6.8	$4\text{CO} \rightarrow 2.25\text{CO}_2 + .334\text{CH}_3\text{COOH} + .124\text{C}_3\text{H}_7\text{COOH} + .025\text{C}_2\text{H}_5\text{OH} + .040\text{C}_4\text{H}_9\text{OH} + .377\text{CELLS}$
6.4	$4\text{CO} \rightarrow 2.26\text{CO}_2 + .316\text{CH}_3\text{COOH} + .152\text{C}_3\text{H}_7\text{COOH} + .018\text{C}_2\text{H}_5\text{OH} + .032\text{C}_4\text{H}_9\text{OH} + .279\text{CELLS}$
6.0	$4\text{CO} \rightarrow 2.32\text{CO}_2 + .260\text{CH}_3\text{COOH} + .142\text{C}_3\text{H}_7\text{COOH} + .050\text{C}_2\text{H}_5\text{OH} + .055\text{C}_4\text{H}_9\text{OH} + .279\text{CELLS}$

Table 21. Continuous, steady-state CO fermentation molar yield coefficients as a function of pH for *B. methylotrophicum*.

pH	Molar Yield Coefficients					
	CO ₂	CH ₃ COOH	C ₃ H ₇ COOH	C ₂ H ₅ OH	C ₄ H ₉ OH	Cells
7.2	0.552	0.102	0.026	0.005	0.008	0.097
6.8	0.562	0.084	0.031	0.006	0.010	0.094
6.4	0.565	0.079	0.038	0.005	0.008	0.070
6.0	0.580	0.065	0.036	0.012	0.014	0.070

substrate towards all the fermentation products. These proportions, shown as percent of total from CO, are given in Table 22 and Table 23 for the carbon and electron partitioning, respectively. The fractions of carbon and electrons going from CO to alcohols approximately double between a pH of 6.4 and 6.0. Steady-state production of 4-carbon compounds, i.e., butyrate and butanol, accounts for over 50% of the total electrons from CO at a fermentation pH of 6.0. Between a pH of 7.2 and 6.0, the partitioning of carbon and electrons to acetate decreases by approximately 35%. The effects of fermentation pH on the ratios of 4-carbon products to acetate for this steady-state pH regime are shown in Figure 26. Even at a pH of 6.0, acetate is the predominant product, on a molar basis, over all 4-carbon products. Thus, in continuous culture (Grethlein et al., 1990), or in continuous culture with cell recycling, operation at a pH of 6.0 does not yield butyrate as the major product compared to acetate, as was observed in batch culture (Worden et al., 1990).

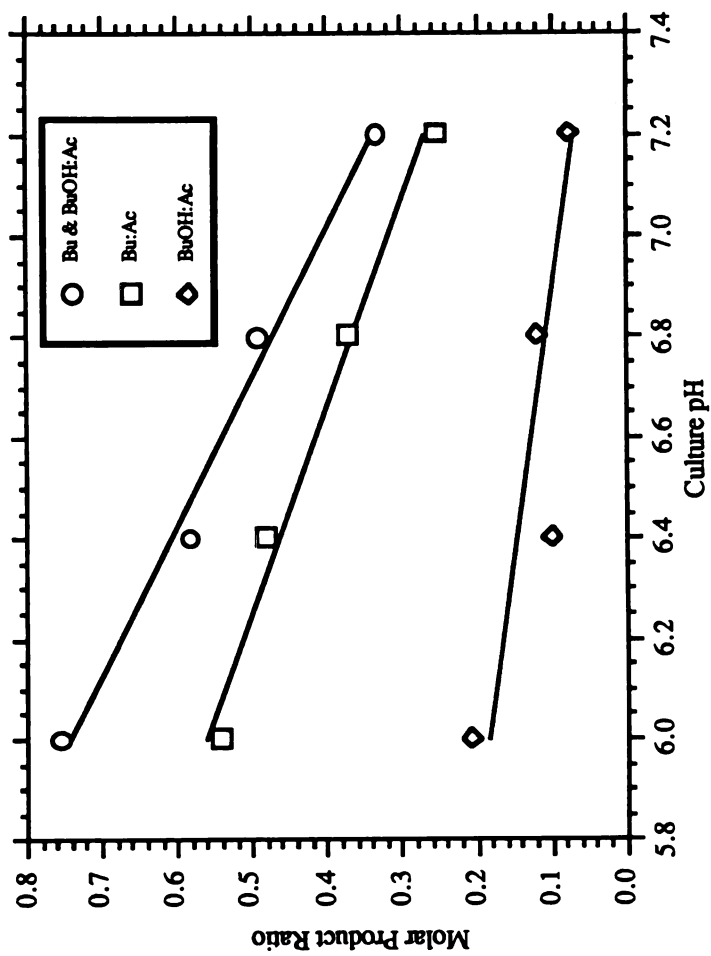
As stated in the previous section, relative calculations such as the fermentation stoichiometries and carbon and electron partitioning values of the steady-state fermentation results are a better means of comparison because of the differences in operating cell densities, fermenter volumes, and also experimental improvements during the course of the study. To emphasize these differences, the actual fermentation parameters and steady-state product concentrations are shown in Table 24. An almost 3-fold variation between the maximum and minimum steady-state operating cell density was observed, and the resulting CO consumption rates also varied over this range. Regardless of pH, maximum product concentrations of 8.7 g/L acetate, 4.6 g/L butyrate, 0.46 g/L ethanol, and 1.2 g/L butanol were observed during steady-state operation. The corresponding increases in fermenter productivities, compared to maximum chemostat product concentrations obtained, are 830% for acetate, 850% for butyrate, 820% for ethanol, 1481% for butanol, and 2440% for cell mass, assuming 100% viability. Thus, the application of cell recycling to the continuous fermentation of CO gas by *B. methylotrophicum* resulted in a 8-9 fold

Table 22. Continuous, steady-state CO fermentation carbon partitioning as a function of pH for *B. methylotrophicum*.

pH	CO ₂	CH ₃ COOH	Carbon Partitioning (%Carbon)			Cells
			C ₃ H ₇ COOH	C ₂ H ₅ OH	C ₄ H ₉ OH	
7.2	55.2	20.5	10.5	1.0	3.2	9.7
6.8	56.2	16.7	12.4	1.2	4.0	9.4
6.4	56.5	15.8	15.2	0.9	3.2	7.0
6.0	58.0	13.0	14.2	2.5	5.5	7.0

Table 23. Continuous, steady-state CO fermentation electron partitioning as a function of pH for *B. methylotrophicum*.

pH	CH ₃ COOH	Electron Partitioning (%Electrons)			Cells
		C ₃ H ₇ COOH	C ₂ H ₅ OH	C ₄ H ₉ OH	
7.2	41.0	26.2	2.8	9.6	20.4
6.8	33.4	31.0	3.8	12.0	19.8
6.4	31.6	38.0	2.7	9.6	14.7
6.0	26.0	35.5	7.5	16.5	14.7



* Legend symbols Bu, BuOH, and Ac stand for Butyrate, Butanol, and Acetate, respectively.

Figure 26. Molar product ratios as a function of culture pH during continuous cell recycle CO fermentation.

Table 24. Continuous, steady-state CO fermentation parameters, product concentrations, and CO consumption rates as a function of pH for *B. methylotrophicum*.

pH	Culture Volume (L)	OD	Average Product Concentrations (g/L)				CO Uptake (mol/hr)
			CH ₃ COOH	C ₃ H ₇ COOH	C ₂ H ₅ OH	C ₄ H ₉ OH	
7.2	1.4	10.3	8.69	3.27	0.315	0.829	0.0218
6.8	1.4	20.6	8.06	4.40	0.459	1.200	0.0360
6.4	1.2	16.3	6.52	4.62	0.282	0.811	0.0248
6.0	1.2	7.0	2.71	2.15	0.397	0.698	0.0124

Table 25. Continuous, steady-state CO fermentation CO consumption rates as a function of fermenter volume and culture OD for *B. methylotrophicum*.

pH	Culture Volume (L)	OD	CO Uptake (mol/hr)	CO Uptake (mol/hr•OD)	CO Uptake (mol/hr•L)	CO Uptake (mol/hr•L•OD)
7.2	1.4	10.3	0.0218	0.00211	0.01556	0.00151
6.8	1.4	20.6	0.0360	0.00175	0.02573	0.00125
6.4	1.2	16.3	0.0248	0.00152	0.02067	0.00127
6.0	1.2	7.0	0.0124	0.00177	0.01031	0.00147

increase in acid production and an 8-14 fold increase in alcohol production.

To compare the CO uptake rates of the four steady-state experiments, the rates can be normalized to both fermenter volume and cell density, as shown in Table 25. The calculated CO consumption rates for each experiment are shown in both Table 24 and Table 25. As shown, there is a 2.9 fold difference between the minimum and maximum CO consumption rates. The effect of fermenter volume can be normalized by calculating the volumetric CO consumption rates, shown in Table 25. Normalizing the CO uptake rates by volume, as shown in Table 25, reduces the difference between the minimum and maximum to a factor of 2.5. Although cell viability was not measured, a specific CO consumption rate can be calculated on a basis of overall cell density, and this normalization results in a 1.4 fold difference between the minimum and maximum uptake rates. A normalization which takes both volume and cell density into account, with the units for CO consumption of $\text{mol/hr}\cdot\text{L}\cdot\text{OD}$, is also shown in Table 25, and this calculated uptake rate results in only a 1.2 fold difference over the range of observed values. These units are equivalent to the specific uptake rate ($\text{mol/hr}\cdot\text{gram cell}$). However, since the viability of the cells was not measured, the units of $\text{mol/hr}\cdot\text{L}\cdot\text{OD}$ will be used henceforth. Nevertheless, if both fermenter volume and cell density are accounted for, the overall CO consumption rate during the steady-state fermentations was essentially constant, and thus the effect of pH on the CO consumption rate between the values of 6.0 and 7.2 can be assumed to be negligible.

It is important to verify the nature of these steady-state systems with respect to the assumption of CO mass transfer as the rate-limiting phenomena. The highest value obtained for the volumetric CO gas consumption was $0.02573 \text{ mol/hr}\cdot\text{L}$, or for the specific CO gas consumption rate, $0.00439 \text{ mol/hr}\cdot g_{\text{cell}}$, calculated using a value of $0.344 g_{\text{cell}}/\text{L}\cdot\text{OD}$, calculated from a dry-weight calibration curve (Lynd et al., 1982; Grethlein, unpub. res.). Calculations from previous batch data (Lynd et al., 1982) have yielded CO consumption rates as high as $0.02 \text{ mol/hr}\cdot g_{\text{cell}}$. The maximum observed specific CO

consumption rate was only 22% of this value, a strong indication that CO mass transfer was limiting the system during the steady-state cell recycle fermentations.

The mechanism for the predictable metabolic shift towards butyrate production and away from acetate production as the fermentation pH is lowered has not been determined experimentally in *B. methylotrophicum*. The least realistic hypothesis for the pH effect can be likened to a deacidification mechanism, where the cell responds to an acidic environment by producing those products which will acidify the environment less. Such products are alcohols or butyrate, which on a carbon-mole basis has only half of the acidification value of acetate. Yet such a simplistic view of an enormously complex regulatory process is somewhat misleading, particularly for *B. methylotrophicum*, where the energetics of CO metabolism are intimately linked to the proton-motive force and the maintenance of a pH gradient across the cell membrane. Many of the current ideas concerning the effect of pH on metabolic regulation, product formation, and cell growth arise from studies with heterotrophic, acidogenic bacteria which derive a large proportion of their metabolic energy from substrate-level phosphorylation. Organisms such as *C. acetobutylicum* and *C. thermoaceticum* are noteworthy examples. In the case of *B. methylotrophicum*, the production of acetic acid from CO has two major consequences, one which centers on the effect of producing acetic acid and ultimately lowering the pH of the environment, and one which centers on the necessity of acid production for maintenance of cellular energetics and growth. The former is the topic of discussion in this chapter, while the latter is discussed primarily in Chapter 5, where the metabolic model attempts to account for the energetics of the continuous cell recycle fermentations.

The intracellular alkalinity of *B. methylotrophicum* is required for a pH gradient across the cytoplasmic membrane to exist and for various transport and membrane linked energetic functions to operate. Mechanisms such as electron-transport, ATP-linked proton pumps, and product excretion all participate in the maintenance of the pH gradient, and can encompass a large proportion of the cells metabolic energy expenditure (Kashket, 1985).

The balance of this gradient is paramount to the cell viability, and disruption of the internal pH frequently results in cell death. For *B. methylotrophicum*, maintenance of the internal pH requires that acidic fermentation products such as acetic and butyric acid be excreted from the cell, along with their requisite protons.

The passive diffusion of most short chain organic acids in chemotrophic, anaerobic bacteria, has been discussed (Thauer et al., 1977), and the accepted mechanism is that the un-ionized, or protonated form of the acid is the species which diffuses across the membrane. The excretion of fermentation products is thus a major mechanism in controlling intracellular alkalinity. Assuming an initial extracellular environment with a pH of 7.0, and *B. methylotrophicum* with a pH of 6.0 for an intracellular environment, the production of acetate during growth on CO would result in diffusion of acetic acid across the membrane and into the extracellular environment, resulting in a pH decrease over time. Since the pK_a of acetic acid is 4.76 (butyric acid is 4.82), the proportion or ratio of unionized to ionized species in an aqueous media can be calculated by the equation

$$\text{ratio} = 10^{(pK_a - pH)}$$

where at a pH of 7.0, the ratio is 0.0058, at a pH of 6.0 the ratio is 0.058, at a pH of 5.5 the ratio is 0.182, at a pH of 5.0 the ratio is 0.575, and of course the ratio is 1 at a pH of 4.76. As calculated, a higher proportion of undissociated species accumulates for acetic acid as the pH nears 5.0, and this proportion can freely diffuse back into the cell, thereby disrupting the pH gradient.

The exact pH at which the system allows diffusion back into the cell is a function of the cell physiology and the requisite internal pH, for *C. thermoaceticum*, below a pH of 5 the chemical and electrical potentials across the cell membrane collapse (Baronofsky et al., 1984). For *B. methylotrophicum*, the value has not been determined, but based on this mechanism can be assumed to be between 5 and 5.5, from the results observed in the continuous cell recycle fermentations. If the driving force for acetic acid excretion is compromised at low pH, and it follows that a logical cellular response to a shift down in

the extracellular pH would be to produce less acid, and if acid must be produced, to produce less acid per mole of substrate.

This somewhat speculative mechanism for the pH effect on the CO fermentation is supported by the experimental data obtained from batch, continuous, and continuous cell recycle fermentations. However, it does not explain why at low pH the cell does not cease acid production altogether, and switch to alcohol production, as is observed during the solventogenic phase of *C. acetobutylicum*. This question is addressed by an energetic analysis of the fermentation. Interestingly, if the concentration of undissociated acid is the key regulatory factor which inhibits cell functions at low pH, then the pH effect could perhaps be enhanced by continuous extraction of acids from the fermentation broth, particularly during low-pH operation. Another hypothesis arising from this analysis is that the acid uptake results described in Chapter 3 were as much a consequence of the high initial pH as they were of the high acid concentration, since at equilibrium, 10 g/L at a pH of 7.2 results in an external acetic acid concentration of approximately 0.04 g/L, while 2 g/L at a pH of 5.0 results in an external acetic acid concentration of 0.73 g/L. If the external concentration of undissociated acid is the critical species, then the latter case of this calculation would be more harmful to the cell.

4.3.2. Unsteady-State Results

The fermentations conducted at pH values of 5.75 and 5.5 initially exhibited primary butanol production, followed by prolonged oscillations in acetate and butyrate formation. The time-course profiles for these unsteady-state systems are shown in Figure 27 and 28 for the pH values of 5.75 and 5.5, respectively. The oscillations in the pH of 5.5 case are much more distinct, and oscillations in butanol production are also observed. The initial responses of primary butanol production are significant in that they demonstrate a capability in *B. methylotrophicum* for producing butanol as the major product from CO metabolism. However, these responses were transient and were not maintained for over 86 hours in either the pH of 5.5 or 5.75 case.

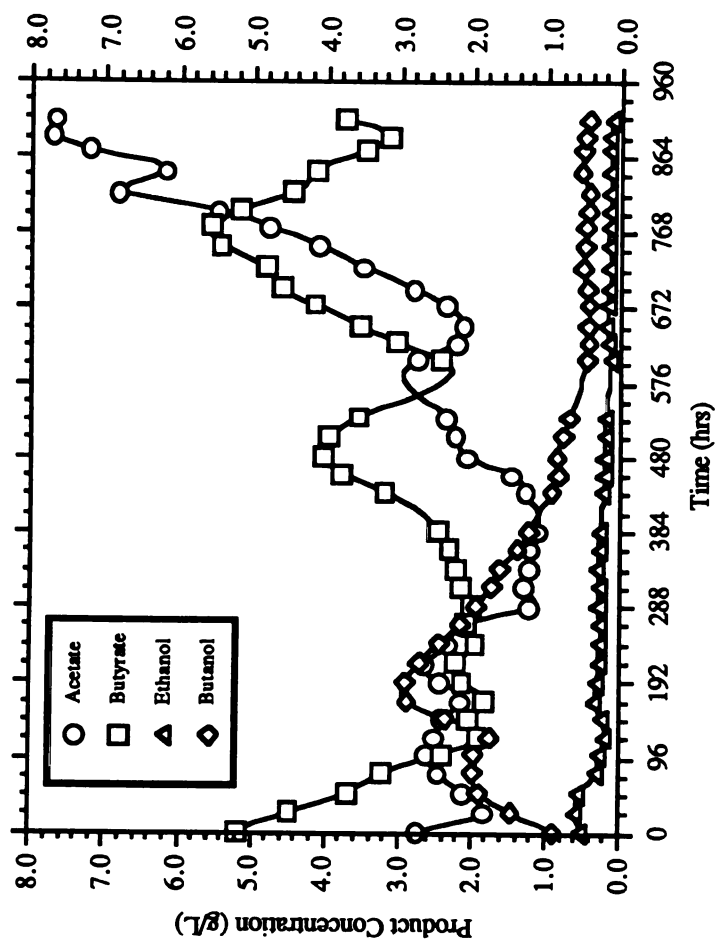


Figure 27. Product concentrations during continuous cell recycle CO fermentation at a pH of 5.75.

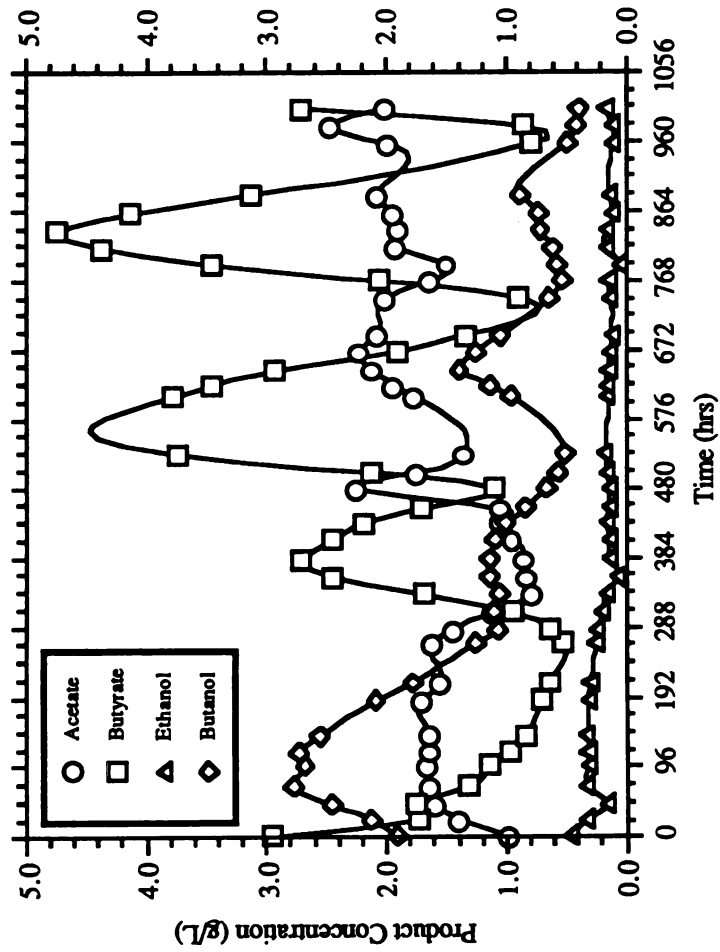


Figure 28. Product concentrations during continuous cell recycle CO fermentation at a pH of 5.5.

Although these initial responses of primary butanol production were only transient responses, they are evidence for a potential alcohol fermentation from CO gas. Table 26 shows the initial fermentation stoichiometries for these two unsteady fermentations during the transient period of primary butanol production. The butanol coefficients in the balanced equations are significantly greater than those in Table 20 for the steady-state experiments.

Table 26. Unsteady-state, initial fermentation stoichiometries as a function of pH for cell recycle fermentation of CO gas.

<u>Culture pH</u>	<u>Fermentation Stoichiometry</u>
5.75	$4\text{CO} \rightarrow 2.36\text{CO}_2 + .126\text{CH}_3\text{COOH} + .074\text{C}_3\text{H}_7\text{COOH} + .021\text{C}_2\text{H}_5\text{OH} + .115\text{C}_4\text{H}_9\text{OH} + .595\text{CELLS}$
5.5	$4\text{CO} \rightarrow 2.40\text{CO}_2 + .112\text{CH}_3\text{COOH} + .049\text{C}_3\text{H}_7\text{COOH} + .029\text{C}_2\text{H}_5\text{OH} + .149\text{C}_4\text{H}_9\text{OH} + .533\text{CELLS}$

Averages of the product concentrations over the time period of primary butanol production were used to obtain these balances. As can be seen in both Figure 27 and Figure 28, the butyrate concentration was decreasing during the initial phase of each experiment. The rate of decrease in both cases is approximately equal to the theoretical washout of the acid, which can be calculated at each data point by assuming complete termination of the butyrate pathway. The resulting washout curves at each data point, as shown in Figure 29 for the experiment at a pH of 5.5, can be compared to the actual butyrate concentrations; concentrations above a given washout curve indicate butyrate production, and concentrations below the washout curve indicate butyrate consumption. As shown, all of the examined data are on or slightly above each of the washout curves, which is a strong indication that butanol production occurred solely due to CO uptake as opposed to butyrate uptake.

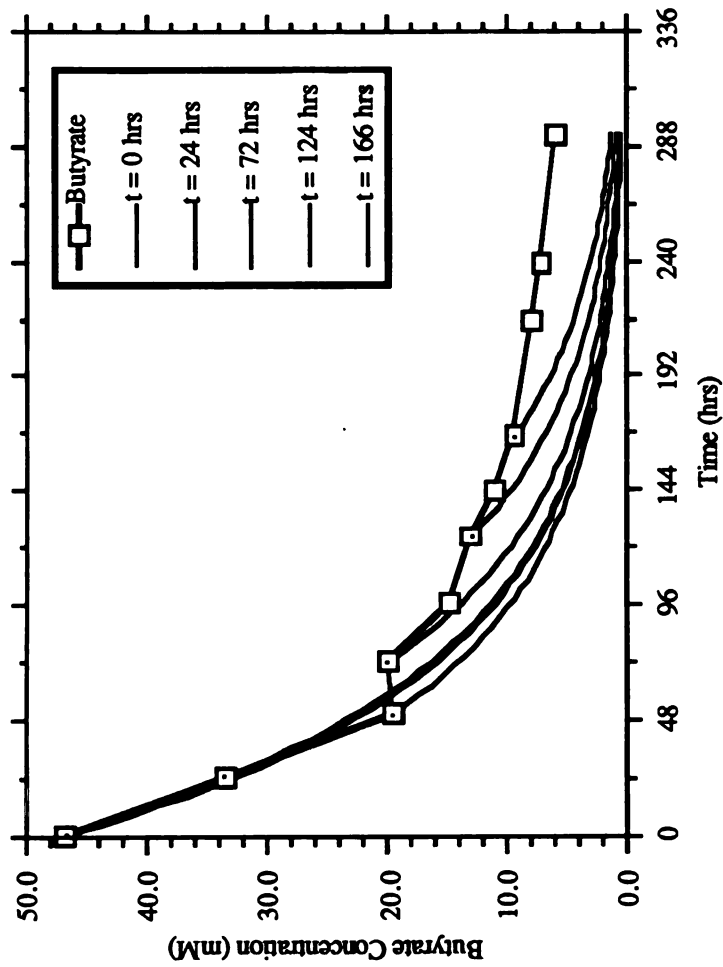


Figure 29. Theoretical and measured washout curves for butyrate during cell recycle fermentation at a pH of 5.5.

Time zero in Figures 27 and 28 is the point at which the pH had reached setpoint, approximately 2 days after it had been changed from a value of 6.8, which was the standard pH used for system start-up and cell growth. Therefore, the transient period of butanol production from CO gas, although a real phenomena, could be interpreted as a result of the experimental procedure, as opposed to a response to fermentation pH. It is reasonable to assume, with the results obtained in Chapter 3, that the high concentrations of both acetate and butyrate, resulting from the system start-up at high pH, were an influential variable in the observed transient butanol production.

When compared on a basis of carbon and electron partitioning during this initial time period, as shown in Table 27 and Table 28, butanol alone accounts for as much as 44% of the total available electrons in the CO feed at a pH of 5.5. The relative increase in the cell mass term is not entirely clear. One hypothesis is that cell death is significantly greater at pH values below 6.0. This hypothesis is supported indirectly by the results indicating that a viable culture could not be maintained at pH values below 5.5, i.e., at 5.35 and 5.1.

The oscillations observed for acetate and butyrate production at low pH suggest that the energetics of CO metabolism may be a controlling factor during these fermentations, since formation of these products results in ATP synthesis. Table 14 in Chapter 3 shows the theoretical net substrate-level ATP and electron yields for each product from CO. These values were obtained from known and proposed metabolic pathways for CO metabolism in *B. methylotrophicum* (Grethlein et al., 1991b). One hypothesis to explain the oscillatory phenomena is that production of acids and alcohols is regulated by the available cellular energy (ATP), and only when the ATP levels in the cells are in excess of a critical concentration does significant formation of products other than acetate occur. If such a hypothesis were true, then maximizing the cellular energetics during CO metabolism, possibly by using more reduced co-substrates, could alleviate metabolic requirements for acetate production. The construction and analysis of a metabolic model for CO fermentation in *B. methylotrophicum* is the subject of Chapter 5, and the use of co-

Table 27. Continuous, initial unsteady-state CO fermentation carbon partitioning as a function of pH for *B. methylotrophicum*.

pH	CO ₂	CH ₃ COOH	Carbon Partitioning (%Carbon)			Cells
			C ₃ H ₇ COOH	C ₂ H ₅ OH	C ₄ H ₉ OH	
5.75	59.0	6.4	7.4	1.0	11.5	14.9
5.5	56.2	5.6	4.9	1.5	14.7	13.3

Table 28. Continuous, initial unsteady-state CO fermentation electron partitioning as a function of pH for *B. methylotrophicum*.

pH	CH ₃ COOH	Electron Partitioning (%Electrons)			Cells
		C ₃ H ₇ COOH	C ₂ H ₅ OH	C ₄ H ₉ OH	
5.75	12.6	18.5	2.2	34.5	31.3
5.5	11.2	12.2	4.4	44.1	28.0

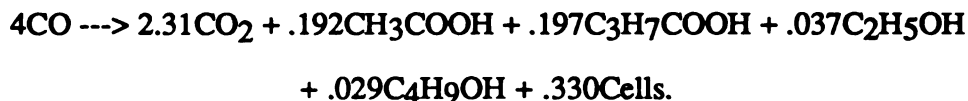
-substrates such as acetate, are described below.

4.3.3 Death Phase Results

The death regime at pH values of 5.35 and 5.1 was indicated by steady washout of all fermentation products after achieving the pH setpoint in the fermentation system. These studies were therefore of no practical value, except in that a time-dependent analysis of the washout curves was the first evidence, albeit indirect, for acetate and butyrate uptake mechanisms in *B. methylotrophicum*.

4.3.4. Cosubstrate Results

The hypothesis of energetic limitations during CO fermentation at low pH and the results for acid uptake presented in Chapter 3 prompted a preliminary investigation as to the potential for use of cosubstrates such as acetate or methanol concurrent with CO gas. The purpose of using acetate was to inhibit acetate formation during CO metabolism, and thus regulate the metabolism more towards butyrate, as was observed in the batch bottle experiments. This fermentation was conducted with an external acetate concentration of 5.7 g/l at a pH of 5.9, and steady-state was achieved. The fermentation stoichiometry was,



which shows that in the presence of acetate, butyrate is the primary product from CO. The carbon and electron partitioning is shown in Table 29. Although alcohol production was not affected significantly relative to the previous steady-state results, the percent of electrons contained in 4-carbon products during this fermentation exceeded 57%, which is the highest value ever observed for this organism growing on CO gas. This fermentation was typical in all other respects, with a normalized CO consumption rate of 0.00138 mol/hr•L•OD, which falls approximately at the average of the other steady-state values calculated. CO conversion for this fermentation was 17.8%.

Table 29. Continuous, steady-state CO fermentation carbon and electron partitioning at a pH of 5.9 in the presence of acetate for *B. methylotrophicum*.

	(%Carbon)	(%Electrons)
Product:		
CO ₂ :	57.8	0.0
CH ₃ COOH:	9.6	19.2
C ₃ H ₇ COOH	19.7	49.2
C ₂ H ₅ OH	1.9	5.6
C ₄ H ₉ OH	2.9	8.7
Cells	8.2	17.4

4.4. Summary Discussion of Fermentation Results

The key limitation of the cell recycle studies was the reliance on the carbon and available electron balances for calculation of CO consumption and cell mass production. One possible source of error which was calculated not to be a significant factor was the possibility of product stripping by the CO gas leaving the system, a conclusion determined using equilibrium calculations (Rauolt's Law) based on the typical concentrations of soluble products and flow rates observed during the fermentations. Besides analytical techniques, the other most likely source of error was in the measurement of liquid and gas flow rates, which was done using calibrated pumps and flow meters. These issues must be kept in mind when discussing the fermentation results.

One interesting set of calculations based on acid and alcohol production from CO are the free energies of formation, or ΔG° values, for the theoretical reactions of acetate, butyrate, ethanol, and butanol production. these values are shown in Table 30, where the equations are balanced in carbon and oxygen only. As shown, all of the formation reactions are sufficiently exergonic to drive ATP synthesis, which has a theoretical energy requirement of 7.3 kcal/mol.

Table 30. Standard free energies of reaction for CO conversion^a.

Reaction	ΔG° (kcal/g-mol CO)
$4\text{CO} + 2\text{H}_2\text{O} \rightarrow 2\text{CO}_2 + \text{CH}_3\text{COOH}$	-9.8
$10\text{CO} + 4\text{H}_2\text{O} \rightarrow 6\text{CO}_2 + \text{C}_3\text{H}_7\text{COOH}$	-9.7
$12\text{CO} + 5\text{H}_2\text{O} \rightarrow 8\text{CO}_2 + \text{C}_4\text{H}_9\text{OH}$	-9.0
$6\text{CO} + 3\text{H}_2\text{O} \rightarrow 4\text{CO}_2 + \text{C}_2\text{H}_5\text{OH}$	-8.1

^aFrom Worden et al., 1991.

Several conclusions relating directly to the feasibility of the coal-derived synthesis gas conversion concept were drawn during the cell recycle fermentation study. The use of cell recycle increased overall cell densities 10-20 fold and increased product concentrations 5-10 fold, compared to continuous fermentations without cell recycling. Since the previous non-cell recycling fermentations and these studies were all conducted at the same dilution rate, the corresponding increases in the volumetric productivities of the cell recycle fermentations was also 5-10 fold. Long-term (6-8 weeks) continuous operation was achieved without significant changes in operating conditions due to membrane fouling or life. Alcohol production during CO metabolism was measured at all pH values tested, and a capacity for primary butanol formation directly from CO gas was observed at pH values below 6.0. Three metabolic regimes were observed due to fermentation pH, with stable, steady-state operation at pH values of 6.0 and above, oscillations at pH values of 5.75 and 5.5, and cell death at pH values below 5.5. These findings have strengthened the feasibility of an anaerobic fermentation process based on coal-derived synthesis gas.

CHAPTER 5

METABOLIC MODELING AND FERMENTATION ANALYSIS

5.1. Objectives and Principles of the Model

Results from both the metabolic tolerance studies in Chapter 3 and the cell recycle fermentation studies in Chapter 4 suggested that regulation of CO metabolism in *B. methylotrophicum*, specifically in the production of acetate relative to butyrate and alcohols, was a function not only of pH but perhaps also of the energetic limitations. To produce any compounds besides acetate, as shown previously in Table 14, the cell must expend energy on a substrate-level basis. The relationship between low pH inhibition of acetate production and loss of ATP generation from decreases in acetate production suggest that these two antagonistic factors are the key mechanisms which ultimately determine product stoichiometry during CO fermentation. Thus, in order to more fully analyze the data obtained during the cell recycle fermentations, the energetics of CO fermentation in *B. methylotrophicum* must be taken into account.

From a teleological standpoint, a bacterial cell has the main purpose of performing work, in the form of transport, motility, and biosynthesis processes, in order to reproduce in and colonize an environment. The energy needed to support these functions comes from the metabolism of substrates obtained from the external environment. The efficiency of energy extraction during cell growth on chemical substrates is of paramount importance to a microorganism's ability to survive, particularly in a competitive environment.

The energy requirements for the physiological functions listed above are met by the use of energy-rich intermediates, primarily in the form of ATP. Several terms are frequently used when considering this energy metabolism, including the cell yield, Y_S (g cells/mol substrate), the ATP yield, Y_{ATP} (g cells/mol ATP produced), and the ATP gain, G_{ATP}

(mol ATP/mol substrate). However, the calculation of Y_{ATP} requires a knowledge of the ATP gain, since

$$Y_{ATP} = (Y_S/G_{ATP})$$

and this raises the problem of experimentally determining these values. Y_S can be obtained by plotting substrate consumption versus the dry weight of cells produced, and taking the inverse of the slope; for *B. methylotrophicum*, this value has been determined as 3.4 g cells/mol CO (Lynd et al., 1982). If G_{ATP} is known, then Y_{ATP} can be calculated by the above equation. Typically, a value of 10.5 g/mol is assumed for most anaerobic bacteria, a value which has been found to be relatively invariant in a wide range of species (Bauchop and Elsdon, 1960). However, this value is based on heterotrophic metabolism with glucose as the energy source, and cannot be assumed to be accurate for other substrates, particularly 1-carbon compounds (Stouthamer, 1979).

This fact becomes clear when it is realized that values of Y_{ATP} are calculated based on known metabolic pathways, typically for glucose, and thus the calculation of Y_{ATP} is dependent on the known production of ATP per mole of substrate. Specifically, and as discussed previously, there are two main contributing mechanisms to the generation of ATP in a bacteria, SLP and ETP. Since the SLP portion of energy generation is that used to calculate Y_{ATP} , values for Y_{ATP} cannot be readily obtained from organisms with no net energy generation from SLP, such as *B. methylotrophicum*. The question then arises as to how to analyze such organisms from an energetic standpoint, without such key information. In general, this problem prevents definite conclusions about the magnitude of Y_{ATP} in such systems (Stouthamer, 1988). This point has to be considered in the development of an energetic equation for cell mass production, as described below.

5.2. Development of the Metabolic Model

The use of a fermentation equation to describe the energetics of cell formation during cell metabolism has been suggested as a means of verifying and analyzing fermentation

product data and associated parameters such as maximum theoretical product yields (Papoutsakis, 1983; Papoutsakis, 1984; Papoutsakis and Meyer, 1985a; Papoutsakis and Meyer, 1985b; Vallino and Stephanopoulos, 1990). Essentially, these "metabolic modelling" equations are balanced equations for carbon, ATP, and reducing equivalents, or electrons, derived from known metabolic pathways (Papoutsakis, 1983). The application of this type of analyses is that by measuring product formation during fermentation, the various extents of intracellular metabolic reactions and their selectivities can be calculated, as a function of only measured product concentrations and cell mass production.

It follows that in this type of fermentation analysis, one of the most significant reactions is the equation relating the production of cell mass to the substrate, ATP, and electron requirements. The stoichiometric equation for biomass production requires knowledge of the cell yields for the particular substrate, a knowledge of Y_{ATP} , and also calculation of the available electron content of the cell mass and the substrate, so that a stoichiometric coefficient for the required electrons can be obtained. The final result is a lumped equation for biomass production which relates molar substrate, electron equivalents, and ATP requirements to cell mass formation.

The method stipulates that the fermentation equation for cell mass is incorporated into a system of linear equations for the known metabolic pathways. The rates of the product forming reactions are knowns, the concentrations of intermediate species are assumed to be constant using a pseudo-steady state assumption, and the system of equations is then solved for each of the specific reaction rates. Such a system, depending on the number of known rates, can be solved uniquely, or, in the case of excess fermentation data, can be overspecified, and the best-fit solution to the system of equations obtained using all of the data. The constraints imposed by the ATP and electron balances used in deriving the fermentation equations allow maximum theoretical yields and rate-limiting reactions to be elucidated, in what is known as identifying "gateway sensors" for metabolic pathways.

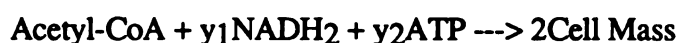
Application of this type of metabolic modelling to the CO fermentations described in Chapter 4 is a method by which the energetics and flow of carbon and electrons during CO metabolism can be studied. However, the method, developed using well-elucidated heterotrophic bacterial fermentation systems (Papoutsakis and Meyer, 1985a; Papoutsakis and Meyer, 1985b), has several limitations when applied to the unicarbonotrophic fermentations by *B. methylophilicum*. These limitations arise from the lack of complete fermentation data, mainly experimental data for cell mass production and CO consumption, and also from the lack of information on the energetics of CO metabolism, specifically to a value for Y_{ATP} . Thus, in order to apply the metabolic model to the present system, several assumptions and estimates had to be incorporated into the model.

During the following derivation and subsequent analysis, all of the known electron carriers in the CO metabolic pathway are referred to as NADH, for the purposes of convenience. This simplification is not intended to imply that NADH is the electron carrier in all of the reactions steps, since some of the specific electron carriers have yet to be determined, or are rubredoxin or ferredoxin based (Saeki et al, 1989a; Saeki et al, 1989b; G. J. Shen and J. G. Zeikus, unpublished results). Since the fermentation equations depend only on the electron balance and not on the specific carrier, this lack of information was inconsequential from the standpoint of the model development.

The first step in the metabolic modelling of the CO fermentations was to determine an equation for biomass production from CO. The absence of net substrate-level ATP production made direct calculation of Y_S impossible. As such, the typical form for the biomass equation,

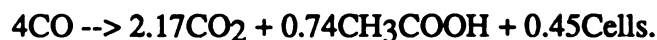


was not applicable, since the molar ATP yield coefficient y_2 was unknown. However, based on the known metabolic pathways, specifically for acetogenic metabolism, it was possible to redefine the biomass equation to the form,



where the coefficients y_1 and y_2 were to be determined empirically. In this form, the units of the yield coefficients are thus mol NADH₂/mol Acetyl-CoA consumed for y_1 and mol ATP/mol Acetyl-CoA consumed for y_2 .

Determination of y_1 and y_2 was accomplished using CO growth phase data during batch bottle experiments (Lynd et al., 1982). This data resulted in a fermentation stoichiometry of



From the raw data, an electron balance was used to calculate y_1 , which was 1.48 mol NADH₂/mol Acetyl-CoA consumed, and which was rounded to 1.5 mol NADH₂/mol Acetyl-CoA consumed. Calculation of y_2 required an assumption of ETP and the stoichiometry of the proton-translocating ATP synthase. The electrons produced by the oxidation of CO to CO₂ were assumed to drive an electron transport chain as suggested by Zeikus et al, (1985), and a standard ratio of 3 moles protons per mole ATP produced was assumed (Niedhardt, 1987). The ATP production via ETP could thus be determined using Lynd's data. From the known SLP contribution, taken from the pathway of CO metabolism and acetate formation (See Figure 5), the net overall ATP consumption, and thus the ATP requirement for cell mass production, was then calculated. This value was found to be 2.0 mol ATP/mol Acetyl-CoA consumed, which interestingly results in a Y_S value of 0.5 mol ATP/mol CO, or a Y_{ATP} value of 6.8 g cell/mol ATP.

A system of linear equations was set-up based on the developed pathway for CO metabolism in *B. methylotrophicum*, but including pathways for ethanol and butanol formation (J. S. Shieh, unpublished results). A detailed diagram of this pathway, including the hypothesized flow of electrons during electron transport phosphorylation, is shown in Figure 30. This scheme is an extension of that suggested by Zeikus et al, (1985). It must be emphasized that the actual electron carriers in some of the reactions have not yet been determined, although NADH is used as a generic carrier in Figure 30.

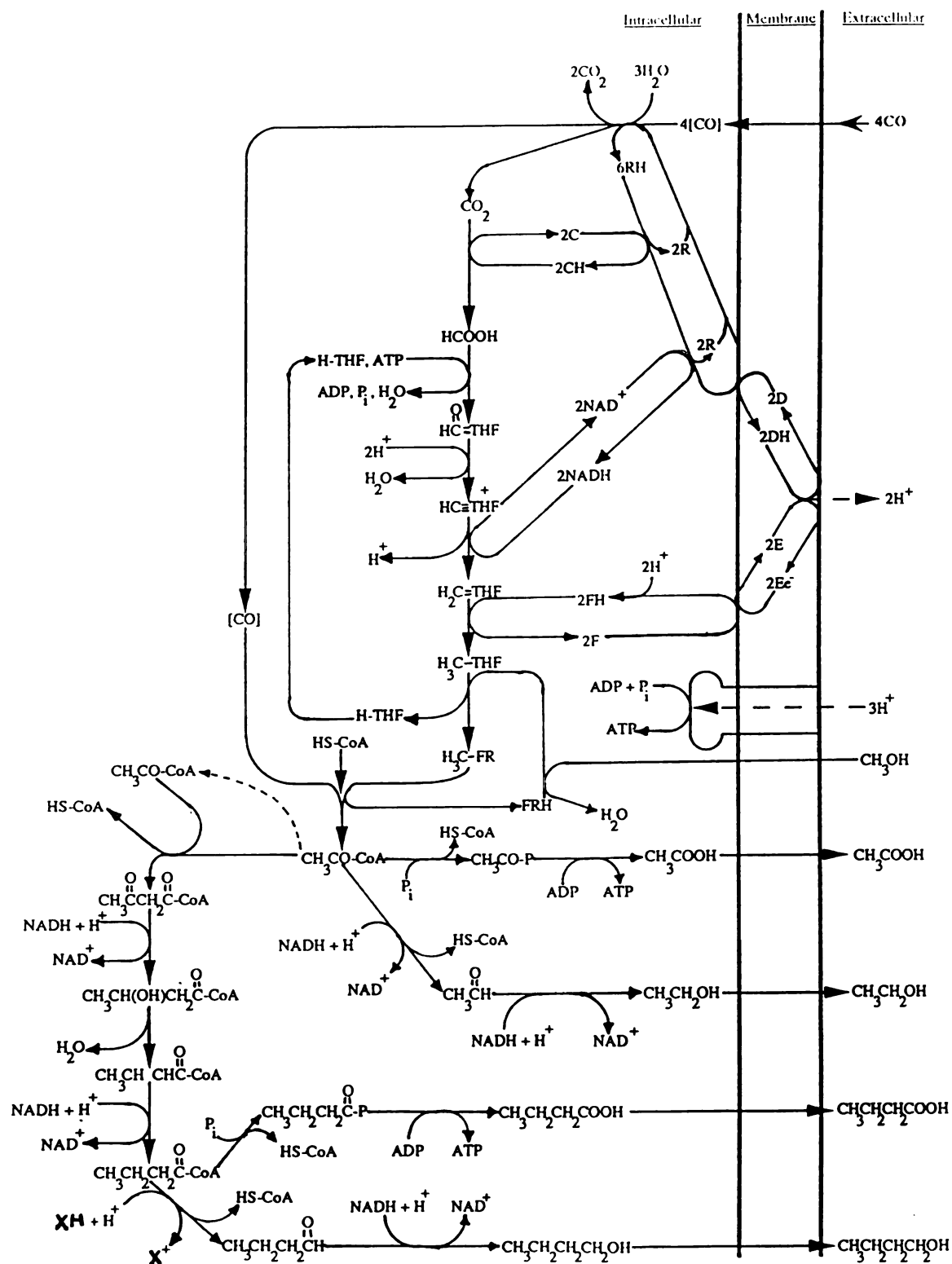


Figure 30. Known and proposed metabolic pathways for carbon and electron flow during CO metabolism in *B. methylotrophicum*.

Letters indicate unknown electron carriers, with F indicating ferredoxin and R indicating rubredoxin. The equations were developed from each of the major reaction steps, where



is the reaction for oxidation of CO to CO₂. For the 6-step tetrahydrofolate-mediated conversion of the bound CO₂ group to the bound CH₃OH group, or CH₃O•, an overall reaction is

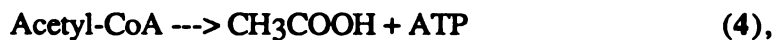


and for the condensation reaction to form acetyl-CoA,

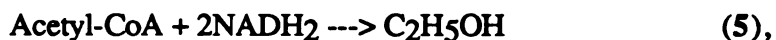


is the carbon-balanced equation.

Acetyl-CoA participates in several pathways, including the formation of acetate, with the overall reaction



and for the formation of ethanol,



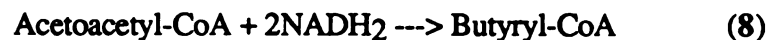
and for the formation of cell mass,



and the formation of acetoacetyl-CoA,



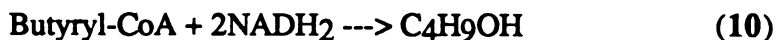
Acetoacetyl-CoA is the precursor to butyryl-CoA in a 3-step reaction sequence simplified by the overall reaction



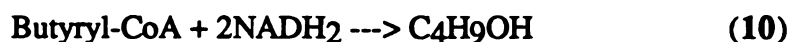
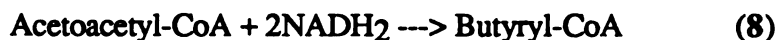
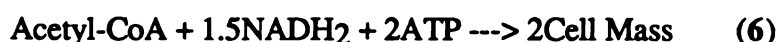
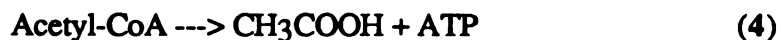
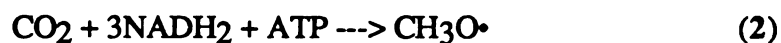
which then can form either butyrate by



or butanol by



The complete system of fermentation equations for this pathway, balanced in carbon, ATP, and electrons (NADH), is thus



If the rates of the ten reactions 1-10 are given as a-j, then all of the reactants, products, and intermediate concentrations are thus a function of these 10 equations, where

$$\text{NADH}_2 = (\text{a} - 3\text{b} - 2\text{e} - 2\text{f} - 2\text{h} - 2\text{j})$$

$$\text{CH}_3\text{O}^\bullet = (\text{b} - \text{c})$$

$$\text{Acetyl-CoA} = (\text{c} - \text{d} - \text{e} - \text{f} - \text{g})$$

$$\text{CH}_3\text{COOH} = (\text{d})$$

$$\text{C}_2\text{H}_5\text{OH} = (\text{e})$$

$$\text{Cell Mass} = (2\text{f})$$

$$\text{Acetoacetyl-CoA} = (0.5\text{g} - \text{h})$$

$$\text{Butyryl-CoA} = (\text{h} - \text{i} - \text{j})$$

$$\text{C}_3\text{H}_7\text{COOH} = (\text{i})$$

$$\text{C}_4\text{H}_9\text{OH} = (\text{j})$$

and where the ATP balance, because of the presence of ETP, was not used to specify the system.

Several pseudo-steady state assumptions were then invoked on all the intracellular reaction intermediates, leaving 5 independent equations:

$$\begin{array}{ll}
 \text{NADH}_2 & : \quad (a - 3b - 2e - 1.5f - 2h - 2j) = 0 \\
 \text{CH}_3\text{O}^\bullet & : \quad (b - c) = 0 \\
 \text{Acetyl-CoA} & : \quad (c - d - e - f - g) = 0 \\
 \text{Acetoacetyl-CoA} & : \quad (0.5g - h) = 0 \\
 \text{Butyryl-CoA} & : \quad (h - i - j) = 0.
 \end{array}$$

The measurable or calculated species, acetate, butyrate, butanol, ethanol, CO, CO₂, and cell mass, comprise the other specifications, resulting in a system of 10 total equations with 5-independent and 5-dependent equations. If all of the species concentrations were measured, this system could conceivably be overspecified with 12 total knowns or equations (7 measurable rates and 5 independent equations) and 10 unknowns (rates a-j). Unfortunately, depending on the CO fermentation system, only 5 measurable quantities were available in any given experiment, and thus the system is uniquely specified. Yet some of the unmeasurable species can be calculated from the carbon and available electron balances, to overspecify the system.

This issue is addressed for each of the specific cases of the model, applied below to the chemostat experiments conducted previously in order to verify the overall approach. The model is then applied to the steady-state cell recycle experiments using different specifications, and then also in a preliminary approach to modelling the unsteady-state cell recycle experiments.

5.3. Application to Chemostat Results

The model developed above was first applied to the previously obtained steady-state chemostat data in order to verify the approach and to determine some of the energetic parameters which are possible to calculate using the metabolic model. The system of equations described above was solved with data for acetate, butyrate, ethanol, butanol,

and cell mass production, and with the 5 independent equations; it was thus a unique system of equations with 10 knowns and 10 unknowns. The method of solution was Gaussian elimination, or row-reduction techniques. The following solutions were obtained, where r_{Ac} , r_{Bu} , r_{Et} , r_{Bh} , and r_{CM} are the measured rates of acetate, butyrate, ethanol, butanol, and cell mass production, respectively:

$$a = 3[r_{Ac} + r_{Et} + 0.5r_{CM} + 2(r_{Bu} + r_{Bt})] + 2r_{Et} + 0.75r_{CM} + 2(r_{Bu} + r_{Bt}) + 2r_{Bh}$$

$$b = r_{Ac} + r_{Et} + 0.5r_{CM} + 2(r_{Bu} + r_{Bt})$$

$$c = r_{Ac} + r_{Et} + 0.5r_{CM} + 2(r_{Bu} + r_{Bt})$$

$$d = r_{Ac} \quad e = r_{Et} \quad f = 0.5r_{CM} \quad g = 2(r_{Bu} + r_{Bt}) \quad h = r_{Bu} + r_{Bt}$$

$$i = r_{Bu} \quad j = r_{Bh}.$$

A spreadsheet was then used to apply the chemostat fermentation data to these solutions. All of the rate data, as a function of pH, were normalized to the cell density for these calculations, which thus yielded reaction extents. Some of the important calculations were the molar consumption and production extents for CO and CO₂, shown in Figure 31. These extents were relatively constant over the tested range of pH values. As a check on the validity and accuracy of the model, the ratio of CO consumption to CO₂ production calculated using the model can be compared to the molar ratios calculated using carbon and available electron balances, as were shown previously in Table 17. This comparison is made in Table 31. As shown, there is less than a 6% difference in all of the calculated values. The model was thus verified and the accuracy, relative to the carbon and electron balancing method, was high. Other important calculations were the ratio of acetyl-CoA derived products to butyryl-CoA derived products, which includes cell mass, and also the ratio of 2-carbon products to 4-carbon products, which does not include cell mass. These values are shown in Figure 32, where as seen previously, almost a 7-fold decrease in the 2-carbon to 4-carbon product ratios occurs between a pH of 6.8 and 6.0. Finally, the energetics of CO metabolism were calculated by assuming ETP based on the pathways shown in Figure 30. A ratio of 3 moles of protons consumed to every mole of ATP

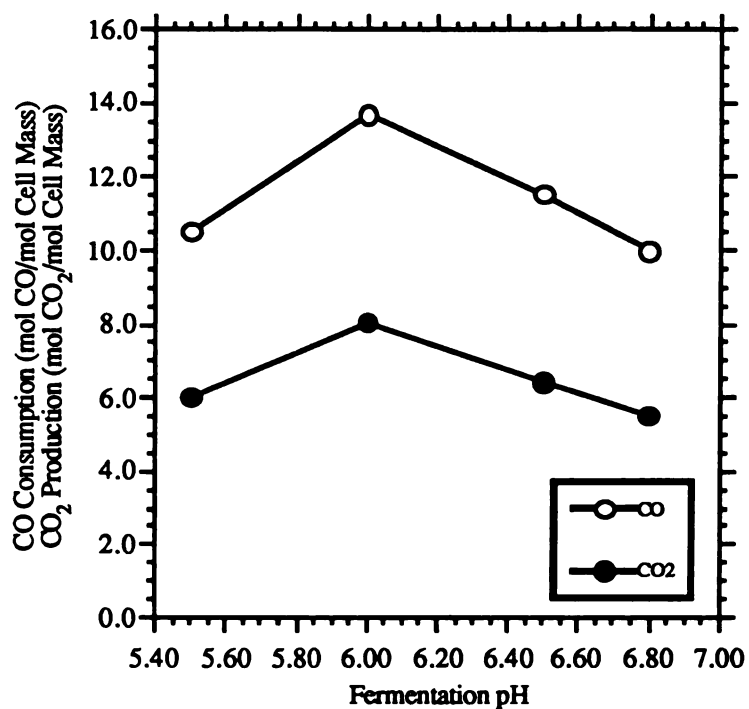


Figure 31. Molar consumption and production rates for CO and CO₂ gas as a function of fermentation pH during steady-state, continuous, culture.

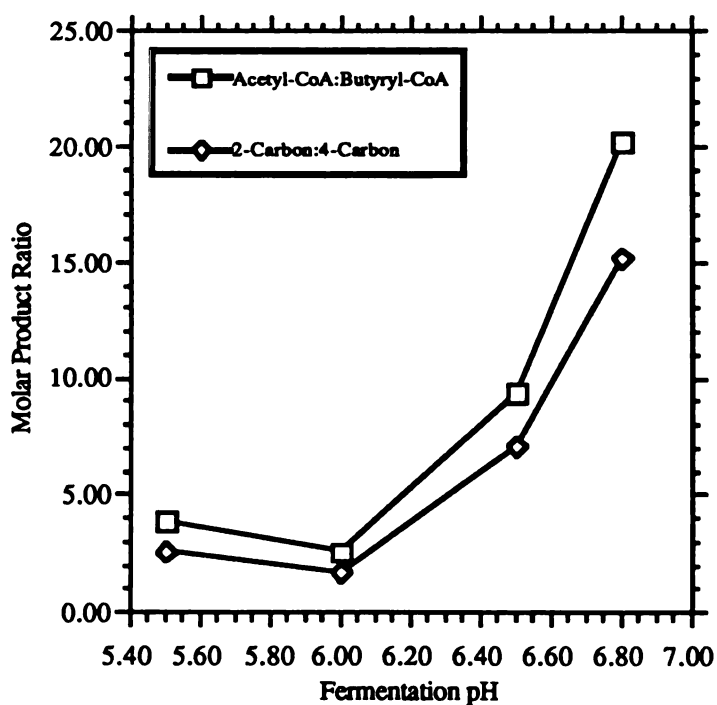
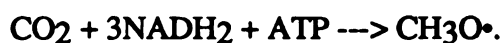


Figure 32. Molar product ratios as a function of fermentation pH during steady-state, continuous culture.

Table 31. Comparison of CO:CO₂ ratios from chemostat culture between metabolic model and carbon and electron balancing calculations.

Culture pH	CO:CO ₂ ratio		Percent Difference
	Metabolic Model Calculation	Carbon and Electron Calculation	
6.8	1.805	1.914	5.69
6.5	1.792	1.878	4.58
6.0	1.704	1.762	3.29
5.5	1.749	1.835	4.69

produced was assumed (Niedhardt, 1987), and the protons calculated by the reaction extent of (b),



The relative theoretical ATP contributions calculated for ETP, SLP, and also the total theoretical ATP production for the chemostat fermentations, normalized to the total CO consumption, are shown in Figure 33 as a function of pH. As has been described previously, substrate-level reactions consume ATP during production of all products other than acetate, as observed by the negative contribution of SLP in Figure 33. However, with the calculated contribution of ETP, the net ATP generation during CO metabolism was positive, and did vary somewhat with pH. This method of energetic analysis is therefore consistent with the hypothesis that during autotrophic or unicarbonotrophic growth, ATP deficits during catabolism are compensated for by an active ETP mechanism, which results in positive ATP production and thus cell growth.

Overall, the results of the test of the model on the chemostat data were encouraging, with all of the calculated values for CO consumption, CO₂ production, product ratios, and energetics being consistent with either previous calculations or current theory. It was thus

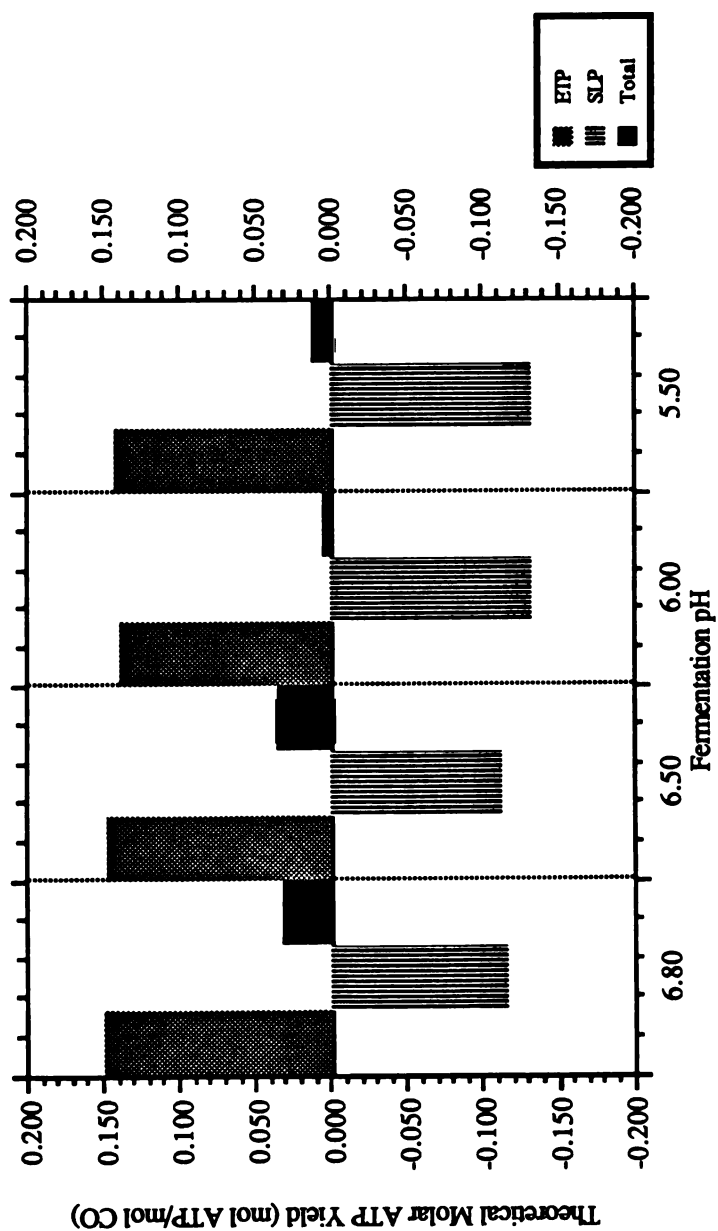


Figure 33. Theoretical molar ATP yield via electron-transport and substrate-level phosphorylation as a function of fermentation pH during continuous culture.

determined that this method of metabolic modelling was applicable to the analysis of the cell recycle fermentations, as described below.

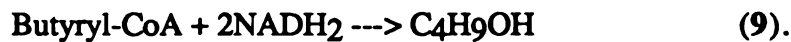
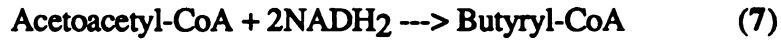
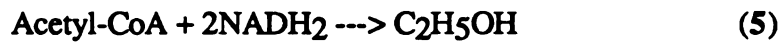
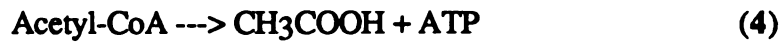
5.4. Application to Steady-State Cell Recycle Fermentation Results

The application of the metabolic model to the steady-state continuous cell recycle fermentation results was different from the application to the chemostat data in several ways. First was that instead of cell mass, CO₂ production was the fifth measured variable. Second, the variability of the raw data from the cell recycle experiments, as shown in Table 24, required normalization of the data prior to solution of the system of equations. Solutions to the rates of reactions are thus best compared in the units of mol/hr•L•OD, as described previously. The steady-state results were analyzed in 5 separate cases. Case 1 was a unique solution to the system of equations but without the addition of the fermentation equation for cell mass production, i.e., the reaction rates for only extracellular products were obtained. Case 2 is the so-called base-case, and should be considered as the representative case for this system. In Case 2, the system was uniquely specified, and CO consumption and cell production calculated. Case 3-5 were applications of calculated data from the carbon and available electron balances in order to overspecify the system. In Case 3, the system was overspecified with the calculated value for CO consumption. In Case 4, the system was overspecified with the calculated value for cell mass production. In Case 5, both the value for CO consumption and the value for cell mass production were used to overspecify the system.

5.4.1. Case 1: Uniquely Specified System: No Cell Mass Production

In Case 1, the system was set-up without an equation for the production of cell mass from acetyl-CoA. This case was evaluated to determine the contribution, or lack of contribution, of cell production on the overall energetics of the CO fermentations. The system of equations used was





and since there are only 9 equations with solutions a-i, the independent relationship

$$\text{NADH}_2 = (\text{a} - 3\text{b} - 2\text{e} - 2\text{g} - 2\text{i})$$

was not used to solve the system. Instead, the system was solved with the remaining 4 independent equations, and the 5 measured variables rAc, rBu, rEt, rBh, and rCO₂.

Gaussian elimination was used to solve this unique system of equations, with solutions of

$$\text{a} = \text{rCO}_2 + \text{rAc} + \text{rEt} + 2(\text{rBu} + \text{rBt})$$

$$\text{b} = \text{rAc} + \text{rEt} + 2(\text{rBu} + \text{rBt})$$

$$\text{c} = \text{rAc} + \text{rEt} + 2(\text{rBu} + \text{rBt})$$

$$\text{d} = \text{rAc} \quad \text{e} = \text{rEt} \quad \text{f} = 2(\text{rBu} + \text{rBt}) \quad \text{g} = \text{rBu} + \text{rBt}$$

$$\text{h} = \text{rBu} \quad \text{i} = \text{rBh}.$$

with calculation of unknowns such as the rate of CO consumption (rCO), the rate of electron production/consumption (rNADH), and the rate of ATP production via SLP, ETP, and their combined total (rSLP, rETP, rATP) by the equations

$$\text{rCO} = (\text{a} + \text{c})$$

$$\text{rNADH} = (\text{a} - 3\text{b} - 2\text{e} - 2\text{g} - 2\text{i})$$

$$\text{rSLP} = (\text{d} + \text{h} - \text{b})$$

$$\text{rETP} = 2/3(\text{b})$$

$$\text{rATP} = (\text{d} + \text{h} - \text{b} + 2/3(\text{b})).$$

Figure 34 shows the results if the data are not normalized to fermenter volume or cell density, where large variations in the calculated rates for CO consumption and cell density are observed. However, if the data are normalized, the CO consumption rates are considerably smoothed over the pH range, as shown in Figure 35. Subsequently, all of the data presented will be normalized in this manner. Figure 36 shows the molar production and consumption of CO and CO₂, respectively. These ratios are also relatively constant over the pH range. Also, in Figure 37 are the acetate to butyrate ratio and the 2-carbon to 4-carbon product ratio as a function of pH. These ratios are both approximately halved as the pH is decreased from 7.2 to 6.0. In Figure 38 are the molar yields for ATP generation, where once again, the SLP contribution is negative, but with positive production overall as a result of the ETP contribution. Importantly, there is also an observed trend of decreasing ATP production as the pH decreases, which is due to an increase in the ATP deficit during SLP, as shown by the larger negative values for SLP as the pH drops from 7.2 to 6.0. This observation, even though Case 1 is not representative of the actual biological system since cell mass was not accounted for, is an important aspect of the pH effect, and is discussed in detail for the more appropriate cases below. Finally, as a check on the accuracy of the metabolic model to the cell recycle data, rNADH can be broken down into the electron-producing and electron-consuming reactions, as shown in Figure 39. Since the net production of electrons, or NADH, should be the electron requirement for cell production, this value should be positive, as is indicated.

The results for Case 1 indicate that the metabolic model, as for the chemostat data, is consistent when applied to the cell recycle data. Furthermore, as discussed in Chapter 4, Case 1 has reemphasized the need for normalization of all fermentation rate data to both fermenter volume and culture density, in order to fully compare the calculated reaction rates. The production of ATP as a function of fermentation pH was also observed to be dynamic, and is detailed in a later section.

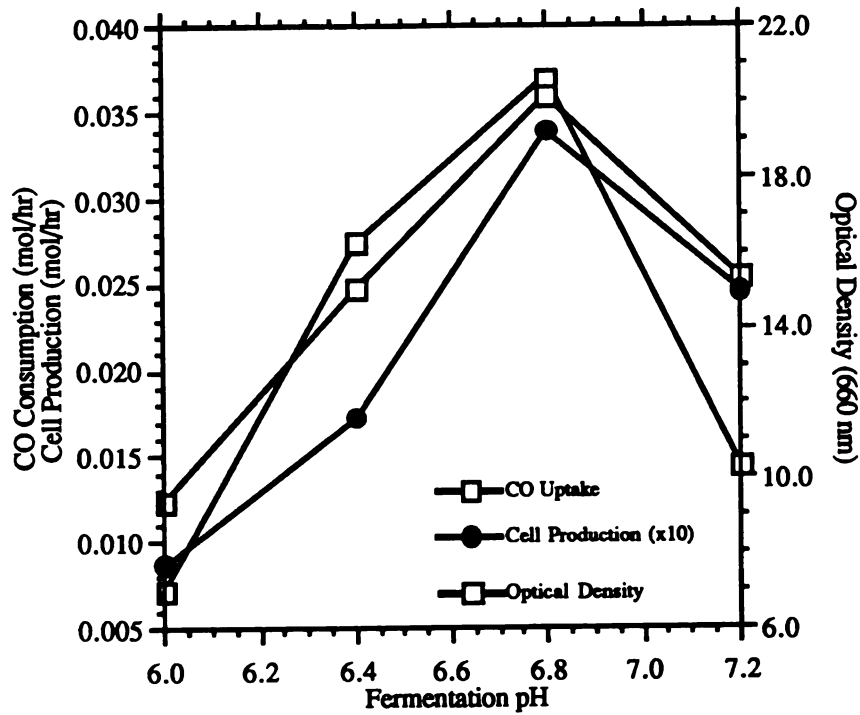


Figure 34. Steady-state CO consumption, cell production, and optical density as a function of pH for continuous cell recycle fermentation.

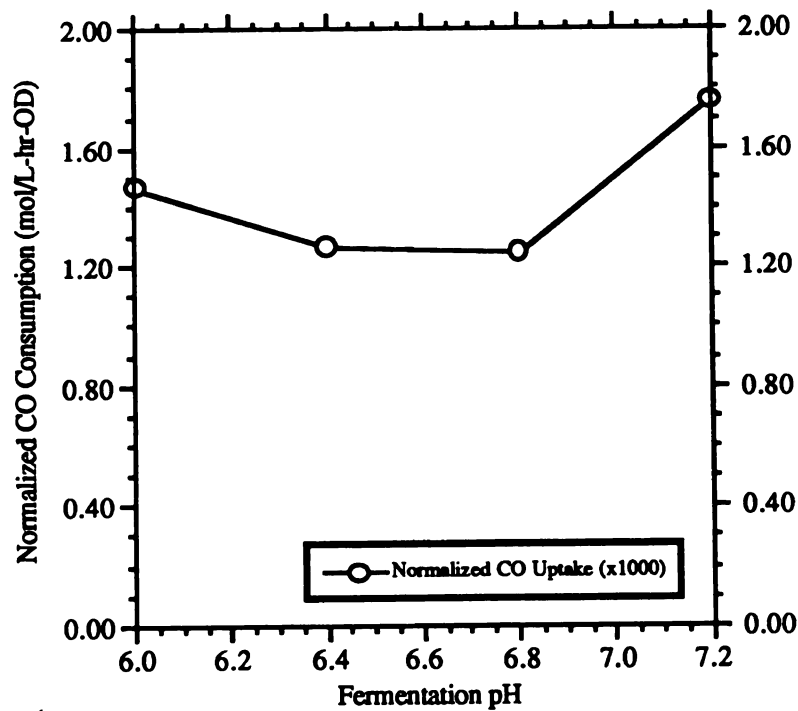


Figure 35. Normalized CO consumption rates for continuous cell recycle fermentation as a function of pH.

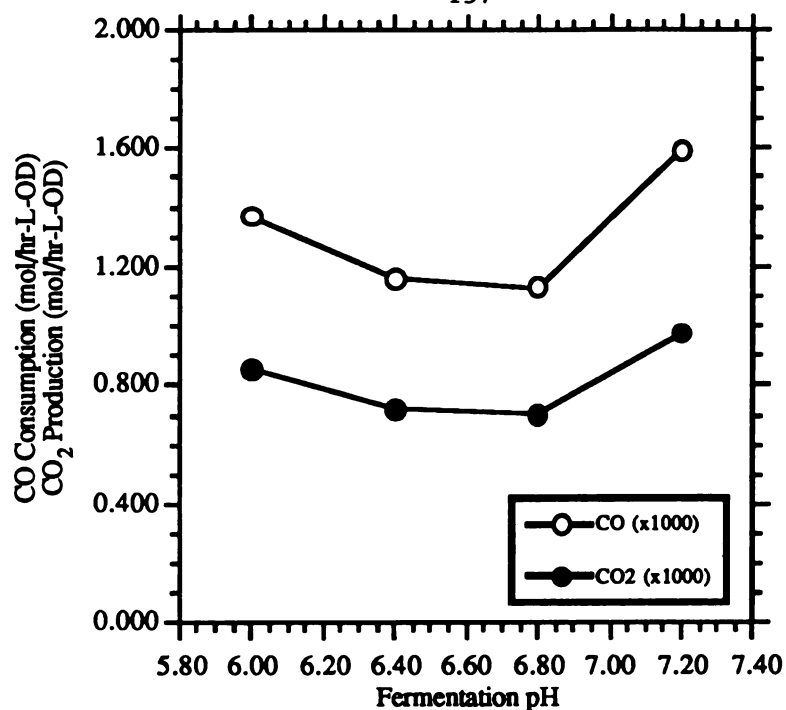


Figure 36. Normalized molar gas consumption and production rates as a function of pH during steady-state, continuous cell recycle fermentation: Case 1.

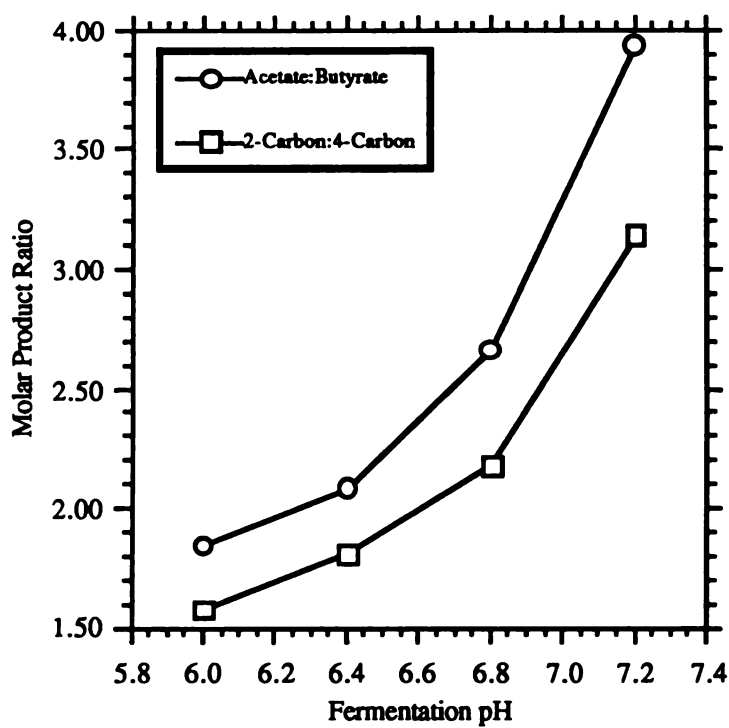


Figure 37. Molar product ratios as a function of pH during steady-state, continuous cell recycle fermentation: Case 1.

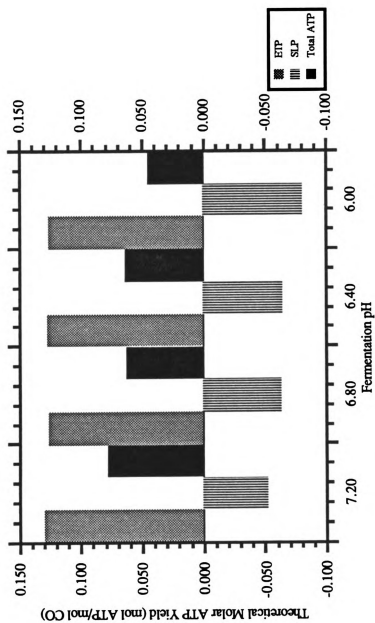


Figure 38. Theoretical molar ATP yields via electron-transport and substrate-level phosphorylation vs. pH during steady-state cell recycle fermentation: Case 1.

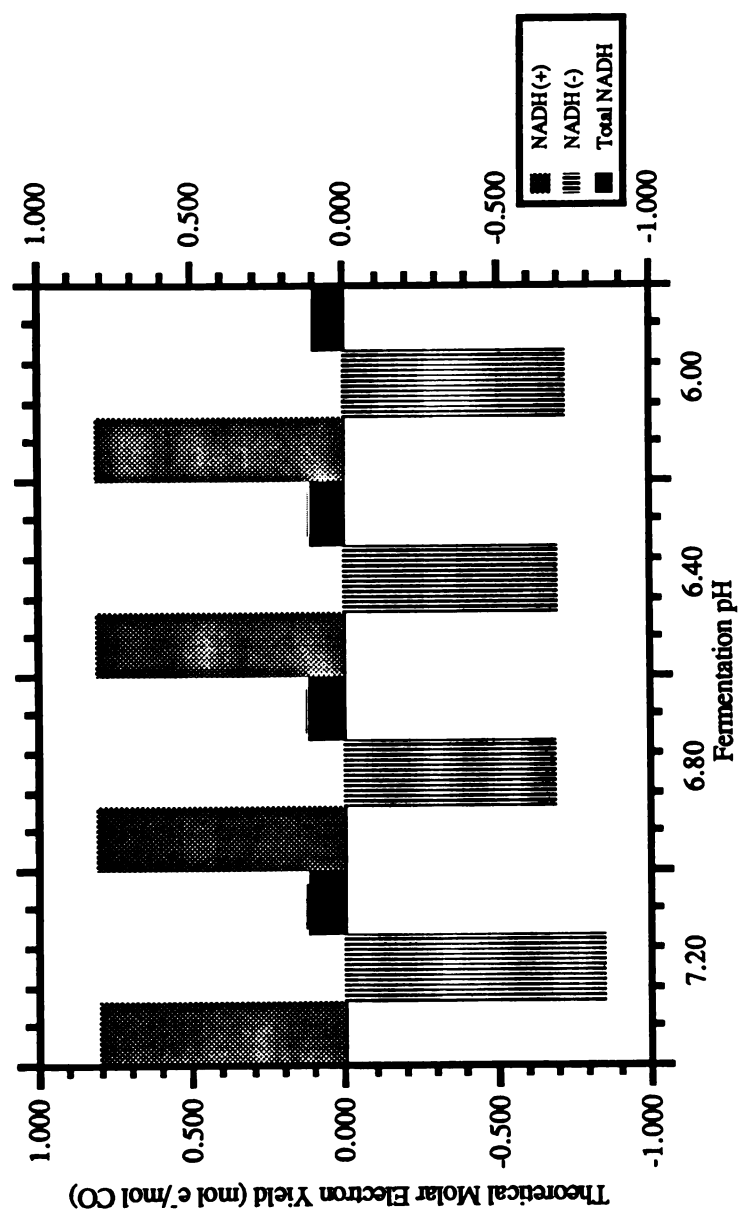
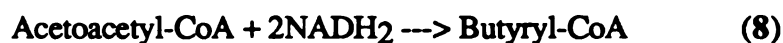
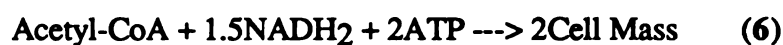
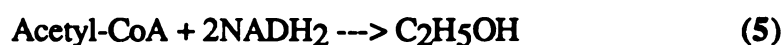
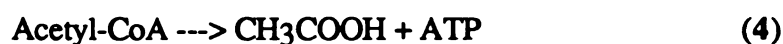
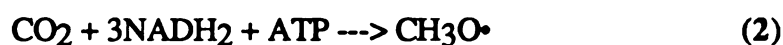


Figure 39. Molar electron yields as a function of pH during steady-state cell recycle fermentation: Case 1.

5.4.2. Case 2: Uniquely Specified System

For an accurate analysis of the cell recycle fermentation results, the production of cell mass, or more specifically the proportioning of carbon and electrons to cell mass, must be accounted for in the metabolic model. Case 2 includes the derived equation for cell mass production from acetyl-CoA into the system of equations,



with rates a-j for reactions 1-10. The 5 independent equations

$$\text{NADH}_2 \quad : \quad (\mathbf{a} - 3\mathbf{b} - 2\mathbf{e} - 1.5\mathbf{f} - 2\mathbf{h} - 2\mathbf{j}) = 0$$

$$\text{CH}_3\text{O}^\bullet \quad : \quad (\mathbf{b} - \mathbf{c}) = 0$$

$$\text{Acetyl-CoA} \quad : \quad (\mathbf{c} - \mathbf{d} - \mathbf{e} - \mathbf{f} - \mathbf{g}) = 0$$

$$\text{Acetoacetyl-CoA} \quad : \quad (0.5\mathbf{g} - \mathbf{h}) = 0$$

$$\text{Butyryl-CoA} \quad : \quad (\mathbf{h} - \mathbf{i} - \mathbf{j}) = 0$$

are used to solve the system with the rate data rAc, rBu, rEt, rBh, and rCO₂. The solution set for this unique system (10 equations or knowns and 10 unknowns) is

$$\mathbf{a} = \mathbf{rCO}_2 + 3/7[\mathbf{rAc} + \mathbf{rEt} + 2(\mathbf{rBu} + \mathbf{rBt}) + \Omega]$$

$$\mathbf{b} = 3/7[\mathbf{rAc} + \mathbf{rEt} + 2(\mathbf{rBu} + \mathbf{rBt}) + \Omega] \quad \mathbf{c} = 3/7[\mathbf{rAc} + \mathbf{rEt} + 2(\mathbf{rBu} + \mathbf{rBt}) + \Omega]$$

$$\mathbf{d} = \mathbf{rAc} \quad \mathbf{e} = \mathbf{rEt} \quad \mathbf{f} = 3/7\Omega - 4/7(\mathbf{rAc} + \mathbf{rEt} + 2\mathbf{rBu} + 4\mathbf{rBh})$$

$$\mathbf{g} = 2(\mathbf{rBu} + \mathbf{rBh}) \quad \mathbf{h} = \mathbf{rBu} + \mathbf{rBh} \quad \mathbf{i} = \mathbf{rBu} \quad \mathbf{j} = \mathbf{rBh}.$$

and where $\Omega = 2/3(r\text{CO}_2 - 2r\text{Et} - 2r\text{Bu} - 4r\text{Bh})$, which were all obtained again by Gaussian elimination.

The molar consumption and production rates for CO and CO₂ are shown in Figure 40 for the Case 2 results, and with the addition of the cell mass equation there is an increase in those rates compared to the Case 1 results. To again compare the results of the model with previously calculated values for CO consumption and CO₂ production, as shown in Figure 36, the carbon and available electron balance values, shown previously in Table 20, were used. This comparison is given in Table 32. The accuracy, upon comparison, is

Table 32. Comparison of CO:CO₂ ratios from steady-state cell recycle culture between metabolic model and carbon and electron balancing calculations for Case 2.

Culture pH	CO:CO ₂ ratio		Percent Difference
	Metabolic Model Calculation	Carbon and Electron Calculation	
7.2	1.747	1.810	3.48
6.8	1.715	1.778	3.54
6.4	1.718	1.770	2.94
6.0	1.683	1.724	2.38

excellent, with less than 4% difference in all cases.

The ratio of acetyl-CoA to butyryl-CoA derived products and 2-carbon to 4-carbon derived products is shown in Figure 41, and these ratios are consistent in that compared to the results in Figure 37, the ratio of acetyl-CoA to butyryl-CoA derived products has increased relative to Case 1, while the ratio of 2-carbon to 4-carbon products remains essentially unchanged. In Figure 42, the molar ATP production is presented, and an interesting observation is that the total ATP production is positive only because of the ETP component. Unlike what was observed in Case 1, the total molar ATP production in Case

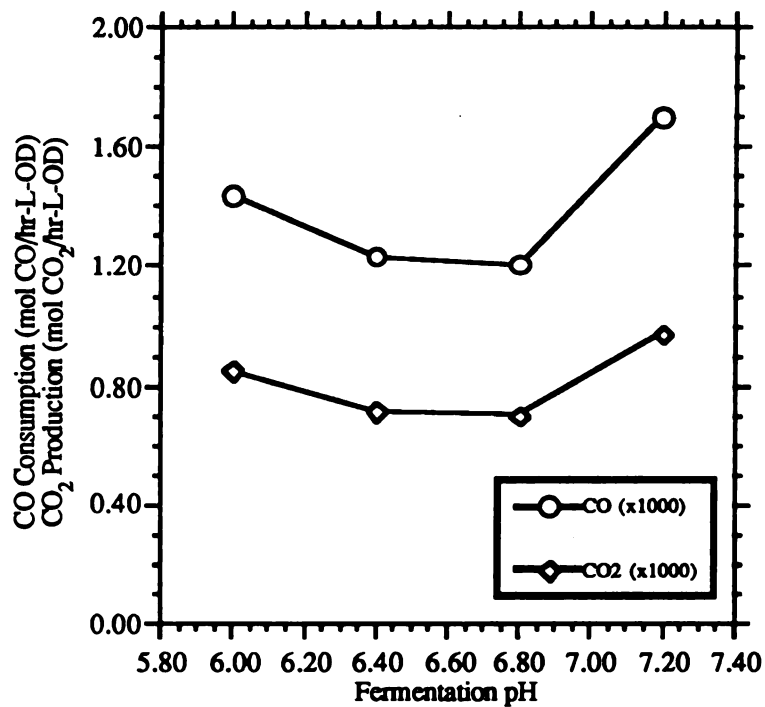


Figure 40. Normalized molar gas consumption and production rates as a function of pH during steady-state cell recycle fermentation: Case 2.

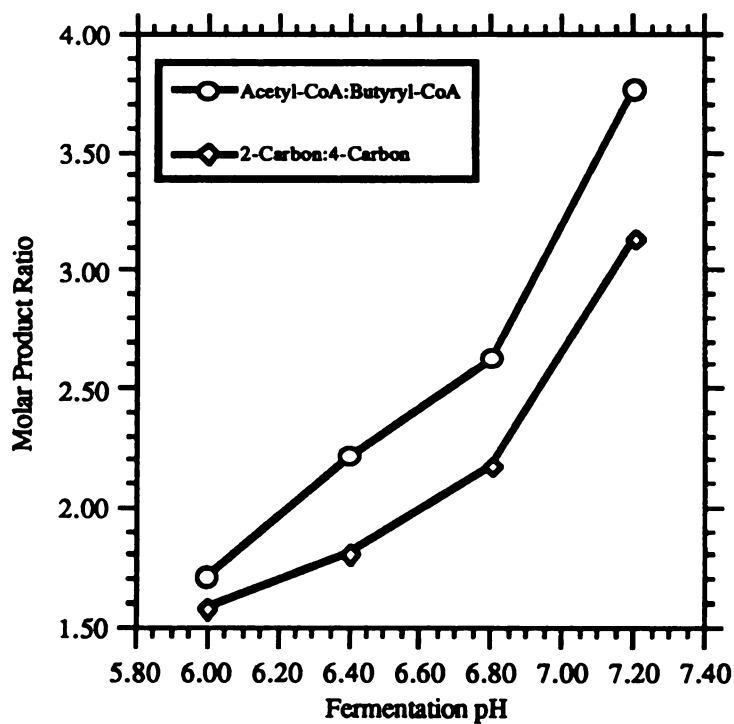


Figure 41. Molar product ratios as a function of pH during steady-state cell recycle fermentation: Case 2.

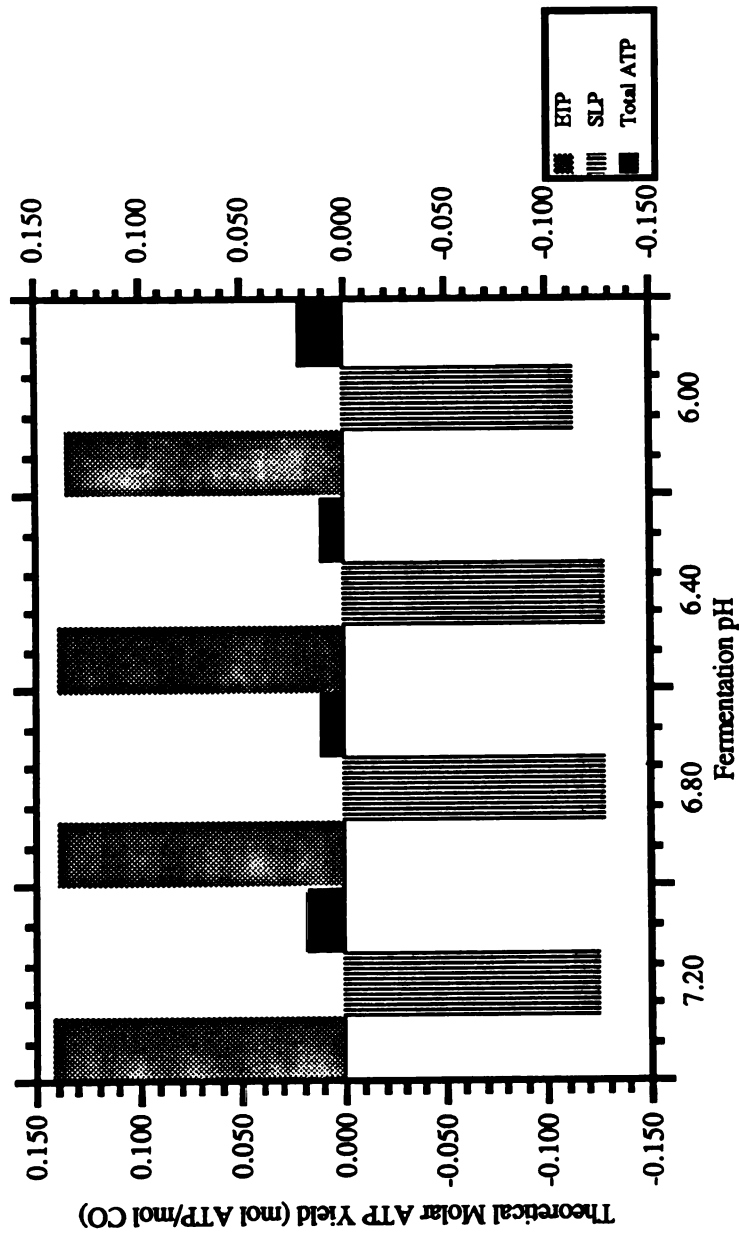
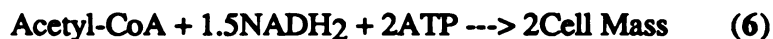


Figure 42. Theoretical molar ATP yields via electron-transport and substrate-level phosphorylation vs. pH during steady-state cell recycle fermentation: Case 2.

2 is highest at a pH of 6.0 and lowest at the intermediate values of 6.8 and 6.4. The actual data are, in moles ATP produced/moles CO consumed, 0.0175, 0.0111, 0.0116, and 0.0221 for the pH values of 7.2, 6.8, 6.4, and 6.0, respectively. The molar cell production of these same experiments was calculated as 0.000076, 0.000046, 0.000048, and 0.000019, for the pH values of 7.2, 6.8, 6.4, and 6.0, respectively, all in units of mol cells/hr·L·OD. The fermentation equation for cell mass production, which reflects an ATP consuming process, can thus be concluded to be an important equation in the cellular energetics, with decreased cell mass production resulting in a increase in ATP yield. This result is opposite to the effect of the relative decrease in acetate production as the fermentation pH is decreased during CO metabolism in *B. methylotrophicum*, which results in a decrease in the ATP yield. Under the conditions of this analysis, the relationship between these two antagonistic trends is complicated. Nevertheless, the coefficient for ATP in the cell mass equation



is therefore a critical value which requires careful derivation for accurate energetic analysis.

The majority of ATP obtained from the ETP mechanisms must be used to support the catabolic reactions which consume ATP via SLP. This point supports the argument for cosubstrate addition such as CH₃OH, which could alleviate the negative effect of SLP on the overall energetics of CO metabolism, but only in a relative manner, since decreases in the flow of electrons in the ETP cascade would result from relative decreases in CO consumption. This effect could well be analyzed by incorporating a cosubstrate reaction into the model system of equations. The calculated value for total NADH shown in Figure 43, which is multiplied by a factor of 10 in the graph, can be taken as the relative error of the solution set for this system, since the NADH balance must equal zero by the pseudo-steady state assumption. This closure of the system was achieved with high accuracy, as the relative error shown is approximately 3% in all cases.

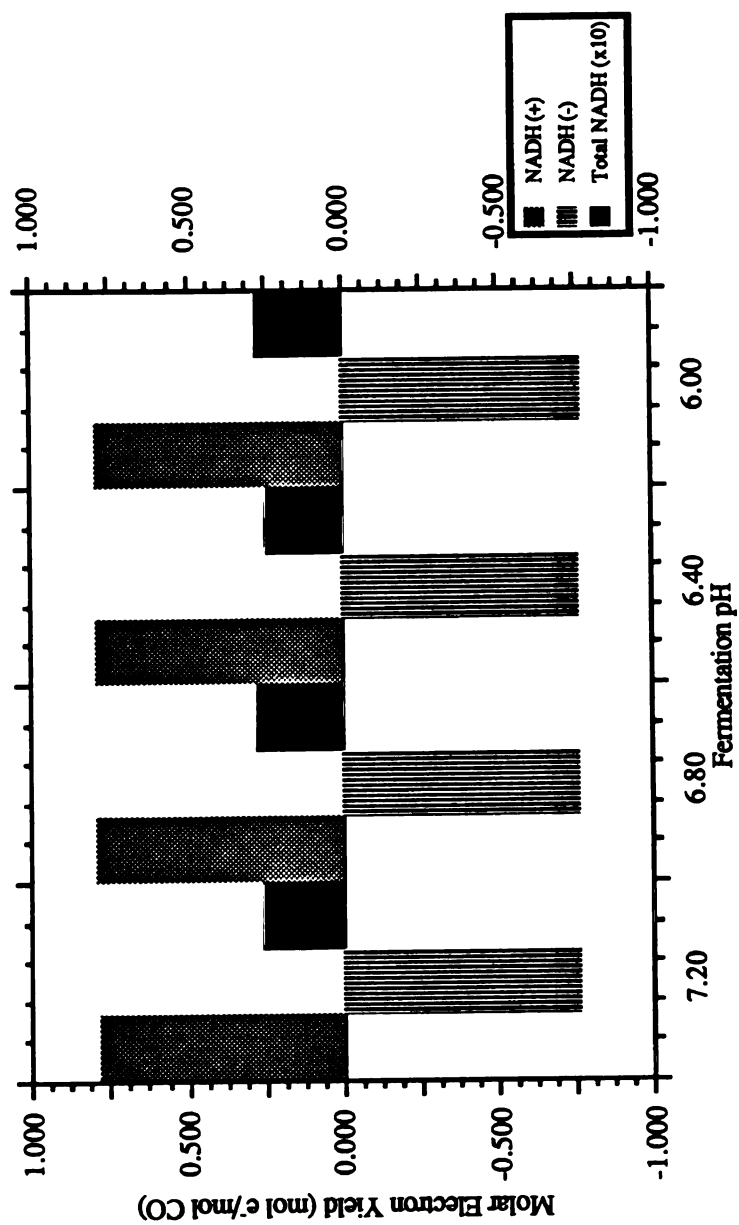


Figure 43. Molar electron yields as a function of pH during steady-state recycle fermentation: Case 2.

An important parametric study which was conducted with the Case 2 system of equations was the effect of the proton-translocating ATP synthase stoichiometry on the yields of ATP via ETP as a function of pH, and also on the total yield of ATP. This stoichiometry was assumed in all cases to be 3 protons for every mole of ATP produced. The effect of this stoichiometry was investigated by varying the ratio from 2.5-3.0, which are typical values (Niedhardt, 1987). The results of this study are shown in Figure 44. As shown, a constant increase in the proton/ATP ratio results in a linear decrease in both the ETP yield of ATP and also the overall ATP yield, as expected. Since the actual existence of ETP in *B. methylotrophicum* has not yet been conclusively proven, particularly as to the existence of a proton translocating ATP synthase, the choice of the proton/ATP ratio was not a significant factor in the development of this metabolic model.

5.4.3. Cases 3-5: Overspecified Systems

The use of overspecified systems when solving the fermentation system of equations can theoretically show the accuracy of the data, by selective overspecification comparison methods. In this study, there were only enough measured variables to completely specify the system. By using calculated values for cell mass production and CO consumption shown in Chapter 4, however, it is possible to overspecify the system of equations, and this is the focus of Cases 3-5. Solution of an overspecified system cannot be accomplished by row-reduction methods, but requires a least-squares solution of the form,

$$[A] [x] = [r]$$

$$[x] = (A^T A)^{-1} A^T [r]$$

where $[r]$ is the vector set of known reaction rates, $[A]$ a matrix of the system of equations, and $[x]$ the solution vector $a-j$.

The same analyses for Case 2 were conducted with Cases 3-5 except that in Case 3, the calculated value for CO consumption was used, in Case 4, the calculated value for cell mass production was used, and in Case 5, both calculated values were used. The validity of using values based on carbon and electron balances of the fermentation data is suspect,

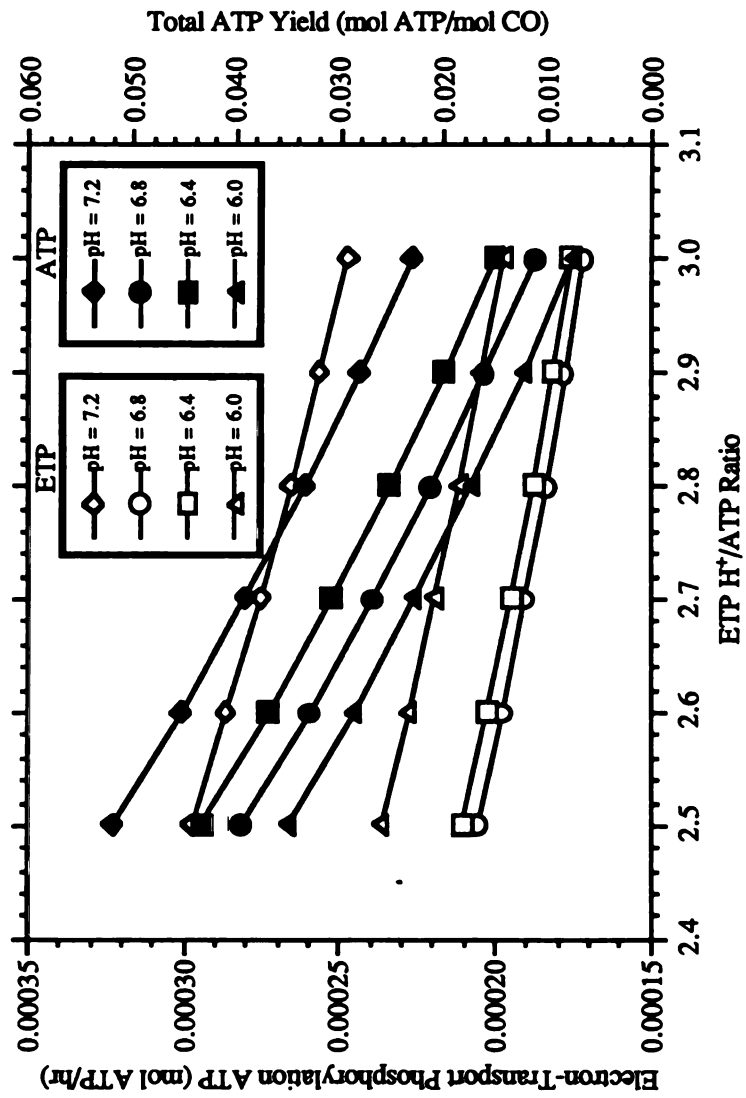


Figure 44. Electron-transport phosphorylation and total ATP yields as a function of ETP H^+/ATP ratio during steady-state, continuous cell recycle fermentation.

since the system of fermentation equations is itself a system of carbon and electron balances. For example, in Case 3, the specified ethanol production rate at a pH of 6.4 was 0.000006 mol/hr•L•OD, but the solution obtained gave a value of 0.000026 mol/hr•L•OD. In Case 4, the specified ethanol production rate at a pH of 7.2 was 0.000009 mol/hr•L•OD, but the solution obtained gave a value of 0.000085 mol/hr•L•OD. Other similar examples indicate that the electron balance in the system of equations was severely affected.

The overall results from the overspecified cases are shown in Figures 45, 46, 47, and 48. In Figure 45, the molar CO consumption and CO₂ production are shown to be invariant with respect to Case 2. In Figure 46, the 2-carbon to 4-carbon product ratios for Cases 3-5 are quite variant compared to Case 2, relatively invariant compared to each other at low pH, and variant compared to each other at high pH. Figure 47 shows the same trend, where compared to Case 2, the molar ATP yield is much higher in the overspecified cases, a result due primarily to calculated rates of cell mass formation which were much lower than in Case 2 at pH values above 6.0. As stated previously, the molar electron yield should equal zero because of the pseudo-steady state assumption invoked in the development of the metabolic model. Case 2 was shown to be relatively accurate in this regard. But, as seen in Figure 48, Cases 3-5 are more accurate, particularly at low pH, in achieving closure of the electron balance, a result due to the anomolous variations observed in the spread-sheet data. Therefore, although the accuracy of the the results for Cases 3-5 are good, the solutions for several of the specified parameters, as discussed above, where not consistent with the specifications used to solve the system of equations, and are thus not representative of the actual solution of that system.

5.5. Application to Unsteady-State Cell Recycle Fermentation Results

The system of fermentation equations used to solve for the steady-state reaction rates is equally applicable to the unsteady-state results in theory (Papoutsakis, 1984; Papoutsakis

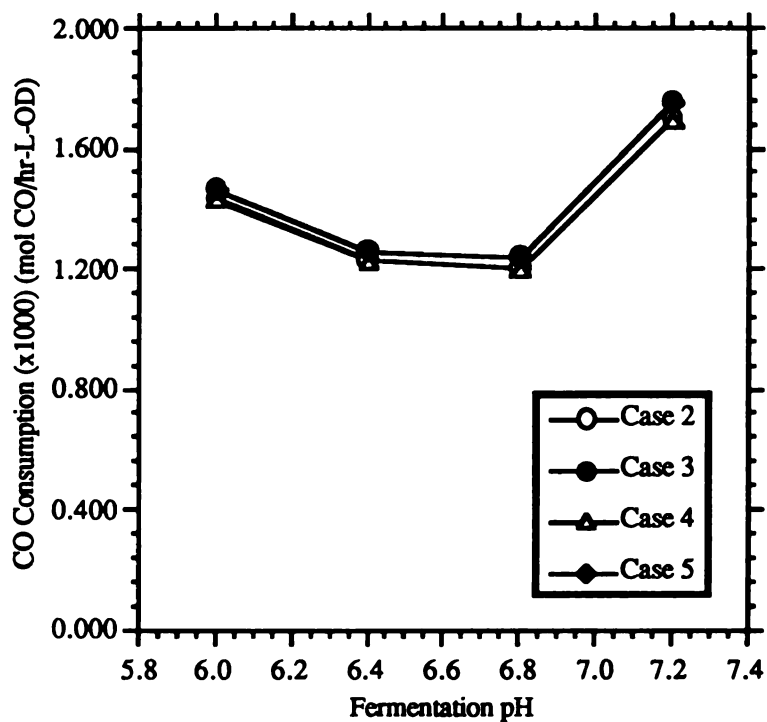


Figure 45. Molar CO consumption for Cases 2-5 as a function of pH during steady-state cell recycle fermentation.

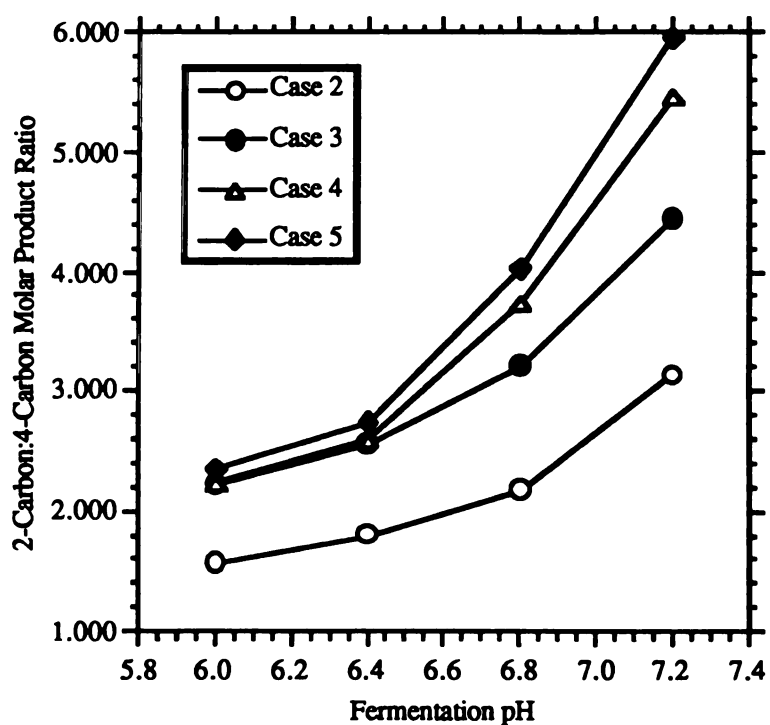


Figure 46. Molar product ratios for Cases 2-5 as a function of pH during steady-state cell recycle fermentation.

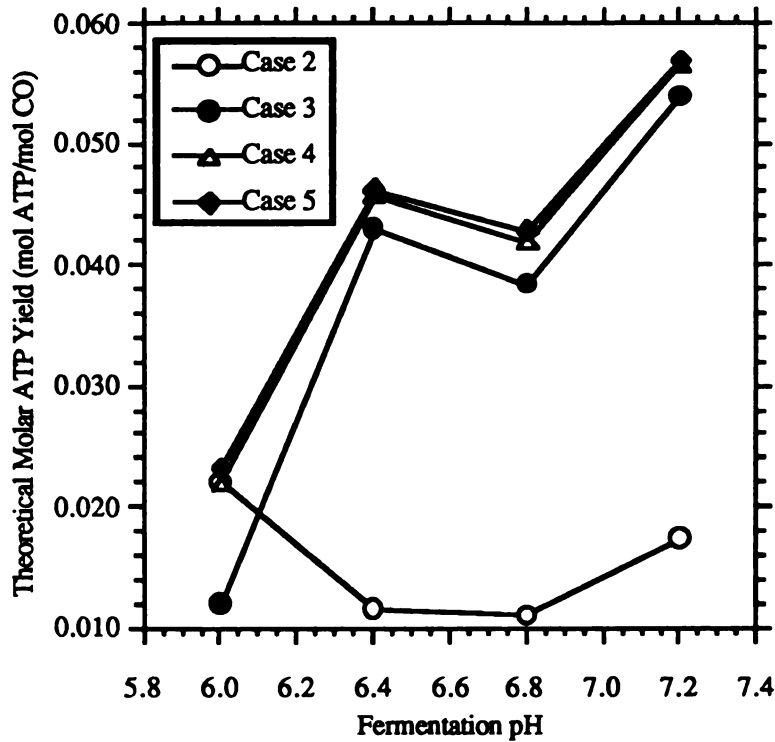


Figure 47. Theoretical molar ATP yields for Cases 2-5 as a function of pH during steady-state cell recycle fermentation.

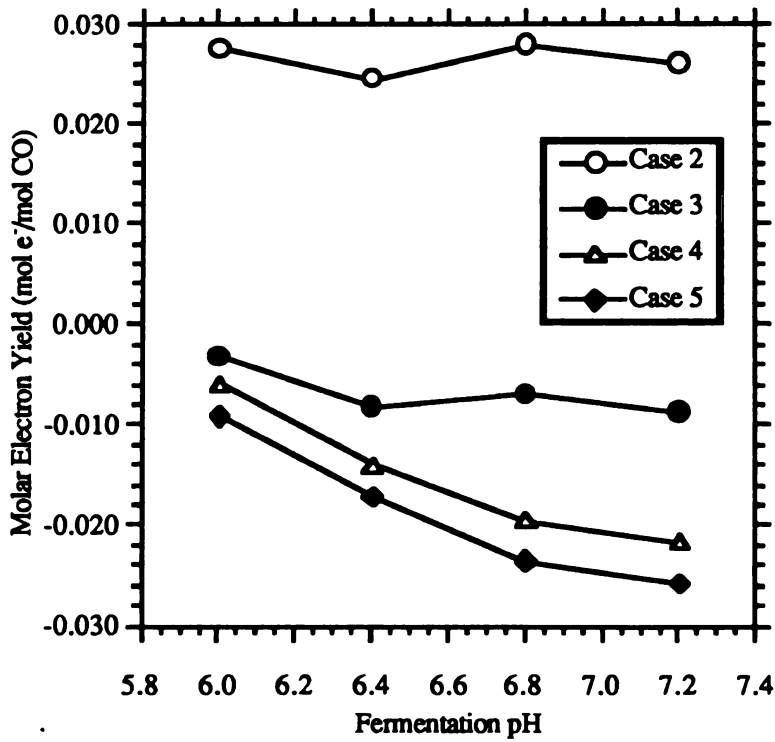


Figure 48. Theoretical molar electron yields for Cases 2-5 as a function of pH during steady-state cell recycle fermentation.

and Meyer, 1985a), but to do so requires more rate information from the fermentations. A generic mass balance on a continuous, constant volume reactor as a function of time is

$$V_R \cdot (dC/dt) = F_i C_i - F_o C_o + V_R R_G$$

where the subscripts i and o correspond to the flows in and out of the reactor, respectively, and where V_R is the reactor volume, C the concentration of the species, F the flow rates, and R_G the species generation or production term. Defining D , the liquid dilution rate, as F/V_R and assuming the concentration of species C in the incoming stream is 0, then

$$(dC/dt) = -DC_o + R_G$$

and at steady-state,

$$R_G = DC_o$$

which was the equation used to calculate the known rates of acetate, butyrate, ethanol, and butanol formation for the steady-state analysis above. In the unsteady-state case,

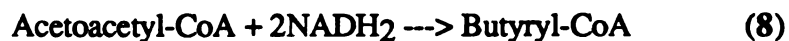
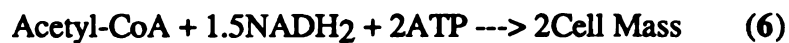
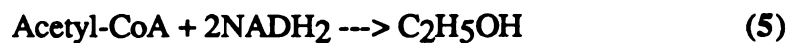
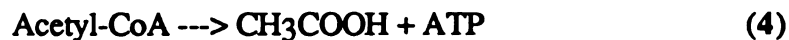
$$R_G = (dC/dt) - DC_o$$

and to solve this equation requires a value for dC/dt .

In an unsteady-state system, the terms in the above equation can potentially assume different values at each time point, or in the context of the cell recycle fermentation, at each data point. Therefore, to apply the system of fermentation equations and solve for the rates of reaction, not only will the values for dC/dt have to be obtained, but the system of equations will have to be solved for each separate data point. These complications distinguish the unsteady-state case from the steady-state case.

To obtain values for dC/dt , the fermentation data for each of the species from the cell recycle fermentation data at a pH of 5.5 were plotted separately as a function of time, similar to what was shown in Figure 28. The method of graphical differentiation was then applied to obtain dC/dt at each data point for each of the 5 species, acetate, butyrate, ethanol, butanol, and CO_2 . These data, along with the calculated values for DC_o at each point were used to solve the system of equations derived from





with solutions **a-j** for equations 1-10, and which was uniquely specified with the 5 independent equations

$$\text{NADH}_2 \quad : \quad (\mathbf{a} - 3\mathbf{b} - 2\mathbf{e} - 1.5\mathbf{f} - 2\mathbf{h} - 2\mathbf{j}) = 0$$

$$\text{CH}_3\text{O}^\bullet \quad : \quad (\mathbf{b} - \mathbf{c}) = 0$$

$$\text{Acetyl-CoA} \quad : \quad (\mathbf{c} - \mathbf{d} - \mathbf{e} - \mathbf{f} - \mathbf{g}) = 0$$

$$\text{Acetoacetyl-CoA} \quad : \quad (0.5\mathbf{g} - \mathbf{h}) = 0$$

$$\text{Butyryl-CoA} \quad : \quad (\mathbf{h} - \mathbf{i} - \mathbf{j}) = 0$$

and the rate data r_{Ac} , r_{Bu} , r_{Et} , r_{Bh} , and r_{CO_2} at each point. The solution set for this unique system (10 equations or knowns and 10 unknowns) is the same, since the system of equations is the same, as for Case 2, described above, namely

$$\mathbf{a} = r_{\text{CO}_2} + 3/7[r_{\text{Ac}} + r_{\text{Et}} + 2(r_{\text{Bu}} + r_{\text{Bt}}) + \Omega]$$

$$\mathbf{b} = 3/7[r_{\text{Ac}} + r_{\text{Et}} + 2(r_{\text{Bu}} + r_{\text{Bt}}) + \Omega] \quad \mathbf{c} = 3/7[r_{\text{Ac}} + r_{\text{Et}} + 2(r_{\text{Bu}} + r_{\text{Bt}}) + \Omega]$$

$$\mathbf{d} = r_{\text{Ac}} \quad \mathbf{e} = r_{\text{Et}} \quad \mathbf{f} = 3/7\Omega - 4/7(r_{\text{Ac}} + r_{\text{Et}} + 2r_{\text{Bu}} + 4r_{\text{Bh}})$$

$$\mathbf{g} = 2(r_{\text{Bu}} + r_{\text{Bh}}) \quad \mathbf{h} = r_{\text{Bu}} + r_{\text{Bh}} \quad \mathbf{i} = r_{\text{Bu}} \quad \mathbf{j} = r_{\text{Bh}}.$$

where $\Omega = 2/3(r_{\text{CO}_2} - 2r_{\text{Et}} - 2r_{\text{Bu}} - 4r_{\text{Bh}})$, and which were all obtained again by Gaussian elimination. This solution set allowed calculation, as a function of time, of all the same fermentation variables.

Shown in Figure 49 are the normalized CO consumption and CO₂ production values. Immediately it is evident that the fermentation at a pH of 5.5 cannot possibly be mass transfer limited, since the rate of CO consumption exhibits strong and distinct oscillations over the entire fermentation time-course. However, the maximum rates of CO consumption are comparable to those observed in the steady-state cases (Figure 40), on the order of 0.00125 mol/hr•L•OD. The production of CO₂ exhibits the same oscillatory phenomena. The molar yields of both butyrate and acetate were also calculated. Figures 50 and 51 show the molar acetate yield and molar butyrate yield as a function of time, respectively. Oscillations are also observed in these values, and thus normalization to the oscillating CO consumption rate does not dampen the oscillations in acetate and butyrate production rates. Finally, the theoretical molar ATP yields, normalized to the CO consumption rates, are shown in Figure 53. The ATP yield from the ETP contribution is constant over time, which is expected since this contribution is calculated from the single reaction in the system of equations,



and since the rate of CO₂ production is oscillating as a result of the oscillating rate of CO consumption, normalization of the ETP rate of ATP generation would be expected to dampen those oscillations. However, as seen in the figure, the ATP yields from SLP do show oscillations, and those oscillations are directly reflected in the oscillations in the total ATP yields. This result could be expected from the results seen in Figures 50 and 51, where the oscillations in acetate and butyrate production are independent of CO consumption, and thus the normalized SLP contribution, which is largely due to the contributions from the acid forming reaction steps, would not be dampened by oscillations in CO consumption.

From Figure 52, the overall theoretical ATP yield is negative over the entire time-course, which is not consistent with known biological phenomena. However, the magnitude of the ATP yields is consistent with those shown in Figure 42, particularly for

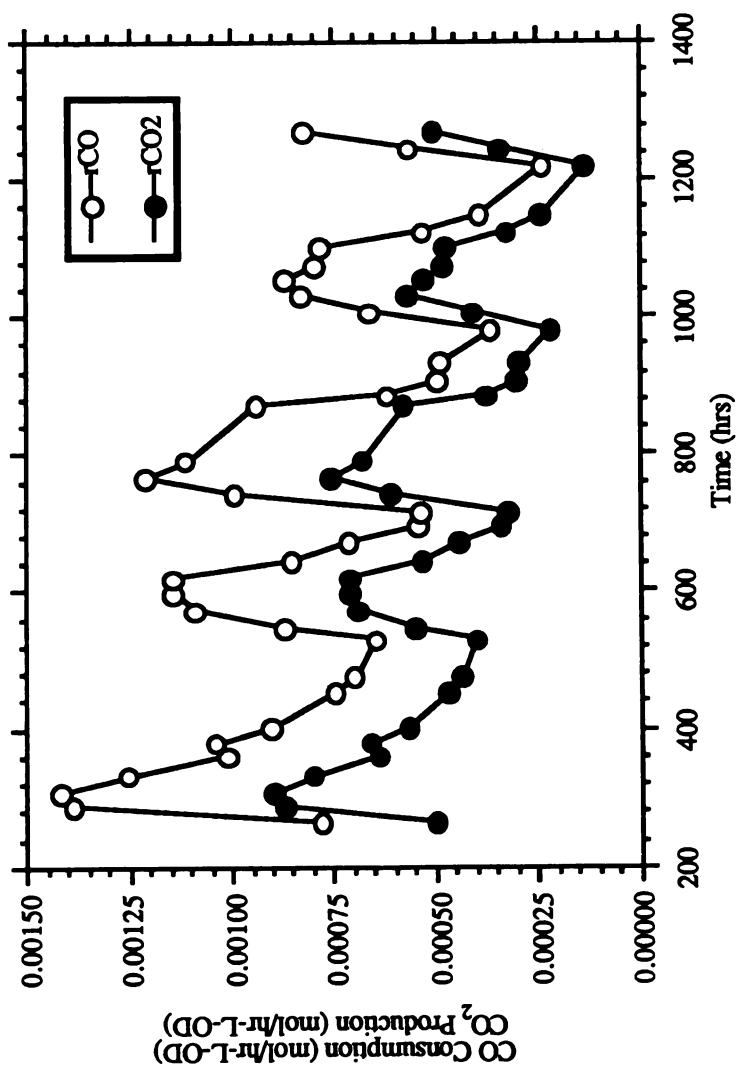


Figure 49. Normalized molar gas consumption and production rates as a function of time during unsteady-state cell recycle fermentation at a pH of 5.5.

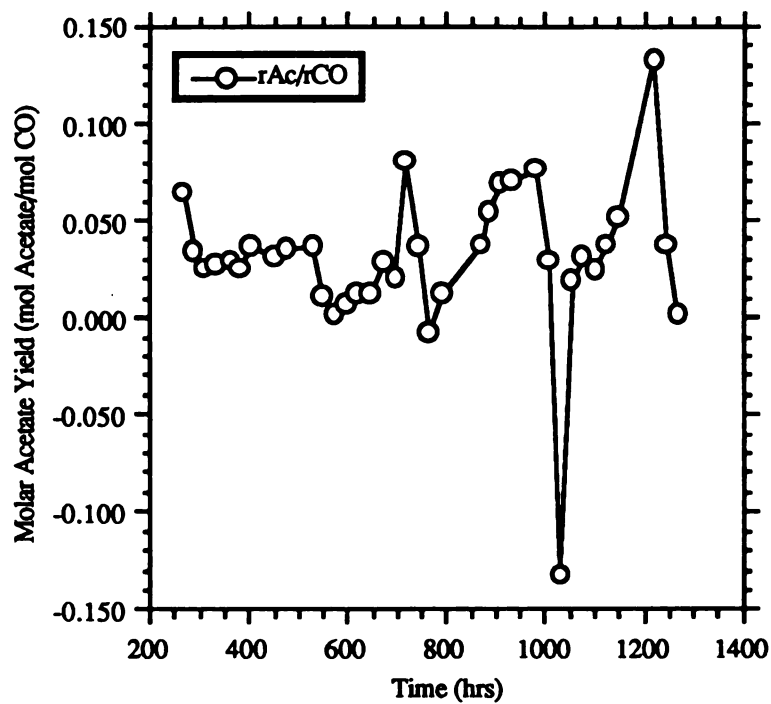


Figure 50. Molar yield of acetate during unsteady-state cell recycle fermentation at a pH of 5.5.

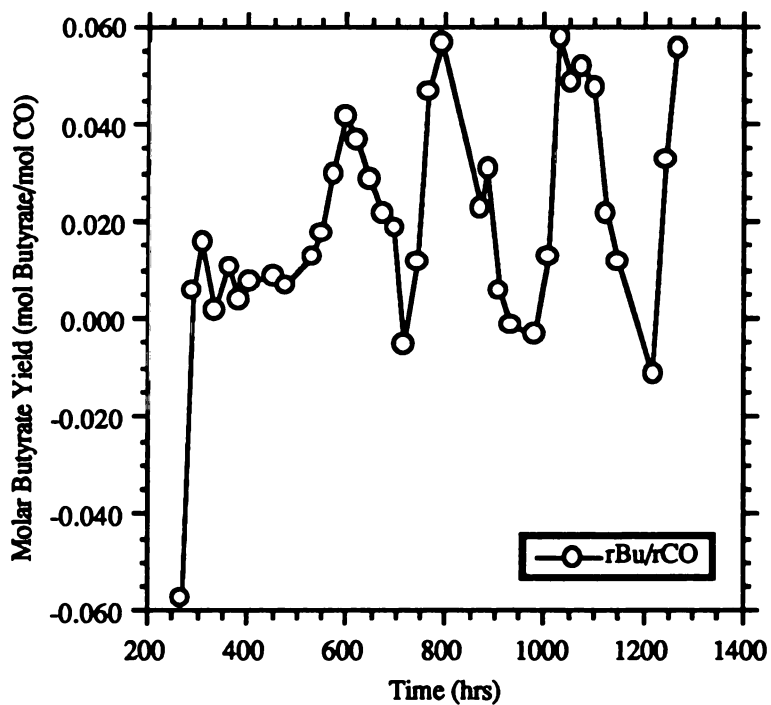


Figure 51. Molar yield of butyrate during unsteady-state cell recycle fermentation at a pH of 5.5.

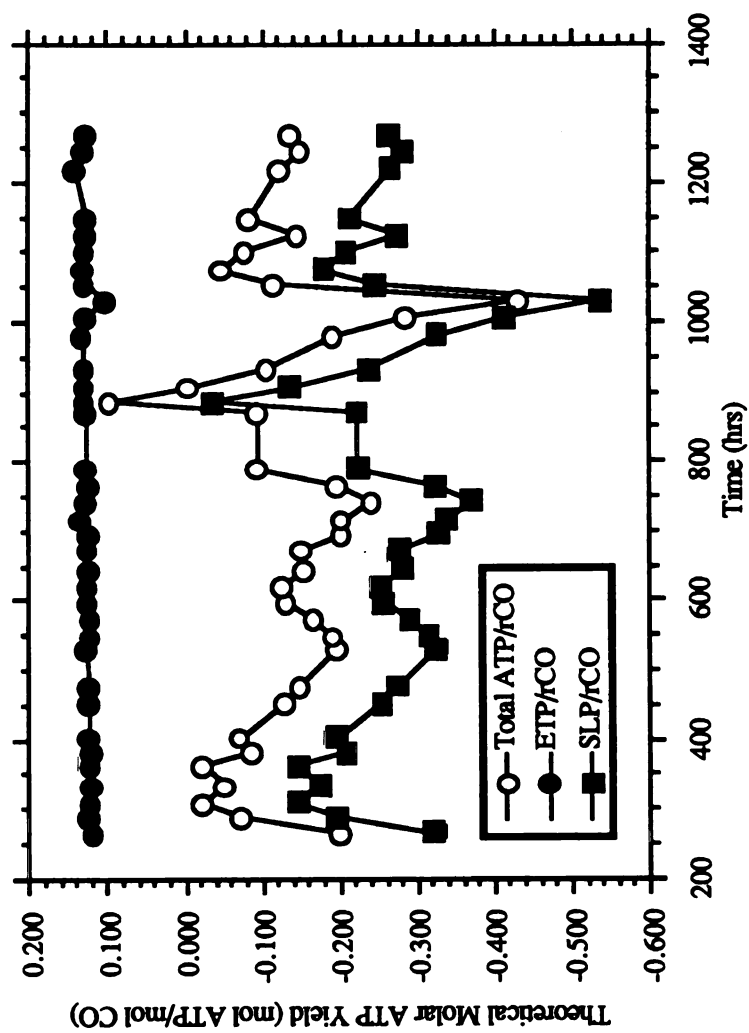
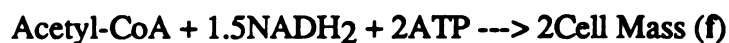


Figure 52. Theoretical molar ATP yields via electron-transport and substrate-level phosphorylation during unsteady-state cell recycle fermentation at a pH of 5.5.

the ETP contribution. Direct comparison with the results in Figure 42 at a pH of 6.0 show that the average SLP contribution is much less (more negative) at a pH of 5.5 than at a pH of 6.0, which is consistent with the reduced acetate production observed. It is therefore reasonable to assume that the negative ATP yield at a pH of 5.5 is not a result of the model, since the model accurately calculated the magnitudes of the ETP contribution and CO consumption rates. It is also apparent that the negative ATP yield cannot be a function of the chosen proton-translocating ATP synthase stoichiometry, since although that was shown to influence the contribution of ETP in Figure 44, the influence of that variable is not of the same magnitude as the changes observed in Figure 52. The possibility of an inaccuracy in the fermentation equation for cell mass production,



is one potential source of error, although the Case 2 system was solved with a high degree of accuracy using this equation.

One possible explanation for the negative theoretical ATP yields is that not all of the electron-transport mechanisms were included in the model. There has been some evidence (G. J. Shen and J. G. Zeikus, unpublished results) indicating that the electron carrier (X) for the reaction



is membrane bound, which is indirect support for its participation in an electron transport pathway. If true, then the energetics of butyrate production would be much more favorable than indicated in this study, due to the additional ATP generation from the ETP-linked step. Other mechanism of ATP synthesis, specifically solute-transport or monovalent ion-linked systems are also possible but purely speculative at this time.

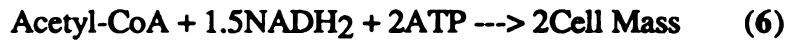
5.6. Limitations of the Model

The metabolic model developed for the cell recycle fermentation results has wide potential in conducting analysis of various fermentation pathways, both from CO and from

other substrates, in *B. methylotrophicum*. With the long-term nature of the typical CO fermentation, such a technique is invaluable. However, there are several limitations of this model, particularly in the assumptions and specifications used to develop the system of equations.

It is important to realize that although the energetic analysis was based on known metabolic pathways, such an analysis is no substitute for actual measurement of species such as ATP. This limitation is reflected in the term "theoretical", which is used as a qualification on the ATP yields presented in this chapter. In general, one can safely conclude the ATP yields calculated by the model are indicative of the general trends of ATP charge in the cell, but not reflective of the actual species concentrations.

The effect of the cell mass equation on the overall theoretical yields for ATP and electrons was found to be significant, particularly for the Case 2 results, where the ATP yield was greater at a pH of 6.0, presumably from a decrease in the production of cell mass. This equation,



requires more detailed development and analysis, both as to its applicability and to the specific values for the coefficients for NADH₂ and ATP. Results which were not shown have indicated that the coefficients are extremely important for calculation of cell mass production, since in all cases analyzed, equation 6 was used to solve the electron balance for NADH₂, where

$$\text{NADH}_2: (a - 3b - 2e - 1.5f - 2h - 2j) = 0,$$

or specifically,

$$(a - 3b - 2e - 2h - 2j) = 1.5f$$

which is why the cell production rates were not highlighted in this analysis.

Finally, the issue of applying a pseudo-steady state assumption to unsteady-state fermentation data requires more careful consideration, since the fluxes of NADH₂ (and potentially of all the intermediates) in the cell would be expected to change during

oscillations in CO consumption. The addition of another piece of data such as CO consumption could alleviate this problem by eliminating the need for reliance on the NADH₂ balance.

CHAPTER 6

CONCLUSIONS AND RECOMMENDATIONS

The research contained in this dissertation dealt with biological conversion of CO gas to acids and alcohols, using *Butyribacterium methylotrophicum*. The investigation was focused in three major areas: metabolic regulation and tolerance, cell recycle fermentation, and metabolic modeling. Several conclusions and observations were made during the course of this work, as discussed below.

Batch studies were conducted to determine the effect of H₂S on the growth and metabolism of *B. methylotrophicum*. H₂S concentrations in the range of those present in typical synthesis gas mixtures were examined. Growth rates and product compositions were unaffected by total liquid phase sulfide concentrations ranging from 0.0 to 2.0 mmol/L, which corresponds to an H₂S partial pressure of approximately 0-1.4%. An analysis of the effect of H₂S equilibrium partitioning, media pH, and gas-liquid equilibration rates on the experimental system was also conducted.

B. methylotrophicum can convert CO or hydrogen and carbon dioxide to acetic acid. Studies have shown that the CO metabolism of this organism can be shifted in favor of butyric acid and ethanol and butanol by lowering the fermentation pH. In this work, growing cells of *B. methylotrophicum* were incubated with CO gas under varying conditions of external alcohol concentration, acid concentration, and broth pH. Concentrations of ethanol and butanol above 3.0 g/L were found to be toxic to the cells. However, preliminary stationary phase experiments showed no inhibition at concentrations of 5 g/L and 7 g/L for ethanol and butanol, respectively. Under conditions of high pH and high acetate concentration (>8 g/L), *B. methylotrophicum* exhibited consumption of both CO and acetate, with net production of butyrate, butanol, ethanol and cell mass. Similarly, under conditions of high pH and moderate butyrate concentration (>2

g/L), *B. methylotrophicum* exhibited consumption of both CO and butyrate, with net production of acetate, butanol, ethanol and cell mass. These studies indicate that regulation of CO metabolism in *B. methylotrophicum* can be achieved in both the growth and stationary phases using a variety of environmental conditions.

Fermentation studies were conducted using a cell recycle system integrated with a chemostat to increase cell density and bias the cell population towards the stationary (resting) state. Results indicate three metabolic regimes for this system. Between pH values of 6.0 and 7.2, steady-state operation was achieved, and a 5-10 fold increase in acid and alcohol production was observed relative to chemostat operation without cell recycle. At pH values of 5.75 and 5.5, oscillations in butyrate and acetate production were observed, with relatively steady alcohol production. Importantly, butanol was the major product over a 72 hour period during initial start-up of the continuous cell recycle system. At pH values of 5.35 and 5.1, the cells exhibited a death phase response. These results have demonstrated that during high cell density, high productivity CO fermentation, fermentation pH induces specific metabolic responses. Furthermore, these responses give insight to the mechanisms controlling product formation, specifically 4-carbon products, directly from CO gas.

A metabolic model was developed to analyze the cell recycle fermentation data. This comprised a system of linear equations based on known metabolic pathways for CO metabolism in *B. methylotrophicum*. The model incorporated a hypothetical reaction for generation of ATP via electron-transport phosphorylation, as well as known substrate-level phosphorylation routes for ATP synthesis. The theoretical molar yields for ATP were shown to be a function of fermentation pH, and to be strongly dependent on the rate of cell mass production. ETP was concluded to be a required portion of the overall energetics, based on the energetic analysis of steady-state results. A preliminary analysis of unsteady-state results suggested that further, as yet unknown ATP generating pathways, either ETP-based or via some other mechanism, must be present in *B. methylotrophicum*. Oscillations

in net theoretical ATP yields were shown to be concomitant with oscillations in acetate and butyrate formation, indicating that the net ATP charge could play a regulatory role in directing carbon and electron flow during CO metabolism.

The mechanism of the pH effect, where low pH values inhibit acetate formation and cell growth, is complicated and not fully understood. A case for mass-action effects, or feedback inhibition of acetate formation, was presented based on known regulation mechanisms in other organisms. This mechanism presumes the regulatory species is the protonated form of the acid, and thus regulation of metabolism is a function of both concentration and of pH. Since formation of acetate is the main reaction contributing to ATP synthesis via SLP, the regulatory effects of pH and of ATP charge, if present, would be interdependent. Although the data support this theory, confirmation of the several hypotheses requires a biochemical analysis of both carbon and electron flow and of the cellular energetics.

Experimentally, several improvements in the present system are needed for further development, both of which center on data acquisition. By far, the major limitation with the present work is the reliance on carbon and electron balances for calculation of key fermentation parameters such as cell mass production, CO uptake, and CO₂ production. The use of an inert tie-component in the gas substrate, to allow calculation of CO and CO₂ gas partial pressures, is a potential solution to this issue. One study that is of paramount importance is a parametric sensitivity analysis on the fermentation equation for cell mass production used in the metabolic model. Small variations in the magnitudes of the coefficients for electron and ATP requirements can potentially result in large differences for calculated reaction rates, based on the electron balance for NADH. The equation for cell mass production should thus be closely examined and its accuracy confirmed.

The success of the cell recycle fermentations in increasing fermentation productivity, roughly 8-10 fold, and of elucidating a capacity for primary production of butanol from CO gas, has greatly enhanced the potential of the synthesis gas bioconversion concept.

However, there are still several important issues which must be addressed for this system, most of which deal with the reaction rate for CO uptake. Other organisms have exhibited much faster rates of growth and product formation from CO, but produced only acetate and ethanol. A strong potential exists for finding an organism capable of high CO uptake rates as well as formation of 4-carbon products such as butyrate and butanol. Thus, an isolation effort directed at finding new and improved microorganisms may be the most promising direction for future work.

Another area of research with some promise is in the use of cosubstrates such as methanol during CO metabolism, or perhaps just methanol alone. These approaches would facilitate increases in reaction rates, and are not outside the realm of synthesis gas feedstock utilization. A specific methanol to butanol fermentation would perhaps be the goal of such work, since acetate from methanol and CO is already well established commercially. *B. methylotrophicum* has exhibited the versatility for such approaches. However, whether with *B. methylotrophicum* or some other organism, the ultimate potential for biological conversion of synthesis gas will require further development for such processes to become a commercial reality, in the face of current chemical technology.

APPENDIX

APPENDIX

Review of the Carbon and Electron Balancing Method

The method of carbon and electron balancing for determination of biological fermentation stoichiometries is a powerful tool when data for consumption or production of one or two species is unavailable. These balances also allow calculation of carbon and electron recovery in the fermentation products. Carbon balancing, as detailed below, is simply a material balance on the reaction, based on the moles of carbon atoms reacted. Electron balancing is a balance on the available electron equivalents and is analogous to an energy balance on the fermentation reaction.

Specifically, electron balances are derived from molecular energy changes associated with changes in oxidation number due to electron transfer between species. The atomic oxidation number is characteristic of the valence electron(s) of the atom, which stoichiometrically guide the reaction and which for carbon containing compounds can assume several values. The energy content of carbohydrate molecules is related to the oxidation number, with highly reduced compounds being energy-rich. Changes in oxidation number arise from electron transfer between species, often coupled to redox reactions involving electron carriers such as NADH.

Within this setting, the reductance degree of a compound is defined as the number of electrons available for transfer in oxidative catabolism, and is established on a basis of one gram atom carbon. For atoms, several reductance degrees are,



and thus for several compounds can be calculated as



and *ad infinitum*. The reductance degree therefore forms a basis for energy balancing biological reactions where the total electrons supplied by the reactants, or substrates, must equal the total electrons obtained by the products. The material balance for carbon is also achieved in this fashion.

As a specific example related to calculations made during this study, the carbon and electron balances for a 100% CO batch fermentation will be illustrated. Fermentation data include product concentrations of acetic acid, butyric acid, and cell mass, but no data is obtained for CO consumption and CO₂ production. For this anaerobic reaction, a typical stoichiometry is of the form



where the lower case letters represent total moles of each species, with the cell mass term expressed with a molecular formula based on one gram-mole of carbon. If this general reaction is balanced with respect to available electron contents, with the Cells term having a previously derived value of 4.21 for *B. methylotrophicum*, the resulting equation is

$$a(2) + b(0) + c(0) \rightarrow d(0) + e(8) + f(20) + g(4.21)$$

which is equivalent to

$$a(2) \rightarrow e(8) + f(20) + g(4.21).$$

The product concentration data for acetate, butyrate, and cell mass is then converted to total moles and inserted in this equation, where

$$a(2) \rightarrow 0.10(8) + 0.0031(20) + 0.015(4.21)$$

and the value for **a**, the total moles CO consumed, calculated. This value is

$$\mathbf{a} = 0.4624 \text{ moles CO consumed.}$$

If the reaction is then balanced with respect to carbon, the equation is of the form



which upon insertion of the total carbon atoms in each molecular formula yields

$$a(1) \rightarrow d(1) + e(2) + f(4) + g(1).$$

The product data is then inserted and the value of **b**, the moles CO₂ produced, calculated from

$$0.4624(1) \rightarrow d(1) + 0.10(2) + 0.0031(4) + 0.015(1)$$

which yields

$$b = 0.2350 \text{ moles CO}_2 \text{ consumed.}$$

The overall carbon and electron balance for the fermentation can now be normalized to an arbitrary amount of substrate, in this case 4 moles of CO, which results in a final fermentation balance of



which is a representative balance derived for 100% CO batch fermentation.

LIST OF REFERENCES

LIST OF REFERENCES

- Abbanat, D. R. and J. G. Ferry. 1990. Synthesis of Acetyl Coenzyme A by Carbon Monoxide Dehydrogenase Complex from Acetate-Grown *Methanosarcina thermophila*. *J. Bacteriol.* 172:7145-7150.
- Agreda, V. H. 1988. Acetic Anhydride from Coal. *Chemtech.* Apr:250-253.
- Baer, S. H., H. P. Blaschek, and T. L. Smith. 1987. Effect of Butanol Challenge and Temperature on Lipid Composition and Fluidity of Butanol-Tolerant *Clostridium acetobutylicum*. *Appl. Environ. Microbiol.* 53:2854-2861.
- Bajpai, R. K. and E. Iannotti. 1988. In Handbook on Anaerobic Fermentations, L. E. Erickson and D. Yee-Chak Fung, eds., Marcel Dekker, Inc., New York, pp. 207-241.
- Barik, S., S. Prieto, S. B. Harrison, E. C. Clausen, and J. L. Gaddy. 1988. Biological Production of Alcohols from Coal Through Indirect Liquefaction. *Appl. Biochem. Biotechnol.* 18:363-378.
- Barker, H. A. 1944. *Butyribacterium*, a New Genus of Gram-Positive Nonsporulating Anaerobic Bacteria of Intestinal Origin. *J. Bacteriol.* 47:301-305.
- Baronofsky, J. J., W. J. A. Schreurs, and E. R. Kashket. 1984. Uncoupling by Acetic Acid Limits the Growth of and Acetogenesis by *Clostridium thermoaceticum*. *Appl. Environ. Microbiol.* 48:1134-1139.
- Bassler, E. J. and R. G. Sperhac. 1986. Recommendations for a U.S. Synthetic Fuels Policy. *Energy Progress.* 6:197-199.
- Bauchop, T. and S. R. Elsdon. 1960. The Growth of Microorganisms in Relation to Their Energy Supply. *J. Gen. Microbiol.* 23:457-469.
- Bloomstran, M. A. and B. E. Davis. 1984. Opportunities in Underground Coal Gasification. *Energy Progress.* 4:74-77.
- Bonzel, H. P. and R. Ku. 1973. Adsorbate Interactions on a Pt(110) Surface. I. Sulfur and Carbon Monoxide. *J. Chem. Physics.* 58:4617-4624.
- Bowles, L. K. and W. L. Ellefson. 1985. Effects of Butanol on *Clostridium acetobutylicum*. *Appl. Environ. Microbiol.* 50:1165-1170.

- Braun, M., F. Mayer, and G. Gottshalk. 1981. *Clostridium aceticum* (Wieringa), a Microorganism Producing Acetic Acid from Molecular Hydrogen and Carbon Dioxide. *Arch. Microbiol.* 128:288-293.
- Brock, T. D., D. W. Smith, and M. T. Madigan. 1984. Biology of Microorganisms. Prentice-Hall, Inc., Englewood Cliffs, NJ.
- Carroll, J. J. 1990. Reliably Predict the Solubility of H₂S in Water. *Chem. Eng.* Oct:227-229.
- Chinchen, G. C., Mansfield, K., and M. S. Spencer. 1990. The Methanol Synthesis: How Does It Work? *Chemtech.* Nov:692-699.
- Clark, J. E., S. W. Ragsdale, L. G. Ljungdahl, and J. Wiegel. 1982. Levels of Enzymes Involved in the Synthesis of Acetate from CO₂ in *Clostridium thermoautotrophicum*. *J. Bacteriol.* 151:507-509.
- Conn, A. L. 1981. Why Synthetic Fuels? *Energy Progress.* 1:62-67.
- Cumare, F. E., R. E. Meissner III, and J. B. Hamlin. 1984. Sulfur Management of Coal Processing Complexes. *Energy Progress.* 4:205-213.
- Daniels, L., G. Fuchs, R. K. Thauer, and J. G. Zeikus. 1977. Carbon Monoxide Oxidation by Methanogenic Bacteria. *J. Bacteriol.* 132:118-126.
- Das, A., J. Hugenholtz, H. van Halbeek, and L. G. Ljungdahl. 1989. Structure and Function of a Menaquinone Involved in Electron Transport in Membranes of *Clostridium thermoautotrophicum* and *Clostridium thermoaceticum*. *J. Bacteriol.* 171:5823-5829.
- Datta, R. 1981. Production of Organic Acid esters from Biomass-Novel Processes and Concepts. *Biotechnol. Bioeng. Symp.* 11:521-532.
- Datta, R. and J. G. Zeikus. 1982. Anaerobic Bioconversion of One-Carbon Compounds. *Dev. Ind. Microbiol.* 23:131-140.
- Datta, R. and J. Ogletree. 1983. Methanol Bioconversion by *Butyribacterium methylotrophicum* - Batch Fermentation Yield and Kinetics. *Biotechnol. Bioeng.* 25:991-998.
- Datta, R. and G. F. Andrews. 1991. Mass and Energy Balances for Coal-Based Microbial

Systems. Second International Symposium on the Biological Processing of Coal, Workshop 2. May 1-3, San Diego, CA.

Diekert, G. B. and R. K. Thauer. 1978. Carbon Monoxide Oxidation by *Clostridium thermoaceticum* and *Clostridium formicoaceticum*. *J. Bacteriol.* **136**:597-606.

Diekert, G. B., E. G. Graf, and R. K. Thauer. 1979. Nickel Requirement for Carbon Monoxide Dehydrogenase Formation in *Clostridium pasteurianum*. *Arch. Microbiol.* **122**:117-120.

Diekert, G. B. and M. Ritter. 1982. Nickel Requirement of *Acetobacterium woodii*. *J. Bacteriol.* **151**:1043-1045.

Diekert, G. B., G. Fuchs, and R. K. Thauer. 1985. Properties and Function of Carbon Monoxide Dehydrogenase from Anaerobic Bacteria. In Microbial Gas Metabolism, R. K. Poole and C. S. Dow, eds., Academic Press, London, pp. 115-130.

Drake, H. L., S. Hu, and H. G. Wood. 1980. Purification of Carbon Monoxide Dehydrogenase, a Nickel Enzyme from *Clostridium thermoaceticum*. *J. Biol. Chem.* **255**:7174-7180.

Drake, H. L. 1982a. Occurrence of Nickel in Carbon Monoxide Dehydrogenase from *Clostridium pasteurianum* and *Clostridium thermoaceticum*. *J. Bacteriol.* **149**:561-566.

Drake, H. L. 1982b. Demonstration of Hydrogenase in Extracts of the Homoacetate-Fermenting Bacterium *Clostridium thermoaceticum*. *J. Bacteriol.* **150**:702-709.

Dry, D. E. 1981. Catalysis: Science and Technology, J. J. Anderson and M. Boudart, eds., Springer-Verlag, Berlin, Vol. 1, pp. 159-256.

Dry, D. E. 1987. In Industrial Chemicals via C₁ Processes, D. R. Fahey, ed., ACS Symposium Series 328, ACS, Washington, DC, pp. 18-34.

Ecklund, E. E. and G. A. Mills. 1989a. Alternative Fuels: Progress and Prospects-Part 1. *Chemtech.* **Sept**:549-556.

Ecklund, E. E. and G. A. Mills. 1989b. Alternative Fuels: Progress and Prospects-Part 2. *Chemtech.* **Oct**:626-631.

Ehrler, J. L. and B. Juran. 1983. The Future of C₁ Chemistry. *Chemtech.* **Mar**:188-192.

- Eickmeyer, A. G. and H. A. Gangriwala. 1981. Acid Gas Removal in Synfuels Production. *Energy Progress*. 1:9-12.
- Elliott, J. I. and L. G. Ljungdahl. 1982. Isolation and Characterization of an Fe-S₂ Ferredoxin (Ferredoxin II) from *Clostridium thermoaceticum*. *J. Bacteriol.* 151:328-333.
- Erickson, L. E., J. G. Minkevich, and V. K. Eroshin. 1978. Application of Mass and Energy Balance Regularities in Fermentation Processes. *Biotechnol. Bioeng.* 20:1595-1621.
- Erickson, L. E. and M. D. Oner. 1983. Available Electron and Energetic Yields in Fermentation Processes. *Ann. NY Acad. Sci.* 413:99-113.
- Exxon Company, USA. 1979. Energy Outlook 2000. Houston, TX.
- Frank, M. E. 1982. Methanol: Emerging Uses, New Syntheses. *Chemtech.* June:358-362.
- Fuchs, G., U. Schnitker, and R. K. Thauer. 1974. Carbon Monoxide Oxidation by Growing Cultures of *Clostridium pasteurianum*. *Eur. J. Biochem.* 49:111-115.
- Fuchs, G. 1986. CO₂ Fixation in Acetogenic bacteria: Variations on a Theme. *FEMS Microbiology Reviews.* 39:181-213.
- Goar, B. G. 1986. Sulfur Recovery Technology. *Energy Progress.* 6:71-75.
- Gottwald, M., J. R. Andreessen, J. LeGall, and L. G. Ljungdahl. 1975. Presence of Cytochrome and Menaquinone in *Clostridium formicoaceticum* and *Clostridium thermoaceticum*. *J. Bacteriol.* 122:325-328.
- Grethlein, A. J. 1989. Bioconversion of Carbon Monoxide for production of Mixed Acids and Alcohols. MS Thesis, Dept. of Chemical Engineering, Michigan State University, East Lansing, MI.
- Grethlein, A. J., R. M. Worden, M. K. Jain, and R. Datta. 1990. Continuous Production of Mixed Alcohols and Acids from Carbon Monoxide. *Appl. Biochem. Biotechnol.* 24/25:875-884.
- Grethlein, A. J., R. M. Worden, B. K. Soni, M. K. Jain, and R. Datta. 1991a. Influence of Hydrogen Sulfide on the Growth and Metabolism of *Butyrivibrio*

methylophilum and *Clostridium acetobutylicum*. *Appl. Biochem. Biotechnol.* In Press.

Grethlein, A. J., R. M. Worden, M. K. Jain, and R. Datta. 1991b. Evidence for production of n-Butanol from Carbon Monoxide by *Butyribacterium methylophilum*. *J. Ferm. Bioeng.* In Press.

Grethlein, H. E. and L. R. Lynd. 1986. Distillation Systems and Methods. US Patent 4,626,321., December 2.

Haggin, J. 1981a. C1 Chemistry Development Intensifies. *Chem. Eng. News*. Feb. 23, 59:39-47.

Haggin, J. 1981b. Fischer-Tropsch: New Life for Old Technology. *Chem. Eng. News*. Oct. 26, 59:22-32.

Haggin, J. 1986. C1 Chemistry: Growing Field Despite Crude Oil Price Drop. *Chem. Eng. News*. May 19, 64:7-13.

Haggin, J. 1991. Coal. *Chem. Eng. News*. June 17, 69:20-31.

Hammesfahr, F. W. and P. L. Winter. 1984. Underground Coal Gasification: The Leading Technology for Lower-Priced Gas from Coal. *Energy Progress*. 4:193-195.

Hartmanis, M. G., T. Klason, and S. Gatenbeck. 1984. Uptake and Activation of Acetate and Butyrate in *Clostridium acetobutylicum*. *Appl. Microbiol Biotechnol.* 20:66-71.

Hatanaka, H., E. Wang, M. Taniguchi, S. Iijima, and T. Kobayashi. 1988. Production of Vitamin B₁₂ by a Fermentor with a Hollow-Fiber Module. *Appl. Microbiol. Biotechnol.* 27:470-473.

Hegedus, L. L. and R. W. McCabe. 1981. Catalyst Poisoning. *Catal. Rev. Sci. Eng.* 23:377-476.

Hermann, M., F. Fayolle, R. Marchal, L. Podvin, M. Sebald, and J. P. Vandecasteele. 1985. Isolation and Characterization of Butanol-Resistant Mutants of *Clostridium acetobutylicum*. *Appl. Environ. Microbiol.* 50:1238-1243.

Heubler, J. and J. C. Janka. 1980. In Kirk-Othmer Encyclopedia of Chemical Technology, 3rd ed., John Wiley and Sons, New York, 11:410-446.

- Horowitz, W. H. and M. P. Bryant. 1984. *Peptostreptococcus productus* Strain That Grows Rapidly with CO as the Energy Source. *Appl. Environ. Microbiol.* **47**:961-964.
- Hugenholtz, J. and L. G. Ljungdahl. 1989. Electron Transport and Electrochemical Proton Gradient in Membrane Vesicles of *Clostridium thermoautotrophicum*. *J. Bacteriol.* **171**:2873-2875.
- Iborra, M., J. F. Izquierdo, J. Tejero, and F. Cunill. 1988. Getting the Lead Out with Ethyl Tert-Butyl Ether. *Chemtech.* **Feb**:120-122.
- Imler, D. L. 1985. An Update on the Great Plains Coal Gasification Project. *Energy Progress.* **5**:226-228.
- Ivey, D. M. and L. G. Ljungdahl. 1986. Purification and Characterization of the F₁-ATPase from *Clostridium thermoaceticum*. *J. Bacteriol.* **165**:252-257.
- Kalfadelis, C. D. and H. Shaw. 1980. In Kirk-Othmer Encyclopedia of Chemical Technology, 3rd ed., John Wiley and Sons, New York, **11**:447-489.
- Keim, W. 1987. In Industrial Chemicals via C₁ Processes, D. R. Fahey, ed., ACS Symposium Series 328, ACS, Washington, DC, pp. 1-16.
- Kenealy, W. R., T. E. Thompson, K. R. Schubert, and J. G. Zeikus. 1982. Ammonia Assimilation and Synthesis of Alanine, Aspartate, and Glutamate in *Methanosarcina barkeri* and *Methanobacterium thermoautotrophicum*. *J. Bacteriol.* **150**:1357-1365.
- Kerby, R. and J. G. Zeikus. 1983. Growth of *Clostridium thermoaceticum* on H₂/CO₂ or CO as Energy Source. *Curr. Microbiol.* **8**:27-30.
- Kerby, R., Niemczura, W., and J. G. Zeikus. 1983. Single-Carbon Catabolism in Acetogens: Analysis of Carbon Flow in *Acetobacterium woodii* and *Butyribacterium methylotrophicum* by Fermentation and ¹³C Nuclear Magnetic Resonance Measurement. *J. Bacteriol.* **155**:1208-1218.
- Kerby, R. and J. G. Zeikus. 1987a. Anaerobic Catabolism of Formate to Acetate and CO₂ by *Butyribacterium methylotrophicum*. *J. Bacteriol.* **169**:2063-2068.
- Kerby, R. and J. G. Zeikus. 1987b. Catabolic Enzymes of the Acetogen *Butyribacterium methylotrophicum* Grown on Single-Carbon Substrates. *J. Bacteriol.* **169**:5605-5609.

- King, D. L., J. A. Cusumano, and R. L. Garten. 1981. A Technological Perspective for Catalytic Processes Based on Synthesis Gas. *Catal. Rev. Sci. Eng.* 23:233-263.
- Kolaian, J. H. and W. G. Schlinger. 1982. The Texaco Coal Gasification Process. *Energy Progress.* 2:228-233.
- Lee, H. H. 1985. Heterogeneous Reactor Design. Butterworth Publishers, Boston, MA.
- Lepkowski, W. 1991. Energy Policy. *Chem. Eng. News*. No. 24, 69:20-31.
- Linden, J. C. 1988. In Handbook on Anaerobic Fermentations, L. E. Erickson and D. Yee-Chak Fung, eds., Marcel Dekker, Inc., New York, pp. 59-80.
- Ljungdahl, L. G. 1986. The Autotrophic Pathway of Acetate Synthesis in Acetogenic Bacteria. *Ann. Rev. Microbiol.* 40:415-450.
- Loubiere, P., C. Mariotto, G. Goma, and N. D. Lindley. 1986. Application of the Physiological Characteristics of the Methylophilic Metabolism of *Eubacterium limosum* To Improve the Biotechnological Production of Butyric Acid. In Biology of Anaerobic Bacteria, H. C. Dubourguier, ed., Elsevier Science Publishers, Amsterdam, pp. 117-123.
- Lupton, F. S., R. Conrad, and J. G. Zeikus. 1984. CO Metabolism of *Desulfovibrio vulgaris* Strain Madison: Physiological Function in the Absence or Presence of Exogenous Substrates. *FEMS Microbiol. Lett.* 23:263-268.
- Lynd, L. H., R. Kerby, and J. G. Zeikus. 1982. Carbon Monoxide Metabolism of the Methylophilic Acidogen *Butyribacterium methylophilicum*. *J. Bacteriol.* 149:255-263.
- Lynd, L. H. and J. G. Zeikus. 1983. Metabolism of H₂-CO₂, Methanol, and Glucose by *Butyribacterium methylophilicum*. *J. Bacteriol.* 153:1415-1423.
- McCullough, G. R., S. C. Roberts, and M. J. van der Burgt. 1982. Shell Coal Gasification Process. *Energy Progress.* 2:69-72.
- Mangold, E. C., M. A. Muradaz, R. P. Ouellette, and O. G. Farah. 1982. Coal Liquefaction and Gasification Technologies, Ann Arbor Science Publishers, Inc., Ann Arbor, MI.
- Mayer, F., D. M. Ivey, and L. G. Ljungdahl. 1986. Macromolecular Organization of F₁-

- ATPase Isolated from *Clostridium thermoaceticum* as Revealed by Electron Microscopy. *J. Bacteriol.* **166**:1128-1130.
- Mayfield, G. G. and V. H. Agreda. 1986. The Eastman Chemical Process for Acetic Anhydride from Coal. *Energy Progress.* **6**:214-218.
- Meyer, O. and H. G. Schlegel. 1983. Biology of Aerobic Carbon Monoxide-Oxidizing Bacteria. *Ann. Rev. Microbiol.* **37**:277-310.
- Michel-Savin, D., R. Marchal, and J. P. Vandecasteele. 1990. Butyrate Production in Continuous Culture of *Clostridium tyrobutyricum*: Effect of End-Product Inhibition. *Appl. Microbiol Biotechnol.* **33**:127-131.
- Mills, G. A. 1976. Catalytic Aspects of Synthetic Fuels from Coal. *Catal. Rev. Sci. Eng.* **14**:69-82.
- Moench, T. T. and J. G. Zeikus. 1983. Nutritional Growth Requirements for *Butyribacterium methylotrophicum* on Single Carbon Substrates and Glucose. *Curr. Microbiol.* **9**:151-154.
- Moore, J. S. and W. J. Shadis. 1988. Automotive Fuels Today and Tomorrow. *Chemtech.* Sept:554-561.
- Moriera, A. R., D. C. Ulmer, and J. C. Linden. 1981. Butanol Toxicity in the Butylic Fermentation. *Biotechnol. Bioeng. Symp.* **11**:567-579.
- Nakamura, S. 1990. From Syngas to Glycol- In One Step. *Chemtech.* Sept:556-564.
- Niedhardt, F. C. 1987. *E. coli* and *Salmonella thyphimurium*: Cellular and Molecular Biology. ASM Press, Washington, DC.
- O'Brien, J. M., R. H. Wolkin, T. T. Moench, J. B. Morgan, and J. G. Zeikus. 1984. Association of Hydrogen Metabolism with Unitrophic or Mixotrophic Growth of *Methanosarcina barkeri* on Carbon Monoxide. *J. Bacteriol.* **158**:373-375.
- Oudar, J. 1980. Sulfur Adsorption and Poisoning of Metallic Catalysts. *Catal. Rev. Sci. Eng.* **22**:171-195.
- Pacaud, S., P. Loubiere, and G. Goma,. 1985. Organic Acid Production Methanol Metabolism by *Eubacterium limosum* B2: Effects of pH and Carbon Dioxide on Growth and Organic Acid Production. *Curr. Microbiol.* **12**:245-250.

- Pacaud, S., P. Loubiere, G. Goma, and N. D. Lindley. 1986a. Organic Acid Production During Methylophilic Growth of *Eubacterium limosum* B2: Displacement Towards Increased Butyric Acid Yields By Supplementing with Acetate. *Appl. Microbiol. Biotechnol.* **23**:330-335.
- Pacaud, S., P. Loubiere, G. Goma, and N. D. Lindley. 1986b. Effect of Various Organic Acid Supplements on Growth Rates of *Eubacterium limosum* B2 on Methanol. *Appl. Microbiol. Biotechnol.* **24**:75-78.
- Piel, W. J. 1988. The Role of MTBE in Future Gasoline Production. *Energy Progress.* **8**:201-204.
- Papoutsakis, E. T. 1983. Equations and Calculations for Fermentations of Butyric Acid Bacteria. *Biotechnol. Lett.* **5**:253-258.
- Papoutsakis, E. T. 1984. A Useful Equation for Fermentations of Butyric Acid Bacteria. *Biotech. Bioeng.* **26**:174-187.
- Papoutsakis, E. T. and C. L. Meyer 1985a. Equations and Calculations of Product Yields and Preferred Pathways for Butanediol and Mixed-Acid Fermentations. *Biotech. Bioeng.* **27**:50-66.
- Papoutsakis, E. T. and C. L. Meyer 1985b. Fermentation Equations for Propionic-Acid Bacteria and Production of Assorted Oxychemicals from Various Sugars. *Biotech. Bioeng.* **27**:67-80.
- Ragsdale, S. W., J. E. Clark, L. G. Ljungdahl, L. L. Lundie, and H. L. Drake. 1983a. Properties of Purified Carbon Monoxide Dehydrogenase from *Clostridium thermoaceticum*, a Nickel, Iron-Sulfur Protein. *J. Biol. Chem.* **258**:2364-2369.
- Ragsdale, S. W., L. G. Ljungdahl, and D. V. DerVartanian. 1983b. Isolation of Carbon Monoxide Dehydrogenase from *Acetobacterium woodii* and Comparison of Its Properties with Those of the *Clostridium thermoaceticum* Enzyme. *J. Bacteriol.* **155**:1224-1237.
- Ragsdale, S. W. and H. G. Wood. 1985. Acetate Biosynthesis by Acetogenic Bacteria. *J. Biol. Chem.* **260**:3970-3977.
- Rao, G., P. J. Ward, and R. Mutharasan. 1987. Manipulation of End Product Distribution in Strict Anaerobes. *Ann. NY Acad. Sci.* **506**:76-81.
- Rao, G. and R. Mutharasan. 1988. Altered Electron Flow in a Reducing Environment in *Clostridium acetobutylicum*. *Biotechnol. Lett.* **10**:129-132.

- Rostrup-Nielsen, J. R. 1971. Some Principles Relating to the Regeneration of Sulfur-Poisoned Nickel Catalysts. *J. Catalysis*. **21**:171-178.
- Saeki, K., M. K. Jain, G. J. Shen, R. C. Prince, and J. G. Zeikus. 1989a. Purification and Properties of Ferredoxin and Rubredoxin from *Butyribacterium methylotrophicum*. *J. Bacteriol.* **171**:4736-4741.
- Saeki, K., Y. Yao, S. Wakabayashi, G. J. Shen, J. G. Zeikus, and H. Matsbara. 1989b. Ferredoxin and Rubredoxin from *Butyribacterium methylotrophicum*: Complete Primary Structures and Construction of Phylogenetic Trees. *J. Biochem.* **106**:656-662.
- Schafer, W., M. Trondt, J. Langhoff, W. Konkol, and J. Hibbel. 1988. The Texaco Coal Gasification Process for Syngas and Fuel Gas Generation. *Energy Progress*. **8**:28-38.
- Sharak Genthner, B. R., C. L. Davis, and M. P. Bryant. 1981. Features of the Rumen and Sewage Sludge Strains of *Eubacterium limosum*, a Methanol- and H₂-CO₂-Utilizing Species. *Appl. Environ. Microbiol.* **42**:12-19.
- Sharak Genthner, B. R. and M. P. Bryant. 1982. Growth of *Eubacterium limosum* with Carbon Monoxide as the Energy Source. *Appl. Environ. Microbiol.* **43**:70-74.
- Simbeck, D. R., R. L. Dickenson, and A. J. Moll. 1982. Coal Gasification-An Overview. *Energy Progress*. **2**:42-46.
- Soucaille, P, G. Joliff, A. Izard, and G. Goma. 1987. Butanol Tolerance and Autobacteriocin Production by *Clostridium acetobutylicum*. *Curr. Microbiol.* **14**:295-299.
- Spencer, D. F., M. J. Gluckman, and S. B. Alpert. 1982. Coal Gasification for Electric Power Generation. *Science*. **215**:1571-1576.
- Spencer, D. F., S. B. Alpert, and M. J. Gluckman. 1989. Coal Gasification Plus. *Chemtech*. **July**:444-448.
- Spillman, R. W. 1989. Economics of Gas Separation Membranes. *Chem. Eng. Prog.* **Jan**:41-62.
- Spillman, R. W. and M. B. Sherwin. 1990. Gas Separation Membranes: The First Decade. *Chemtech*. **June**:378-384.

- Stouthamer, A. H. 1979. The Search for Correlation Between Theoretical and Experimental Growth Yields. In Microbial Biochemistry, J. R. Qualyle, ed., University Park Press, Baltimore, pp. 1-47.
- Stouthamer, A. H. 1988. In Handbook on Anaerobic Fermentations, L. E. Erickson and D. Yee-Chak Fung, eds., Marcel Dekker, Inc., New York, pp. 345-437.
- Tanner, R. S., R. S. Wolfe, and L. G. Ljungdahl. 1978. Tetrahydrofolate Enzyme Levels in *Acetobacterium woodii* and Their Implication in the Synthesis of Acetate from CO₂. *J. Bacteriol.* 134:668-670.
- Thauer, R. K., G. Fuchs, B. Kaufer, and U. Schnitker. 1974. Carbon-Monoxide Oxidation in Cell-Free Extracts of *Clostridium pasteurianum*. *Eur. J. Biochem.* 45:343-349.
- Thauer, R. K. 1977. Energy Conservation in Chemotrophic Anaerobic Bacteria. *Bacteriol. Rev.* 41:100-180.
- Udengaard, N. R. and V. Berzins. 1984. Catalytic Conversion of COS for Gas Cleanup. *Energy Progress.* 4:115-117.
- Uffen, R. L. 1976. Anaerobic Growth of a *Rhodopseudomonas* Species in the Dark with Carbon Monoxide as the Sole Carbon and Energy Substrate. *Proc. Natl. Acad. Sci.* 73:3298-3302.
- Uffen, R. L. 1981. Metabolism of Carbon Monoxide. *Enzyme Microb. Technol.* 3:197-206.
- Vallino, J. J. and G. Stephanopoulos. 1990. Flux Determination in Cellular Bioreaction Networks: Applications to Lysine Fermentations. In Frontiers in Bioprocessing, S. K. Sidkar, M. Bier, and P. Todd, eds., CRC Press, Inc., Boca Raton, FL, pp. 206-219.
- Vega, J. L., E. C. Clausen, and J. L. Gaddy. 1989a. Study of Gaseous Substrate Fermentations: Carbon Monoxide Conversion to Acetate. 1. Batch Culture. *Biotechnol. Bioeng.* 34:774-784.
- Vega, J. L., G. M. Antorrena, E. C. Clausen, and J. L. Gaddy. 1989b. Study of Gaseous Substrate Fermentations: Carbon Monoxide Conversion to Acetate. 2. Continuous Culture. *Biotechnol. Bioeng.* 34:785-793.
- Vega, J. L., K. T. Klasson, D. E. Kimmel, E. C. Clausen, and J. L. Gaddy. 1990. Sulfur Gas Tolerance and Toxicity of CO-Utilizing and Methanogenic Bacteria. *Appl.*

Biochem. Biotechnol. **24/25**:329-340.

Verma, A. 1978a. From Coal to Gas. *Chemtech.* **June**:372-381.

Verma, A. 1978b. From Coal to Gas-Part II. *Chemtech.* **June**:626-638.

Vollherbst-Schneck, K., J. A. Sands, and B. S. Montenecourt. 1984. Effect of Butanol on Lipid Composition and Fluidity of *Clostridium acetobutylicum* ATCC 824. *Appl. Environ. Microbiol.* **47**:193-194.

Wiegel, J., M. Braun, and G. Gottsalk. 1981. *Clostridium thermoautotrophicum* Species Novum, a Thermophile Producing Acetate from Molecular Hydrogen and Carbon Dioxide. *Curr. Microbiol.* **5**:255-260.

Wiemer, P. J. and J. G. Zeikus. 1978. One Carbon Metabolism in Methanogenic Bacteria. *Arch. Microbiol.* **119**:49-57.

Wilson, J. S., J. Halow, and M. R. Ghate. 1988. Gasification: Key to Chemicals from Coal. *Chemtech.* **Feb**:123-128.

Wise, D. L., C. L. Cooney, and D. C. Augenstein. 1978. Biomethanation: Anaerobic Fermentation of CO₂, H₂, and CO to Methane. *Biotechnol. Bioeng.* **20**:1153-1172.

Wood, H. G. and L. G. Ljungdahl. 1991. Autotrophic Character of the Acetogenic Bacteria. In Variations in Autotrophic Life, J. M. Shively and L. L. Barton, eds., Academic Press, New York, pp. 201-250.

Worden, R. M., A. J. Grethlein, J. G. Zeikus, and R. Datta. 1989. Butyrate Production from Carbon Monoxide by *Butyribacterium methylotrophicum*. *Appl. Biochem. Biotechnol.* **20/21**:687-698.

Worden, R. M., A. J. Grethlein, M. K. Jain, and R. Datta. 1991. Production of Butanol and Ethanol from Synthesis Gas via Fermentation. *Fuel.* **70**:615-619.

Young, K. D. and W. R. Finnerty. 1991. Mass and Energy Balances for Coal-Based Microbial Systems. Second International Symposium on the Biological Processing of Coal, Workshop 4. May 1-3, San Diego, CA.

Zeikus, J. G. and Wolfe, R. S. 1972. *Methanobacterium thermoautotrophicum* sp. n., an Anaerobic, Autotrophic, Extreme Thermophile. *Science.* **109**:707-713.

- Zeikus, J. G. and V. G. Bowen. 1975. Comparative Ultrastructure of Methanogenic Bacteria. *Can. J. Microbiol.* 21:121-129.
- Zeikus, J. G. 1977. The Biology of Methanogenic Bacteria. *Bacteriol. Rev.* 41:514-541.
- Zeikus, J. G. 1980. Chemical and Fuel Production by Anaerobic Bacteria. *Ann. Rev. Microbiol.* 34:423-464.
- Zeikus, J. G., L. H. Lynd, T. E. Thompson, J. A. Krzycki, P. J. Wiemer, and P. W. Hegge. 1980. Isolation and Characterization of a New, Methylotrophic, Acidogenic Anaerobe, the Marburg Strain. *Curr. Microbiol.* 3:381-386.
- Zeikus, J. G. 1983a. Metabolism of One-Carbon Compounds by Chemotrophic Anaerobes. *Adv. Microb. Physiol.* 24:215-299.
- Zeikus, J. G. 1983b. Chemical and Fuel Production from One-Carbon Fermentations: A Microbiological Assessment. In Organic Chemicals from Biomass, D. L. Wise, ed., Benjamin Cummings, Menlo Park, CA, pp. 359-383.
- Zeikus, J. G., R. Kerby, and J. A. Krzycki. 1985. Single-Carbon Chemistry of Acetogenic and Methanogenic Bacteria. *Science.* 227:1167-1173.

MICHIGAN STATE UNIV. LIBRARIES



31293009085733